# INFORMATION TO USERS

This manuscript has been reproduced from the microfilm master. UMI films the text directly from the original or copy submitted. Thus, some thesis and dissertation copies are in typewriter face, while others may be from any type of computer printer.

**The quality of this reproduction is dependent upon the quality of the copy submitted.** Broken or indistinct print, colored or poor quality illustrations and photographs, print bleedthrough, substandard margins, and improper alignment can adversely affect reproduction.

In the unlikely event that the author did not send UMI a complete manuscript and there are missing pages, these will be noted. Also, if unauthorized copyright material had to be removed, a note will indicate the deletion.

Oversize materials (e.g., maps, drawings, charts) are reproduced by sectioning the original, beginning at the upper left-hand corner and continuing from left to right in equal sections with small overlaps.

ProQuest Information and Learning
300 North Zeeb Road, Ann Arbor, MI 48106-1346 USA
800-521-0600

# UNIVERSITY OF CINCINNATI

July 19 19 54

*I hereby recommend that the thesis prepared under my supervision by* ROMAN OSADCHUK

*entitled* TRANSFORMATIONS IN NODULAR CAST IRON

*be accepted as fulfilling this part of the requirements for the degree of* DOCTOR OF PHILOSOPHY

*Approved by:*

Roy O. McDuffie

John F. Kahles

Robert H. Price

Form 668—G.S. and T.C.—1M—4-51

# TRANSFORMATIONS IN NODULAR CAST IRON

A dissertation submitted to the
Graduate School of Arts and Sciences

of the University of Cincinnati
in partial fulfillment of the requirements
for the degree of

DOCTOR OF PHILOSOPHY

1954

by

Roman Osadchuk

B.A.Sc. University of Toronto 1950
M.S. University of Cincinnati 1952

## ACKNOWLEDGEMENT

The author is indebted to the International Nickel Company Inc., who made this work possible through the grant of a Fellowship at the University of Cincinnati, and who supplied the irons for the second part of this investigation. Special appreciation is due to Mr. C. T. Haller of the International Nickel Company, for his suggestions and excellent cooperation.

The author wishes to thank Dr. R. O. McDuffie, Professor F. E. Westermann and the rest of the faculty for their advice and generous assistance.

TABLE OF CONTENTS


| | Page |
|---|---|
| Introduction | 1 |
| Theories of Graphite and Cementite Formation | 10 |
| Theories of Nodular Iron Formation | 26 |
| Purpose of This Investigation | 34 |
| **Part I** | |
| Liquid to Solid Transformations | 36 |
| Experiment I | 41 |
| Observations | 60 |
| Experiment II | 62 |
| Discussion of Experimental Results | 65 |
| The Mechanism of Graphite Spherulite Formation and Growth in Hypoeutectic Cast Irons | 70 |
| Formation of Flake Versus Nodular Graphite in Hypoeutectic Cast Irons | 80 |
| Summary of Spherulite Formation and Growth in Hypoeutectic Nodular Irons | 83 |
| **Part II** | |
| Solid to Solid Transformations | 85 |
| Experimental Methods and Apparatus | 87 |
| T - T - T Diagrams | 99 |
| Discussion of Experimental Results | 105 |
| Discussion of the Microstructures | 129 |
| Photomicrographs | 138 |

ABSTRACT

The work in this thesis is divided in two parts. Part I has to do with the liquid to solid transformations in nodular iron while Part II is concerned with the sub-critical transformation of austenite and pearlite in nodular cast irons.

In Part I two experiments were carried on the solidification of nodular iron in order to determine the mechanism of the formation and growth of graphite spherulites. Small specimens were melted in a specially designed induction furnace and quenched in a brine solution from various points on the cooling curve. The temperature was recorded by a thermocouple connected to the Speedomax recorder which recorded the cooling curve of the specimen. After quenching the specimens were observed under the microscope.

The results indicate that the graphite nodules are formed during the "horizontal" portion of the cooling curve. The nodules grow during the so called "eutectic solidification" although strictly speaking eutectic solidification does not occur in nodular iron. The graphite nodules are surrounded by a shell of austenite while they are very small and the

graphite nodule grows in a shell of austenite, as the liquid transforms to solid. As a result of this investigation a new theory for the formation and growth of graphite spherulites is proposed.

The objective of the experiments in Part II was the determination of T-T-T diagrams for the four nodular cast irons and the determination of the end of graphitization of pearlite and austenite below the critical temperature.

Small specimens were prepared from keel blocks. These specimens were then homogenized and austenitized in a dry argon atmosphere and transformed at various temperatures in liquid metal baths. The specimens were quenched in water after various intervals of transformation and observed under the microscope.

As a result of these experiments four T-T-T diagrams are presented together with the $M_s$, $M_f$, and the two critical temperatures for each alloy. The effect of homogenization and nodule count is also indicated. Isothermal reaction curves, percent of martensite vs temperature curves, and photomicrographs are included in this text. Hardness of completely transformed structures is given in the table. A graph indicating the comparison of the hardness of the matrix and the overall hardness of the nodular cast iron

No. 4 for completely transformed structures vs transformation temperature is also presented. The results show that the hardness of the matrix is about six Rockwell units higher than that indicated by the overall hardness of the iron.

# INTRODUCTION

Cast iron is a complex alloy consisting primarily of iron, carbon and silicon in which the carbon appears as graphite and/or as carbide. Cast iron also contains minor alloying elements or impurities such as manganese, sulphur, and phosphorus which modify its structure to some extent. For simplicity and practical purposes cast iron may be considered as a ternary alloy of iron, carbon, and silicon.

A common definition of cast iron is steel plus graphite and/or carbide. This definition is quite appropriate since the matrix of cast iron is similar in its behavior to steel of the same composition. As in the case of steel, special alloying elements such as nickel, molybdenum chromium, etc., may be added to cast iron to produce specific properties. The main difference between steels and cast iron as far as composition is concerned is that cast irons have more carbon and silicon than steels. Steels range from 0-1.5% carbon while cast irons range from 2-4.5% carbon although there is no definite demarkation line between steel and cast irons which would indicate where steels end and where cast irons begin. Cast irons which are less than eutectic in composition are called hypoeutectic, while those greater than eutectic composition are called hypereutectic.

Cast irons may be conveniently classified under four groups, namely:

1. Gray Cast Iron
2. White Cast Iron
3. Malleable Iron
4. Nodular Cast Iron, also know as ductile iron, etc.

Gray cast iron contains a large percentage of its carbon in the form of flake graphite after casting. The mechanical properties depend to a great extent upon the amount, shape and distribution of the graphite as well as upon the characteristics of the matrix. The low strength of graphite makes it act as voids (with a notch effect) in the structure when a tensile stress is applied, and for this reason gray cast iron has a low tensile strength and is considered a weak material. However, gray cast iron has a good compressive strength. Structurally gray cast iron may be considered as a matrix of hypoeutectoid, eutectoid or hypereutectoid steel with flakes of graphite in it.

Gray cast iron is the most widely used of all cast irons and its tonnage production exceeds all cast irons combined. The reason for its wide industrial use is its good corrosion resistance, good machinability, good damping properties, fairly good wear resistance and above all it is

the cheapest of all industrial alloys. Although its strength and its toughness are not too good, nevertheless they are good enough for most industrial applications. Gray cast irons are widely used in automotive industry, agricultural equipment, pipes, flanges, fittings, as well as in manufacturing, transportation, mining and household appliance industries. Chemical composition of gray cast irons ranges from 1-3% silicon and from 2.5-3.8% total carbon, and their tensile strength from 20,000-70,000 psi. Slow cooling promotes graphite formation while rapid cooling promotes carbide formation. Therefore proper combination of cooling rate and composition is necessary to produce gray iron.

White cast iron is extremely hard and quite brittle because practically all of the carbon occurs as iron carbide. For example, 3.3% carbon would give a structure which would be approximately 50% iron carbide, and for that reason white iron has properties similar to iron carbide. White irons are used mainly where high hardness and good wear resistance are desired and where low strength is permissible. Because of their brittleness and non-machinability white cast irons have a very limited use. Another use of white cast iron is in the production of malleable iron which is described below. The chemical composition of white cast irons differs from

gray iron in that white irons have low silicon content, usually less than 1%. Low silicon content, high content of carbide stabilizers, and fast cooling rate favor the formation of white iron. The microstructure of white cast iron is massive carbides in the matrix of one or more of the transformation products of austenite.

Malleable iron is produced by annealing white cast iron of the proper chemical composition. The microstructure of standard malleable iron is composed of temper carbon in a matrix of ferrite. Temper carbon consists of aggregates of graphite which are formed during annealing of white cast iron. It is also possible to have other types of malleable iron for example perlitic malleable iron consists of temper carbon in a matrix of pearlite; thus the matrix may consist of any one or more of the transformation products of austenite. The chemical composition of malleable iron is usually from 0.8-1.6% silicon and 2-3% carbon. The percentage of silicon should be low enough to prevent precipitation of graphite during cooling, and high enough to give fairly rapid decomposition of carbide during annealing. The annealing temperatures range from 1500-1700°F for several days in order to convert carbide to temper carbon and austenite. The whole process of slowly heating to annealing temperature, holding at annealing temperature and slow cooling to room temperature takes about one week, and after that cycle is

complete, standard malleable iron is obtained. During slow cooling the austenite is converted to ferrite and graphite and this process is known as subcritical graphitization. The most common alloying elements that are added to malleable cast iron are copper and molybdenum in order to increase the tensile strength.

Malleable iron has higher ductility and higher tensile strength than gray cast iron and is used where greater strength and higher resistance to shock is required. It is easily machinable, soft and has poor abrasion resistance. Its uses are similar to those of gray cast iron outlined previously. The chief disadvantage of malleable iron is its much greater cost due to long heat treatment cycle, and for that reason it is not used as extensively as gray cast iron.

Nodular cast iron is similar in chemical composition to gray cast iron and it only differs in that graphite is in spheroidal form instead of flakes. Nodular irons are produced by adding a small amount of magnesium and cerium to cast irons containing from 1.5-3% silicon and about 2.5-4% carbon. The magnesium content of these cast irons is very small and is about 0.1% magnesium or less. This type of iron contains spheroids of graphite in a matrix of pearlite,

ferrite or both in the as cast condition depending on the silicon content and the cooling rate. The higher the silicon content and the slower the cooling rate the more ferrite is present. Magnesium is added to the laddle containing molten metal before metal is poured and the temperature is usually kept low, just above freezing point, since at high temperature magnesium vaporizes readily and the efficiency of solution in iron is decreased.

The properties of nodular iron are superior to those of gray cast iron because the graphite is in the form of spherulites and the continuity of the matrix is not interrupted as seriously as in gray iron. It has been stated earlier that the reason why malleable irons show greater strength is because graphite is in the form of aggregates (temper carbon) or patches of carbon, and the same reason is also applicable to nodular iron. The graphite in gray iron occurs in various shapes and exists as flakes or lamellae which act as stress-raisers by interrupting the continuity of the matrix and thus making the iron brittle and weak. As pointed out earlier malleable irons are quite expensive because of long heat treatment, and ordinary gray cast irons are too weak and brittle for some applications. Nodular irons possess the good properties of both irons and do not require the long and expensive heat

treatment as do malleable irons. At the present time however the cost of modular iron is greater than that of gray iron because the foundries have little experience in its production, and therefore have difficulty in meeting certain specifications. This is expected to be only temporary because the first publications on the production of nodular iron by the addition of cerium or magnesium appeared only about six years ago.

Since the subject of this thesis deals primarily with nodular iron, it will be discussed in more detail later. For the present only a brief introduction was given in order to show the relationship of nodular cast iron to other cast irons and to cite some of the important advantages and disadvantages of each type.

The influence of carbide and graphite on the mechanical and physical properties of cast irons was discussed above with reference to the four main types of cast irons. It should be pointed out that mechanical properties are also influenced by the type of microstructure of the matrix. For example the properties will depend to some extent whether the matrix is ferritic, martensitic, perlitic, bainitic, austenitic, etc. As was stated earlier in the definition of cast irons the matrix may be considered

as steel of similar composition. The microstructure of the matrix in cast iron as in the case of steel will depend on the cooling rate from austenitizing temperature and on the composition of the matrix. In order to predict the microstructure of the matrix at some definite cooling rate or to obtain a certain desireable microstructure it is necessary to know something about the kinetics of austenite decomposition at various temperatures. This information is most readily obtained from curves for the isothermal transformation of austenite. These curves are commonly known as "S" curves, T-T-T curves or I-T curves. The I-T curve is usually a plot of temperature versus log of time of isothermal start and end of transformation for a particular alloy. The start and finish are not definitely defined but start is usually taken as 1% transformed and finish as 95-99% transformed. Sometimes 50% or any other percent of transformation is recorded. In the case of steel there are thousands of such curves in literature and their use is well known in heat treating circles. T-T-T curves are just as important in heat treatment as equilibrium phase diagrams are in interpreting the number of phases in a given alloy at equilibrium.

From a T-T-T curve one can tell at a glance what will be the microstructure at a given temperature and how

long it takes to obtain that microstructure. It is possible to select a proper temperature in order to get a desired microstructure. It is also possible to predict approximately the type of microstructure that could be obtained at a given cooling rate. For this reason the study of isothermal transformations is very important in metallurgy and is now being applied to many non-ferrous alloys such as titanium and zirconium base alloys.

By applying isothermal treatment to alloys many fundamental principles have been clarified and many more will be explained in the future. In the text of this thesis an extensive use was made of the isothermal treatment in both solid-solid transformations and in liquid-solid transformations in nodular cast irons.

## THEORIES OF GRAPHITE AND CEMENTITE FORMATION

The appearance of graphite in cast irons has puzzled most of the early investigators and many explanation accounting for the formation of graphite in cast irons and carbide in steels were proposed. Even at the present time there is little reliable experimental evidence which would explain why in one case we get carbide and in another we get graphite. The most commonly accepted explanation at the present time postulates that the true and stable equilibrium diagram should be iron-graphite and that iron-iron carbide diagram is metastable and therefore is not a true equilibrium diagram but a metastable diagram where cementite is quite persistant. There have been several experiments designated to show that cementite is unstable from a thermodynamic point of view below the eutectic temperature. However the authors that carried out these experiments arrived at various conclusions, some claiming that cementite is unstable below the eutectic temperature while others claim that it is unstable only below the eutectoid temperature but stable above the eutectoid temperature. Some also claimed that cementite is stable below the eutectic temperature but becomes unstable in the presence of silicon, as in the case of cast irons. It is a well known fact that if there is more than 1%

silicon present in cast irons the decomposition of cementite is very rapid and the stable system is iron-graphite and not iron-iron carbide. This fact is not too apparent in the absence of silicon and in pure low carbon alloys. However the present trend is to consider iron-iron carbide as metastable and iron-graphite as stable even in pure iron-carbon alloys.

In order to have a better understanding of the transformations in cast iron a brief discussion of the iron-iron carbide and iron-graphite equilibrium diagrams is in order. An excellent discussion of these two systems is in the book by Samuel Epstein[1].

Selected Iron-Iron Carbide Diagram:

This diagram is based on many experiments of different authors and the most probable values were selected for plotting this diagram. It should be pointed out that the diagram is based only on experimental evidence and no consideration was given to thermodynamic calculations. The thermodynamic calculations were omitted because data on which they are based are not too reliable. The value and sign of the free energy of formation of cementite is still a controversial point. Factors such as, purity of materials, degree of attaining equilibrium and the

precision of measurements used in experiments are very important in determining equilibrium diagrams.

There are many regions in the iron-iron carbide diagram that are not too well established and some of the most important ones are, the curve denoting maximum solubility of cementite in liquid iron, the liquidus and solidus curves are not too accurate, and the contour of the curve denoting the maximum solubility of cementite in austenite.

From practical viewpoint metallurgists are interested more in the rate of approach to equilibrium rather than in true equilibrium and although determination of equilibrium in very pure iron-carbon alloys is of little practical importance in the heat treatment of commercial alloys, it is nevertheless of primary importance because the true equilibrium diagram may clarify some of the fundamental metallurgical problems and give us better picture of the effect of alloying elements.

The Iron-Graphite Diagram:

The iron-graphite phase diagram originated from the concept of the metastability of cementite rather than from experimental work. The concept of metastability was introduced in order to explain the formation of graphite

in cast irons. Early investigators such as Charpy, Heyn and others concluded that the least stable form is the first to appear on solidification or on precipitation from a solid solution, and that the metastable phase has a lower freezing and transformation temperature. The stable phase is also less soluble in liquid and solid solutions than the metastable phase. This concept offers a convenient means of representing the observed behavior in cast irons and it is generally conceded that graphite is more stable than cementite. Although this concept is simple and appears to be quite sound, nevertheless there are some questions raised after the proponents failed to establish experimentally beyond any doubt the contour of the iron-graphite diagram.

There are many difficulties in establishing experimentally the boundaries of iron-graphite system, for example, cementite is quite persistent in pure iron carbon alloys, and the outline of the iron-carbon diagram appears to be only slightly displaced from the metastable diagram and the displacements are of the same magnitude as the uncertainties in the location of the iron-cementite diagram. Although the iron-graphite diagram has not been established experimentally there is some evidence to support its existence, and the existence of graphite

eutectoid and graphite eutectic is generally conceded. In the most recent investigation on graphitization of high purity iron carbon alloys Cyril Wells[2] has shown that cementite is unstable below 1200°C and above 1200°C graphite is unstable and cementite is stable. Wells also established that graphite eutectoid in pure iron carbon alloys is at about 740°C and at .7% carbon and plotted the iron graphite equilibrium diagram in the vicinity of the eutectoid, thus giving weight to the existence of iron-graphite eutectoid. Since cementite is stable above 1200°C and graphite is metastable above this temperature Wells[2] proposed a modified stable iron-carbon equilibrium diagram.

The two equilibrium diagrams iron-graphite and iron-iron carbide diagrams are usually superimposed and the results is known as the "double diagram". Among the earlier investigators that supported the idea of a double diagram were, Roozeboom, Charpy, Bendicks, Heyn and Upton. Other investigators such as Honda, Sauveur and Hatfield maintained that if graphite never forms directly from the melt the iron graphite lines should not be included in the equilibrium diagram. Many other investigators such as Bolton, Northcott, May and Heike concluded that graphite

forms only upon decomposition of cementite but did not take a definite stand against the double daigram.

Although the argument for the double diagram is not completely settled the present tendency is in support of the double diagram and iron-iron carbide diagram is considered metastable. Also it is generally conceded that graphite may form directly from the liquid and this eliminated the chief objection to the double diagram.

Discussion of Graphite Formation

In the past metallurgists neglected the study of phase transformations in cast irons because these transformations are much more difficult to study and because cast irons were considered as cheap and brittle alloys which could be improved very little by heat treatment.

For this reason very few precise and conclusive data are available and the whole subject is highly controversial. As pointed out earlier, cast irons may be considered as ternary iron-carbon-silicon alloys, and that silicon is very important factor in graphitization and causes graphitization to occur rapidly enough for commercial utilization. It is a well known fact that silicon speeds up graphitization but the mechanism is not clearly understood. Hatfield considered that some of the silicon is

present in the carbide and thus causing the carbide to decompose readily.

The question of the mechanism of the graphitization of cementite is very important in graphitization of malleable iron and heat treatment of ductile irons. Seltz, McDonald and Wells[3] from thermodynamic considerations arrived at conclusions that cementite is unstable in the presence of austenite saturated with carbon and free graphite below 1200°C and that cementite is unstable below 800°C and stable above that temperature relative to pure austenite and pure graphite. This would explain why cementite is more persistent in low carbon steels and less persistent in high carbon steels and cast irons.

Another important question is whether graphitization takes place from decomposition of carbide only or from solid solution or both. There is some evidence to indicate that it takes place from both, solid solution and carbide, and it would be interesting to know whether silicon speeds up graphitization by making carbide less stable, acting as catalyst, or having some influence on the decomposition from solid solution.

Norbury[4] believed that both finely divided graphite and the coarse graphite flakes form directly on solidification. The finely divided graphite forms on super-

cooling and the coarse flake graphite on normal slow cooling. Kase on the other hand concluded from his experiments on solidification of cast irons that only cementite forms on solidification and that graphite flakes form as a result of decomposition of cementite. Hanemann and more recently Boyles[5] have shown that graphite forms directly during the solidification arrest or interval and that graphite flakes extend into ledeburitic areas. Hanemann also showed that the time of graphite formation at the eutectic temperature of chilled and then reheated samples up to the melting point takes 3,500 sec. while graphite forms in 50 seconds during solidification from liquid. This would seem to rule out the possibility that the graphite that formed during solidification resulted from the decomposition of cementite. Although the iron graphite eutectic has not been definitely established, at least eutectic-like structures are observed but no one however has shown satisfactorily the appearance of the iron graphite eutectoid. Many investigators have tried to show the existence of graphite eutectoid but their evidence is not convincing.

Mechanism of Freezing of Gray Cast Irons:

Mechanism of freezing of cast irons is discussed in detail by Boyles[5] and some of the important features

are outlined below in order to show the similarities between these irons and ductile irons discussed in the experimental section of this thesis. In hypoeutectic alloys freezing begins with the formation of dendrites of primary austenite, followed by crystallization of eutectic liquid from independent centers within the interstices of the dendrites. This is similar to other alloy systems in which eutectic appears. The dendrites grow until the eutectic solidification starts. Crystallization of the eutectic liquid begins at centers which grow equally in all directions, forming a cell-like structure. The graphite flakes do not appear until this cellular structure starts forming, that is until eutectic starts to freeze. The flakes grow rodially from the centers of eutectic crystallization, forming colonies of graphite flakes and austenite. After the solidification is complete the flake structure is established and is not changed appreciably during cooling to room temperature. Graphite flakes grow according to their natural inclinations and the austenite component of the eutectic is trailing along obediently. As the graphite flakes grow outward and become more separated new centers of graphite are nucleated in the spaces between them. Each graphite crystal has a nucleus and the number of graphite nuclei formed along the advancing

front of solidification determines the total number of graphite flakes formed in a given colony. The size of the flakes depends on the rate of nucleation and the rate of growth. If the rate of nucleation is very rapid relative to the rate of growth of the individual graphite crystals, small flakes will be produced. There are three important and independent types of nucleation during freezing of gray cast irons.

1) Nuclei of primary austenitic dendrites
2) Nuclei of centers of the eutectic solidification which give rise to cellular structure and to a colony of graphite flakes
3) Nuclei of the individual graphite flakes which form during growth of the eutectic colonies.

The characteristic graphite patterns found in gray cast iron are classified by the American Society for Testing Materials and illustrated on the chart by photomicrographs designated as Types A, B, C, D, and E.

In type A graphite is of uniform distribution and random orientation and is the most common type of structure found in gray cast iron. In this type of structure the austenite formed during eutectic freezing merged with that of the primary austenite dendrites to form a continuous mass. MacKenzie demonstrated by models that the graphite flakes formed in this type consisted of "whorl" type resembling a motor boat propeller or a fan. This would indicate that the graphite flakes do not form a continuous path of weakness through the metal as often loosely stated by metallurgists.

Graphite in type B is in the form of rosette groupings of random orientation. In this iron each rosette represents a center of crystallization of eutectic liquid and is a result of radial growth of eutectic colonies of graphite and austenite. In other words the center of each rosette is the center of the cell described previously.

In type C graphite consists of superimposed large flakes which are sometimes called kish flakes over small flakes. Both types of flakes are of random orientation. Type C is usually found in hypereutectic alloys and freezing for these alloys is somewhat different. Whether

kish flakes (large long flakes) form directly from the melt or whether they form from decomposition of cementite is not settled as yet, but the important thing is that they exist as graphite in the melt just before freezing of the eutectic. The mechanism of solidification of hypereutectic alloys is not known at the present time and it is impossible to say whether the eutectic freezes in the same way as described previously for hypoeutectic irons.

Type D consists of very small graphite flakes randomly oriented and without exhibiting radial type of growth. The graphite is confined to the spaces between the dendrites and the primary dendrites are perfectly outlined by a mixture of graphite and iron. This type of graphite is usually found in thin sections and is associated with rapid rate of nucleation. It is considered to form directly from the liquid as described previously although there is some disagreement on that issue. These cast irons are hypoeutectic and are usually associated with a fairly rapid cooling rate.

Graphite in type E is of preferred orientation and outlines the primary dendrites by interdendritic segregation. These cast irons are usually strongly hypoeutectic and therefore the primary dendrites are

crowded together. It is believed that because of this the graphite flakes formed during freezing of the eutectic were forced to develop in the narrow spaces between the dendrides which resulted in preferred orientation.

In the case of hypoeutectic irons it may be said that constituents formed during freezing of the eutectic occupy the interstices of the primary dendrites, and for this reason the graphite flakes and the phosphide eutectic are restricted by the size and distribution of dendrites.

Segregation During Freezing of Cast Irons

Segregation during freezing is of primary importance in heat treatment of cast irons and the effect of segregation on the rate of isothermal transformation in nodular irons will be demonstrated by the experimental evidence in this thesis. In order to understand this problem better it is necessary to point out that segregation during freezing takes place in two stages.

1) Segregation between the primary dendrites and the liquid
2) Segregation due to cellular growth of the eutectic during freezing. This segregation takes place from the crystallization centers

of the eutectic outward into the boundaries of the cells.

Boyles[5] has shown that sulphur and phosphorus segregate in the boundaries of the eutectic cells and this results in increase in the amount of pearlite in these regions. He also pointed out that subsequent recrystallization as the iron passed through the transformation range did not alter the distribution of the sulphide. It is important to point out that many impurities and alloying elements may segregate in cell boundaries or between the dendrites and have an important effect on the rate of isothermal transformation. He also found that in cast irons containing manganese where the structure was partially ferrite and partially pearlite, the pearlite segregated in the boundaries of cell structure and as the content of manganese increased more pearlite formed.

It is only proper to point out at this stage that there are many factors which affect the solidification structure of cast irons and which will not be discussed here in detail. Besides those that behave in the orthodox manner such as composition, other factors which are less understood such as inoculation, effect of gases or

atmosphere, inclusions, effect of undercooling, and effect of minor alloying elements are very important and any one or more of these may change the structure completely. The reason why they are so important is that these factors have great influence on the nucleation of eutectic cell, graphite, and cementite. Also the stability of cementite, surface energy or tension, and diffusion may be affected by these factors. For example Boyles has found that when a calcium-silicon was added as inoculant it increased the number of nuclei from which eutectic cells or colonies of graphite flakes start and decreased the total number of nuclei from which individual flakes grow during freezing. The whole problem is so complex and so undeveloped that no further discussion will be given to this topic except to point out that it is very important in dealing with cast irons.

## Nodular Cast Iron

History:

It is rather difficult to establish who was the first investigator that discovered how to produce nodular iron, and the origin of the nodular graphite may never be definitely established. There are several references

of the occurence of nodular iron in prewar German and American literature and patents. It is true that there have been several photomicrographs of perfect nodules produced before World War II and one of them is found in Volume II of the book entitled "Metals" by Carpenter and Robertson. However the information in prewar literature is not too definite and the production of nodular iron in these references is believed to be accidental.

The first definite and detailed publication of the production of nodular cast iron was an article titled "Graphite Formation in Cast Irons and Nickel-Carbon and Cobalt-Carbon Alloys, and Nickel-Iron-Carbon Alloys", by Morrogh and Williams published in the Journal of the Iron and Steel Institute Volume 158, March, 1947. In this article the discovery of Cerium process was presented. It may therefore be stated that the history of "nodular iron" began in 1947 and "nodular iron" is only several years old. The Cerium process was described and illustrated by Morrogh in three papers published during 1947 and 1948.

In the discussion of papers by Morrogh and his associates the American "magnesium process" was introduced. In 1948 there appeared also two papers in Germany one by Piwowarsky and one by Adey. Finally in 1949 the "magnesium process" was described and illustrated by

Gagnebin, Mills, and Pilling in the Iron Age February 17, 1949 and by Donoho in the American Foundryman February, 1949.

Theories of Nodular Iron Formation

There are more than a dozen theories on nodular iron formation but none of them are too convincing and they are not supported by experimental evidence. Very little precise work has been done on solidification of nodular iron and temperature control in many experiments was not precise enough to make any definite conclusions. The theories are also divergent in their views and not many of them can be reconciled. At the present time there is no theory that can be acceptable. Delport[6] reporting on the discussion at the International Foundry Congress in 1951 on "Nodule Formation" summarized the views expressed at that time under three hypothesis as follows:

1) The nodule makes its appearance in the solid state by decomposition of ledeburitic cementite.

2) The nodule appears in the liquid by precipitation of carbon from hypereutectic elements (interdendritic in the case of hypoeutectic irons; this primary precipitation causes the remaining liquid to be

composed of ledeburitic eutectic and it solidifies as ledeburite. Cementite is very rapidly decomposed into austenite and carbon which migrates to the existing nodules. In brief nodules appear in the liquid and grow rapidly in the solid by decomposition of the cementite.

3) Precipitation and growth in the supersaturated austenite. This hypothesis implies complete solidification as mixed crystals and therefore a displacement toward the right of the eutectic point. In other words nodular cast iron gives no eutectic and it always solidifies as mixed crystals.

The hypothesis (2) and (3) are the most favorable.

Morrogh and Williams propose the following sequence of events in solidification of nodular irons:

1) The formation of proeutectic graphite spherulites followed by metastable solidification of the eutectic complex to ledeburite and the subsequent graphitization of the carbide phase. It was claimed that Mg and Ce stabilized the carbide during freezing but since carbide is unstable at high temperature it decomposes to form solid nodules.

Pellini and Dunphy propose the following sequence of events during solidification of hypoeutectic cast iron treated with magnesium:

1) The solidification of dendrites of austenite beginning at the liquidus temperature and continuing to the temperature at which the normal eutectic consisting of flake graphite and austenite would occur.

2) Suppression of the normal flake graphite eutectic during which interval graphite precipitates from localized regions of supersaturated interdendritic liquid in a spherulitic crystallization mode.

3) Solidification of the remaining eutectic liquid as an austenite iron carbide complex, and rapid malleabilization of the structure resulting in growth of the graphite particles. They also concluded from their experiments that nodules form during very short time corresponding to the beginning of the horizontal part of the cooling curve, immediately prior to the start of the eutectic reaction, and that localized pools of hypereutectic liquid provide genesis conditions similar to hypereutectic melts. They claim that no nodules form during eutectic solidification.

Krynitsky[7] and Stern concluded from their experiments that nodules are formed in the melt during solidification and graphite patches are produced after solidification by decomposition of carbides and this is similar to Morrogh's views. They also observed radial and non radial structures of graphite and cores consisting of inclusions.

Iitaka[8] advanced the theory that six sided columnar crystals of graphite are produced from nuclei under free growth conditions at high temperature. These crystals are weak and break by slipping along their basal planes

because of the relative movement of the graphite and the molten metal. This gives flake graphite. On the other hand crystals which do not break by slippage grow into granules and lumps. These lumps are plastic at high temperature but their surface tension is insufficient to cause them to become globular. If however magnesium or cerium is present in the iron in amounts greater than the solubility at solidification then the excess separating as vapor is absorbed in part by the growing graphite. The increase in surface tension resulting from absorption of the metal vapour causes the graphite to become globular.

Bounin and Ivantzoff[9] conclude from their experiments that graphite in regular cast irons seems to grow while in contact with the liquid phase during the eutectic interval whereas in magnesium treated irons the graphite particles grow in an envelope of austenite which isolates them from the liquid metal. The space required for growth of the graphite is provided by self diffusion of the iron atoms within the austenite. This self diffusion is increased by the addition of silicon because of the difference in size between silicon and iron atoms which results in weakening of the atomic bonds in the austenite and alters its space lattice.

Just recently De Sy[10] proposed a similar theory to the one outlined above. He also claims that spherulite

originates and grows in a supersaturated austenite and since austenite in the vicinity of the nodule may be considered homogeneous single phase the growth would be equal in all directions which would result in spherulitic growth of nodules. Since self diffusion of iron is much slower than the diffusion of carbon the shape of the graphite would be controlled as stated by Bunin by the speed of evacuation of the iron atoms enveloping the graphite, and since self diffusion of iron atoms in homogeneous phase is equal in all directions the graphite will have spheroidal shape. The nodular iron is believed to solidify without the eutectic but in a mixed crystal system forming supersaturated austenite in which graphite precipitation occurs beginning at a certain degree of supersaturation and spherulitic graphite growth follows by a peritectic transformation reaction. The carbon is continually withdrawn from the austenite solution and replaced at the expense of the carbon in the melt. Thus carbon migrates from liquid through the austenite surface layer to the graphite spherulite. For magnesium treated cast irons austenite is believed to be highly supersaturated as indicated by the cooling curves, (high supercooling of eutectic and freezing takes place at a much lower temperature). Magnesium decreases

graphite nuclei formation by eliminating graphite nuclei mainly through reduction of silica particles which in turn results in supercooling and austenite supersaturation.

The experimental evidence on solidification of ductile irons in this thesis seems to support part of the theory of Bunin and De Sy and is discussed in experimental section. The experimental evidence that De Sy furnishes in support of his theory is the fact that magnesium treated highly hypereutectic iron does not reject kish (spherulitic) graphite while the ordinary irons reject large quantities of kish graphite. Although the nodular irons show definite spherulite flotation as shown by the micrographs consisting of clusters of nodules in the upper part of the casting, the phenomena is not difficult to explain. The clusters are due to flotation of small austenite grains which have been lightened by the precipitated graphite spherulites.

Render[11] in his experiments reached the following conclusions regarding nuclei formation.

1) There is a central spot present in many nodules which is not graphite and which has properties much different from the surrounding graphite.

2) Nucleus is probably associated with each nodule.

3) The nuclear material is quite hard, and has a strong tendency to chip or flake.

4) The nucleus usually has a somewhat distorted regular polygonal form. Elongated or rectangular, nuclei are rarely found.

5) The nucleus is possibly of hexagonal habit.

6) The nucleus is apparently unaffected by a wide range of dilute acids and is relatively inert.

7) The graphite of which the nodule is composed is not a single crystal but is rather a growth of many crystals crystallographically arranged.

8) Formation of spherulitic graphite in nodular iron is possibly caused by precipitation on a kindred nucleus.

It should be pointed out that the presence of descrete nucleus in spherulitic nodules has not been

proven, although there are many articles on this subject.

Scobie[12] in his discussion of Nodular Iron Symposium attended by nearly 100 metallurgists in September 1950 brought out the following controversial points.

1) (a) Nodules form spontaneously; (b) they form around a small non-metallic inclusions; (c) they precipitate on graphite nuclei.
2) (a) There is a high degree of segregation of graphite nodules; (b) there is no segregation.
3) (a) Nodules contain a nucleus; (b) they do not contain a nucleus.

It is clear therefore that the theory of nodular iron transformations is in its infancy at the present time and much more experimental evidence is necessary in order to explain some of these phenomena.

## PURPOSE OF THIS INVESTIGATION

In ordinary gray cast irons the common heat treatments such as "ferritizing", spherodizing, martempering and austempering are not used very extensively because gray cast iron is quite brittle and the costly operation of heat treatment does not improve its properties appreciably. This perhaps accounts for the fact that very little work has been done on the isothermal transformations in cast irons. Not many "S" curves on cast irons are available in literature and even those that are published, are incomplete and uncertain. Nodular iron on the other hand is more ductile and stronger than gray cast iron and "S" curves can be of great value as a guide to improving its properties just as they have been used in the case of steel. Because of their susceptability to heat treatment, there probably will be more demand for nodular alloy cast irons in the future. In order to carry out properly any particular heat treatment such as austempering, martempering and spherodizing it is desireable to know the rates of transformation and the type of microstructure produced at some given temperature. This facilitates the task of choosing a correct temperature and time for a particular heat treatment. This type of information is readily available from isothermal transformation

curves ("S" curves) for that particular material. Since no complete "S" curves have been produced up to the start of this investigation as far as the author knows, it was decided that research of this type would be quite useful from a practical as well as a theoretical point of view. It was anticipated that a detailed isothermal study would shed some light on such basic fundamentals as the existence of a graphite eutectoid, the mechanism of subcritical graphitization, and the effect of some of the principal alloying elements in nodular cast iron on isothermal transformations.

Another part of the research which was undertaken, was for the purpose of solving the basic problem of how and when the graphite nodules form. This is very important, because it has not been established whether the nodules form from the decomposition of cementite, supersaturated austenite, or directly from the liquid. This information is of basic fundamental importance and any experimental evidence in this field may aid in settling the old argument as to the mechanism of graphite formation in cast irons.

PART I

## LIQUID TO SOLID TRANSFORMATIONS

The solidification of metals or alloys may be considered as a liquid to solid type of a reaction. This type of a reaction involves the nucleation of one or more of the solid phases and the growth of these phases by diffusion of atoms from the liquid to the solid. The rate of solidification depends on the rate of removal of heat, and the temperature at which solidification takes place depends on the cooling rate and the rate of nucleation of a solid phase. If the rate of nucleation of a solid phase is low, then solidification will take place at a lower temperature for a given cooling rate. A rapid cooling rate results in a lower solidification temperature because there is not enough time for the nucleation of a solid phase at the higher temperature, and the solidification begins at some lower temperature because at that temperature there is sufficient time for the formation of nuclei of a solid phase. Because of the low rate of nucleation of most of the solids, the liquid metal may be supercooled below their equilibrium solidification temperature. Once the metal starts to solidify in the supercooled liquid the solidification is very rapid and the evolved heat of solidification tends to raise the temperature of the liquid.

The remaining liquid then may even freeze at the equilibrium solidification temperature if the cooling rate is sufficiently low.

In the process of freezing there is an interchange of atoms between solid and liquid at a solid-liquid interface. The observed rate of freezing as pointed out by Chalmers[14] is the difference of the rates at which atoms leave the surface of the solid and join unto the surface of the solid from the liquid. If the two rates are equal the interface between the liquid and the solid is stationary.

As stated previously nucleation of the solid phase is very important in liquid to solid reactions. In the absence of impurities which act as nuclei, most of the common metals may supercool up to one fifth of their melting temperature. Supercooling of metals is very important from a practical point since it influences the structure of the metals after solidification is complete. In the case of cast irons supercooling determines whether the cast iron will freeze according to the stable or metastable system, what crystal size and shape will be and the distribution of chemical elements, cavities, etc.

In freezing of eutectic systems where two solid phases may form, the phenomena of nucleation is complicated

because one phase may aid in nucleation of the other. In the case of complex alloy systems where several phases may form during solidification the whole mechanism of freezing is very complicated and only the theory of the binary eutectic freezing is well developed. Little is known about the mechanism of freezing of the ternary and quaternary eutectics.

The mechanism of the solidification of cast irons is even more complex because cast irons may solidify according to either the stable and/or the metastable system. The mechanism of graphite formation either in nodular or gray iron is still a controversial point. Some authors claim that graphite forms directly from the liquid while others claim that it is a decomposition product of carbide. It has been shown experimentally by Boyles[5] and other that type A and type B flake graphite are formed directly from the liquid during the eutectic interval of solidification and that the mixture of austenite and flake graphite may be considered as a eutectic product.

The method used in determining the mechanism of nodular graphite formation described below was the well known procedure of quenching into water or cold brine solutions. In order to explain some of the phenomena

occuring during solidification of nodular iron a vertical section of Iron-Carbon-Silicon phase diagram for 2% silicon is represented on Fig. 1.

Several months were spent on preliminary investigation of the production of nodular iron in a specially designed induction furnaces in order to solve some of the problems such as reproducibility, elimination of flake graphite, design of induction melting furnaces etc. All furnaces in this investigation were designed and made by the author in order to meet certain requirements in these experiments. A 50 kilowatt Tocco induction unit was used in melting the iron for this investigation.

As a result of these preliminary investigations, the following conclusions were reached.

1) The best results were obtained when the magnesium alloy was added at a low temperature just above the freezing point of the cast iron. This gave pure nodules with minimum addition of the magnesium alloy.

2) The nodules formed in the vicinity of the eutectic temperature. This conclusion was reached after quenching small specimens having a radius of 0.5" in a large cold copper mold. The nodules were present in large quantities only when the metal was poured from a temperature at which it was in a "pasty" condition, and that temperature

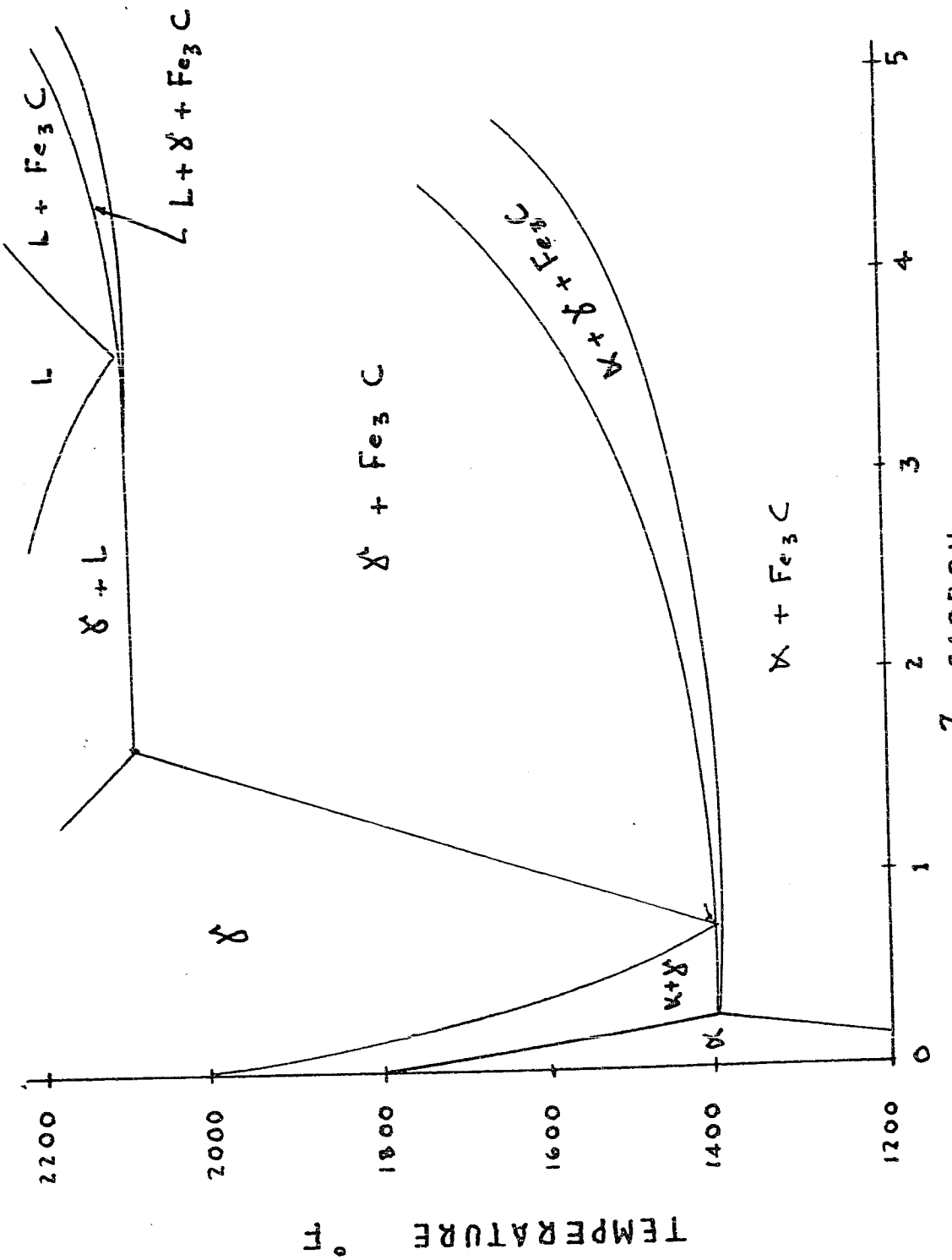


FIGURE I. SECTION THROUGH THE TERNARY DIAGRAM OF Fe - C - Si SYSTEM (2% Si)

corresponds to the temperature of the "horizontal" on the cooling curve (Fig. 2) and it is sometimes called the eutectic temperature. No nodules were formed from a temperature appreciably above this "eutectic" temperature of the alloy.

In all experiments the magnesium was added as an alloy of 80% copper and 20% magnesium, and the composition of cast irons ranged from 2-3% silicon, 2.5-4% carbon, 0.3-0.8% manganese, 0.75-3% nickel, 0.02-0.04% phosphorus, 0.01-0.02% sulphur, and 0.1-1.0% copper. As a result of these preliminary experiments two experiments were carried out which are described below. The materials used in these two experiments were similar in composition to commercial hypoeutectic and eutectic nodular cast irons and no attempt was made to prepare high purity alloys.

## EXPERIMENT I

In the first experiment the cast iron was melted in an induction furnace in a cylindrical graphite crucible and heated up to about 2500-2600°F. The samples were held at this temperature for some time in order to get a homogeneous liquid. The liquid was then cooled to just above the melting point (2200°F) and then the copper-magnesium

FIG. 2

COOLING CURVE FOR HYPOEUTECTIC NODULAR IRON

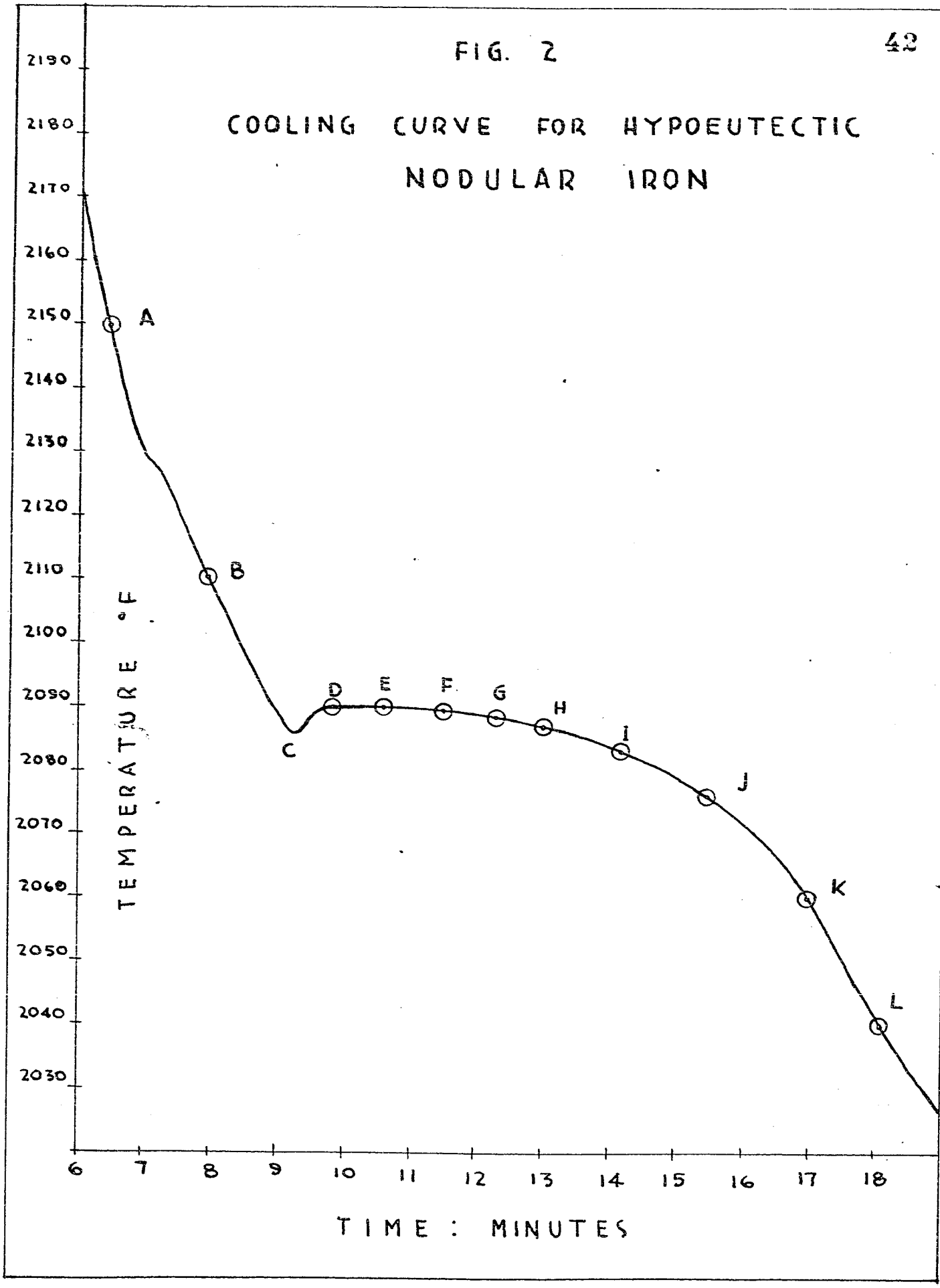

alloy was added in order to produce spheroidal graphite. The metal was stirred with a graphite rod to get a better mixing of the liquid. After a few minutes of stirring the liquid was reheated to 2400°F and held at that temperature for about 5-10 minutes. The liquid then was cooled slowly and the cooling curve was recorded on a Speedomax recorder. The samples were then quenched in a cold aqueous solution of sodium hydroxide (approximately 15% of sodium hydroxide by weight), from various points which are designated by the letters on the cooling curve diagram, Fig. 2. Each sample letter has the same letter on the cooling curve (Fig. 2). In all these samples the thermocouples were never taken out nor the Speedomax stopped until the temperature was well below the freezing point. Thus the temperature at the time of quenching was always recorded by the Speedomax, and the time of quenching was no more than one or two seconds. The graphite crucible that contained the metal was cylindrical in shape having the following dimensions:

Outside diameter = 2 inches

Inside diameter = 1 1/4 inches

Height = 4 inches

The cast iron samples after quenching were 2 inches long

and 1 1/4 inches in diameter. Thin walled fused silica tubes closed at one end were used as thermocouple protectors and a new tube had to be used for each sample. The samples were cut on a cut-off wheel, polished and either heat tinted or etched and observed under the microscope. Figures 5-21 are photomicrographs of these samples. The sample letters refer to the letters on the cooling curve (Fig. 2).

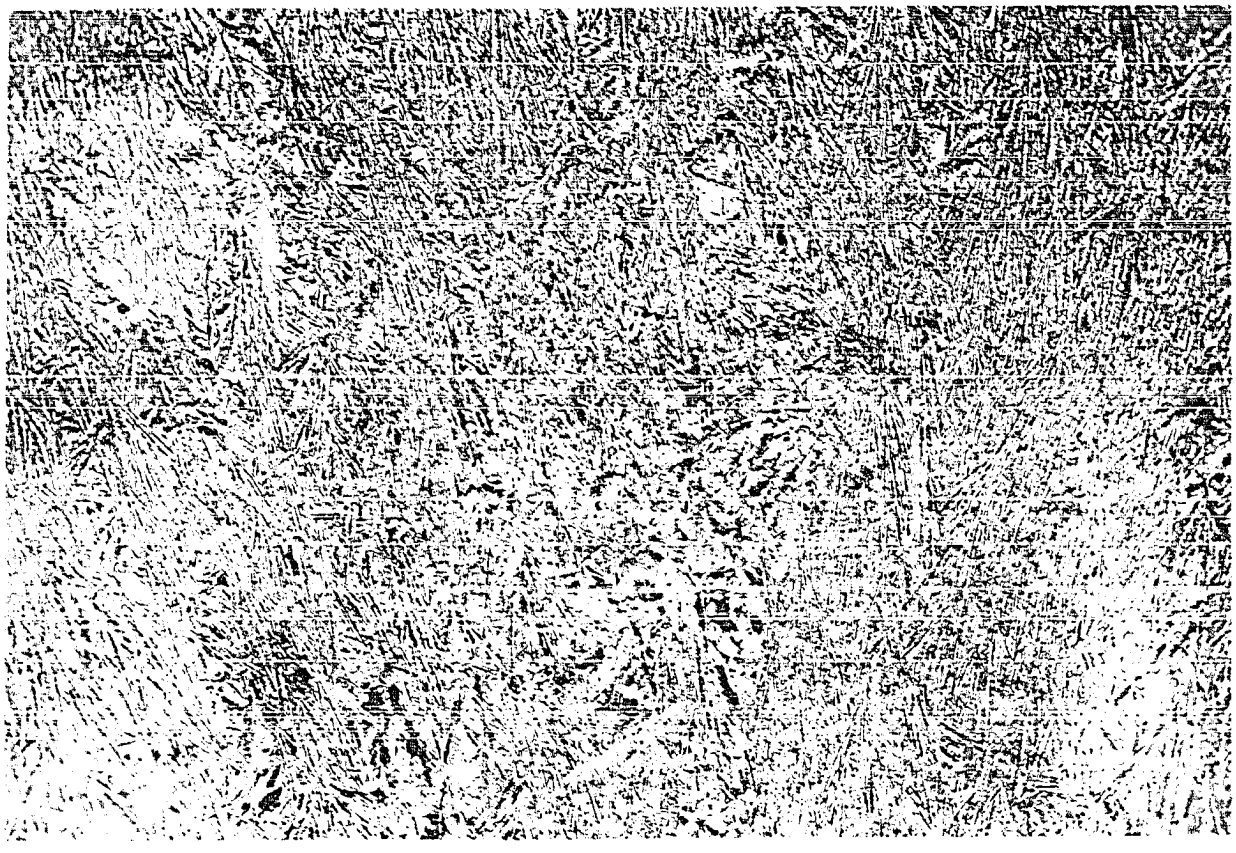

FIG. 5

Sample (a), quenched from the point (a) on the cooling curve. Fine structure of ledeburite. Heat tinted. 100 X.

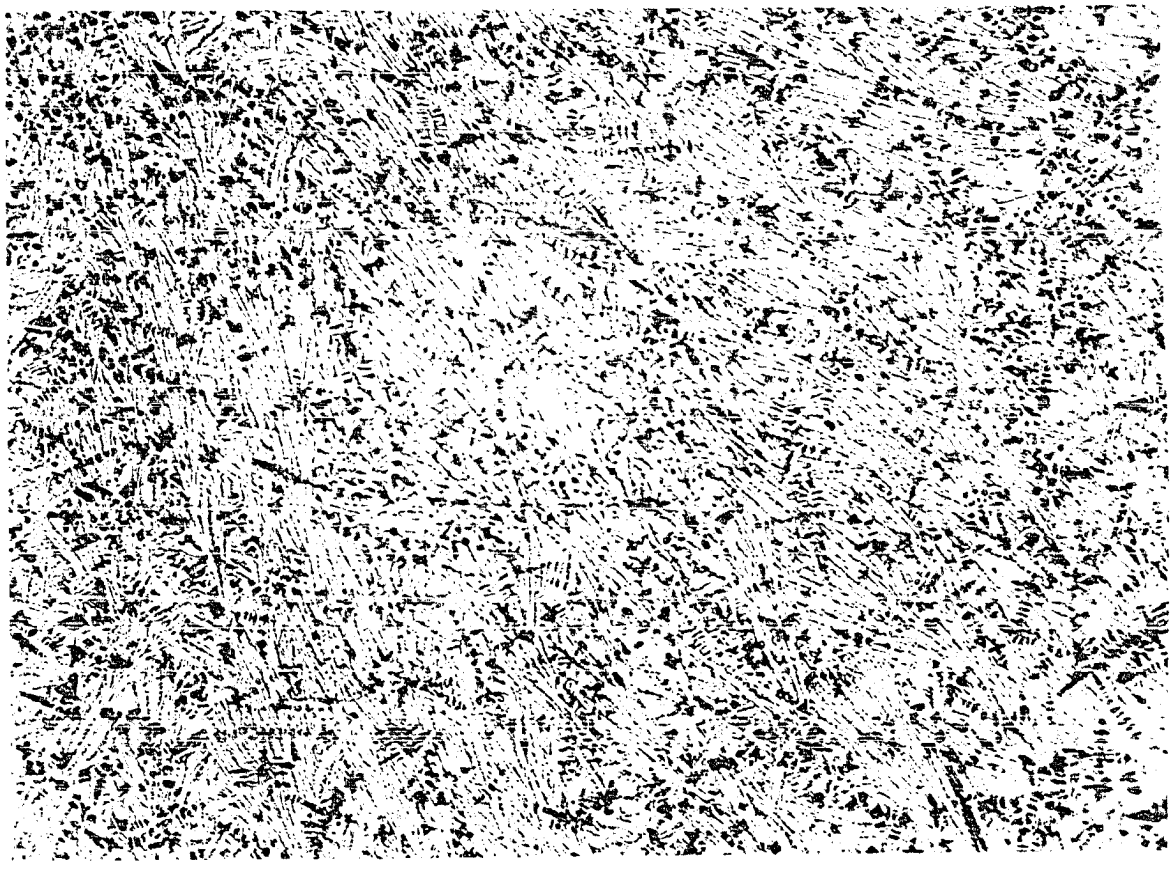

FIG. 6

Sample (b), quenched from the point (b) on the cooling curve. This sample was heat tinted first and then re-polished for a short time on the last wheel in order to show more contrast between primary austenite dendrites and ledeburite. The structure shows only austenitic dendrites and fine ledeburite. 100 X.

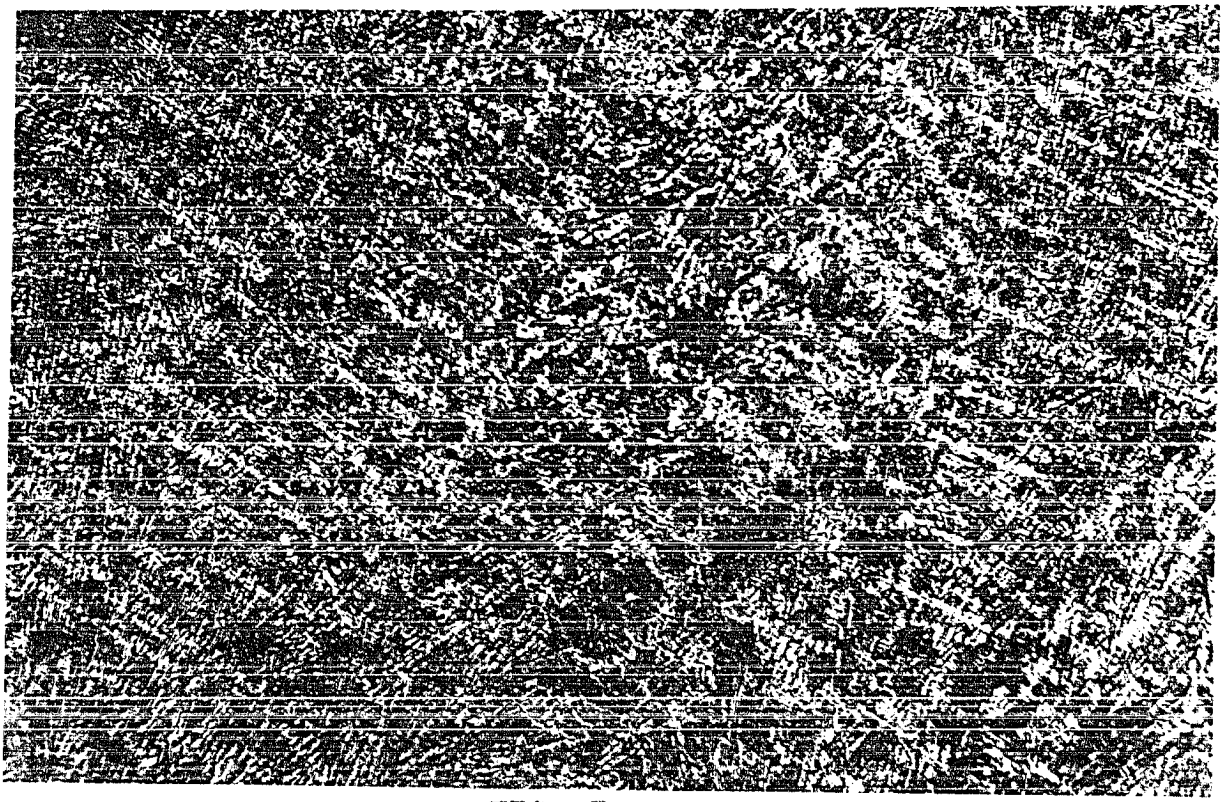

FIG. 7

Sample (c), quenched from the point (c)(Fig. 2). The structure consists of austenitic dendrites, fine ledeburite, and only several very small nodules. No nodules are visible in this photomicrograph but they are visible in Fig. 8. Heat tinted and repolished. 100 X.

FIG. 8

The sample sample as in Fig. 7 except it was slightly repolished after heat tinting in order to get better contrast between dendrites and ledeburite and to reveal the small nodules which could not be noticed easily before repolishing. The two nodules are encircled on the diagram. This is the first point where the nodules begin to appear. 100 X.

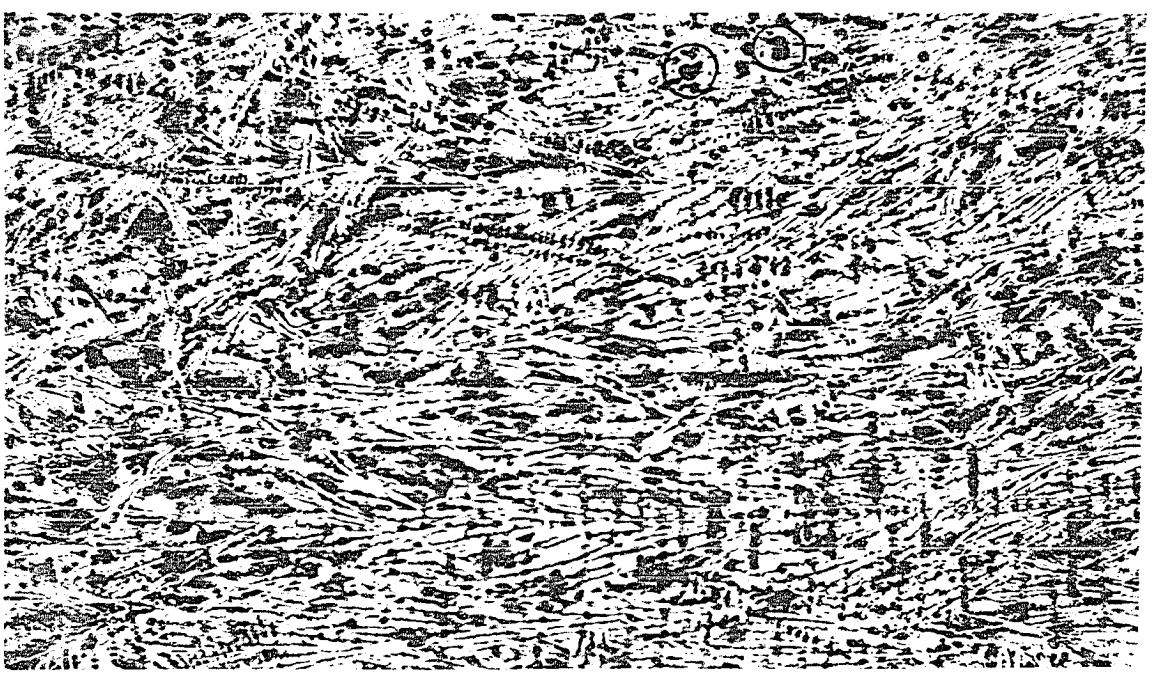

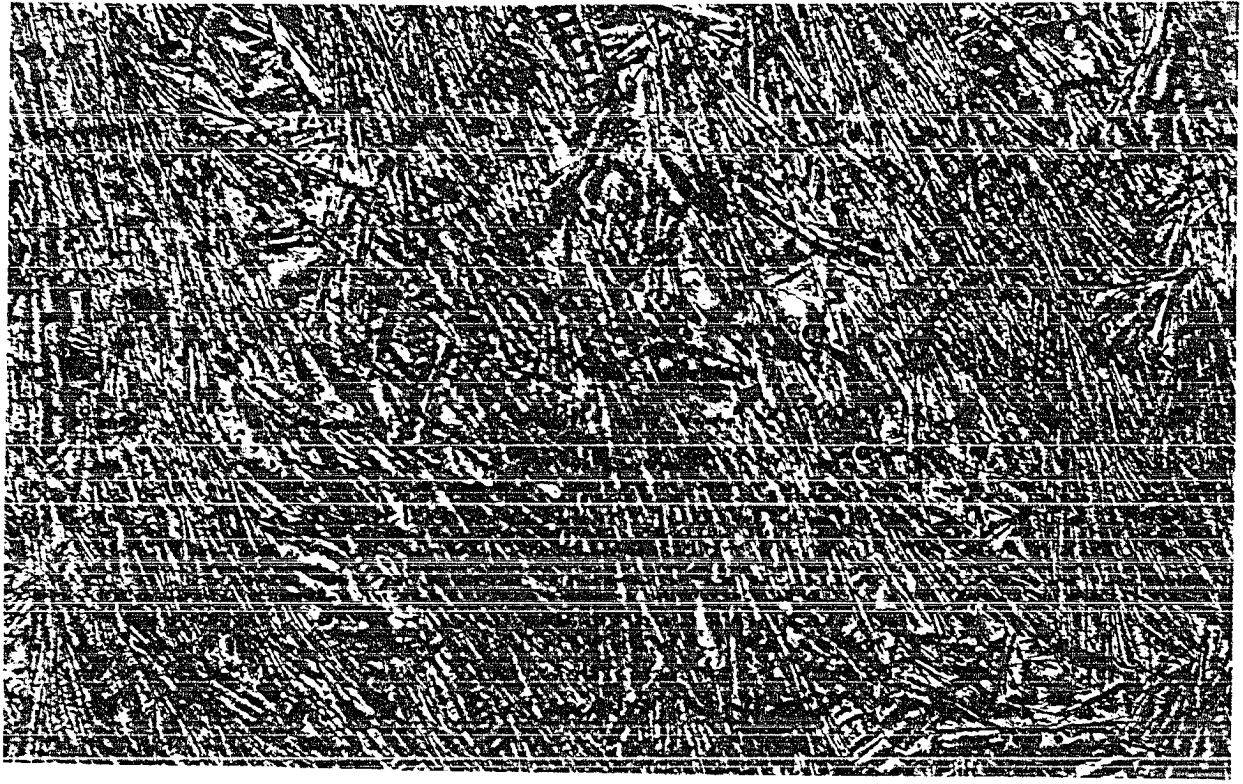

FIG. 9
Sample (d), quenched from the point (d)(Fig. 2). The structure consists of austenitic dendrites, ledeburite and many small graphite nodules surrounded by an austenitic shell. Heat tinted. 100 X.

FIG. 10
The same sample as in Fig. 9 except repolished after heat tinting. Repolishing gives a better contrast between the ledeburite, the austenite dendrites and the austenitic shells surrounding the graphite nodule.

FIG. 11

The same sample as in Figure 9. The sample was tempered for one minute at 750°F and etched with nital. The structure shows the graphite nodule and the austenitic shell around it at a high magnification. The shell in turn is surrounded by ledeburite. 2,000 X.

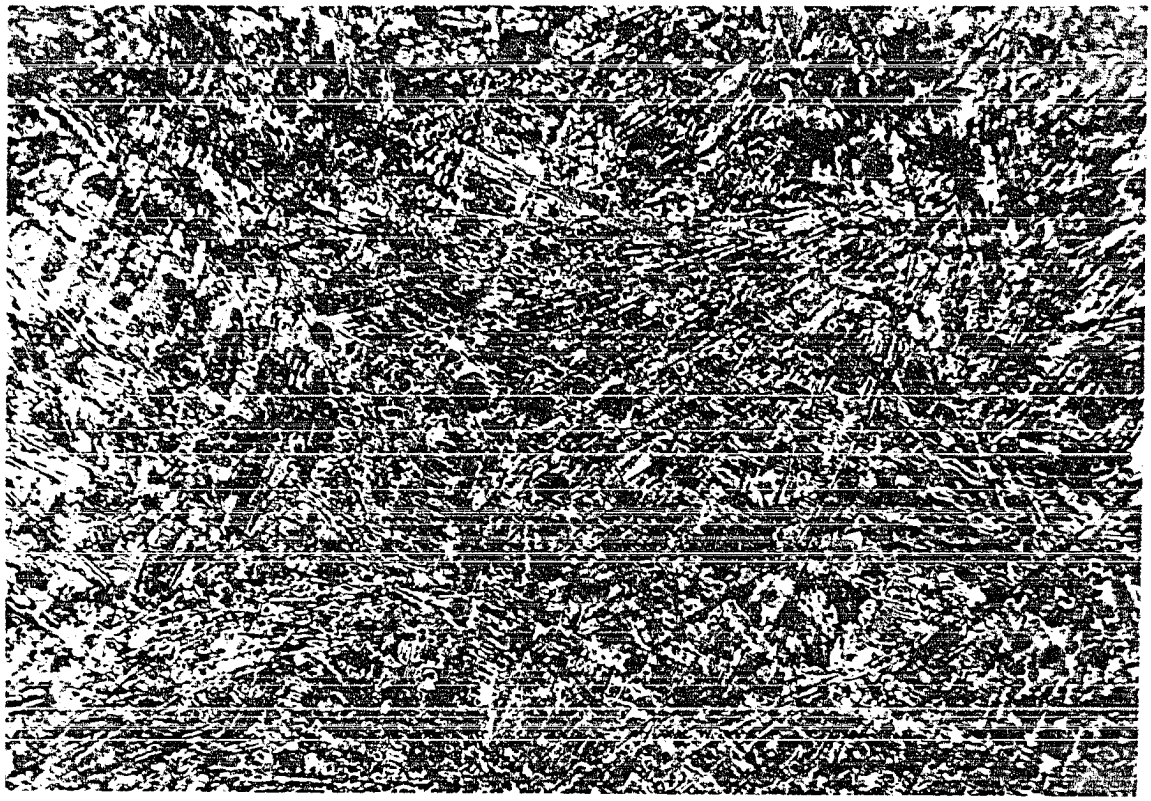

FIG. 12
Sample (e), quenched from the point (e)(Fig. 2). Showing the growth of graphite nodules and the growth of austenitic dendrites. Heat tinted. 100 X.

FIG. 13
The same sample as in Fig. 12 except was tempered for 1 minute at 750°F and etched with nital. The magnification is also higher. 1000 X.

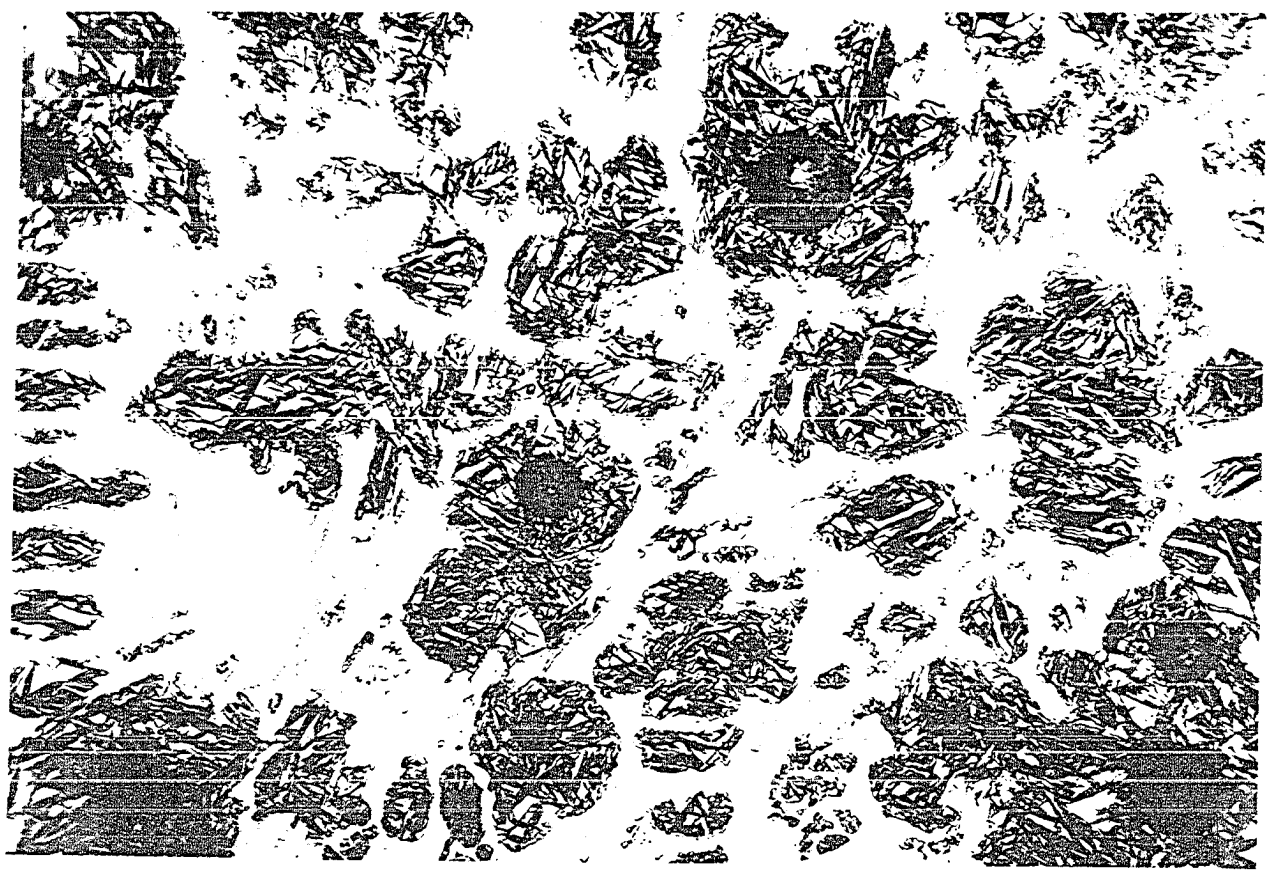

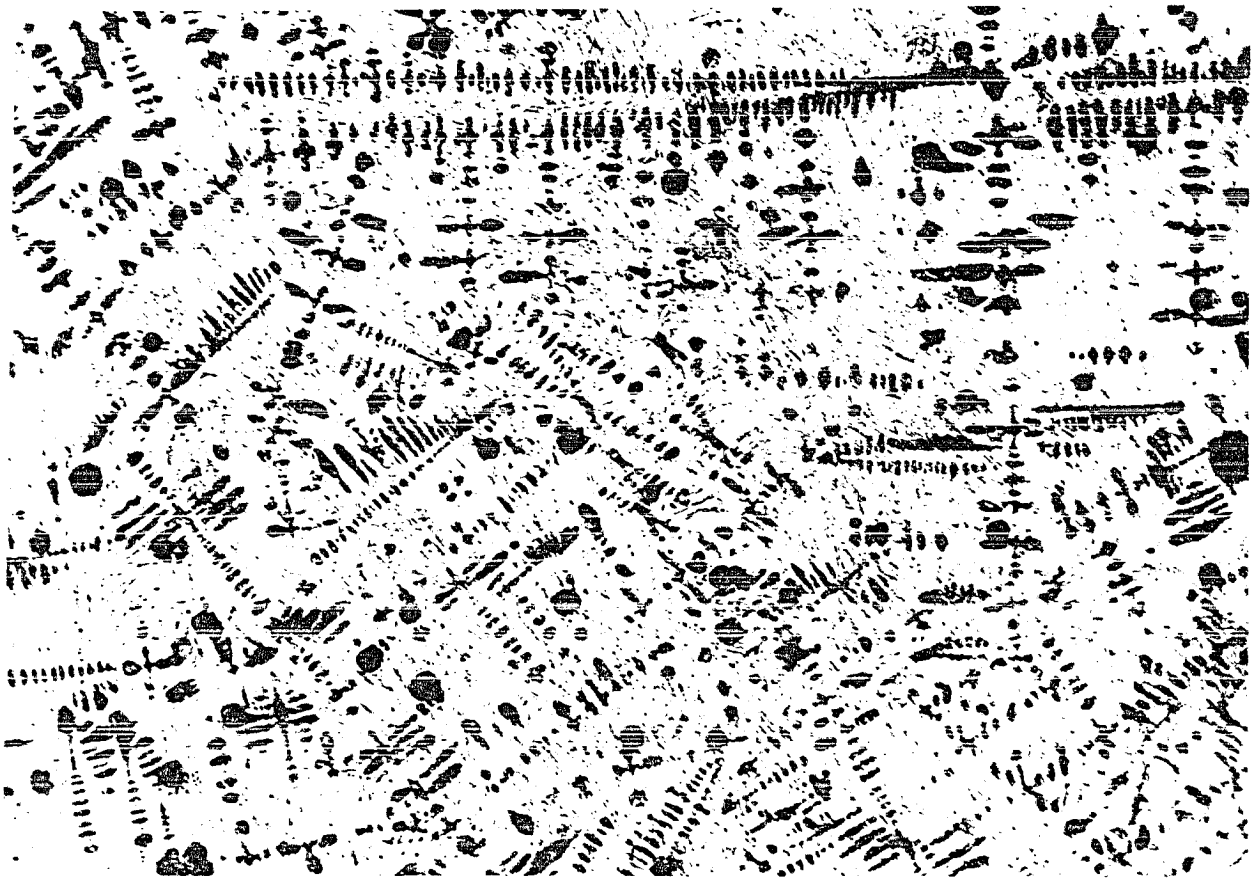

FIG. 14

The same sample as in Fig. 12. Repolished after heat tinting. Reveals graphite nodules better than Fig. 12.

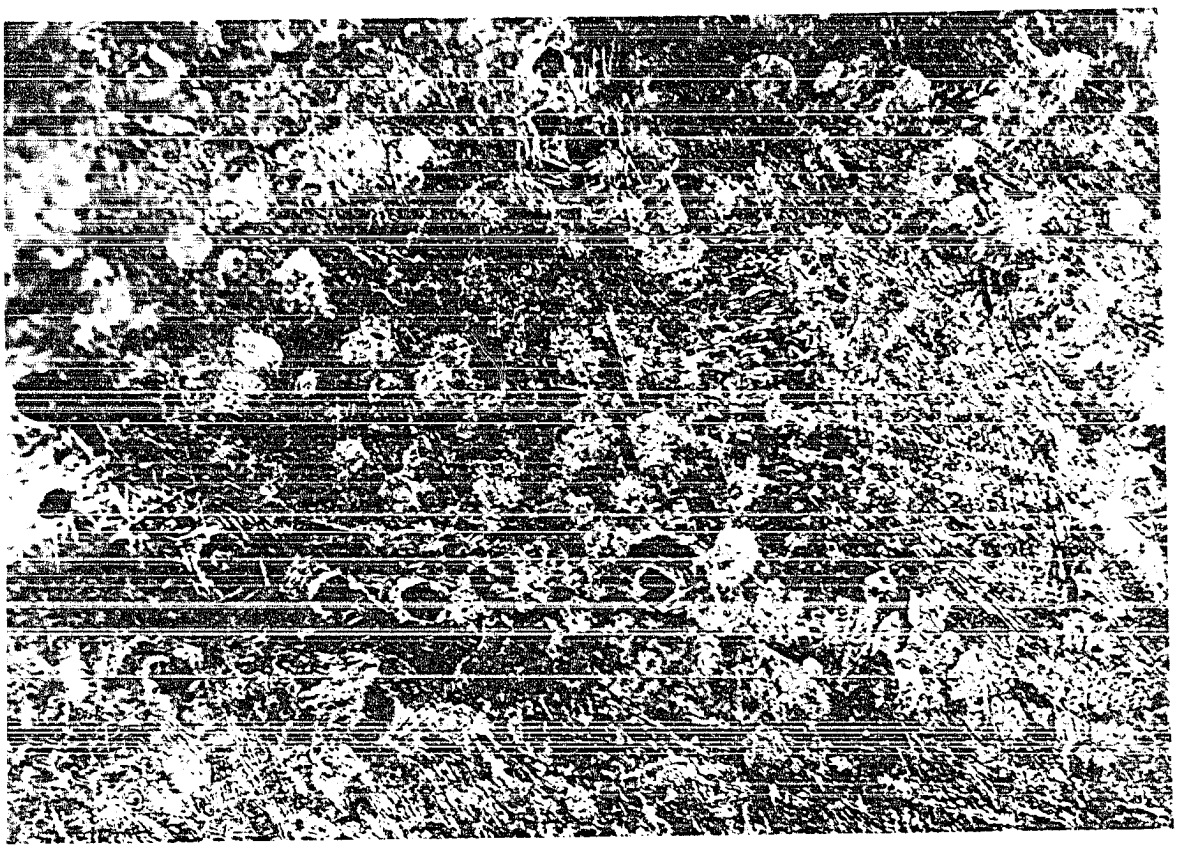

FIG. 15

Sample (f), quenched from the point (f) (Fig. 2). The structure shows that the nodules have a tendency to form near the dendrites and usually lie in a straight or slightly curved line. Heat tinted. 100 X.

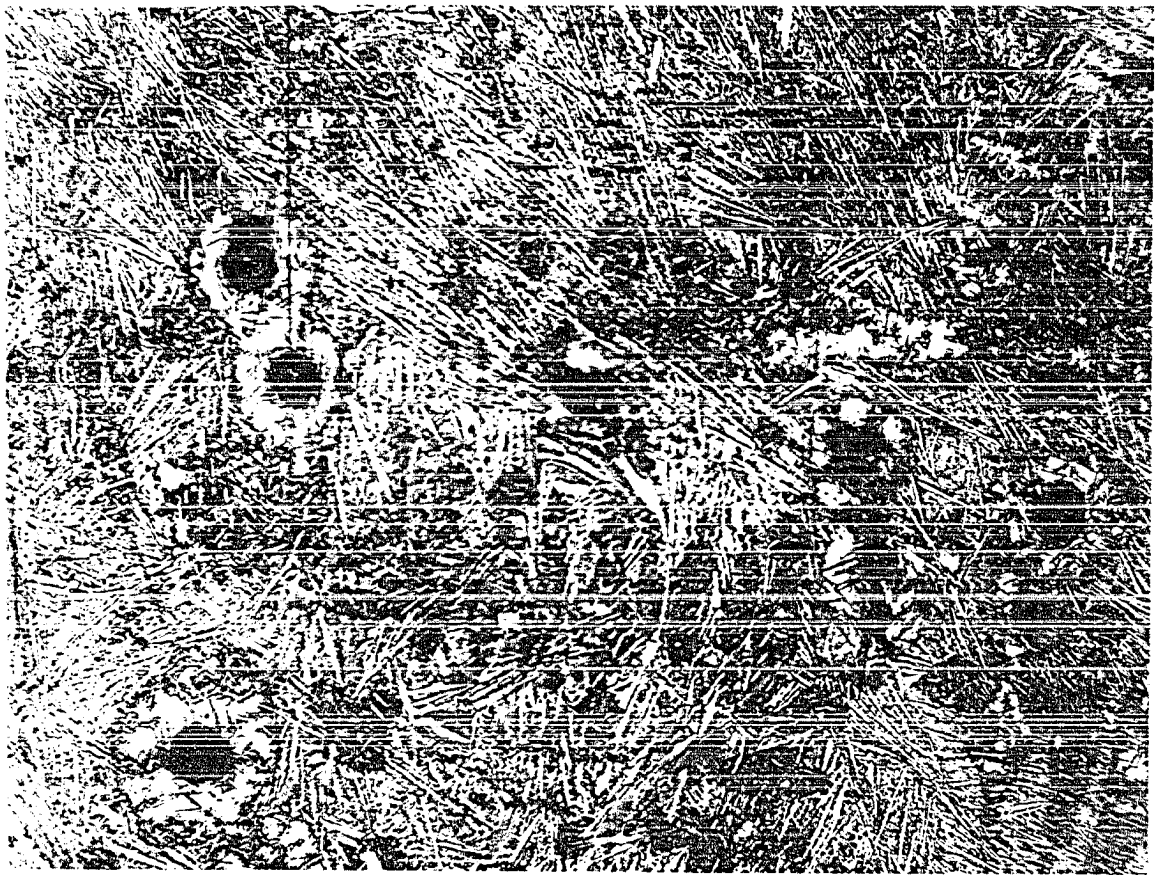

FIG. 16

Sample (g), quenched from the point (g)(Fig. 2). The structure shows the growth of nodules and "shells" of austenite near the dendrites. Heat tinted. 100 X.

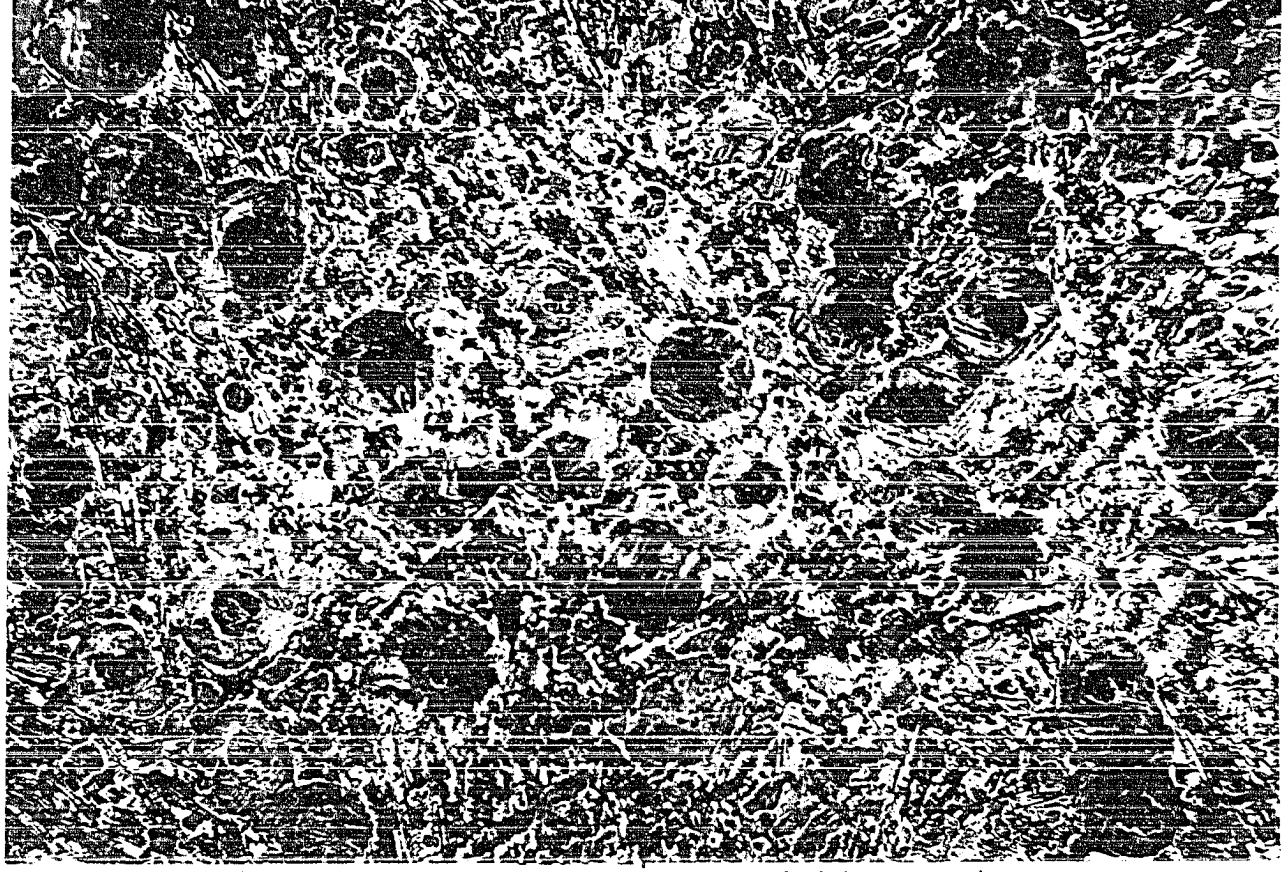

Sample (h), quenched from the point (h)(Fig. 2). The structure illustrates the cellular growth of austenitic shells and graphite nodules. Heat tinted. 100 X.

FIG. 18

The same sample as in Fig. 18. Repolished after heat tinting. The structure shows the independent growth of graphite nodules inside the austenitic shells. The matrix which was liquid before quenching is ledeburite. Some of the cells have already combined and formed large cells. 100 X.

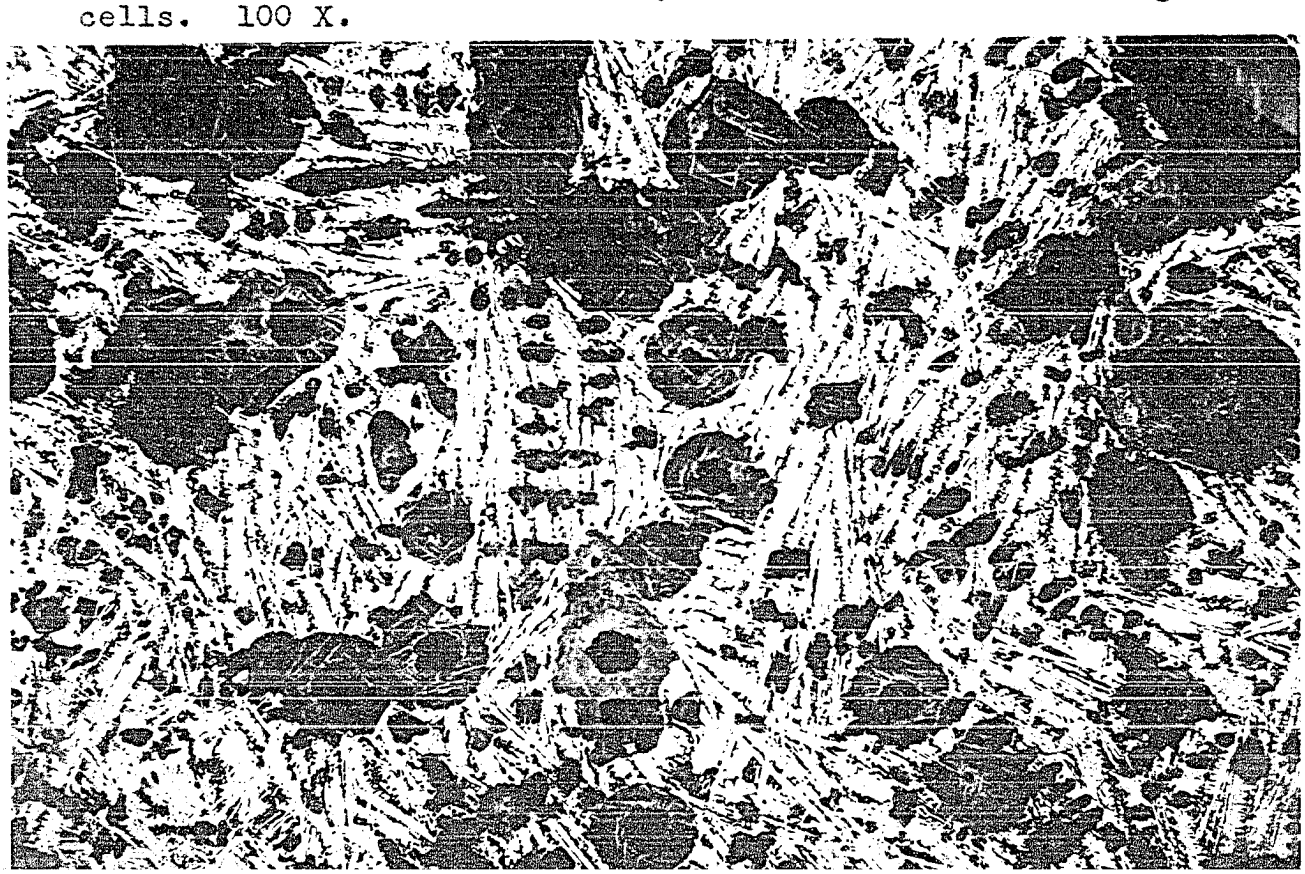

FIG. 19

The same sample as in Fig. 17 but at a higher magnification. A detailed structure showing a graphite nodule and an austenitic shell around it in a matrix of ledeburite. The structure does not show any formation or decomposition of cementite before quenching. All cementite was formed on quenching and consists of eutectic cementite. Heat tinted. 1000X.

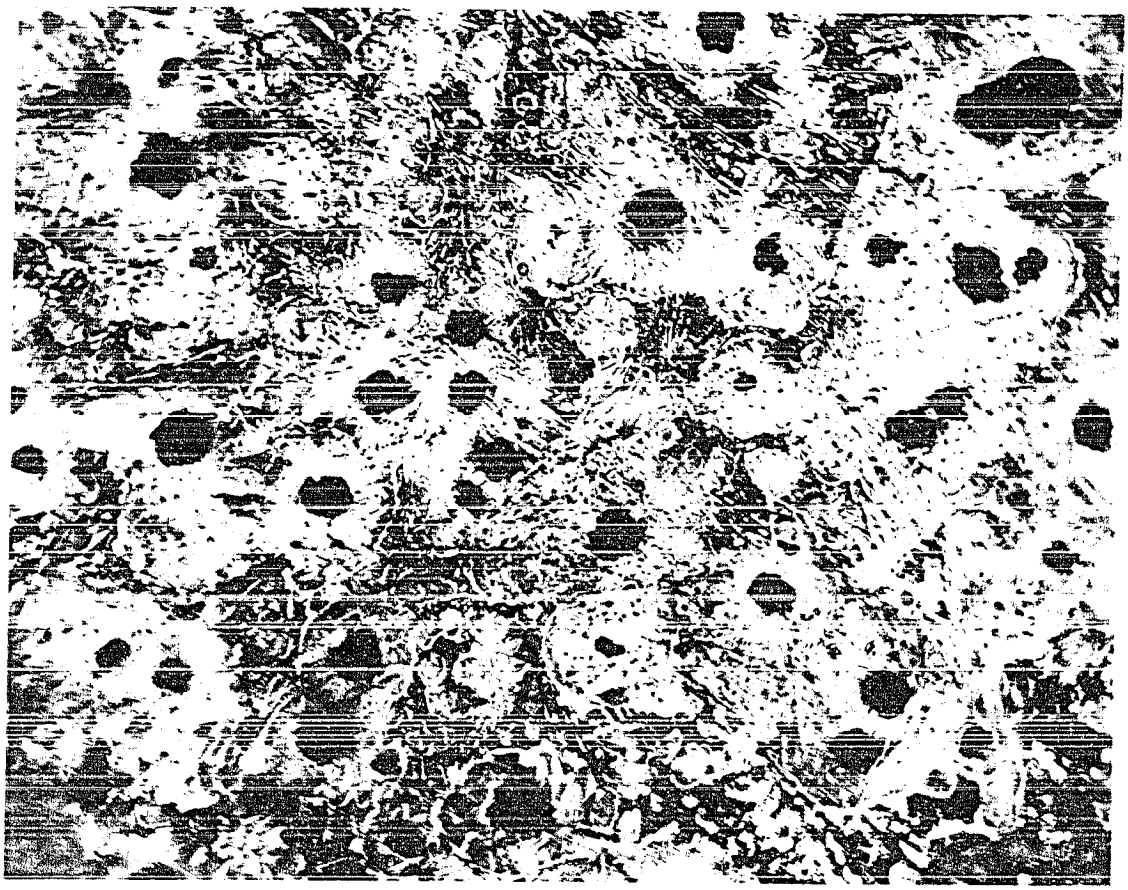

FIG. 20

Sample (i), quenched from the point (i)(Fig. 2). Many cells have already combined to form large cells, and the cellular growth is quite evident. Heat tinted. 100 X.

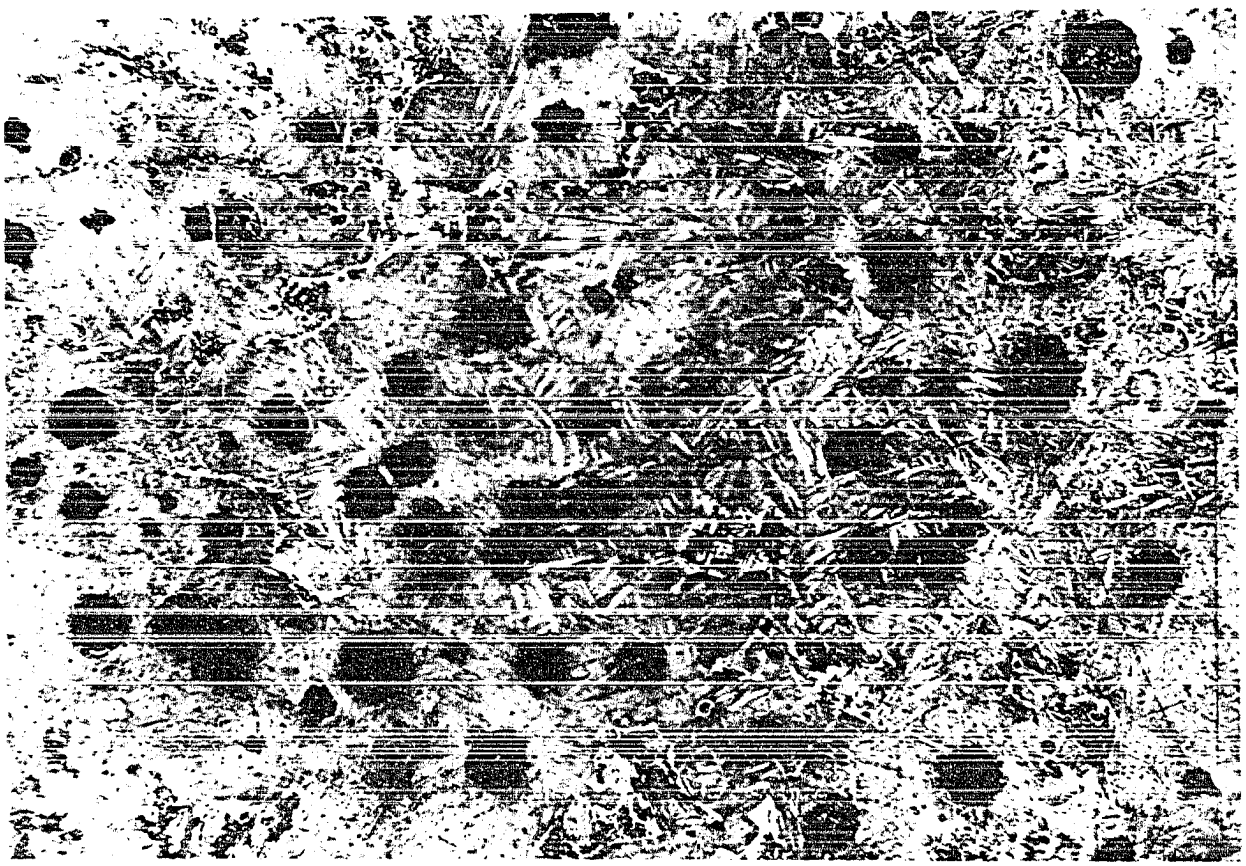

FIG. 21

Sample (j), quenched from the point (j)(Fig. 2). The solidification is nearly complete and no more new nodules form from the liquid. The liquid is at the cell boundaries, and the concentration of impurities in this liquid is responsible for the slow ferritization in these regions. Heat tinted. 100 X.

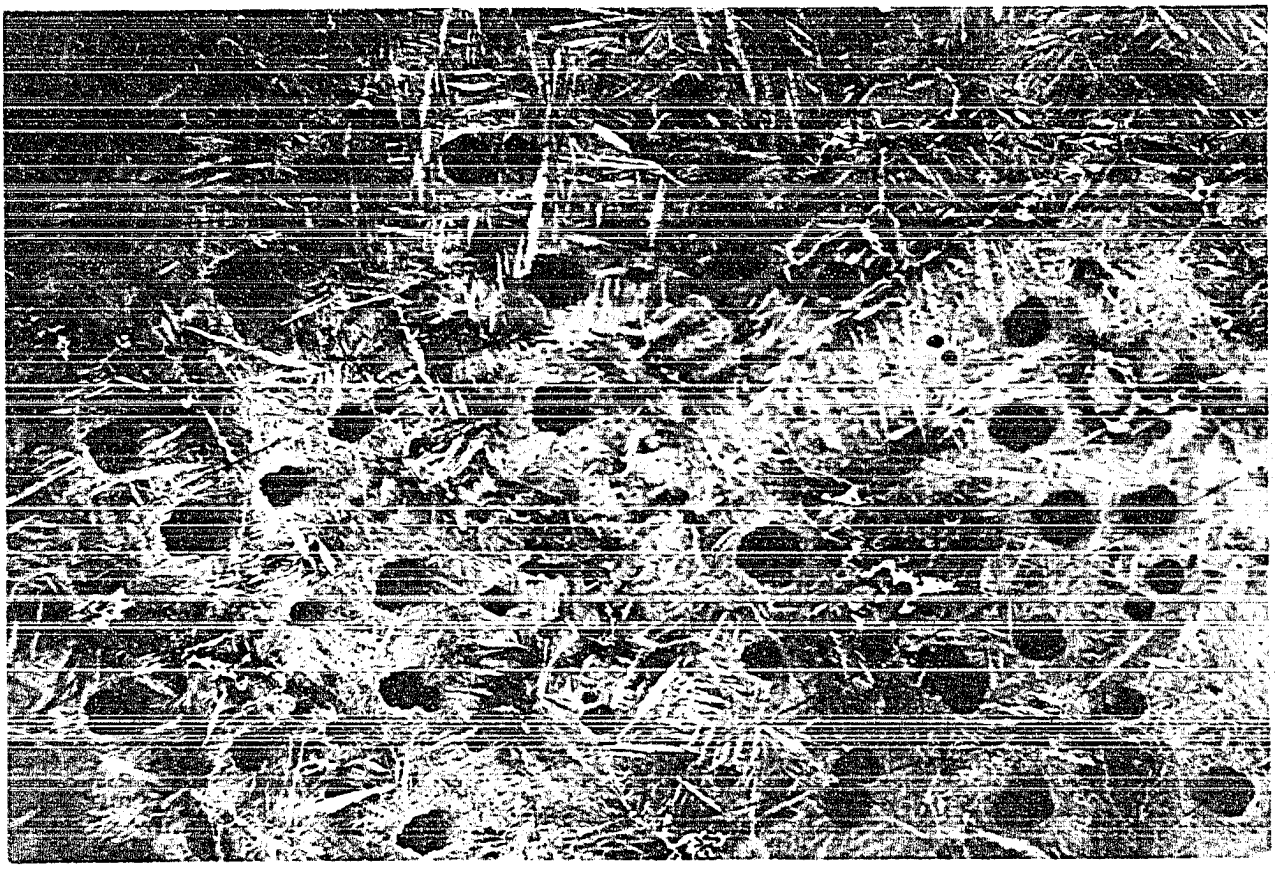

FIG. 22

Sample (k) quenched from point (k)(Fig. 2). Some liquid still present in cell boundaries. Solidification is almost complete. Heat tinted. 100 X.

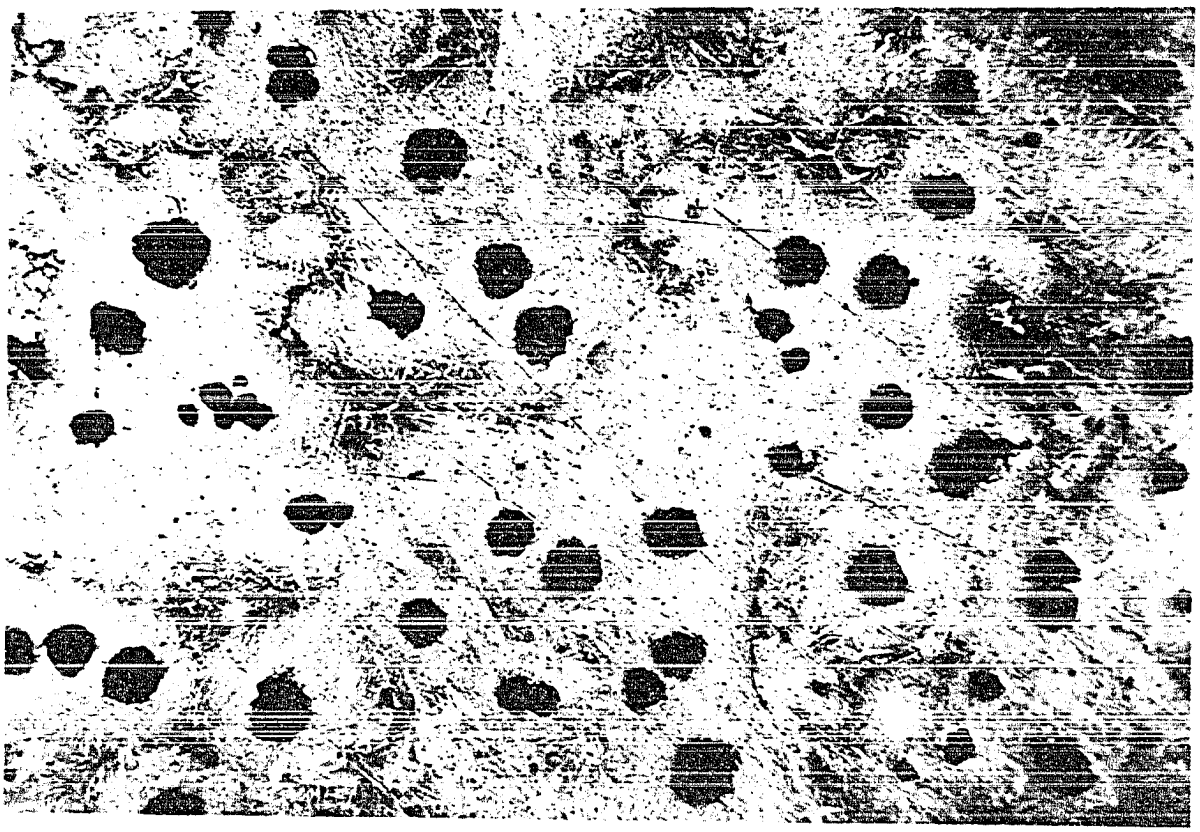

FIG. 23

Sample (1), quenched from point (1)(Fig. 2). Solidification is complete. The structure shows segregation in the cell boundaries.

Observations:

1) Dendrites of primary austenite form first and grow as the temperature is lowered.

2) Nodules of graphite do not form until the horizontal part on the cooling curve is reached.

3) Nodules of graphite are never in contact with the liquid but are surrounded by an austenitic shell.

4) Nodules of graphite usually form beside the austenitic dendrites but not always.

5) Many nodules form independently of the dendrites and are surrounded by the austenitic shell which is in contact with the liquid.

6) At the start of the "horizontal" on the cooling curve, nodules just began to form while at the end of the "horizontal" practically all of the nodules have already formed.

7) If the "horizontal" is the eutectic temperature then it may be said that the nodules form during the eutectic freezing and we have a structure which looks like a "devorced" type of a eutectic.

8) As soon as nodules start forming the liquid freezes in a "cellular" manner rather than dendritic.

9) The first and earliest indication of the formation of a graphite nodule is a "center of crystallization" which consists of a very small graphite nodule surrounded by a thin austenitic shell (Fig. 6), and this "center of crystallization" grows radially in all directions. This gives the appearance of a cell growing in all directions and this growth of the solid phases is termed cellular growth.

10) There was no indication of formation of carbide before quenching nor of decomposition of carbide to form graphite nodules.

11) The last liquid to solidify froze in the cell boundaries and few if any new nodules were formed in these boundaries.

12) The number of nodules increased with the time during the horizontal interval but the rate of nodule formation decreased rapidly after 50% solidification.

13) As the graphite nodule grows in size, so does the austenitic shell around it, and the diameter of the nodule is always approximately equal to the width of the shell provided there is only one nodule in the shell. Thus if

the diameter of the nodule is increased three times, then the width of the shell is also increased approximately three times.

14) It was impossible to establish whether the graphite nodule in its very early state of formation precipitates from the liquid or from the supersaturated austenite.

15) Although its origin of formation was not established, the experiments did show that as soon as the nodule is large enough to be resolved under the microscope it grows in the austenite and not in the liquid.

## EXPERIMENT II

In the second experiment the graphite crucible was also cylindrical in shape but somewhat larger. It was 4 inches high, 3 inches in outside diameter and 2 inches in inside diameter. Two thermocouples were placed inside the crucible, one in the center of the crucible and the other touching the side, both in the same horizontal plane. The thermocouples were protected with fused silica protectors described previously. The procedure of melting and preparing this sample was the same as the one described in the first experiment up to the time when the cooling curve was started.

The cooling of this sample was adjusted so that the metal started to freeze on the outside first, and the outside was completely solid before the inside or the center of the bar started to solidify.

Since one of the thermocouples was indicating the inside temperature of the sample while the other the outside temperature of that sample, the progressive stages of solidification could be observed under the microscope after the sample was quenched when the outside of the sample was completely solid while the inside was still liquid. Thus when the Speedomax recorder which was connected to the thermocouple recording the outside temperature indicated that the solidification was complete and the inside thermocouple showed that the center is still liquid, the sample was quenched in brine with the thermocouples still in the sample. The sample was then cut on half in a plane perpendicular to the thermocouples and across their tips. It was then prepared for microscopic observation.

Observations in the Experiment II

The sample was polished and heat tinted, and the structure observed under the microscope ranged from no nodules at the center to the completion of the formation of nodules at the surface. This experiment confirmed the observations in the first experiment and the structures

representing various stages of solidification were identical with those in the first experiment in showing the development of nodules from the center of the mold to the outside.

No photomicrographs are included from this experiment because they are identical to those for the first experiment. In traversing from the center to the outside of the casting, the center consisted only of ledeburite, followed by a matrix of ledeburite containing small dendrites which became larger in size until few traces of widely spaced small graphite nodules were found usually adjacent to the dendrites. Farther away from the center, the dendrites became larger and the number of nodules increased rapidly in number and size. Some of the nodules formed away from the dendrites while others formed near the dendrites and near other nodules. Nodules also were not evenly distributed but were concentrated in long banded zones. The nodules in all cases were surrounded by austenite and there could be one, two or more nodules in one austenitic cell. Still farther away from the center the number of of austenite cells containing one two or more nodules increased and some the cells already started to merge. Near the outside, most of the austenitic cells have already joined and practically all of the nodules have been formed.

Approaching the surface only small quantities of the liquid remain outlining the cell boundaries and the number of nodules is about the same but slightly larger in size. Finally at the surface there is no liquid remaining although heat tinting reveals slightly the cellular structure thus indicating a segregation of alloying elements or impurities during solidification.

## DISCUSSION OF EXPERIMENTAL RESULTS

The experimental evidence as summarized under the subheading of observations in experiments I and II indicates that the graphite nodules form during the so called eutectic freezing of the liquid. It should be pointed out that the discussion in this paper pertains only to the eutectic and hypoeutectic irons since no experimental work was done on hypereutectic irons. It is quite possible however that the same mechanism may be applicable to the hypereutectic cast irons.

Let us discuss some of the hypothesis that appeared in literature regarding the nodule formation with reference to the observations in this paper.

1) One of the hypothesis, which will be called the first hypothesis, states that the nodule makes its appearance in the solid state by decomposition of the ledeburitic cementite.

The experimental results in this paper definitely prove that the nodule appears when the liquid is only partially solid and that it does not form from the decomposition of ledeburite. The indication that the nodule does not form from the decomposition of cementite is shown by the fact that even if some of the ledeburite had formed prior to the quenching, then this ledeburite would be of much coarser structure than the ledeburite formed during quenching. Also the first ledeburite would probably have a different orientation than the one formed during the quench because the direction of heat flow which influences the orientation of ledeburite may be different. Since there was no indication of any ledeburite which was formed before quenching nor any indication of the decomposition of ledeburite, it may be assumed that no ledeburite forms before quenching, and that the nodules do not form from the decomposition of ledeburite. Therefore because the experimental results do not give any support to this theory, but seem to contradict it, the author thinks that this hypothesis is not correct.

The second hypothesis which is well described by Dunphy and Pellini[13] and supported by others, states that the nodule appears in the liquid by precipitation of carbon from the hypereutectic zones. In the case of hypoeutectic iron it is assumed that there are localized pools of

hypereutectic liquid existing near the dendrite arms because the austenitic dendrites are lower in carbon content than the average content of the liquid. The solidification of dendrites is responsible for greater carbon content in the liquid near the dendrite arms, which may even be high enough to give hypereutectic pools in these regions. The hypereutectic pools may also result because of undercooling due to addition of magnesium. In any case whether it be hypoeutectic or hypereutectic irons the nodule forms as a proeutectic graphite and the precipitation of carbon from the liquid continues until the liquid reaches eutectic composition. This remaining liquid then freezes as ledeburite. The cementite from the ledeburite mixture is then very rapidly decomposed, and the graphite is deposited on the existing nodules. In other words this hypothesis postulates that the nodules appear in the liquid and grow rapidly in the solid by decomposition of cementite.

The experimental evidence in this thesis does not support this hypothesis either because the observations show that no ledeburite was formed during the horizontal part of the cooling curve nor at any other time before the samples were quenched. This indicates that the remaining liquid does not solidify as ledeburite as is postulated by the hypothesis, but that the liquid is constantly being depleted of carbon due to the precipitation of graphite on

the existing nodules and this depleted liquid freezes as austenite on the existing austenite.

Although it is impossible to ascertain definitely by microscopic observations whether the first graphite or graphite nucleus originates in the liquid or in the solid austenite, the later stage of nodule formation when the nodule is large enough to be resolved by the optical microscope shows that the graphite nodule is surrounded by austenite.

The third hypothesis which is supported by De Sy, Wittmoser and Bunin and which was described in detail in the section discussing the various theories of nodular iron formation. This hypothesis postulates that nodules precipitate from supersaturated austenite and grow in this austenite by the diffusion of carbon from the liquid through the austenite. The graphite is never in contact with the liquid and since self-diffusion of iron in supersaturated austenite is equal in all directions, the graphite has a spheroidal shape. They argue that the decomposition of ledeburite would not give a spheroidal graphite because the self-diffusion of iron which must make room for the graphite is not equal in all directions.

The experimental evidence in this thesis seems to support part of this hypothesis but the author does not

believe that the nodules originate in the supersaturated austenite because if they did then most of the nodules would be at the dendrites. The experimental results indicate that the nodules may form near the dendrite arms, or independently away from the dendrites but as a rule not inside the dendrites. The author believes that it is not necessary to postulate the condition that the nodules originate from the precipitation of supersaturated austenite, although it may be possible. At the completion of this work the author had a chance to read an article entitled "The Solidification of Nodular Iron" by H. Morrogh published in the Journal of the Iron and Steel Institute, April, 1954. In this paper Morrogh suggests that in the case of hypereutectic irons, nodules form directly from the liquid until the eutectic transformation when they become enveloped by austenite. He also believes that hyper- and hypo-eutectic nodular irons solidify by analogous mechanisms.

The three main hypothesis of nodule formation and their growth have been discussed above, with reference to the experimental observations in this thesis and now a sequence of nodule formation and growth is presented below, based on the experimental results in this thesis and the extensive literature on this subject.

## THE MECHANISM OF GRAPHITE SPHERULITE FORMATION AND GROWTH IN HYPOEUTECTIC CAST IRONS

The first solid phase to form from the liquid is austenite. The skeleton crystals of primary austenite dendrites separate out on cooling and grow down to below the eutectic temperature, depending on the amount of undercooling (supercooling). There must be supercooling in order to get nodular graphite. It is assumed that nucleation of graphite in nodular cast iron is much more difficult than in gray cast iron but that nucleation of graphite can occur above the metastable eutectic (austenite-carbide).

Nucleation of graphite occurs in the liquid because the liquid is unstable with respect to graphite at that temperature. It usually occurs near the dendrites because the carbon content of the liquid is higher in the vicinity of the dendrites due to supercooling and growth of dendrites. The nucleation of graphite may also occur away from the dendrites because of localized composition difference, and ease of graphite nucleation at those points. The graphite may precipitate on both, graphite nuclei and suitable foreign nuclei. As soon as graphite precipitates on one of these nuclei it depletes the liquid of its carbon content around the graphite. This condition induces the nucleation of

austenite in the zone of the liquid which is depleted of carbon. The newly nucleated austenite grows very rapidly (almost spontaneously) into the depleted liquid zone because the liquid in the depleted zone is extremely supercooled. This supercooling is due to lower carbon content and not to any temperature difference of the two liquids. For example a liquid of 1% carbon is supercooled at the eutectic temperature while the liquid of eutectic composition at the eutectic temperature is not supercooled.

The austenite grows much more rapidly in the depleted zone than graphite and it soon surrounds the graphite and isolates it from the remaining liquid. If the graphite precipitates near the austenite dendrite, then the new austenite nuclei do not have to form but the austenite from the dendrite grows very rapidly into the supercooled region developed by the depletion of graphite. The growth of austenite shell therefore is very rapid at the beginning because the supercooling with respect to austenite is great. The amount of supercooling is given by "Z-Y", (Fig. 3). After the austenite shell has been formed, more carbon is deposited on the graphite nodule because the austenite in contact with the graphite is much lower in carbon content than the austenite in contact with the liquid as shown on Fig. 3, where point "I" gives the

FIG. 3

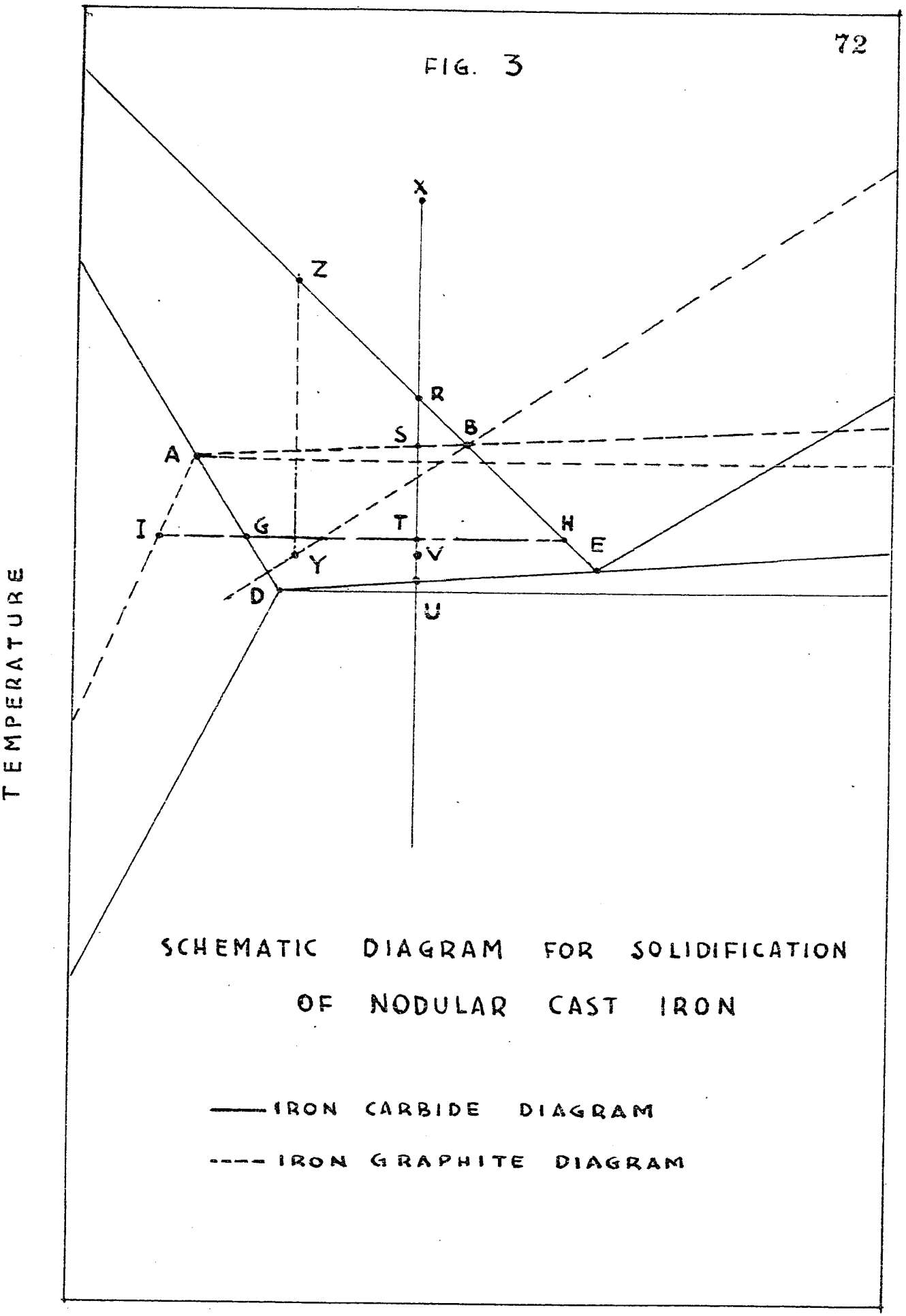


SCHEMATIC DIAGRAM FOR SOLIDIFICATION OF NODULAR CAST IRON

——— IRON CARBIDE DIAGRAM

---- IRON GRAPHITE DIAGRAM

composition austenite in contact with the graphite and point "G" gives the composition of austenite in contact with the liquid.

Because of this carbon concentration gradient the graphite diffuses very rapidly from the liquid through the thin austenite shell surrounding the graphite and is deposited on the existing graphite. In order for the graphite to grow the iron atoms in the austenite-graphite interface have to move out. As stated by Bunin and De Sy[10] the self-diffusion of iron in austenite is equal in all directions and this results in equal removal of iron atoms from the graphite-austenite interface thus giving rise to the growth of spheroidal graphite. If the self-diffusion of iron were not equal in all directions then the graphite would not grow in spheroidal shape but would follow the shape manifested by the removal of iron atoms.

At high temperature the self-diffusion of iron atoms in austenite is quite rapid and nodules can grow very rapidly. The graphite can grow equally in all directions and the basal hexagonal planes of graphite are formed perpendicularly to the direction of growth and to the direction of heat-flow which is produced by crystallization of graphite. In other words the basal planes are perpendicular to the radii of the sphere. This mode of crystallization of graphite results in acicular graphite

crystals radiating from the center of the nodule.

The initial precipitation of graphite from the liquid and the rapid growth of austenite at that time generates appreciable amount of heat and the solidification temperature rises slightly if cooling rate is slow enough. Since the growth of the nodules and the formation of new nodules is not too rapid after the initial rise of temperature the cooling curve does not remain horizontal but gradually starts droping down as shown on Fig. 2. The nodules (spherulites) form and grow during the so called horizontal portion of the cooling curve.

After the formation of the austenite shell around the graphite, the carbon from the liquid diffuses through the austenite and occupies the space vacated by self-diffusion of iron atoms at the austenite-graphite interface. Thus the graphite nodules grow and the heat liberated maintains the temperature which is approximate to the one marked "T" (Fig. 3) and which is the horizontal line on the cooling curve, (Fig. 2) or sometimes called the eutectic temperature, although strictly speaking it is not the eutectic temperature. The growth of nodules depletes the liquid of its carbon content resulting in the formation of more austenite. This austenite forms in the vicinity where the liquid is depleted of its carbon content and that is

around the austenite shell. Thus the austenite shell and the graphite nodule grow simultaneously from the liquid during the horizontal part on the cooling curve, and this temperature is any place between temperatures "S" and "U" (Fig. 3). At the austenite-graphite interface the composition of austenite is given by "I" and the composition of austenite at the liquid-austenite interface is given by "G". The concentration gradient for the diffusion of carbon from the liquid through the austenite is given by "G-I". The austenite grain containing a graphite nodule is called a cell because of its cellular growth. Many such cells originate at the beginning of the horizontal (solidification) and some of these cells form beside the dendrite arms while others form independently. Soon these cells begin to impinge and merge together.

This cellular growth results in segregation of alloying elements and impurities and is quite important in heat treatment of nodular cast irons as will be shown later in the experiment on "S" curves. Finally all the cells merge and the remaining liquid solidifies in the cell boundaries. The final composition of austenite at the end of solidification is given approximately by point "I" (Fig. 3).

This progress of nodule formation and growth is

illustrated by photomicrographs and the cooling curve on Figs. 2-22.

The question now arises regarding the function of magnesium in the formation of nodules. This question is not an easy one to answer and no experimental evidence which would shed some light on the subject is available. However it is well known that the addition of magnesium to cast iron favors the solidification according to the metastable system, and magnesium is considered as strong carbide stabilizer. It is the opinion of the author that when magnesium is added to cast iron, it inhibits the nucleation of graphite from the liquid phase either by removing the foreign nuclei on which graphite may form and/or inhibiting the formation of graphite nuclei from the liquid.

There is some literature[7][11][12][15] for, and some against foreign nuclei in nodular iron. The author believes that although some nodules do have foreign nuclei (material) in them these foreign nuclei are not essential and many nodules do not have them. If there is a suitable foreign material in the liquid on which the precipitation of graphite is facilitated then it will act as a graphite nucleus, and graphite will precipitate on that material. However this condition is not necessary and it is believed that the graphite may precipitate from the liquid without

the aid of any foreign nuclei.

In addition magnesium may lower the temperature for the formation of carbide eutectic or inhibit the nucleation of cementite. This would result in greater temperature difference between the stable and metastable eutectis, which would be desireable for the production of nodular iron because the liquid could be cooled to a lower temperature without any cementite formation.

The most essential condition for the production of nodular iron as postulated in this theory requires that the solidification of the graphite-eutectic be suppressed so that only few graphite nuclei form in the liquid at low temperature and no nuclei at high temperature.

Strictly speaking the eutectic reaction (Liquid to Graphite + Austenite) does not take place in the solidification of nodular iron. When nodular iron solidifies there are several reactions going on simultaneously during the horizontal part of the cooling curve which is sometimes loosely termed the eutectic solidification because the shape of the cooling curve resembles the eutectic solidification, and the temperature is in the vicinity of the eutectic temperature of cast iron. First, the liquid precipitates graphite, then there is a rapid growth of austenite around the graphite and finally the carbon

diffuses from the liquid through the austenite and is deposited on the graphite while the remaining liquid gives austenite. In order for graphite nodules to grow iron atoms must be removed from the austenite-graphite interface and this depends on the rate of self-diffusion of iron atoms at that temperature.

The mechanism of graphite spherulite formation and growth in hypoeutectic irons as discussed above is illustrated schematically on Fig. 4.

SCHEMATIC DIAGRAM FOR THE FORMATION AND GROWTH OF GRAPHITE SPHERULITES (NODULES).



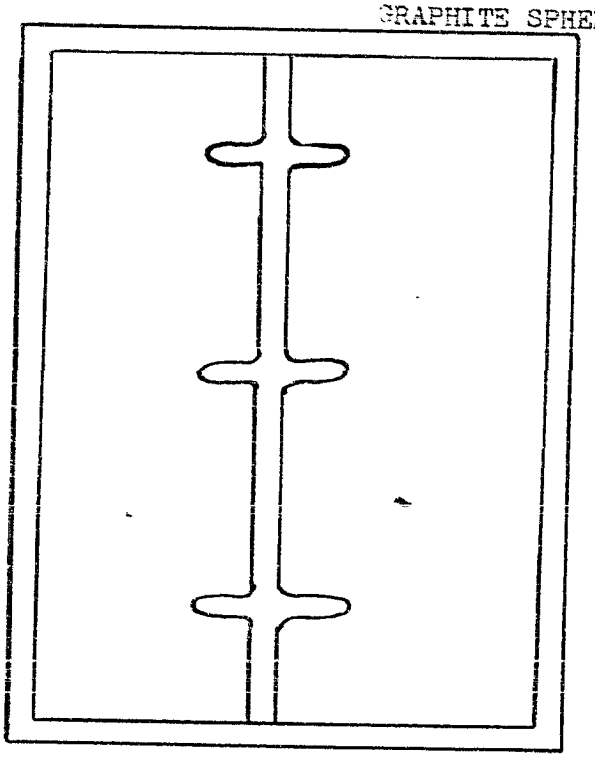

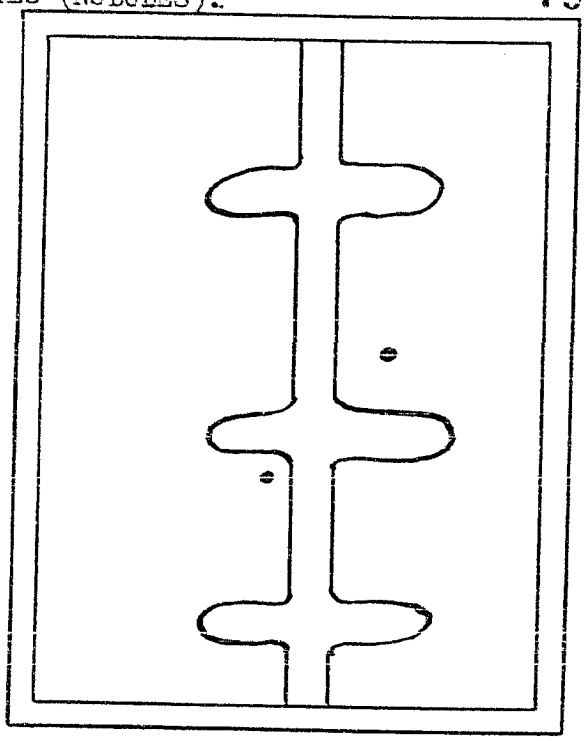

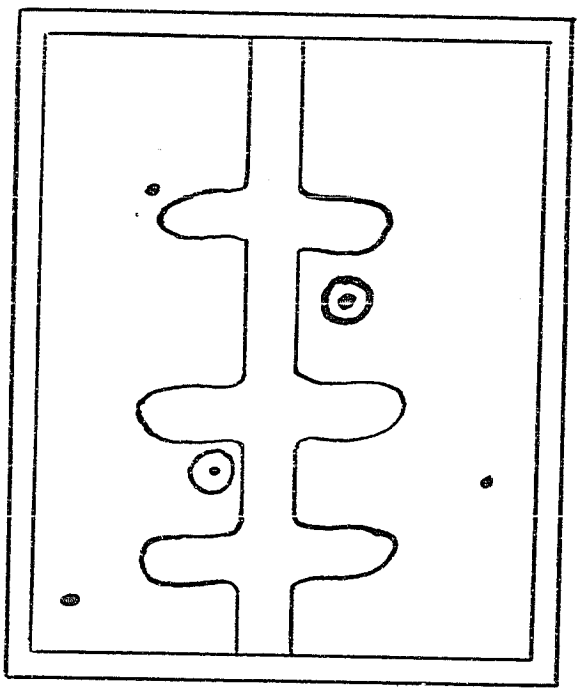

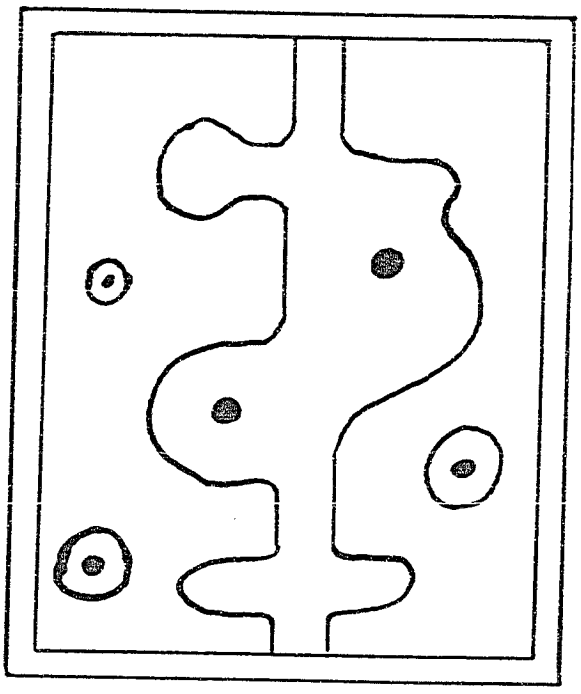

## FORMATION OF FLAKE VERSUS NODULAR GRAPHITE IN HYPOEUTECTIC IRONS

Let us compare the two mechanisms of graphite formation, namely coarse flake graphite of types A and B as described by Boyles[5] and nodular graphite as described in this thesis.

In both, gray cast iron consisting of flake graphite and nodular cast iron consisting of spheroidal graphite, solidification starts with the formation of skeletons of primary austenite dendrites. As the cooling progresses these dendrites grow. When the temperature of iron-graphite eutectic marked "S" on Fig. 3 is reached, or just below that temperature, crystallization of the eutectic liquid in flake gray iron begins according to the eutectic reaction $L \rightarrow G + A$ while in nodular iron the eutectic reaction is suppressed. The graphite in flake gray iron precipitates from the liquid and this precipitation depletes the liquid of some of its carbon content in the neighborhood of graphite and results in nucleation of austenite beside the graphite. Since the supercooling is not too great austenite does not grow too rapidly relative to graphite and therefore graphite is not cut off from the liquid. This austenite restricts the growth of graphite and forces the graphite to grow into the liquid while the austenite grows slowly beside the graphite. This results in the formation of flake graphite. Thus we have edgewise growth of austenite and graphite side by side pushing the liquid interface in front of them. Carbon is deposited directly from the liquid unto the graphite and the graphite is always in contact with the

liquid during solidification. This eutectic solidification begins at independent centers and grows equally in all directions, forming a cell like structure. The nucleation of graphite in flake graphite cast irons is not too difficult and many flakes are formed close together. Because of the ease of nucleation of flake graphite from the liquid appreciable supercooling of the liquid cannot be attained unless very rapid cooling rate is used and this results in solidification according to the metastable system.

Thus the solidification of flake gray iron is truly an eutectic reaction because both graphite and austenite are nucleated in the eutectic liquid and the two phases are always in contact with the liquid while they grow side by side. Therefore the mixture of coarse flake graphite and austenite may be considered as a product of the eutectic reaction.

As stated previously there is no eutectic reaction during solidification of nodular iron because the nucleation of graphite from the liquid is suppressed. Because of this suppression of solidification, nodular iron does not start to freeze until a lower temperature is reached. This temperature is still above the metastable eutectic temperature but low enough to give supersaturated liquid. At this temperature the graphite which precipitates from the liquid is surrounded immediately by rapidly growing austenite

because of the large amount of supercooling which is equal to "Z-Y" as shown on Fig. 3. After the nodule is entraped by the austenite it is no longer in contact with the liquid and it is forced to grow in the solid austenite. Carbon then diffuses from the liquid, through the austenite shell and is deposited on the graphite, while the iron atoms at the austenite-graphite interface are removed equally in all directions in order to make room for the graphite. The graphite therefore grows equally in all directions and becomes spherical in shape.

As soon as precipitation of graphite from the liquid starts the temperature remains more or less constant and the solidification proceeds by cellular growth until the metal is solid. Small quantities of the liquid which is high in alloying elements and impurities such as phosphorus solidify in cell boundaries at a temperature below the temperature given by the "horizontal" of the cooling curve, both in flake graphite iron and nodular graphite iron.

Summarizing the main differences briefly, it may be said that flake graphite originates and grows in the liquid, while nodular graphite originates in the liquid but grows in the solid austenite.

## SUMMARY OF SPHERULITE FORMATION AND GROWTH IN HYPOEUTECTIC NODULAR IRONS

In order to illustrate the mechanism of nodular graphite formation let us take an alloy of composition "X" shown on Fig. 3 and follow chronologically what happens on cooling that alloy from the liquid state. Fig. 3 is used to facilitate this description. As the alloy "X" is cooled temperature "R" is reached where the skeletons of austenite dendrites begin to form. On further cooling the austenite dendrites grow and temperature "S" is reached. Although temperature "S" is the iron-graphite eutectic temperature and iron graphite eutectic should start forming on further cooling, the graphite is not formed at this temperature because the nucleation of graphite is suppressed by the addition of magnesium. Therefore cooling through the temperature "S" and down to temperature "V" only austenite dendrites grow and the composition of the dendrites changes gradually to that of "G" while the composition of the liquid changes to that of "H" at the temperature "T". At the temperature "V" graphite precipitates from the liquid giving a liquid around the graphite precipitate equal to composition "Y" or "Z". The liquid "Z" is greatly supercooled with respect to austenite and is very unstable at that temperature. Because of this great supercooling, the

austenite nucleates in it and grows very rapidly into the depleted zone. This results in the entrapment of graphite in an austenite shell. By this time the temperature has risen to temperature "T" because of the evolution of heat due to the formation of austenite and graphite. At temperature "T" composition of austenite in contact with the liquid is given by "G" and the composition of austenite in contact with graphite is "I". Thus the carbon concentration gradient in the austenite shell is given by "G-I". This results in the diffusion of carbon from the liquid, through liquid-austenite interface, through the austenite shell, and finally deposition of the carbon on the graphite nodule at the austenite graphite interface. This reaction progresses at some time in the vicinity of temperature "T" but although this temperature may remain constant it does not have to do so and usually after about 30% solidification it starts dropping down because there is more heat evolved during the early part of the solidification. This is due to the fact that most of the nodules are formed during the early part of solidification and that during the later part of solidification carbon has to diffuse through greater distances in order to be deposited on the nodule, while the concentration gradient is decreased.

# PART II

## SOLID TO SOLID TRANSFORMATIONS

The subcritical transformations in nodular cast iron may be considered as solid to solid reactions and there are several reactions that may occur depending on the temperature of the transformation. The various reactions that occur below the critical temperature (eutectoid temperature) are listed below.

1) Austenite to Ferrite + Graphite
2) Austenite to Ferrite + Carbide (pearlite)
3) Carbide to Ferrite + Graphite
4) Austenite to Bainite
5) Austenite to Martensite
6) Bainite to Graphite + Ferrite
7) Martensite to Ferrite + Graphite
8) Martensite to Ferrite + Cementite (spheroidal)

Reactions 3, 6, 7, and 8 are secondary reactions, that is the austenite is first transformed to martensite, bainite, and/or pearlite, and they in turn are decomposed into graphite and ferrite if the temperature is high enough. The investigation described in this thesis deals

primarily with reactions 1, 2, 3, 4, and 5.

Solid state reactions are conveniently investigated by isothermal transformation studies which have been well developed and extensively used both in ferrous and non-ferrous metallurgy in recent years. There are many ways of determining the progress of an isothermal transformation. The methods most commonly used are optical metallography, dilatometry, hardness measurements, x-ray diffraction, electrical resistance, and thermal analysis. The metallographic method which was well developed by Bain and Davenport[14] in their original study of steel is the most commonly used in the determination of "S" curves which are also called isothermal transformation diagrams (I-T diagrams) and time-temperature-transformation diagrams (T-T-T diagrams). These diagrams usually show the time for the beginning and end of transformation of austenite at some constant temperature. The beginning and end of transformation are arbitrary values and there are no universally accepted standards that would define definitely the percentage of transformation necessary for the beginning and end of transformation. For this reason the values used for the beginning of transformation range from just a trace of transformation to several percent, while the end of transformation is even less definite and the values range from 95-100% of transformation. The most

accepted values for the beginning of transformation in steels range from 1/2-1% and those for the end of transformation range from 97-99%.

In this investigation the beginning and end of transformation as represented in the I-T diagrams ("S" curves) were determined by optical metallography. For the beginning of transformation the value of 1% was used and for the end the value of 97-100% was used. The procedure used in the determination of the "S" curves in this thesis is described below.

## EXPERIMENTAL METHODS AND APPARATUS

The specimens used in the determination of the T-T-T diagrams, were obtained from 1" x 6" keel blocks. The charge for making these keel blocks was composed of Lyle pig, steel punchings, nickel shot, ferromolybdenum, 50% ferrosilicon and 80% ferromanganese, and was melted in a basic lined 150# induction furnace. Spherulitic graphite was obtained by the standard Inco techniques.

The analyses of the four cast irons used in this investigation are as follows:

| Cast Iron | TC | Mn | Si | Ni | Mo | Cu | S | P |
|---|---|---|---|---|---|---|---|---|
| No. 1 | 3.56 | 0.35 | 2.12 | 3.70 | 0.0 | | 0.016 | 0.020 |
| No. 2 | 3.42 | 0.75 | 2.25 | 3.67 | 0.0 | | 0.014 | 0.014 |
| No. 3 | 3.52 | 0.35 | 2.14 | 3.68 | 1.26 | | 0.016 | 0.030 |
| No. 4 | 3.40 | 0.34 | 2.82 | 0.52 | 0.0 | 0.38 | 0.015 | 0.018 |

Cast Irons No. 1 and No. 2 are nickel alloy cast irons, and the keel blocks are pearlitic in the as cast condition. Cast Iron No. 3 is a molybdenum-nickel cast iron and the cast microstructure of the keel blocks is accicular and very hard. Cast iron No. 4 is a typical low alloy commercial nodular cast iron and the microstructure consists mostly of ferrite and some pearlite.

The legs of the keel blocks were cut off giving 1" x 1" x 6" bars of cast iron from which thin specimens were machined for heat treatment. Small specimens (about 1 cm. x 1 cm. x 0.3-0.4 cm.) were cut from these legs and a small hole was drilled at one corner of each specimen in order to fasten it to a nichrome wire. Cast iron No. 3 which contained molybdenum had to be heat treated at 1200°F in order to soften it for machining. The specimens were then numbered and homogenized in batches of 50 at a time in a dry argon atmosphere. The argon from the tank was

first bubbled through concentrated sulfuric acid in order to remove moisture. It was then passed through a tower packed with glass wool in order to remove bubbles of acid. In order to remove the last traces of $CO_2$ and acid gases, the argon was passed through a second tower containing soda lime. Oxygen was removed next by passing the argon through a tube tightly packed with copper turnings held at about 600°-800°F. The last traces of moisture were finally removed by passing the gas through two long glass tubes, one packed with drierite and the other with anhydrous magnesium perchlorate. Finally the argon entered the tube furnace which was used for homogenizing and austenitizing. After leaving the furnace the argon was bubbled through about 12 inches of concentrated sulphuric acid in order to have higher pressure inside the furnace than the atmospheric pressure, so that even if a small leak developed, there would be less chance of contamination with air and leaks could also be detected more easily. After passing through concentrated sulphuric acid the argon was exhausted to the air.

The samples treated in this dried argon atmosphere showed no oxidation, or decarburization even after one week of treatment. If argon or nitrogen is not treated or dried some decarburization is noticed after prolonged

holding. The specimens were always polished and free from oxide just before they were placed inside the tube furnace for homogenizing or austenitizing.

Fifty specimens were placed in a nickel boat and homogenized for 50 hours at 1700°F under a dried argon atmosphere in a tube furnace. One inch fused silica or Vycor tubes were used in the furnace. The inside thermocouple which was always in contact with the specimens gave the temperature inside the furnace, while another thermocouple was placed near the heating elements of the tube furnace and was connected to the controller so that a constant temperature was maintained at all times. The temperature was recorded on a Micromax recorder. The specimens were placed inside the furnace and the furnace was then sealed with a fast drying lacquer. After the lacquer dried the argon was turned on and the whole system flushed for several hours in order to drive out all the air. After flushing, the furnace was turned on and brought to temperature. After fifty hours at 1700°F the specimens were taken out and quenched in water. This treatment gave a fairly homogeneous austenite. Complete homogenization was not attained even after 100 hours.

The austenitizing was carried out in the same furnace, using the same system for drying the argon. The

specimens were cleaned of any oxide film that might have formed during storing after the homogenizing treatment and fastened to a nichrome wire by passing the wire through the hole drilled at one corner of the specimen. One wire was used for each specimen. The 18 gage nichrome wire was thick enough to be rigid when the sample was quenched in a lead bath. One, two, three, or four of these specimens were placed in the tube furnace which was at 1650°F, and held there for three hours. Since the specimens were thin and small, they reached the temperature of the furnace in a short time. When the specimens were placed in the furnace a slight contamination of the argon atmosphere resulted. This contamination was not serious because the pressure of the atmosphere was greater than the atmospheric pressure.

Another reason was that the volume of the tube and the system was small so that very little oxygen could be present. The small amount of oxygen that did get in during the short time of loading the furnace was absorbed right away by the hot copper turnings after the furnace was closed and as a result no damage was done to the specimens. Austenitizing under these conditions gave better results than austenitizing in neutral salts.

After three hours at 1650°F the specimens were rapidly quenched in a lead bath at a constant temperature,

and held there for various lengths of time in order to determine the beginning and end of transformation at that particular temperature. The specimens were pulled out of the austenitizing furnace by holding the cool end of the nichrome wire and then rapidly immersing the specimens in a lead bath heated in a Hoskins electric resistance pot furnace. The cool end of the nichrome wire was than bent and a weight (silica brick) placed on top of it in order to keep the specimens immersed in the lead bath. The nichrome wire was rigid enough so that it did not bend. The specimens immersed in the lead bath were always near the thermocouple. The tip of the chromel-alumel thermocouple was protected by a specially made iron tip which made a tight fit with the thermocouple insulator. With this protection the thermocouple lasted for more than a month. The thermocouples were changed periodically depending on the temperatures used, in order to avoid failures during the runs which sometime lasted for a week. By changing the thermocouple before it actually failed a lot of time was saved. Another thermocouple was placed near the heating elements of the pot furnace and connected to the controller. The temperature of the isothermal baths was measured by a potentiameter and was maintained within $\pm$ 5°F.

The isothermal baths consisted of pure lead for temperatures from 800°F to 1500°F. The molten lead was covered with a layer of charcoal to keep it from oxidizing at higher temperatures. For temperatures of 500°-800°F, a binary eutectic of lead-tin was used. The isothermal bath for temperatures lower than 400°F consisted of a quaternary eutectic alloy containing 50% bismuth, 27% lead, 13% tin, and 10% cadmium. This quaternary alloy or "Wood's Alloy" was also used for quenching bathsin martensite determination experiments. The volume of the isothermal metal baths was large enough so that only a slight change in the bath was observed when the hot specimens were quenched in it. Metal baths like the ones described above are well suited for this type of work because they provide a neutral atmosphere (protect the specimens from oxidation or decarburization etc.), and give rapid quenching because of their excellent heat conductivity. Thus the specimen when quenched in a molten metal bath reaches the temperature of the bath sooner than if it were quenched into a molten salt bath. Alloy cast iron pots were used as containers for metal baths.

The specimens were removed from the bath after various intervals of time and quenched in ice cold water. They were then ground on a wet belt grinder in order to

remove about one sixteenth of an inch of metal and finished on Nos. 1, 1/0, 2/0 and 3/0 emery papers before being electropolished on a Disa Electro-Polisher for 5-15 seconds. The electrolyte used in polishing was of the following composition:

15 ml of 60% Perchloric acid (Sp. Gr. 1.54)
60 g of Sodium thiocyanate
75 g of Citric acid
800 ml of Ethanol
100 ml of Propanol

After electropolishing the samples were repolished on a silk-covered lap or some other suitable cloth such as Miracloth for about three minutes. The specimens were then etched with nital or picral, or a mixture of both, and examined under the microscope. The percentage of transformation was recorded and as a result of these observations, the beginning (1%) and end (97%) of transformation at a given temperature were plotted on semi-log. graph paper. The results of these experiments are shown on the four T-T-T diagrams in this thesis.

In order to determine the martensite start($M_s$) and

finish ($M_f$) temperatures the specimens were homogenized and austenitized as described previously. The specimens were then quenched in liquid baths, such as woods metal for temperatures from 200° to 500°F, mercury fro 50° to 200°F, and in alcohol cooled with dry ice and liquid air for 0° to -200°F. The specimens were held at the liquid bath just long enough for the specimen to reach the temperature of the bath. This time was less than a minute for temperatures above 0°F and a little over a minute for temperatures below 0°F. The specimens were then immersed in a lead bath at a temperature of 750°F. The specimens were held at this temperature for about 30 seconds just long enough to temper the martensite which formed during the first quench. The specimens were finally taken out and quenched in ice cold water. The tempered martensite when observed under the microscope is black while the untempered martensite or retained austenite are white. The $M_s$ represents 1% martensite and $M_f$ represents 97% martensite. Both of these holding times were too short to form any visible bainite because bainite in these cast irons does not begin to form at these temperatures until much more time is allowed. This metallographic method of martensite determination was developed by Greninger and Troiano[16].

Nodular cast irons are complex alloys of iron and therefore the eutectoid temperature (critical temperature)

is not one definite temperature but is a range of temperature. Thus ferrite starts forming at some higher temperature and the transformation of austenite does not go to completion at this temperature no matter how much time is allowed. The reaction does go to completion at some lower temperature. The same may be said about the heating of nodular iron; at a lower critical temperature only a trace of austenite is formed, while at the higher critical temperature the steel matrix is all austenite. The upper critical temperature is called in this thesis "the upper eutectoid temperature" and the lower critical is called "the lower eutectoid temperature". These temperatures were obtained by heating homogenized specimens to some temperature above 1200°F and holding there for 5 hours in order to determine the amount, if any, of austenite formed. Cold homogenized specimens were attached to one end of a nichrome wire and placed in lead baths held at various constant temperatures ranging from 1200°F to 1600°F. The specimens were held in these baths for 5 hours before quenching in water. The specimens were then prepared for metallographic observations as described previously. Any austenite that formed during holding at these temperatures transformed to martensite upon quenching in water, and this martensite could easily

be detected. The temperature which gave about 1% of martensite (transformed austenite) was called "the lower eutectoid temperature" and was marked on the T-T-T diagram for that alloy. The temperature which gave 99% martensite was called "the upper eutectoid temperature" and it also was drawn on the T-T-T diagram. The determination of these critical temperatures upon cooling gives somewhat lower values for both of them as would be expected.

Finally after the T-T-T diagrams have been determined Rockwell "C" and Rockwell "B" hardness measurements were taken on all specimens which represented the end of transformation. The hardness values at 100°F intervals were tabulated for the four cast irons and they represent the hardnesses that may be attained on complete transformation of austenite at that temperature for that particular alloy. If the transformation was not complete at the end of a week, then no hardness measurements were taken of the partial transformation. Besides taking Rockwell "C" and Rockwell "B" hardness measurements Knoop hardness measurements were taken on the steel matrix of cast iron No. 4 with a Tukon hardness machine in order to show the relationship between the overall hardness of cast iron as shown by Rockwell readings and the hardness of the steel matrix

of the same cast iron. The Knoop hardness numbers were converted to Rockwell "C" or Rockwell "B" for comparison purposes. An average value of five hardness readings was taken as the final value.

The results of these experiments are examplified by "S" curves (T-T-T diagrams) photomicrographs and other pertaining data in this thesis.

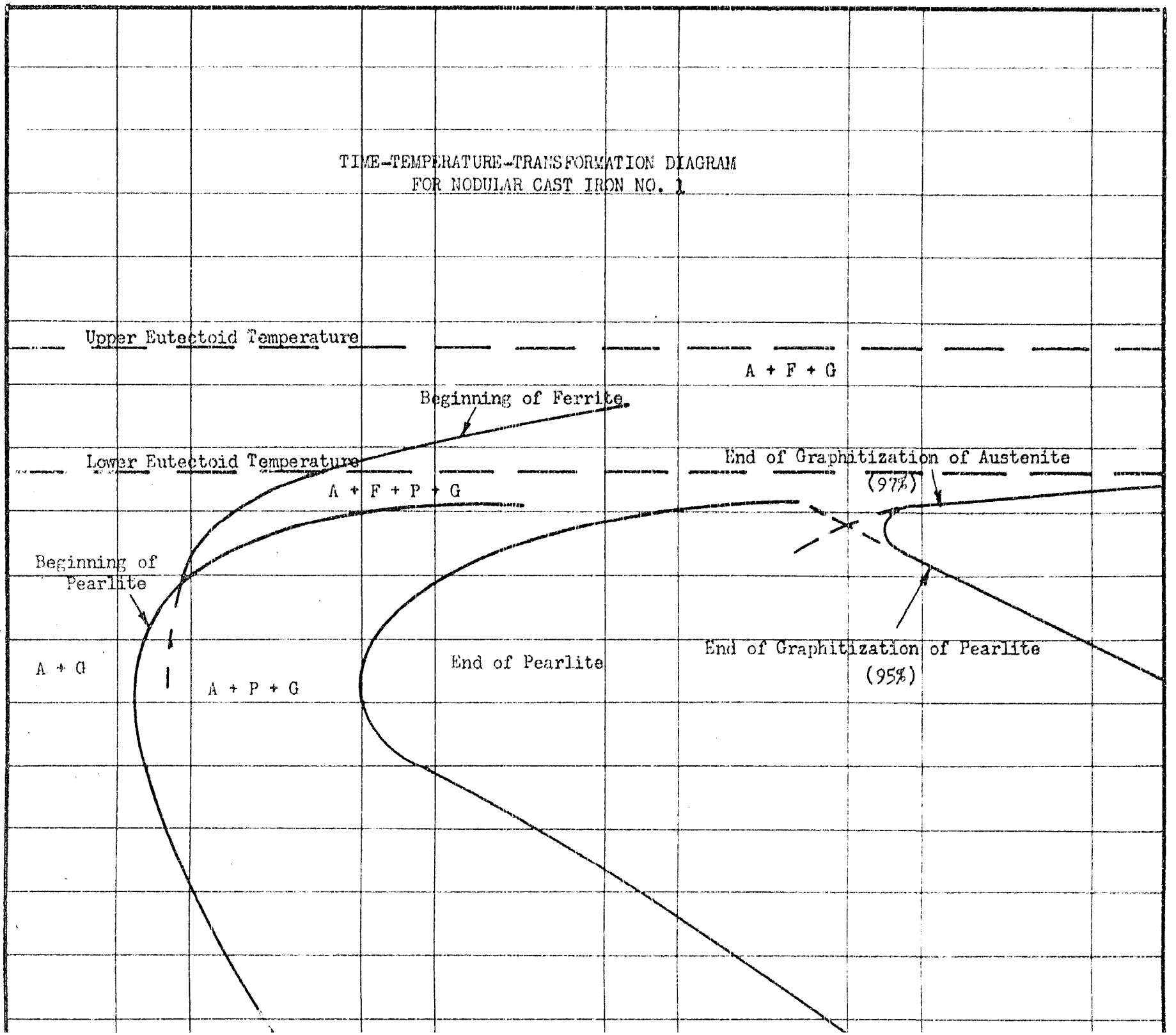

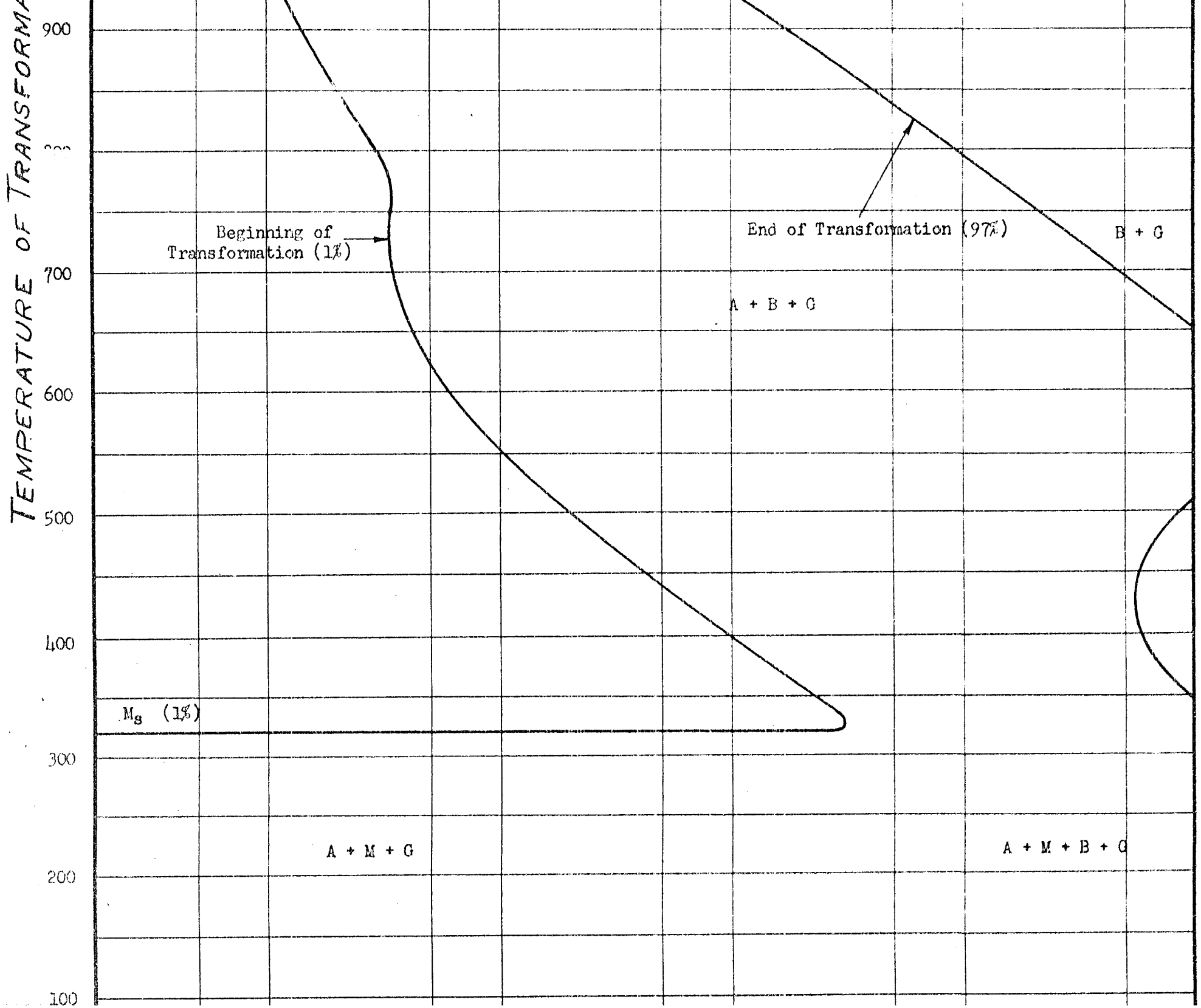

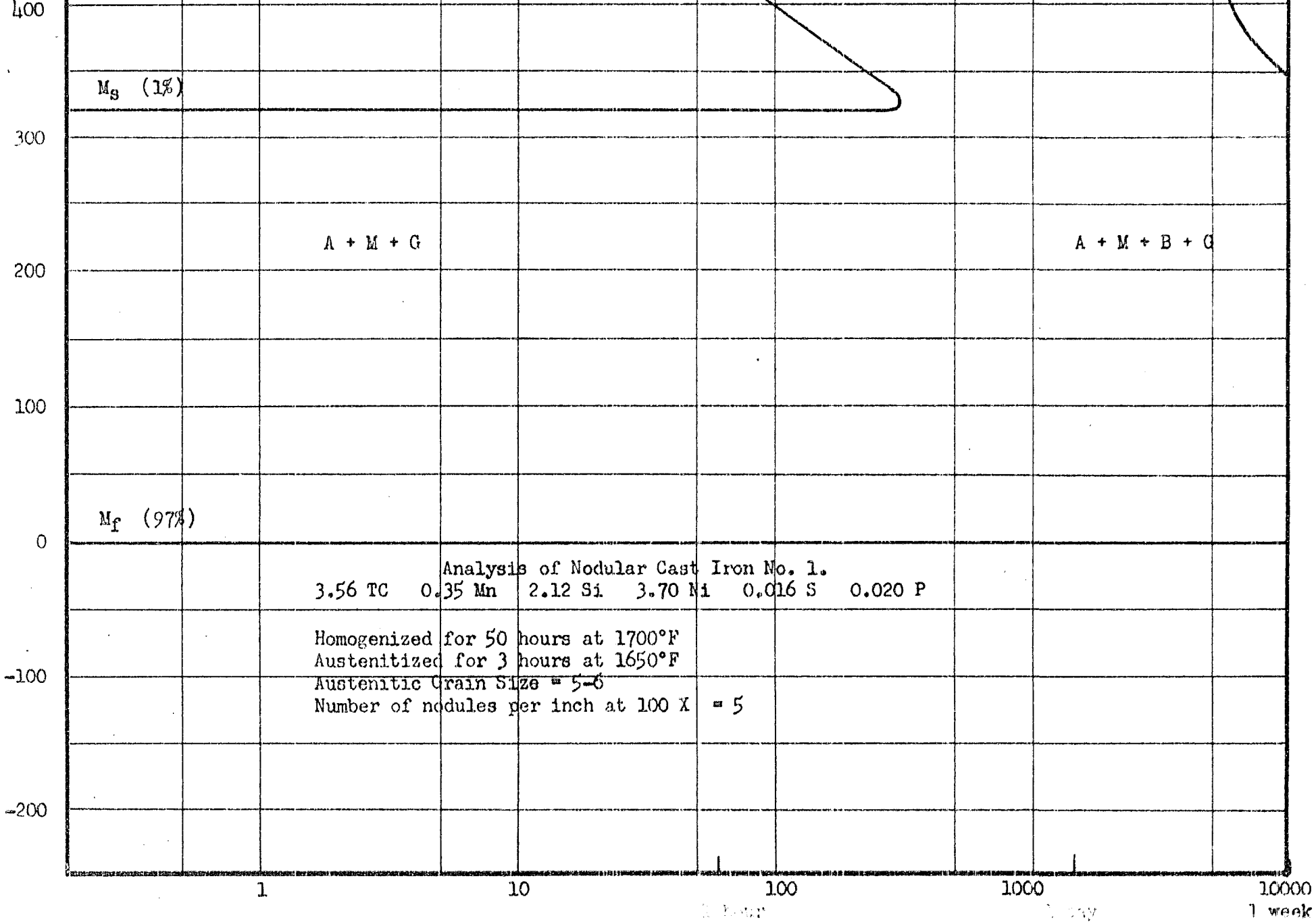


Analysis of Nodular Cast Iron No. 1.
3.56 TC 0.35 Mn 2.12 Si 3.70 Ni 0.016 S 0.020 P

Homogenized for 50 hours at 1700°F
Austenitized for 3 hours at 1650°F
Austenitic Grain Size = 5-6
Number of nodules per inch at 100 X = 5

TRANSFORMATION TIME, MINUTES

Fig. 24

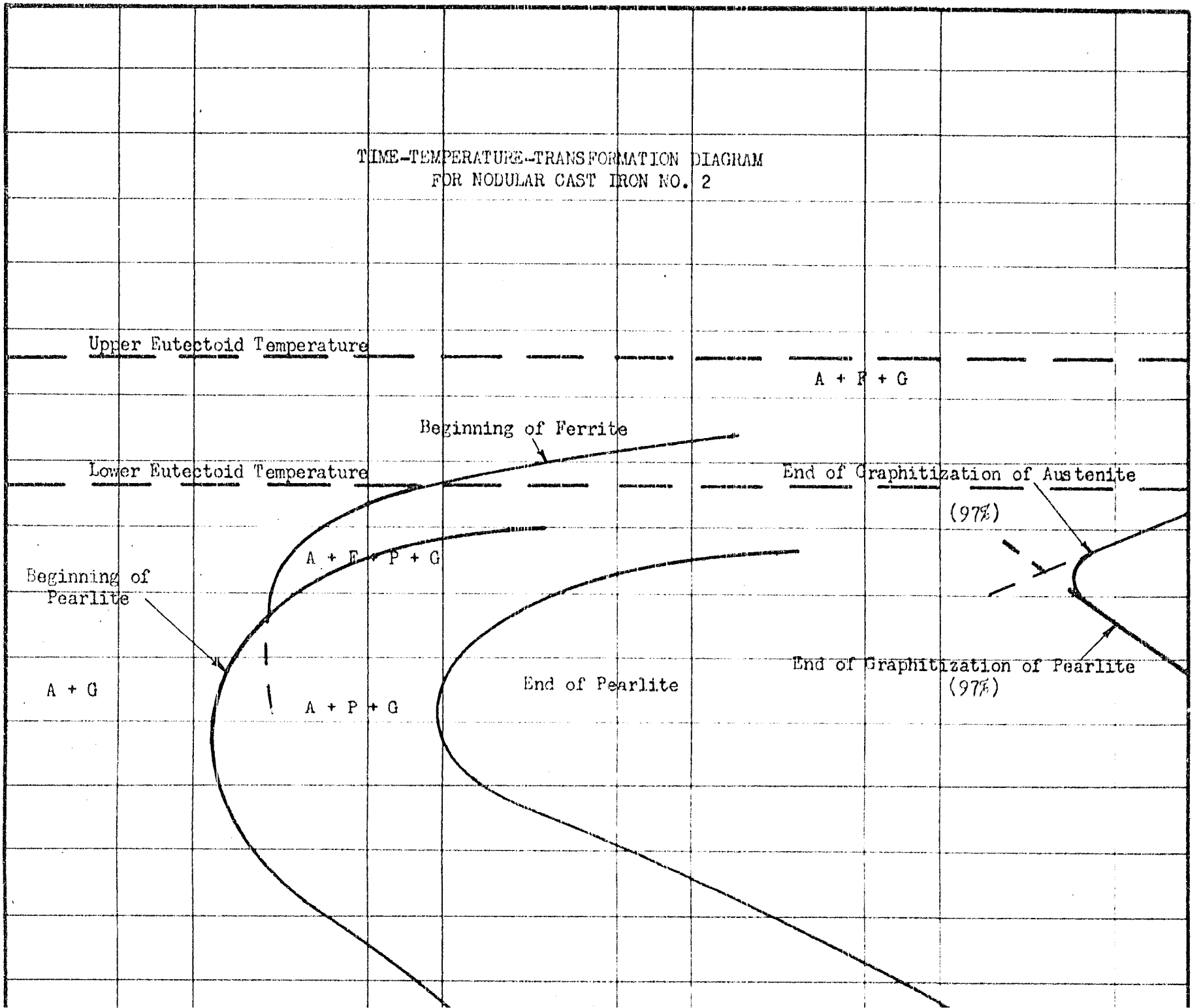

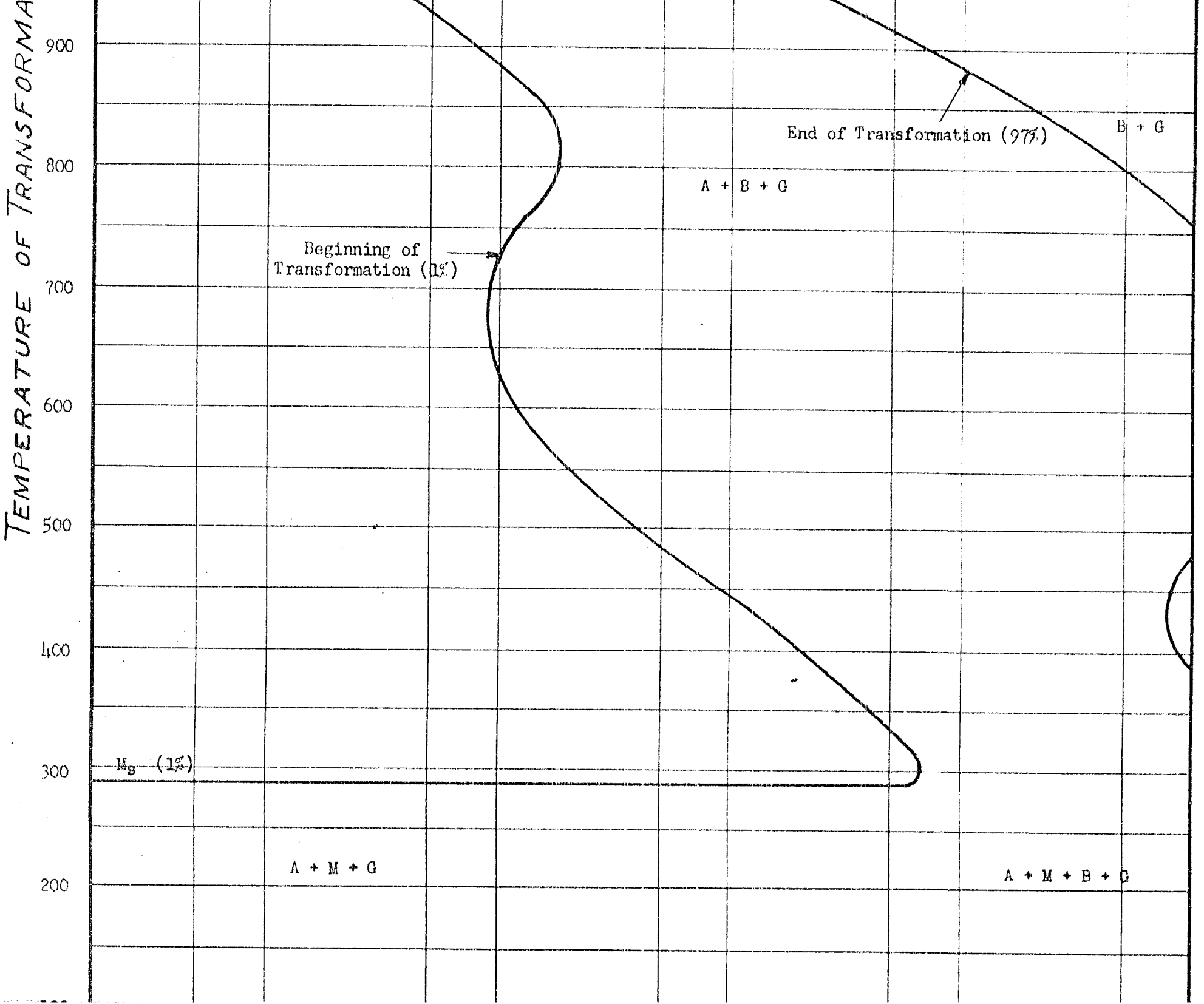

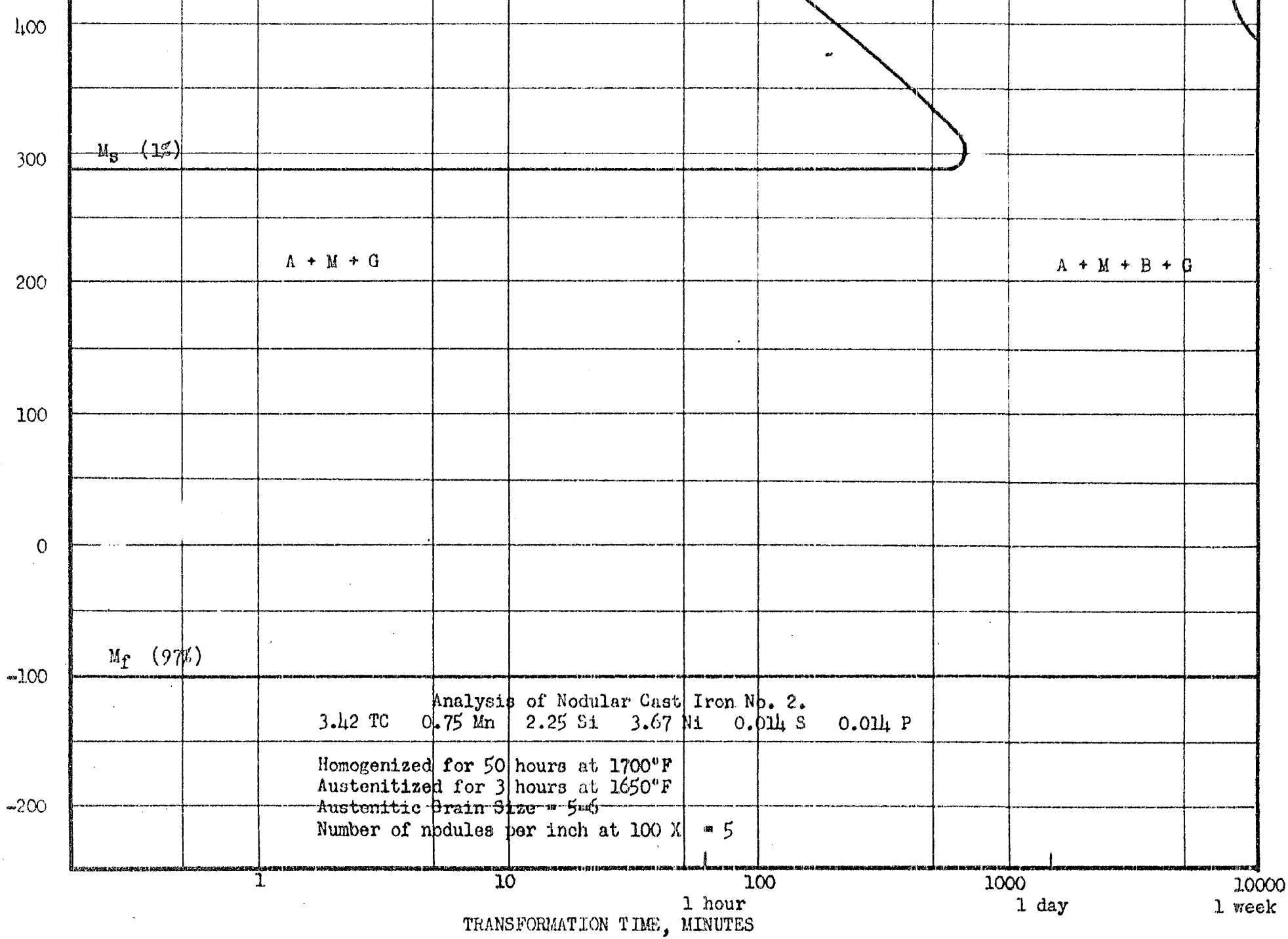


Fig. 25

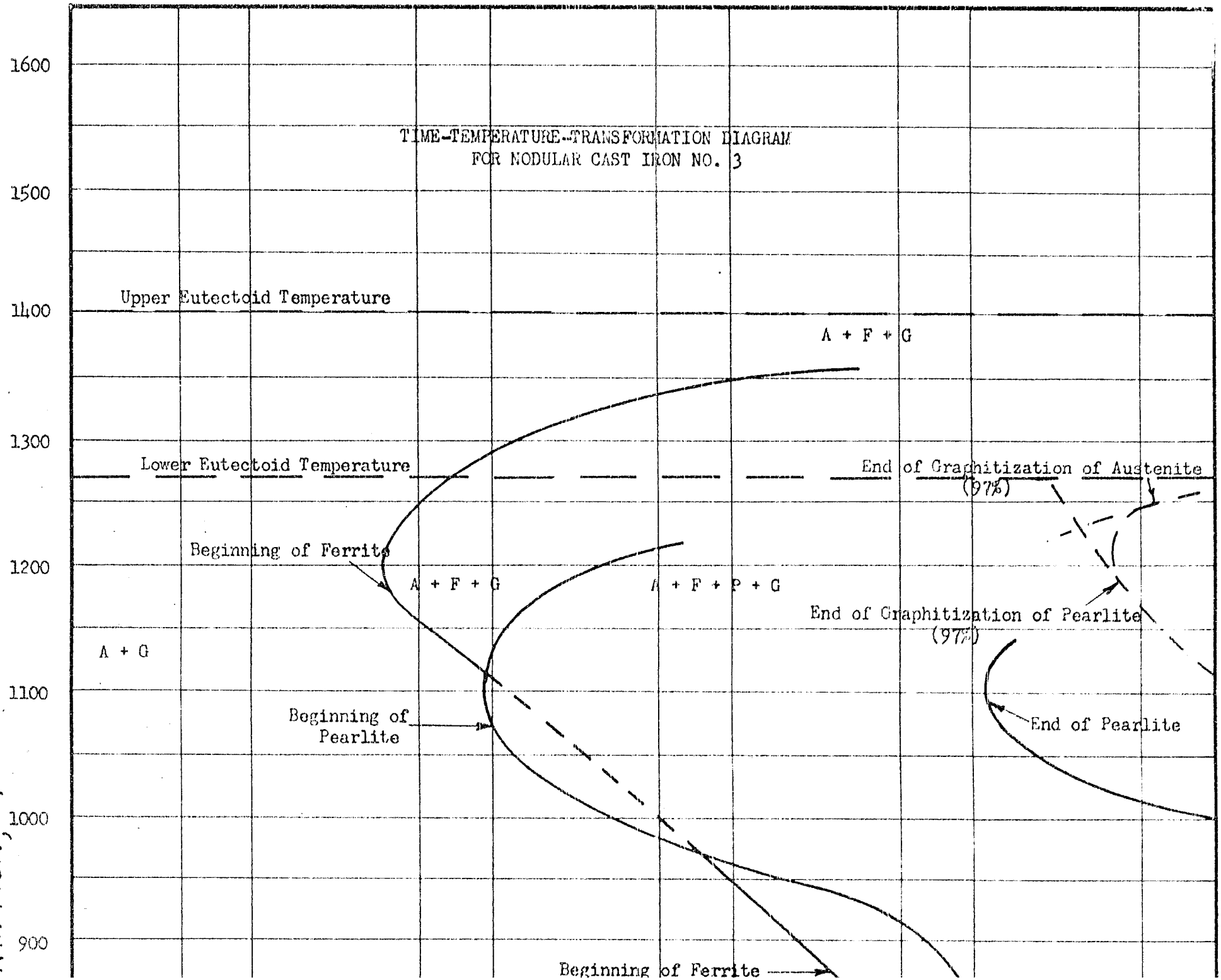

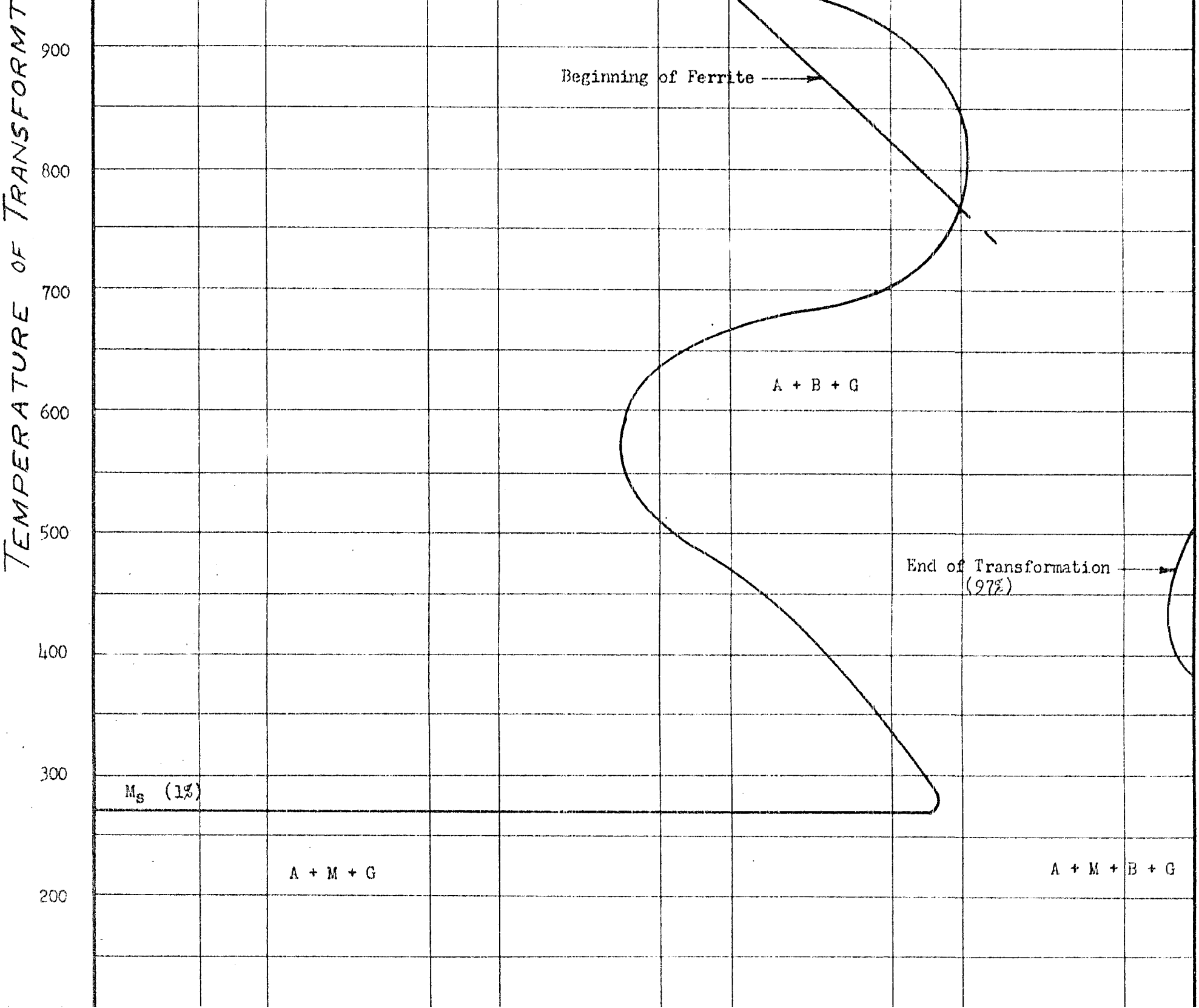

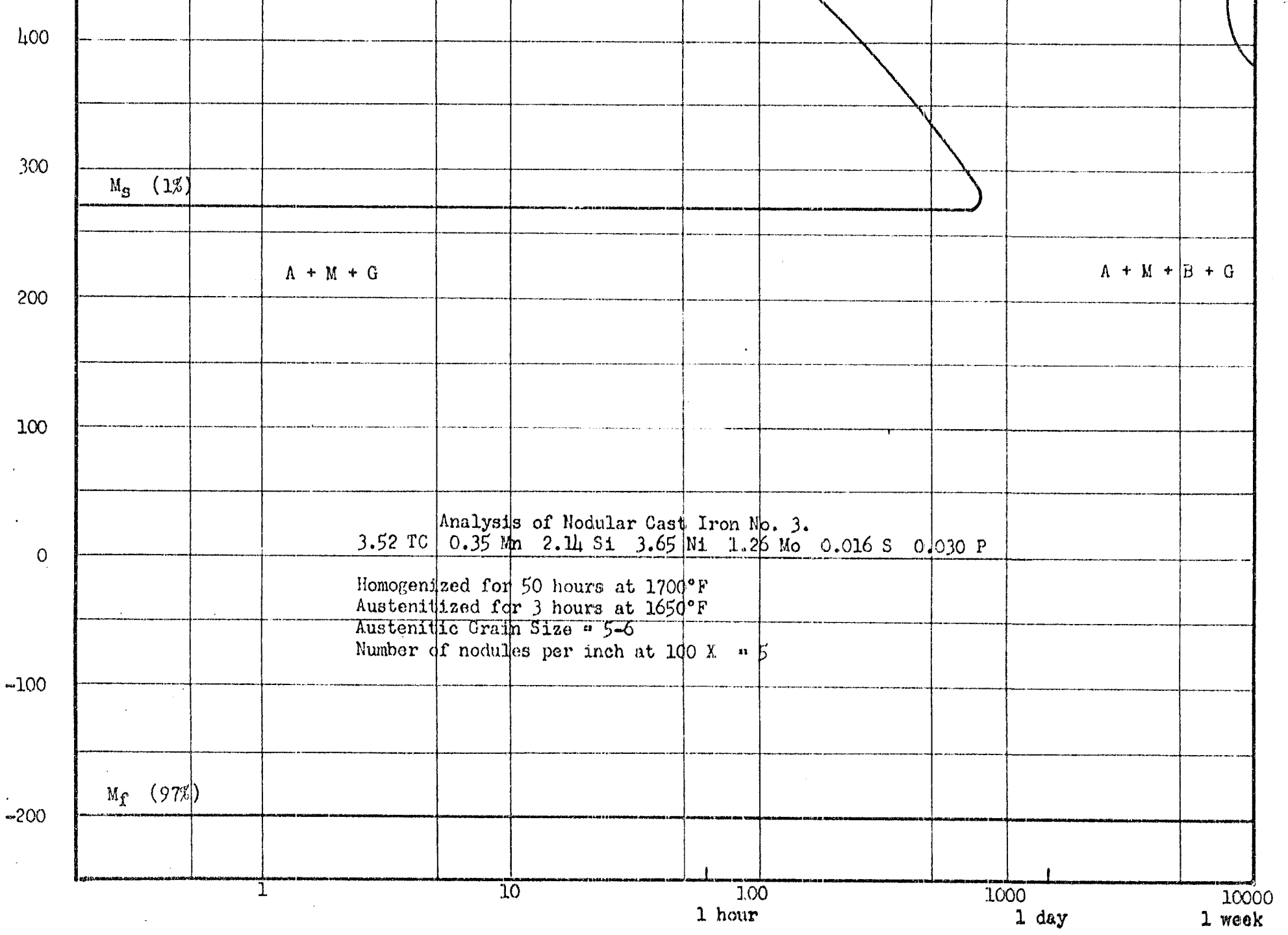


Fig. 26

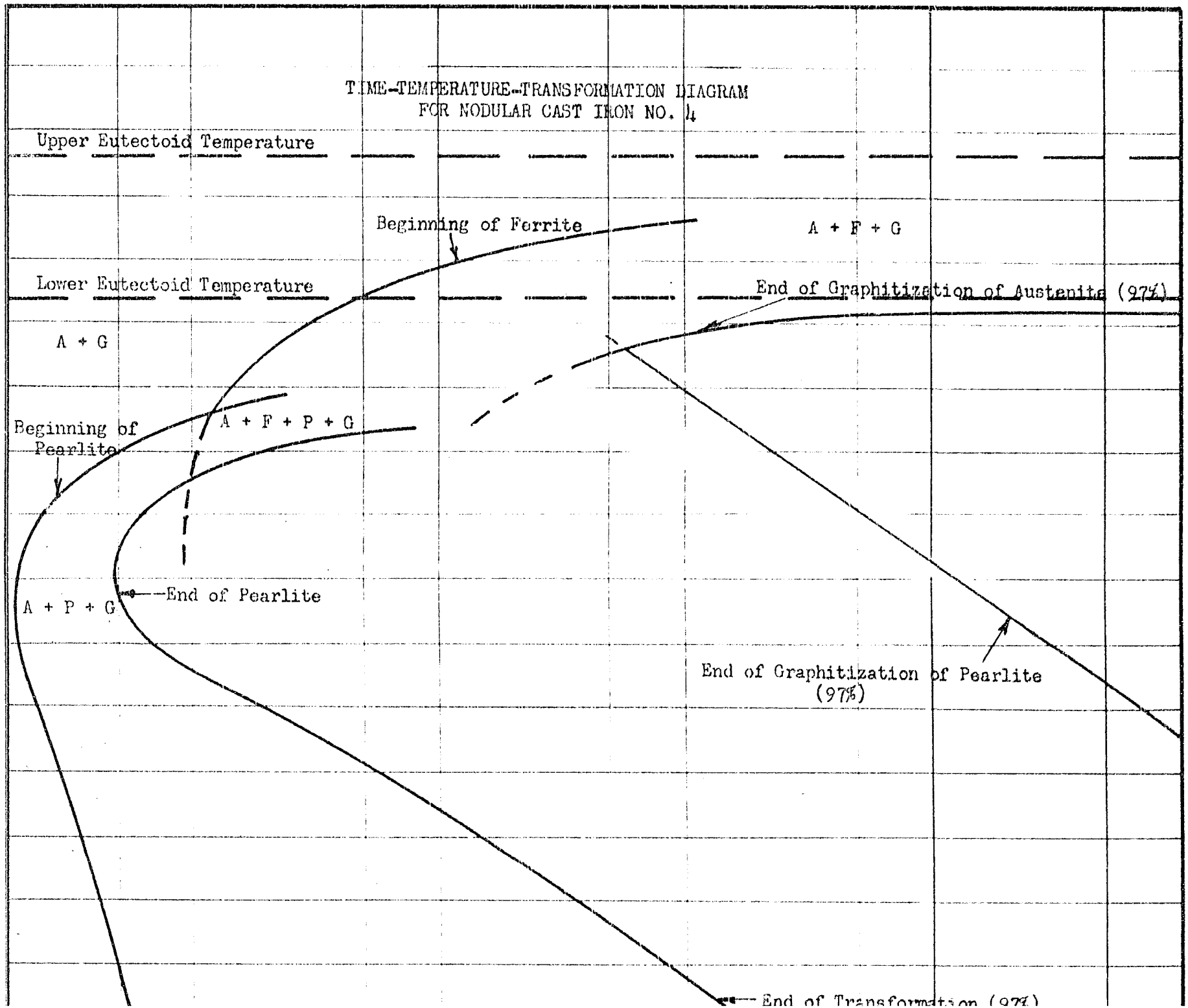

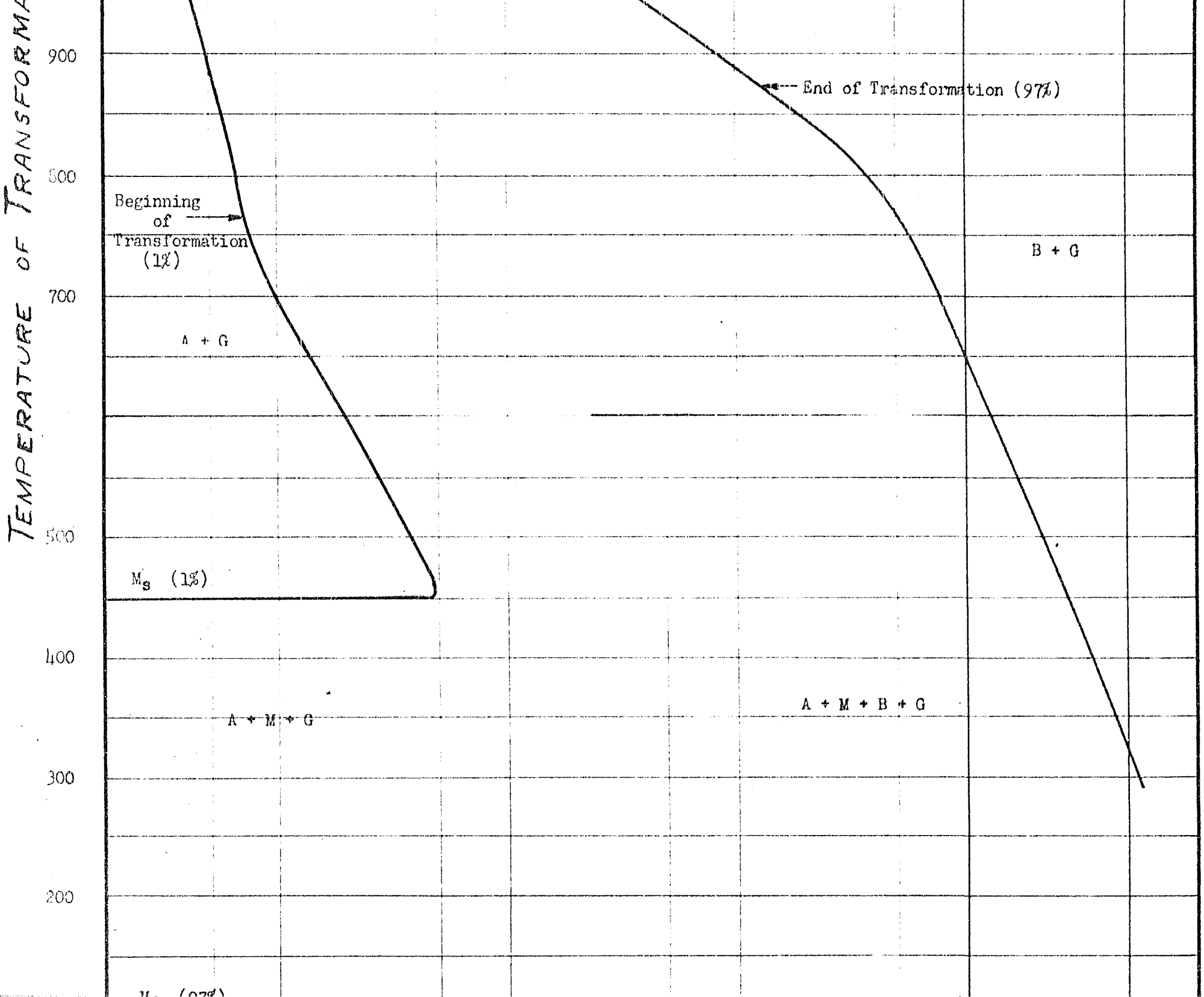

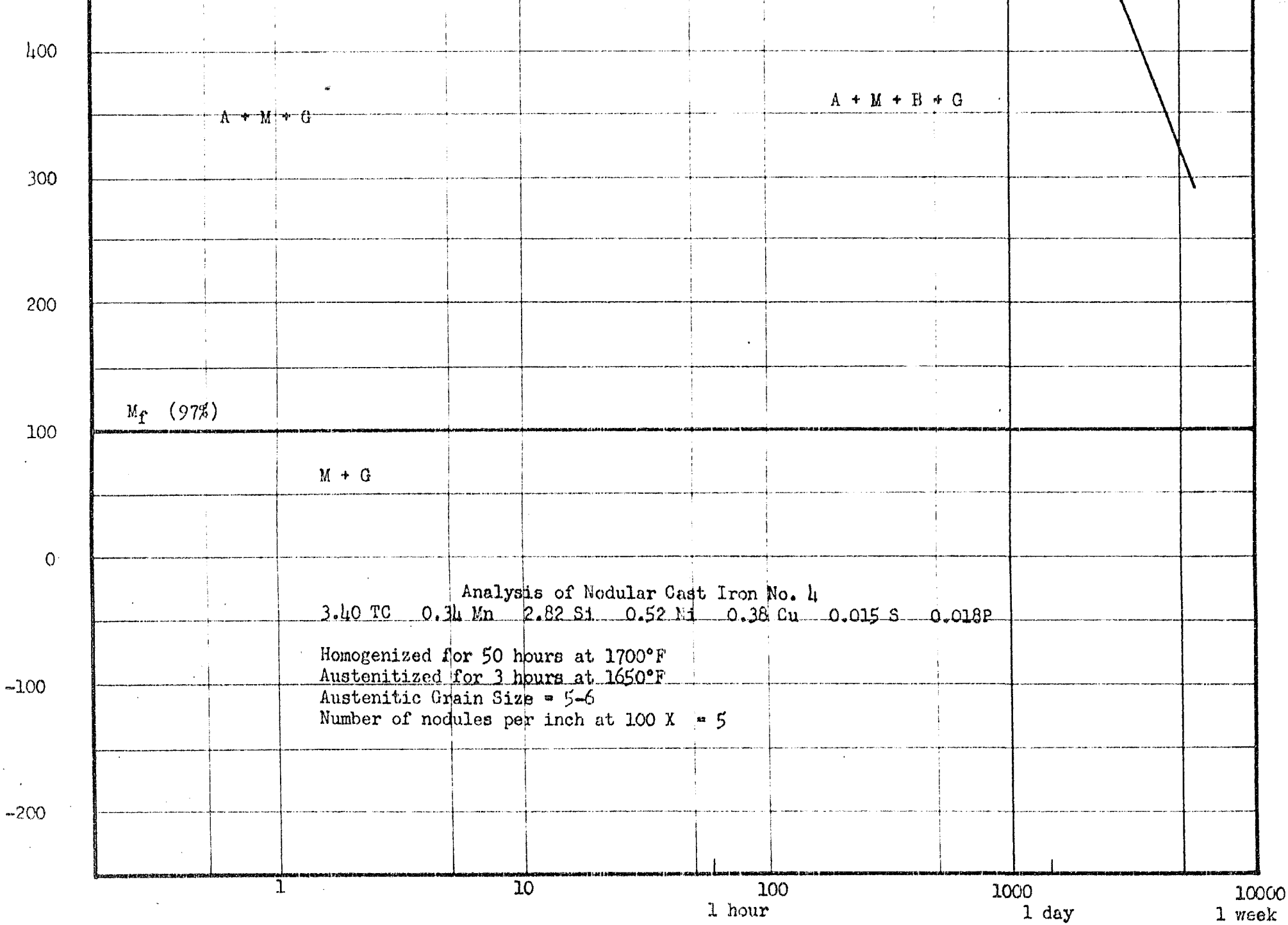


Fig. 27

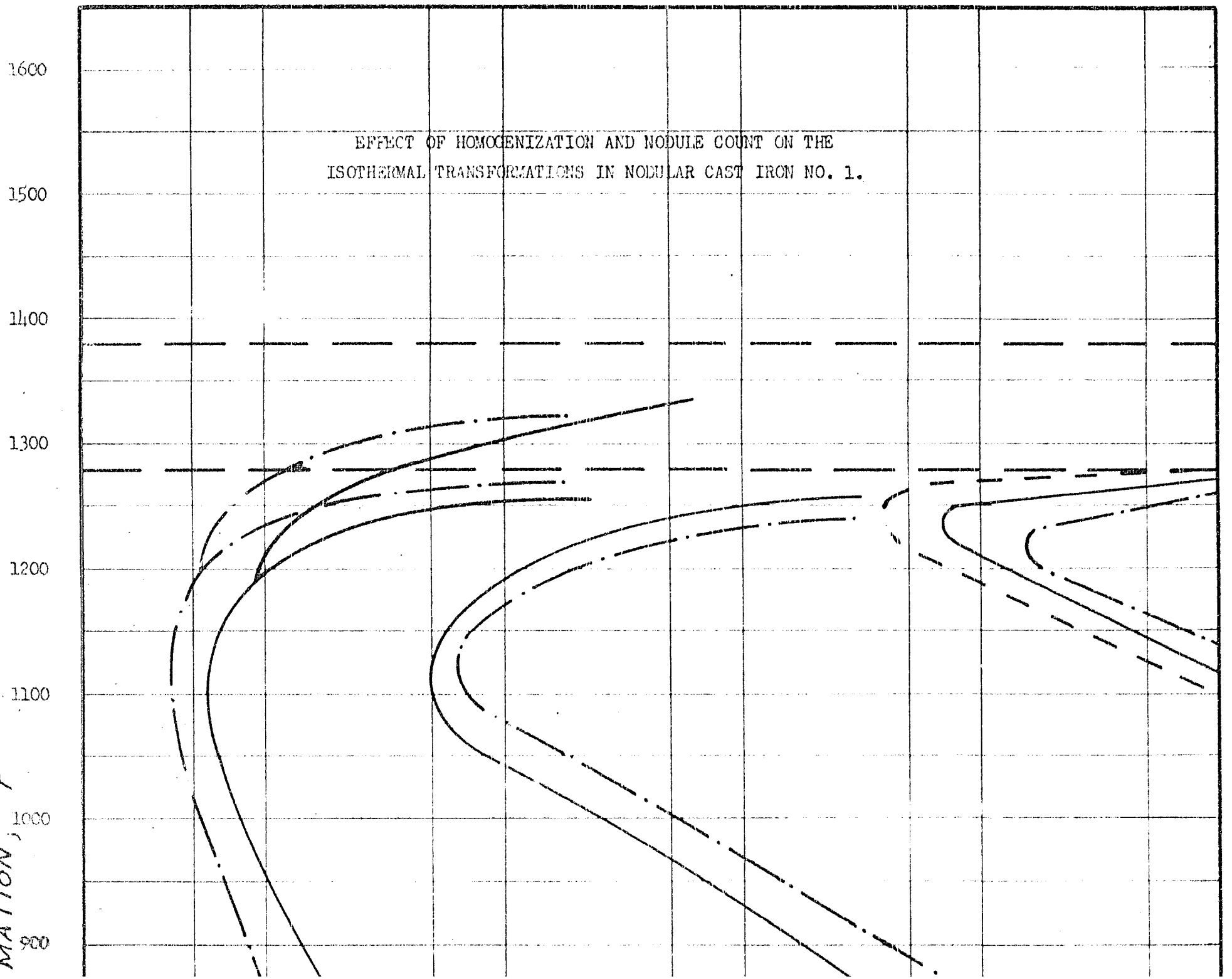

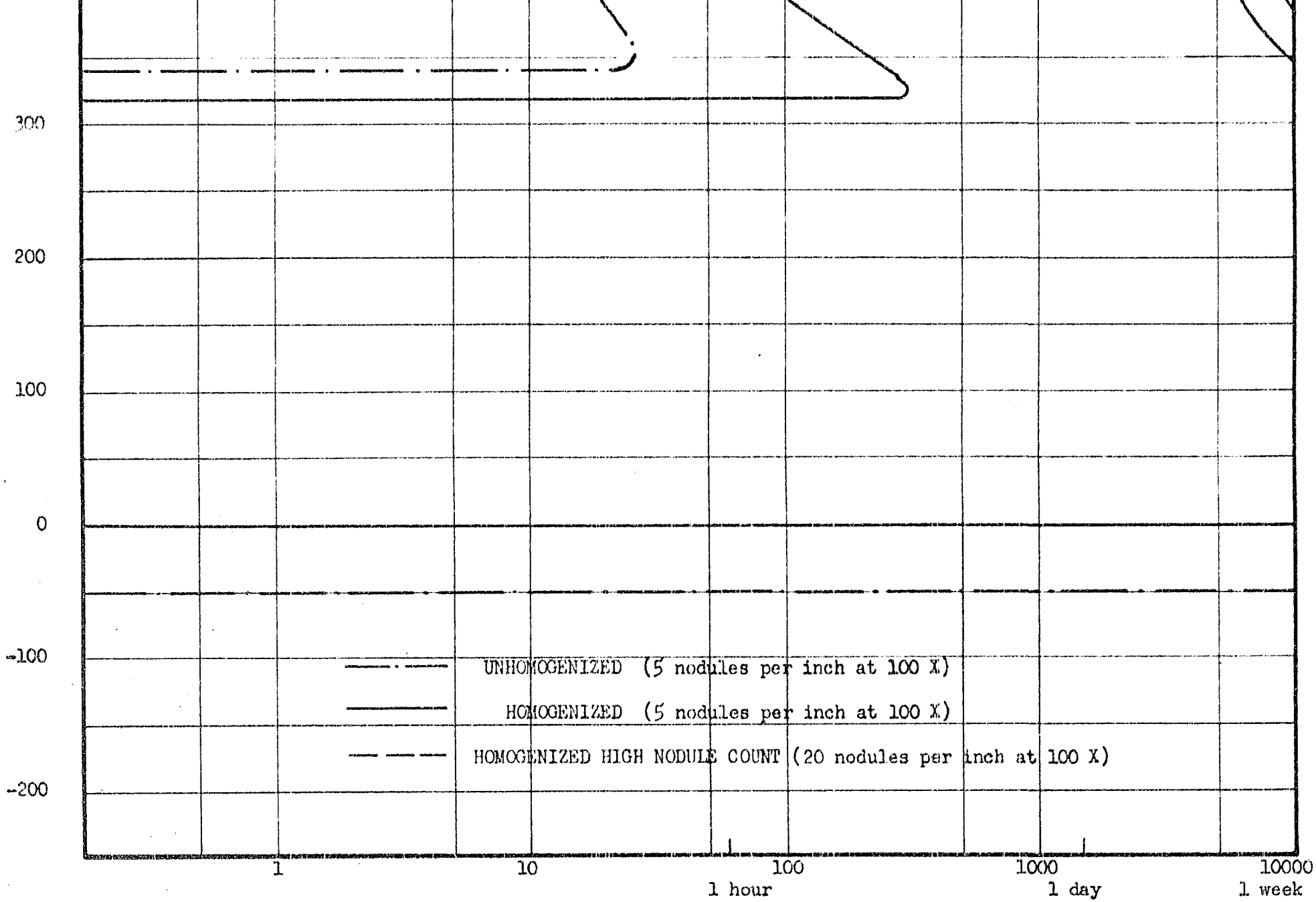


Fig. 28

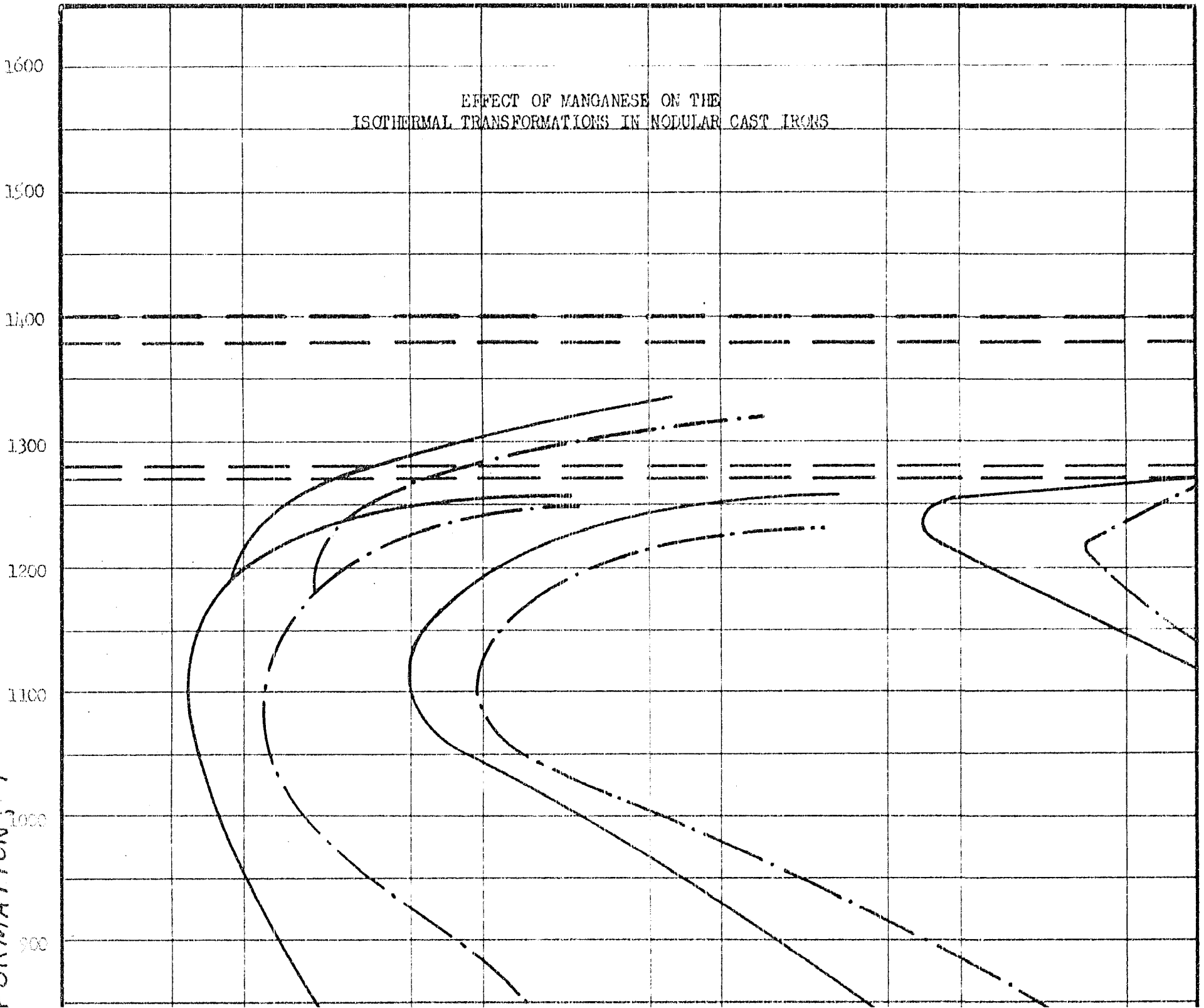

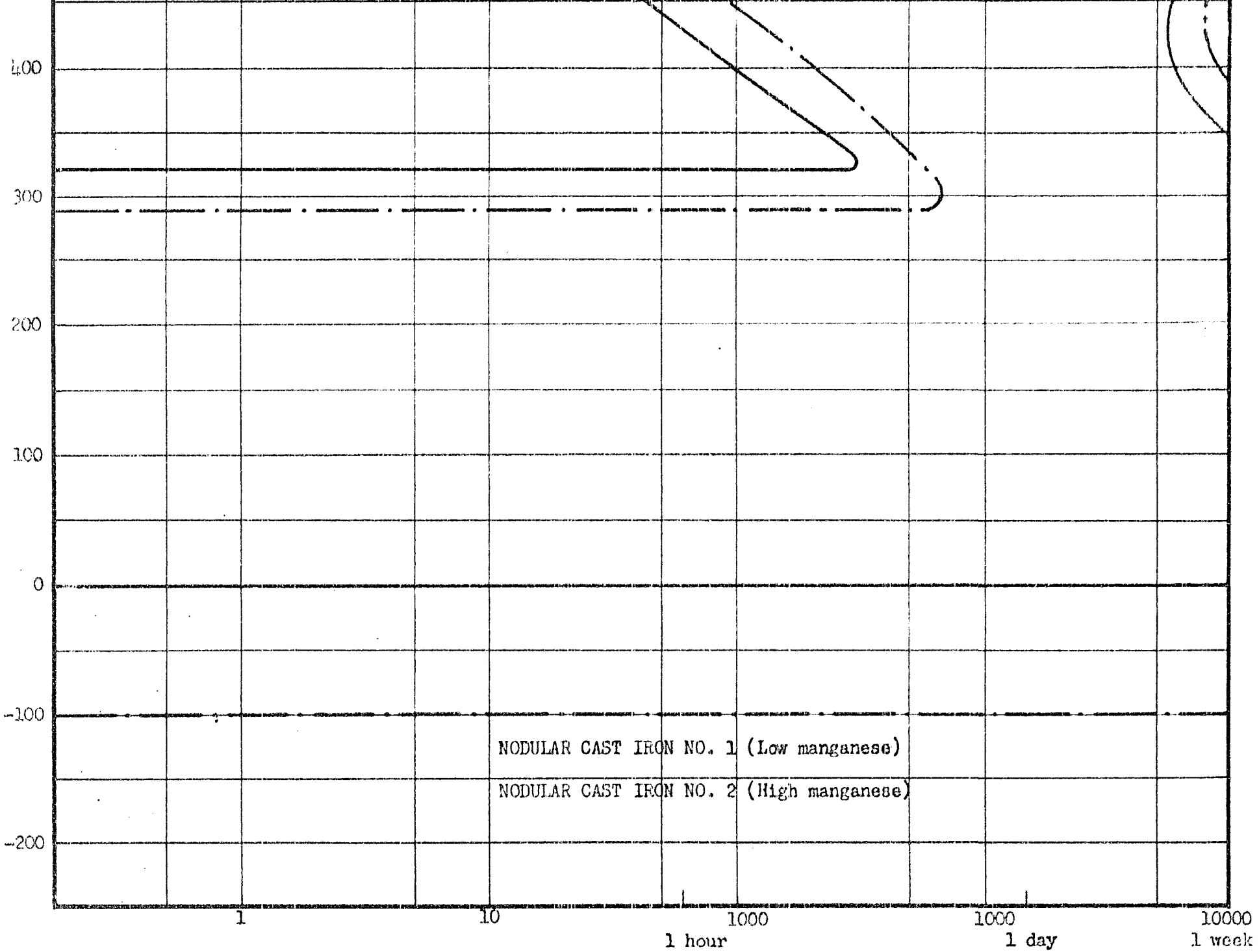


TRANSFORMATION TIME, MINUTES

Fig. 29

## DISCUSSION OF THE EXPERIMENTAL RESULTS

The major portion of the results from the sub-critical transformation experiments is presented in the form of T-T-T diagrams and graphs (Figures 24 to 35). The establishment of accurate T-T-T diagrams for nodular iron is rather difficult because of the inhomogeneities in cast iron. These inhomogeneities can be eliminated to some extent but not completely by a long heat treatment. The segregation of alloying elements and impurities which give rise to an inhomogeneous material is a direct result of the solidification of the cast iron. The segregation in nodular cast iron as stated in Part I of this thesis consists of interdendritic and cellular segregation. The interdendritic segregation is not too serious in nodular cast irons and is readily eliminated by heat treatment. However cellular segregation which usually outlines the cell boundaries is very persistant and is not eliminated completely even by long heat treatments, especially in alloy cast irons. The cellular segregation as was shown in Part I is formed during the so called "eutectic solidification" of nodular cast iron or during the formation and growth of the nodules. The last liquid which freezes in the cell boundaries contains a very large

amount of carbide stabilizers and impurities, and this liquid is responsible for the segregation. For this reason when an unhomogenized nodular cast iron is heat treated to produce ferrite and graphite, the ferrite forms in "shells" around the nodules and even in spherical zones which do not contain any graphite inside. Therefore some authors[17] have concluded that during the subcritical heat treatment the ferrite must start to form around the graphite nodule and grow as a shell of ferrite because graphite is deposited on the existing nodules and the austenite around the graphite nodule is depleted of its carbon content. Thus there is a carbon concentration gradient which is radially away from the nodule and the ferrite shell grows as more carbon is removed. Under this hypothesis the ferrite would always form around the graphite nodule. Brown and Hawkes[17] claim that the reaction of austenite to ferrite and graphite can be controlled so that the ferrite forms in concentric spherical shells around the nodules. This fact, they claim permits the measurement of growth of the ferrite shells as well as the rate of reaction. They measured the thickness of the ferrite shells as a function of time and derived an equation for the reaction. Using this equation and their experimental results obtained from thickness measurements of the ferrite shells they arrived at the conclusion that the reaction is diffusion controlled.

The author does not completely agree with the above theory because in the four nodular cast irons studied the ferrite did not form shells around the nodule as they claimed but formed in grain boundaires, slip planes and also at iron graphite interface, and the austenite to graphite plus ferrite reaction could not be controlled to give only shells around the graphite nodules. The author does agree that there is a carbon concentration gradient as described above and that in very low alloy (non alloy) and unhomogenized nodular cast irons the ferrite forms usually in shells around the nodule, but this is due to segregation of alloying elements and impurities rather than to the carbon concentration gradient alone. When nodular cast iron solidifies the austenitic shell that grows around the graphite is at first low in alloying elements and carbide stabilizers and as solidification progresses the carbide stabilizers are concentrated away from the nodule. Later when nodular iron is heat treated to produce ferrite and graphite the regions which contain low amount of alloying elements and carbide stabilizers form ferrite first, and these regions are usually around the graphite nodule. Thus the mode of formation of ferrite is also dependent on the segregation in nodular cast irons and not only on the concentration gradient of carbon.

The experiments show that nodular cast irons behave similarily to steels in their subcritical transformations except for a few exceptions. For example, although nodular cast irons have high carbon content, the first phase to come out at high temperatures is not carbide as in the case of hypereutectoid steels but ferrite as in hypoeutectoid steels. Also the reaction may go directly from austenite to ferrite plus graphite until all of the austenite is used up.

Ferrite may form directly from austenite without the formation of pearlite over a range of about 150° to 200°F but the range during which austenite may transform completely to ferrite and graphite without any formation of pearlite is quite small, about 25 to 50°F. There is another range at a little lower temperature where pearlite and ferrite form simultaneously from austenite. The experiments show that austenite may transform directly to ferrite and graphite but the experiments failed to establish whether new graphite nuclei were formed during the transformation. The observations seemed to indicate that very few, if any, new graphite particles were formed and the graphite was deposited on the old graphite nodules. This second layer of graphite sometimes was demarkated from the original nodule by a black thin line and usually this

second layer was less compact than the original graphite nodule. This gave the appearance of "duplex" nodules or nodules with shells or crowns of relatively uncompact graphite. It should be pointed out that not every nodule showed this effect, some were unchanged.

In the range of temperatures where pearlite and ferrite formed simultaneously from austenite, pearlite usually formed away from the nodules in segregated regions, that is in areas outlining cell boundaries which were mentioned previously. This supports the assumption that these areas contain more carbide stabilizers. Pearlite in these regions is very persistant and that is why the last 10-20% of pearlite takes much more time to decompose than the first 80%. The last traces of pearlite are always in the cell boundaries.

The reaction of austenite to ferrite plus graphite increases with decrease of temperature, until it is interrupted by the reaction of austenite to pearlite. The reaction of austenite to ferrite plus graphite is more rapid than the reaction of pearlite to ferrite plus graphite, provided the correct temperature for the reaction of austenite to ferrite plus graphite is selected. This temperature is the lowest temperature above which pearlite will not form, or the temperature at which only a trace of pearlite forms. This

temperature is approximately 125° to 175°F above the nose of the "S" curve. Thus the T-T-T diagram is very useful in selecting this temperature. This temperature is in the vicinity of the intersection of the two curves which are labelled "end of graphitization of austenite" and "end of graphitization of pearlite" on the T-T-T diagrams (Figures 24-27). Another interesting phenomenon that occurs in isothermal transformation of alloy nodular cast irons, is the appearance of needles of ferrite just below the nose of the "S" curve. This needle-like ferrite amounts to about 10-15% in the molybdenum-nickel iron (No. 3) and about 5% in the nickel-manganese iron (No. 2). This phenomena is illustrated by photomicrographs in Figures 52, 65, 66, and 67. Generally speaking the microstructures of the steel matrix of the nodular irons which were studied in this thesis are similar to alloy steels such as 4140 etc. These microstructures will be discussed in more detail later.

The effect of homogenization on the isothermal transformations in nodular cast irons is shown in Figure 28. In less homogeneous cast iron the beginning of the transformation curve is shifted to the left (shorter time) and the end of transformation, especially in the bainitic regions, is shifted to the right (longer time). The end

of graphitization curves, namely the "end of graphitization of austenite" and the "end of graphitization of pearlite" are both shifted to the right (longer time).

The effect of "nodular count" (number of nodules per square inch at 100 magnification) is illustrated in Figure 28. The nodule count does not affect the transformation of austenite to pearlite and bainite appreciably, although bainite has a tendency to form near the nodules at the beginning, and therefore the beginning of bainite may be shifted to the left slightly. This shift, however, is small and may be neglected. Therefore it may be stated that the "S" curve is essentially unchanged by nodule count. Nodule count, however does influence the rate of graphitization of both austenite and pearlite. The end of graphitization of austenite and the end of graphitization of pearlite are both shifted to the left (shorter time) with a higher nodule count. The shift is not too great, and the shift due to the alloying elements is more important.

The effect of alloying elements has a profound effect on the beginning and end of transformation and also on the rate of graphitization. For example cast iron No. 4 which has 0.7% more silicon and about 3.2% less nickel than cast iron No. 1 shows a great shift of the "S" curve to the

left, higher $M_s$ and $M_f$ temperatures and an upward shift of the whole "S" curve, approximately 100° to 150°F. The nose of the "S" curve is shifted 100°F higher, the $M_s$ is 150°F higher, and the critical temperatures (upper and lower eutectoid temperatures) are each 150°F higher. This upward shift, which is due to higher silicon and lower nickel contents, has a profound effect on the rate of ferritization. The rate of graphitization is affected in two ways. 1) Graphitization may take place at higher temperatures (150°F higher) which gives greater diffusion and therefore greater graphitization rates. 2) The stability or persistance of austenite and carbide is affected by the alloying elements of silicon and nickel. Looking at the two T-T-T diagrams it is noticed that the curve representing the end of graphitization of pearlite is not changed appreciably and is shifted to the left only slightly while the curve representing the end of graphitization of austenite is shifted 140°F upward thus causing the intersection of the two curves at short time values. Because of the intersection of the two curves at short times, the complete graphitization of No. 4 is more rapid than of No. 1 since the best temperature for graphitization is in the vicinity of the intersection of the two curves. Thus any alloying element which lowers the end of the pearlite graphitization

curve and raises the end of the graphitization of austenite curve, will increase the rate of graphitization in cast iron.

Manganese as shown in Figures 25 and 29 shifts the "S" curve to the right (longer times), lowers the critical temperatures and lowers $M_s$ and $M_f$ temperatures. It also lowers the curve for the end of graphitization of austenite and raises the end of graphitization of pearlite curve. Both of these effects decrease the rate of graphitization. Thus by decreasing the manganese content by 0.30% the graphitization rate is increased by 4 times and the transformation of austenite to pearlite by 2 times.

Molybdenum has a profound effect on the isothermal transformations in nodular cast iron and its effects are illustrated in Figure 26 and photomicrographs (Figures 56 to 72). Molybdenum shifts the pearlite curve, both for the beginning and end of transformation, to the right. The beginning of pearlite transformation is more than ten times longer for one percent of molybdenum while the end of pearlite transformation is about 200 times longer. The start of ferrite curve is also shifted to the right but to a small extent, and this results in the nose of the ferrite curve being more to the left then the nose of the pearlite curve. The micro structure of the pearlite is also different and

will be discussed later. Molybdenum has the greatest effect on the transformation rate of the "intermediate product" or bainite which form at higher temperatures and which is sometimes called constituent "X". This product is described under section on microstructures. The start of constituent "X" is retarded about 300 times for one percent of molybdenum and the end is not known but at the end of one week at temperatures of 900°F and 800°F only about 15-20% of constituent "X" is formed. Another phenomenon that occurs at these temperatures is the formation of needles of ferrite. These needles begin to form before constituent "X" and at the end of a week amount to about 15% or about one half of the transformation products. The acicular bainite curve is shifted very little to the right. An addition of one percent of molybdenum increase the time for the beginning of the acicular bainite by four times. This product forms quite readily at temperatures between 400°F and 550°F because at these temperatures the end is only slightly shifted to the right. The critical temperatures and the $M_s$ temperature are not affected appreciably by one percent of molybdenum and remain essentially the same. The martensite finish ($M_f$) temperature is lowered, however by about 200°F in the alloy studied. The high temperature pearlite is not composed of

nice coarse lamellar pearlite, but consists of a matrix of ferrite with short and widely separated carbide particles. Also the reaction of austenite to ferrite plus graphite does not occur as in previous alloys because the ferrite that is formed in this alloy has small particles of carbide distributed within it, resulting in a staining of the ferrite on etching. Thus at no temperature does cast iron No 3 (nickel-molybdenum) give pure clean ferrite as do the other three alloys. For this reason the curves denoting the end of graphitization are dotted instead of solid lines. This is to differentiate the more or less impure ferrite which has some very stable spheroidal carbides of molybdenum from the rather clean ferrite grains without any precipitated carbides in the other cast irons. Cast iron No. 3 had some complex carbides in the cell boundaries in the as cast condition and this carbide could not be completely eliminated even after four days at 1800°F. The other cast irons No. 1, No. 2 and No. 3, had no massive carbides in the cast condition. The nodule count was the same for all cast irons and at 100 magnification there were 5 nodules per square inch.

Several typical reaction curves are shown in Figures 30, 31, 32 and 33 for the four alloys in this investigation. Generally speaking the reaction curves in these figures are typical isothermal reaction curves for a

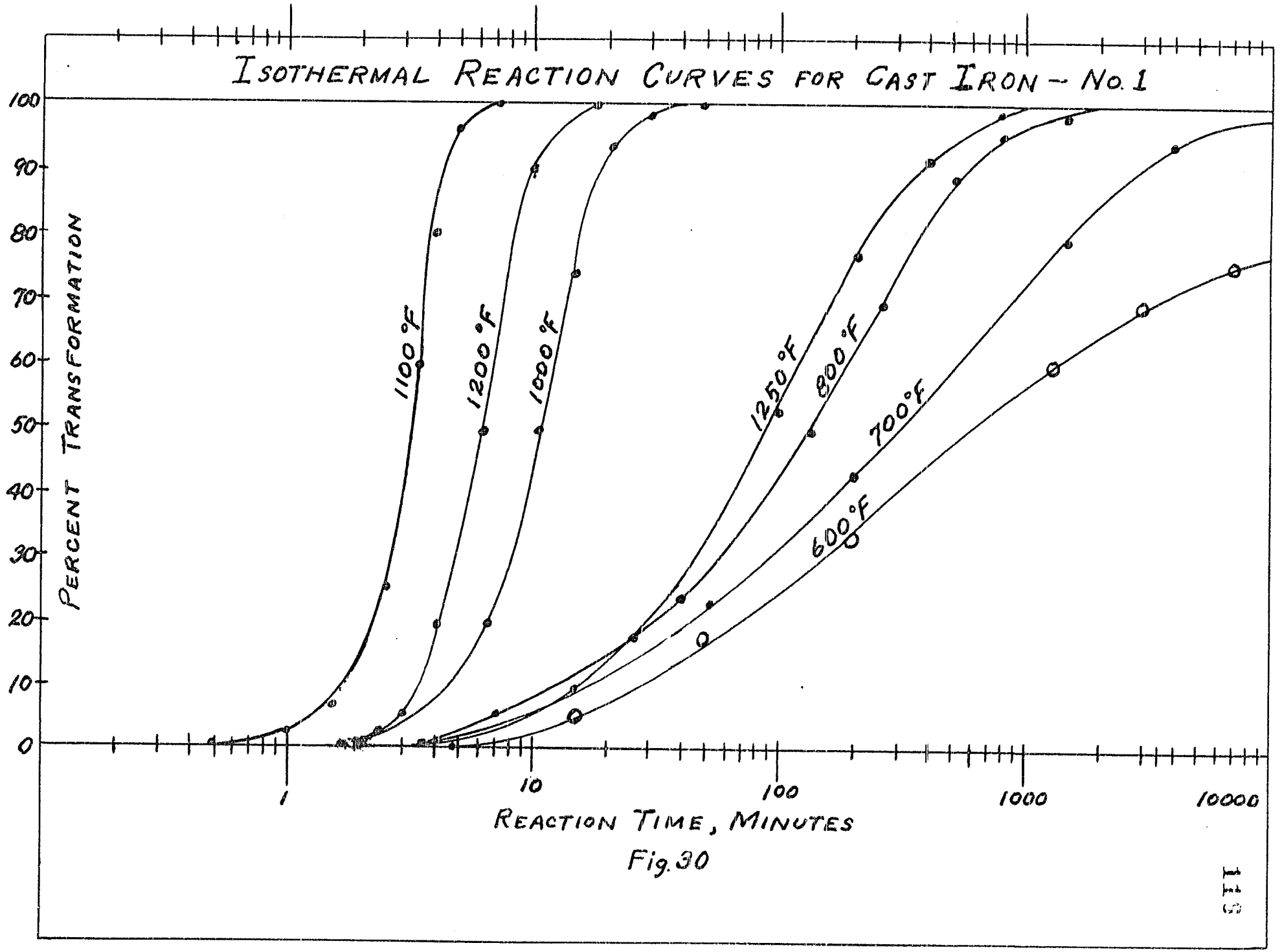


Fig. 30

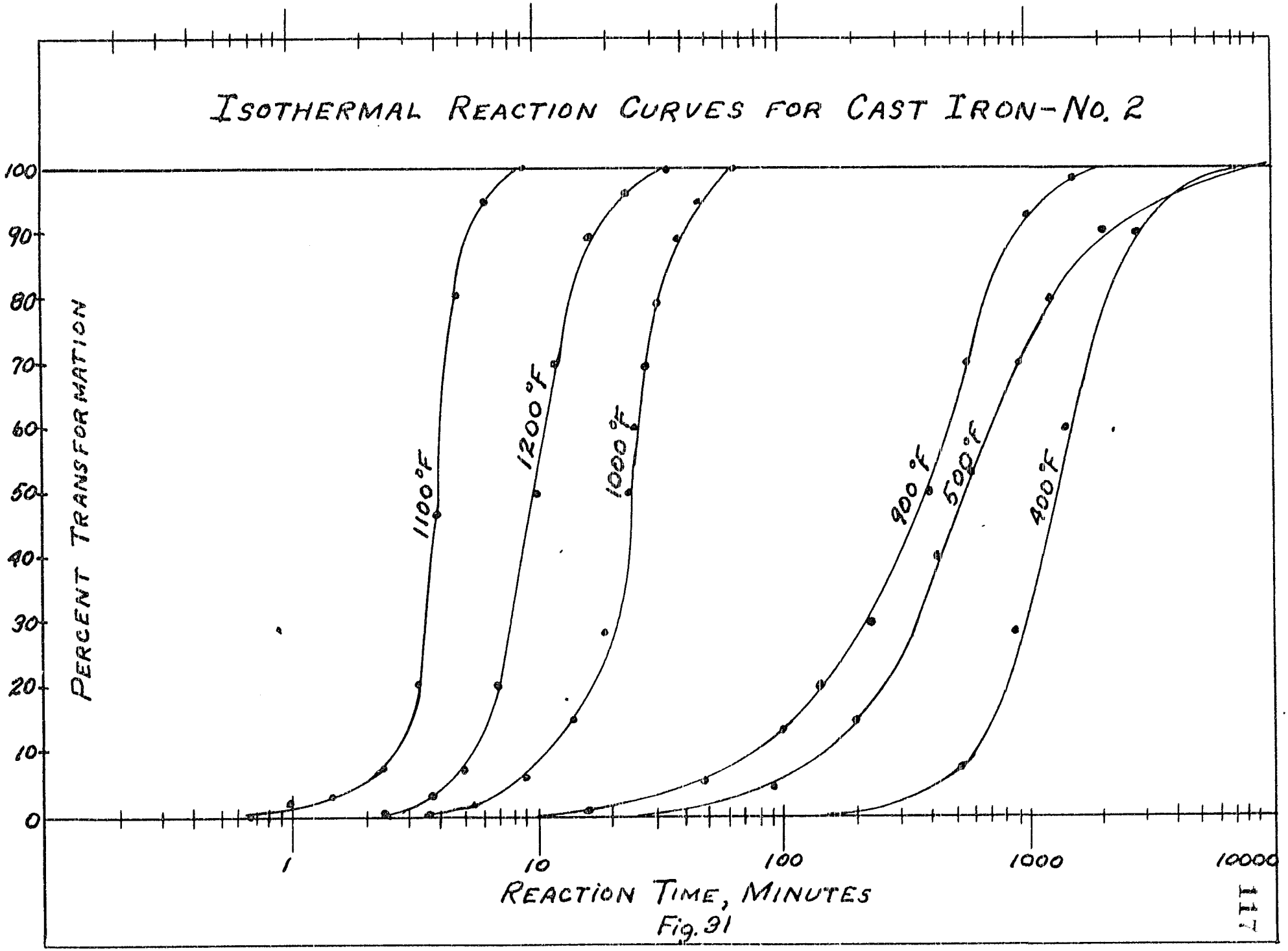


Fig. 31

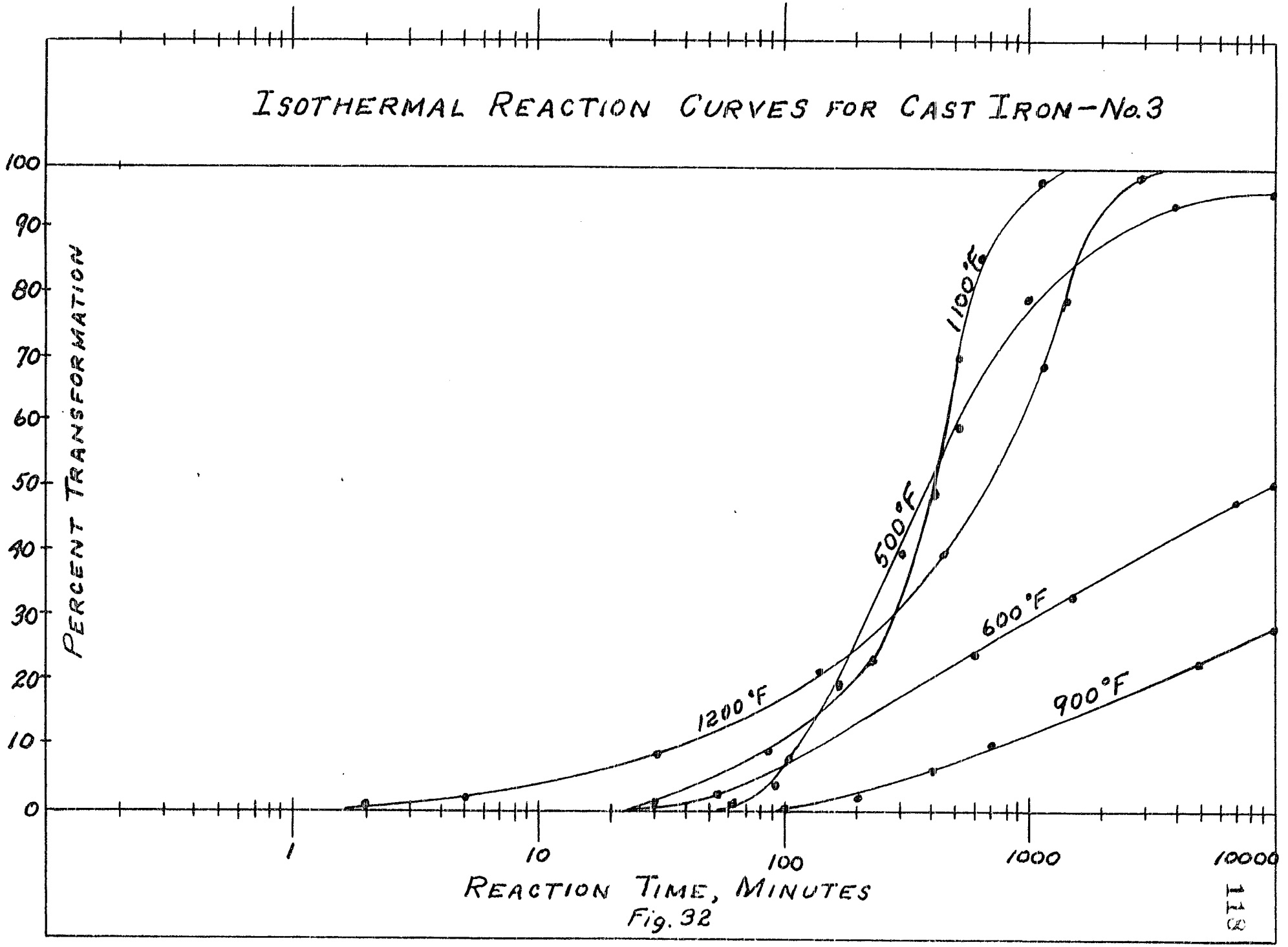


Fig. 32

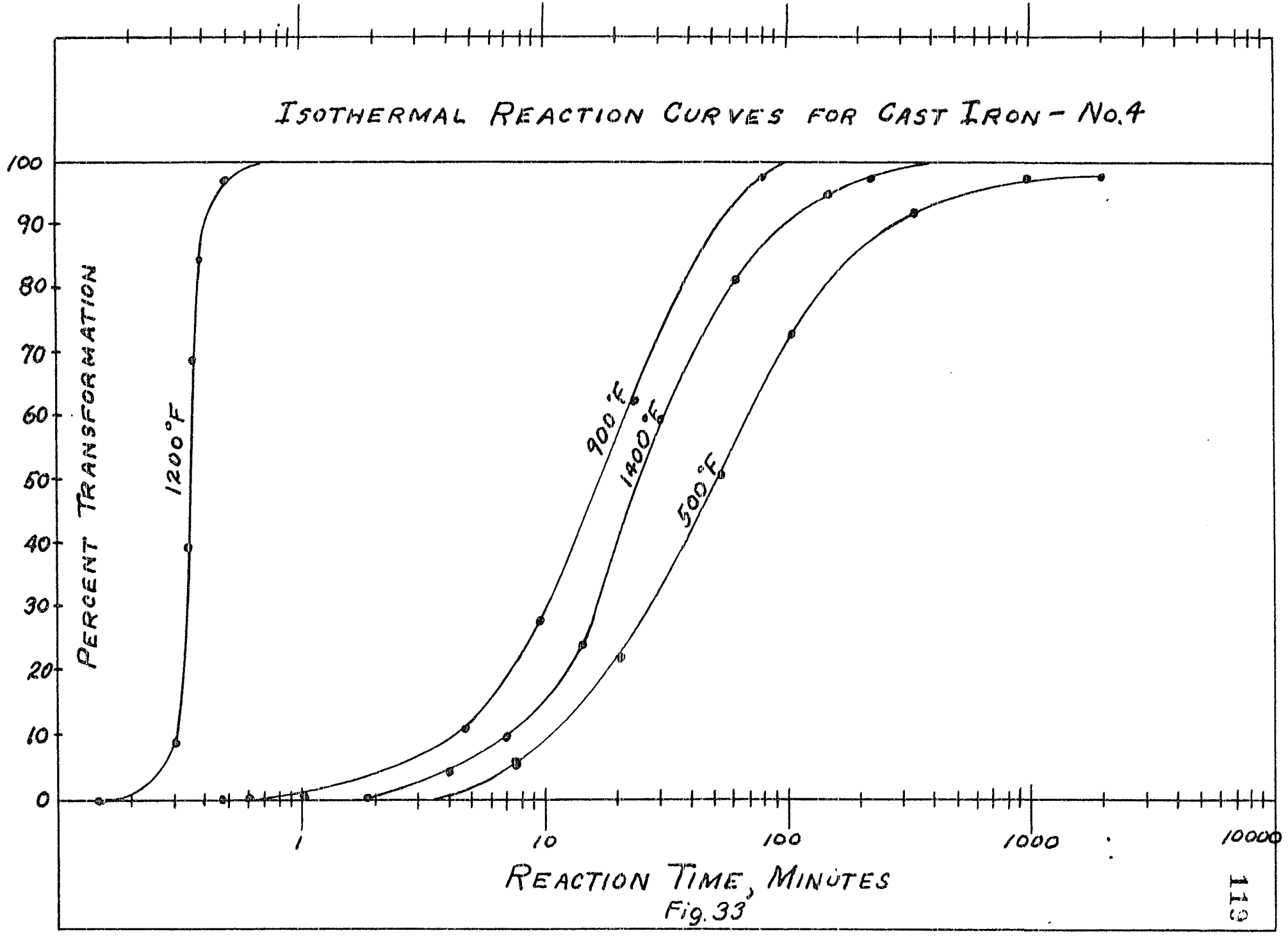


Fig. 33

nucleation and growth process. The shape of the curves for the cast irons No. 1 and No. 2 are identical for all temperatures except that the corresponding reaction curves in the cast iron No. 2 are shifted to the right (longer times). At 1100°F the slope of the reaction curve for the cast irons No. 1 and No. 2 is quite high and the reaction goes to completion in a short time. The slope of the reaction curves is lower above 1100°F and below 1100°F as shown in Figures 30 and 31. The slope of the curves below 1100°F becomes lower with lower temperatures until 500°F where the slope increases considerably and is much higher than for 600°F (Figures 30 and 31). The slope for 400°F is only slightly higher than for 500°F (Figure 31). Below 400°F the slope of the reaction curves again becomes lower as the temperature drops.

The reaction curves for the cast iron No. 3 are all shifted to the right as would be expected from the T-T-T curve for that alloy (Figure 26). The curve for the 1100°F has also the highest slope (Figure 32). Below 1100°F the slope of the curve drops drastically and is lowest for the transformations at 900°F, 800°F, and 700°F (Figure 32). Below 700°F the slope of the curves rises and becomes quite high for 500°F and 400°F (Figure 32). Below 400°F the slope again drops as the temperature drops.

Generally speaking the slopes of the reaction curves for the cast iron No. 4 are higher than for the previous three alloys. In the cast iron No. 4 the highest slope occurs at 1200°F which is the nose of the "S" curve. Below and above 1200°F the slopes become lower Figure 33. In the four cast irons studied in this investigation the highest slope of a reaction curve occurs for the transformation at the nose of the "S" curve.

Curves in Figure 34 show the amount of martensite formed at a given temperature for the four alloys studied in this investigation. As can be seen all four curves are similar in form. They differ only slightly in slope and this difference is greater near the end of transformation or after 75% of transformation. There is less martensite formed per given drop of temperature at the beginning until about 10-15% of martensite. Very little martensite is formed for a given drop of temperature after 90-95% of transformation (Figure 34) and the curves approach 100% transformation assymptotically. This is especially evident in the cast iron No. 3. The temperature interval between the martensite start and martensite finish varies but the range for the four alloys is between 350° to 500°F.

Hardness measurements were taken of all isothermally transformed structures just after the end of transformation.

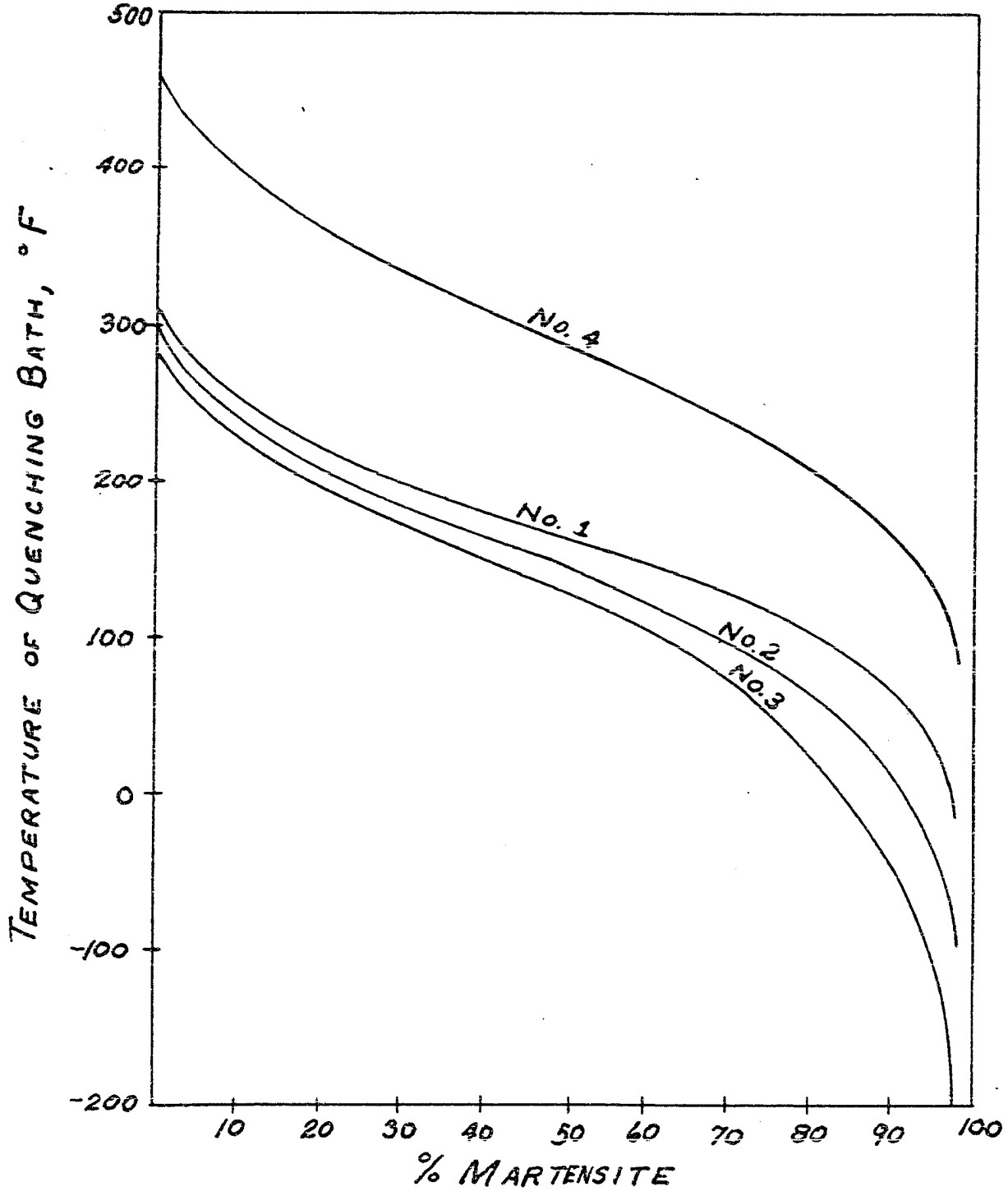


TRANSFORMATION OF
AUSTENITE TO MARTENSITE

Fig. 34

Rockwell "C" and "B" hardness numbers for completely transformed structures at 100°F intervals are given in (Table I) together with the corresponding temperature of the isothermal transformation. These tables show the hardness of the structure which forms at that particular temperature on the completion of transformation. In order to show the difference between the overall hardness of nodular cast irons and the hardness of the steel matrix in cast iron, Knoop hardness measurements were taken of the steel matrix on a Tukon tester using a load of one kilogram. Nodular cast iron No. 4 was selected for this test because completely transformed structures were available for all temperatures of transformation. The results of this test are given in Table II together with the conversion of the Knoop numbers to Rockwell numbers. The overall Rockwell hardness values for the same material are also given in the same table. The comparison of the hardness values of the matrix and the overall hardness values shows that the hardness of the matrix is higher by approximately six Rockwell numbers than the hardness of the nodular iron (overall hardness). The difference between the hardness of the steel matrix and the hardness of the nodular iron for various transformation temperatures is clearly illustrated by curves in Figure 35. The open circles give the overall hardness values of the

Table I

HARDNESS OF COMPLETELY TRANSFORMED STRUCTURES

| | Temperature of Transformation °F | ROCKWELL HARDNESS C.I. No. 1 | C.I. No. 2 | C.I. No. 3 | C.I. No. 4 |
|---|---|---|---|---|---|
| | 0 | 58 RC | 57 RC | 57 RC | 60 RC |
| | 100 | 58 RC | | | 60 RC |
| | 200 | | | | 57 RC |
| | 300 | | | | 52 RC |
| | 350 | 50 RC | | | |
| | 400 | 49 RC | 49 RC | 49 RC | 51 RC |
| | 500 | 47 RC | 47 RC | 46 RC | 49 RC |
| | 600 | | | | 42 RC |
| | 700 | 33 RC | 34 RC | | 34 RC |
| | 800 | 30 RC | 32 RC | | 31 RC |
| | 900 | 29 RC | 33 RC | | 26 RC |
| | 1000 | 28 RC | 31 RC | 27 RC | 24 RC |
| Pearlite | 1100 | 30 RC | 32 RC | 25 RC | 30 RC |
| Ferrite | 1100 | 93 RB | 97 RB | 96 RB | 86 RB |
| Pearlite & Ferrite | 1200 | 25 RC | 28 RC | | 31 RC |
| Ferrite | 1200 | 90 RB | 91 RB | 92 RB | 83 RB |
| | 1225 | 87 RB | 88 RB | 90 RB | |
| | 1250 | 87 RB | 90 RB | 91 RB | |
| Pearlite | 1300 | | | | 29 RC |
| Ferrite | 1300 | | | | 82 RB |
| | 1350 | | | | 86 RB |
| | 1400 | | | | 88 RB |

TABLE II

COMPARISON OF THE OVERALL HARDNESS WITH THE HARDNESS OF THE MATRIX FOR CAST IRON No. 4.

| Temperature of Transformation, °F. | Hardness of the Matrix, Knoop Nos. | Overall Hardness, Knoop Nos. (Converted from Rockwell Nos. to Knoop Nos.). |
|---|---|---|
| 100 | 850 | 732 |
| 300 | 700 | 576 |
| 400 | 680 | 558 |
| 500 | 630 | 526 |
| 600 | 510 | 438 |
| 700 | 425 | 342 |
| 800 | 370 | 318 |
| 900 | 320 | 284 |
| 1,000 | 295 | 266 |
| 1,100 pearlite | 350 | 304 |
| 1,100 ferrite | 215 | 184 |
| 1,200 pearlite | 375 | 326 |
| 1,200 ferrite | 190 | 173 |
| 1,300 pearlite | 350 | 304 |
| 1,300 ferrite | 185 | 170 |
| 1,350 | 210 | 184 |
| 1400 | 220 | 192 |

nodular iron, while the closed circles give the hardness values of the matrix. The dotted curves give the hardness values of ferritic structures between 1100°F and 1400°F. As can be seen from this graph the ferrite formed at 1400°F and 1100°F is slightly harder than the ferrite formed at 1300°F and 1200°F. Another rather striking observation is that the products formed just below the nose of the "S" curve are softer than the fine pearlite formed at the nose of the "S" curve. The nose for this "S" curve is 1200°F and the products formed at 1100°F, 1000°F and 900°F are all softer while those formed at 800°F have about the same hardness as the fine pearlite formed at 1200°F. The softest products are formed at 1000°F. This behavior is different than in plain carbon steels where the transformation productsbelow the nose of the "S" curve are always harder than fine pearlite formed at the nose. The microstructure for the transformation products formed at 1000°F shows that the structure consists of a light etching material which is called constituent "X" in this thesis and is described in more detail in the next section under the microstructure. This structure is a transition structure between pearlite which forms atahigher temperature and acicular bainite which forms atalower temperature and which readily etches dark.

The graphs in Figure 35 help to explain the phenomenon that often nodular cast irons when observed under the

HARDNESS OF COMPLETELY TRANSFORMED STRUCTURES vs TRANSFORMATION TEMPERATURE

CAST IRON No. 4

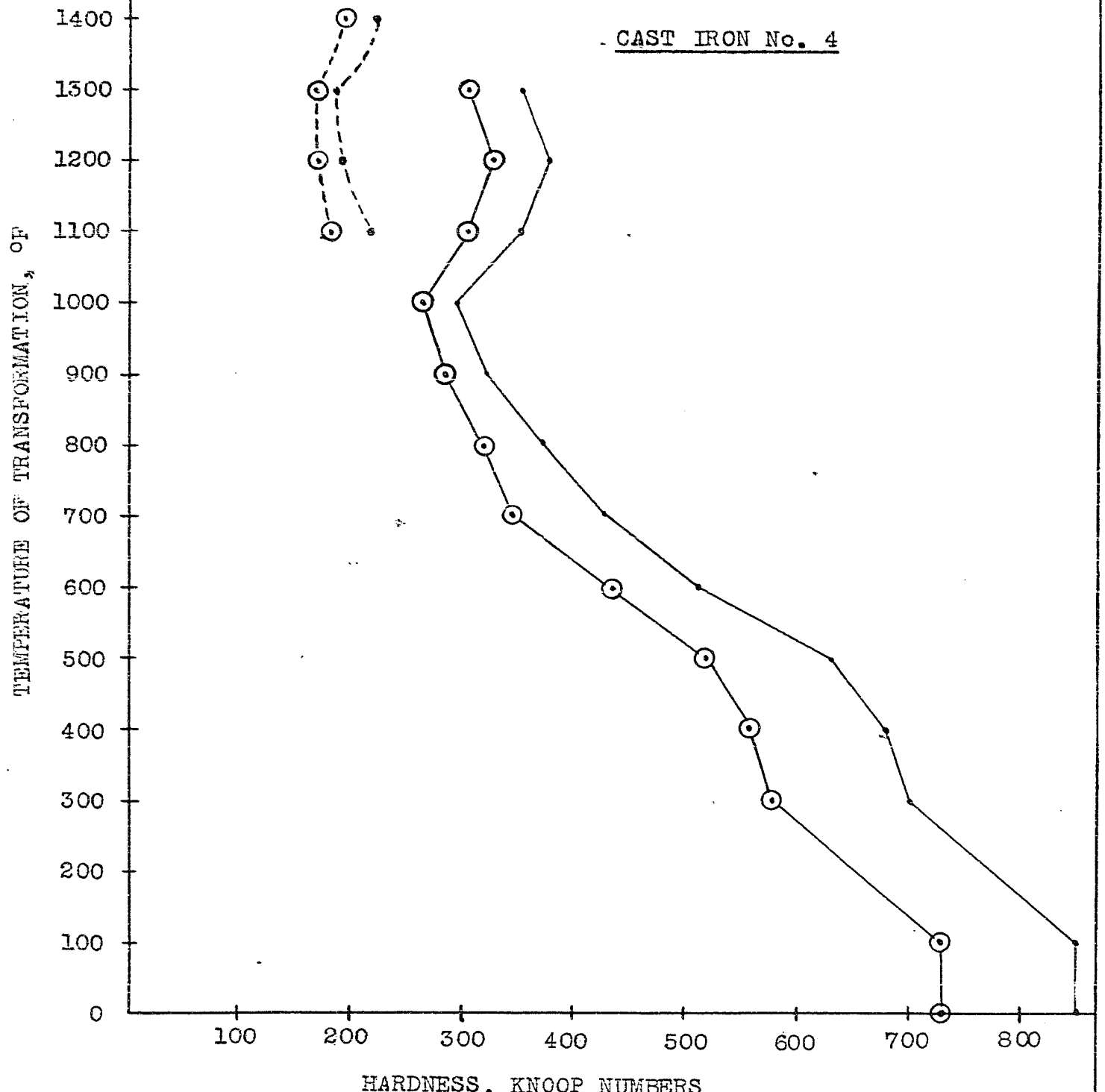


Fig. 35

microscope appear to be martensitic and yet give low hardness values which would indicate bainitic structures. This is due to the presence of graphite nodules which lowers the hardness. For example the Rockwell "C" hardness of completely martensitic nodular cast iron No. 4 is 60 RC while the hardness of the matrix of the same piece is 65 RC. Thus the steel matrix of martensitic nodular irons is about 5-6 RC units higher than the Rockwell hardness value of the same material.

## DISCUSSION OF THE MICROSTRUCTURES PRODUCED ISOTHERMALLY BELOW THE CRITICAL TEMPERATURE

The microstructures of the matrix in nodular cast iron differ from the microstructures of plain carbon steels in the region which separates the lamellar pearlite products from the acicular bainite products. This region is often called the "transition zone" between pearlite and bainite, and the transformation products produced in this zone are called "intermediate products", "transition products", "acicular ferrite" and "constituent X". The occurence of this structure is quite common in alloy steels and the above mentioned names for this structure are found in the literature on alloy steels. The nodular cast irons studied in this thesis are similar in microstructure to the alloy steels such as SAE-AISI grade 4140.

Generally speaking the microstructures of the four alloys studied appear as follows:

At high temperature, just below the critical, ferrite appears. This ferrite may be equiaxed ferrite formed in patches and/or around graphite nodules, grain boundary ferrite and widmanstätten ferrite. At lower temperatures coarse lamellar pearlite forms; the structure becomming

finer as the temperature is lowered until some temperature just below the nose of the T-T-T diagram. At this temperature another structure appears which is called constituent "X" in this thesis (Figs. 44, 54, 71 and 84). This structure occurs about 100°-200°F below the nose of the T-T-T diagram and it separates the lamellar products (pearlite) from acicular bainite. Constituent "X" is light etching structure which becomes speckled as more of it forms. At high magnefication the structure appears to consist of a white matrix with black dots and short dark lines and looks as if it were ferrite with precipitated carbides. The constituent "X" at first appears as rounded needles, light etching feathers or acicular in nature. At lower temperatures this structure becomes more feathery and gradually etches darker. It also becomes more speckled in appearance with the black dots becoming smaller and smaller as the temperature is lowered, until it no longer may be resolved by an ordinary microscope.

Just below the nose of the "S" curve clean white ferrite needles formed together with constituent "X" (Figure 69). These ferrite needles formed before constituent "X" in cast iron No. 3 (Figure 67) and amounted to about 15%. Cast iron No. 2 had some ferrite needles

present but not as much as No. 3. Nodular cast iron No. 1 had only a trace of needles and sometimes there were no needles at all.

As the constituent "X" became darker with lower temperatures it gradually blended into dark etching acicular bainite. This acicular bainite consists of feathers or coarse needles of dark etching structure. These needles or feathers are sometimes oriented along crystallographic planes (Figs. 45, 55, 72, 86, and 87). The coarse dark etching feathers or needles gradually turn to fine dark etching needles. At the $M_S$ temperature bainite consists of very fine, thin dark etching needles. Martensite needles which appear at the $M_S$ temperature are much coarser than bainite needles. The martensitic structure is the same as for steels (Figures 75 and 89) and need not be discussed here.

The microstructures as they appear at approximately 100°F temperature intervals for the four nodular cast irons studied in this investigation are presented below together with comments under each photomicrograph. The microstructures of cast irons No. 1 and No. 2 are the same for a given temperature and the only difference is in the percent of the transformation at a given time interval. Therefore in order to avoid duplication, the microstructures

of cast irons No. 1 and No. 2 are treated together.

Isothermal Transformations in Cast Irons No. 1 and No. 2

Ferrite starts forming at about 1350°F in the grain boundaries but the reaction does not go to completion until about 1270°F, and even at that temperature more than a week is necessary to get a completely ferritic structure. A typical microstructure is shown on Figure 36 in order to illustrate the formation of ferrite in the grain boundaries. At about 1250°F ferrite forms in the grain boundaries, around the graphite nodules and also along the slip planes (Figures 48 and 49). There is more tendency for the ferrite to form along the slip planes in No. 2 than in No. 1 (Figures 36, 37 and 48). Ferrite also forms more rapidly in No. 1 than in No. 2 (Figures 37 and 48). The grains of ferrite formed at 1250°F are equiaxed and show no substructure (Figure 39). At 1200°F the austenite is transformed mostly to coarse pearlite but some ferrite is formed directly especially in No. 1 (Figures 37 and 50). The grains of ferrite which are formed from the decomposition of pearlite show substructure and straining (Figure 40, 64 and 81). Ferrite formed at 1100°F by the decomposition of pearlite shows straining and substructure (Figure 40). The formation of fine pearlite at 1100°F and 1000°F is

illustrated in Figures 51 and 52. At 900°F both the constituent "X" and fine pearlite may form simultaneously. Pearlite forms in the grain boundaries and is dark, while constituent "X" is a light etching speckled structure (Figures 42 and 53). Constituent "X" which forms at 800°F and 700°F is illustrated in Figures 43, 44 and 54. At 600°F acicular or coarse feathery bainite is formed as shown in Figures 45 and 55. As the temperature is lowered the feathers become smaller until they look like fine needles. The microstructures for the acicular bainite formed at 500°F, 400°F, and 300°F are shown in Figures 46, 56, 47, and 57.

Isothermal Transformations in the Cast Iron No. 3.

Formation of ferrite begins at about 1350°F in the grain boundaries of austenite but the reaction does not go to completion until about 1275°F. The grain boundary formation of ferrite is shown in Figure 58. At 1250°F the ferrite that forms stains readily and contains many dispersed small spheroidal carbides. At 1250°F, 1225°F and 1200°F, ferrite and very coarse semi lamellar and spheroidal pearlite forms (Figures 59, 60 and 62). This semi lamellar pearlite is in turn spherodized and decomposed

and the ferrite formed at these temperatures stains readily and contains many fine spheroidal carbides (Figures 60 and 62). At 1100°F which is the nose of the T-T-T diagram, dark unresolvable pearlite forms in the grain boundaries and after some time this dark pearlite becomes surrounded by a white constituent which appears to be ferrite. This light constituent separates pearlite from the untransformed austenite (Figure 63). At the end of a week the structure is all ferrite which shows straining and is stained very easily on etching. The grain boundaries of this ferrite are not clearly revealed by etching (Figure 64). At 1000°F a white structure forms in the grain boundaries that looks like a "light etching pearlite" (Figure 65). It is not certain whether this white constituent that forms in the grain boundaries is a type of ferrite or pearlite. As more time is allowed for the transformation the structure changes and becomes similar to that formed at 1100°F. The structure for 5,000 minutes at 1000°F (Figure 66) shows pearlite (black), ferrite (white) and martensite (gray). The first phase to appear at 900°F consists of many needles of ferrite (Figure 67). This ferrite is different from the one formed at 1000°F and 1100°F. After the formation of these ferrite needles a light etching

constituent forms in the grain boundaries. This constituent darkens somewhat after prolonged etching. The transformation at this temperature is very slow and at the end of a week only about 15-20% of the austenite is transformed (Figure 68). The structure at 800°F consists of about 15% of large white needles of ferrite and about 15% of light etching constituent "X" (Figure 69). At 700°F the ferrite needles disappear and only constituent "X" forms. The formation of constituent "X" is very slow (Figures 70 and 71). The constituent "X" disappears at 600°F and a new phase which is dark etching feathery or acicular bainite appears (Figure 72). This phase forms much more rapidly than constituent "X". However its formation is not so rapid after about 30% of transformation. These feathers of bainite become finer as the temperature is lowered, until at 300°F they look like very fine black needles. This acicular bainite forms usually along crystallographic planes. The acicular bainite structures formed at 500°F, 400°F and 300°F are illustrated in Figures 73 and 74. The amount of martensite that forms at 200°F is illustrated in Figure 75.

Isothermal Transformations in the Cast Iron No. 4

Ferrite starts forming in the grain boundaries and around graphite nodules at about 1500°F. The reaction

goes to completion at about 1410°F. The ferrite forms directly from austenite. The ferrite grains are equiaxed, clean, and fairly large at higher temperatures. Figures 76, 77, and 78 illustrate the formation of ferrite at 1450°F, 1400°F and 1350°F respectively. Figure 77 shows clearly the formation of ferrite directly from the austenite together with the formation of nodules of coarse lamellar pearlite. At lower temperatures ferrite forms around nodules while at higher temperatures it forms preferentially along the grain boundaries. There is much more pearlite formed than ferrite at 1300°F. The ferrite is usually around graphite nodules. Figure 79 shows pearlite and martensite with a few grains of ferrite around the graphite nodules. The ferrite and martensite both are white in this picture. Figures 80 and 81 show the difference between the two types of ferrite formed at 1300°F and 1200°F respectively. As stated previously the ferrite formed at low temperatures shows straining and substructure (Figure 81) while the ferrite formed at higher temperaturesdoes not (Figures 76, 77, and 80). At 1300°F ferrite is equiaxed and without any substructure while at 1200°F it has a substructure. Figure 82 shows the formation of pearlite nodules at the nose of the T-T-T diagram (1200°F) and Figure 83 the formation of pearlite at 1100°F. At 1000°F the structure consists mostly

of light etching constituent "X" and some pearlite (dark), as shown in figure 84. The structure at 900°F is a transition structure between the constituent "X" and bainite. This structure shows both, characteristics of acicular bainite and constituent "X". It etches dark more easily than the constituent "X" but not as easily as acicular bainite. Figure 85 illustrates this transition structure. Structures at 800°F and 700°F consist of dark feathers of bainite. The feathers appear to be mostly oriented along crystallographic planes (Figures 86 and 87). At lower temperatures the feathers become finer until the structure consists of many small needles. This is illustrated on figures 87 and 88, which represent the structures of bainite formed at 700°F, and 500°F respectively. Figure 89 shows the amount of martensite that is formed at 200°F.

PHOTOMICROGRAPHS OF TRANSFORMATION STRUCTURES FOR THE CAST IRON NO. 1

The structures were obtained after austenitizing at 1650°F, quenching and holding at the temperatures and times indicated, and finally quenching in water. The specimens were etched with nital.

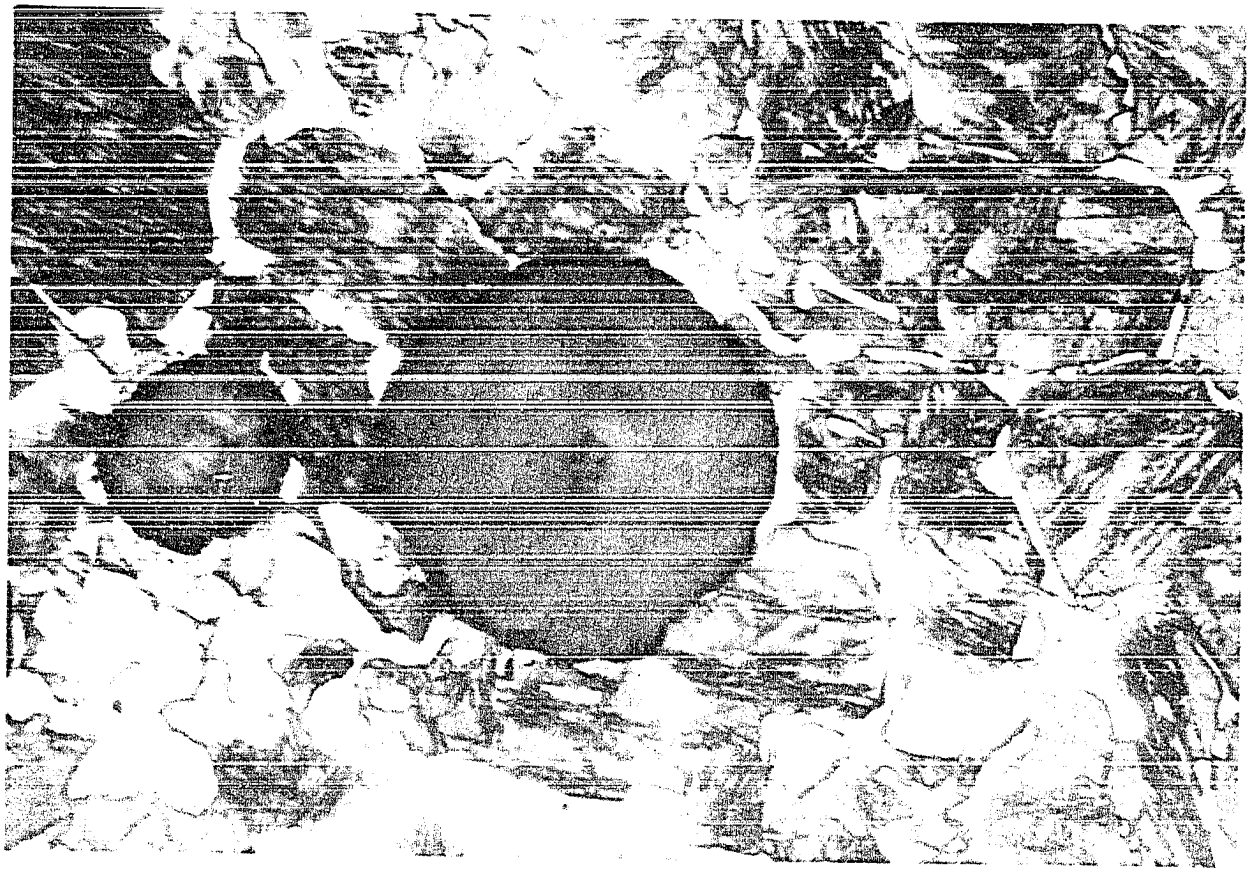

FIG. 36

Transformed at 1275°F for 600 minutes. Ferrite (white) and martensite (gray). 1000 X.

FIG. 37

Transformed at 1250°F for 100 minutes. Ferrite (white) and martensite (gray). 1000 X.

FIG. 38

Transformed at 1250°F for 1,000 minutes. Large and small ferrite grains. 1000 X.

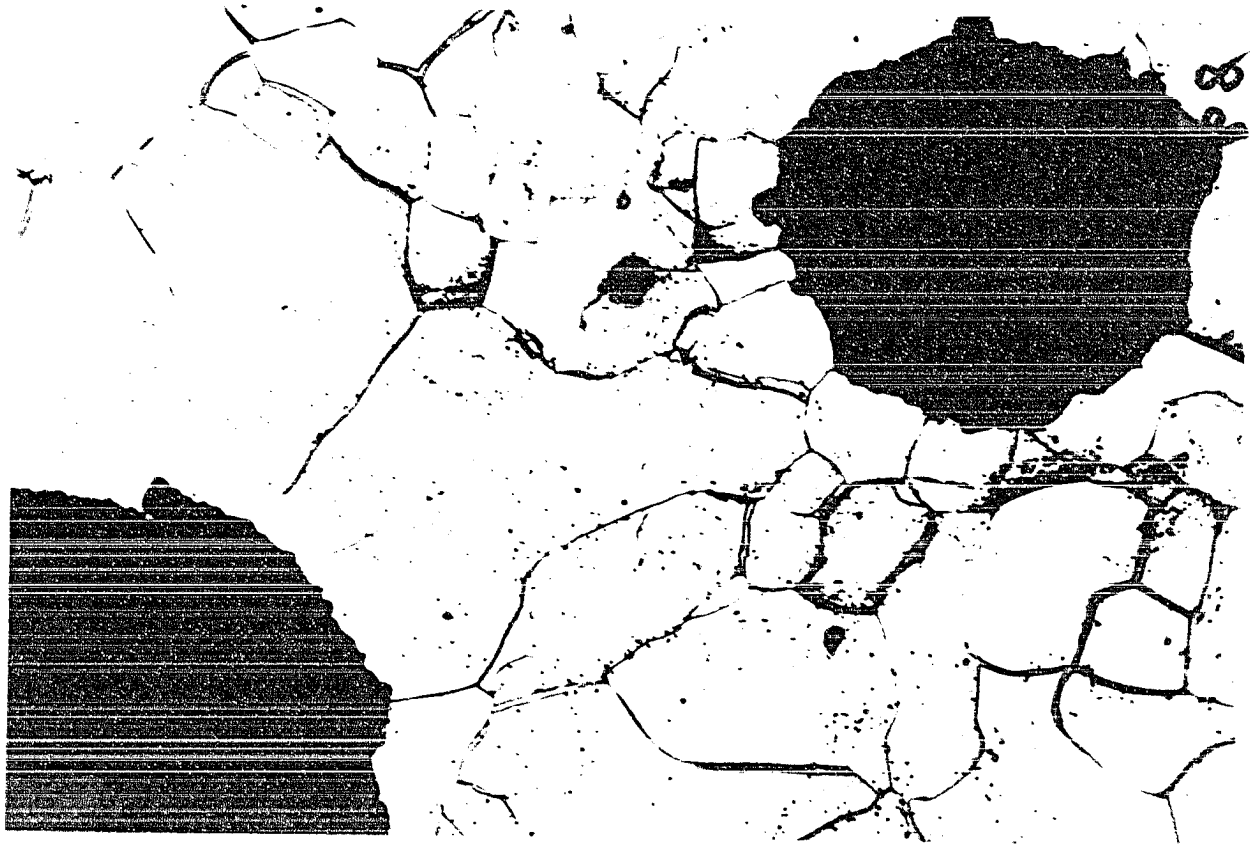

FIG. 39

Transformed at 1250°F for 10,000 minutes. Large unstrained ferrite grains. No substructure. Compare with Fig. 40. 1000 X.

FIG. 40

Transformed at 1100°F for 10,000 minutes (1 week). Small ferrite grains showing substructure and straining. 1000 X.

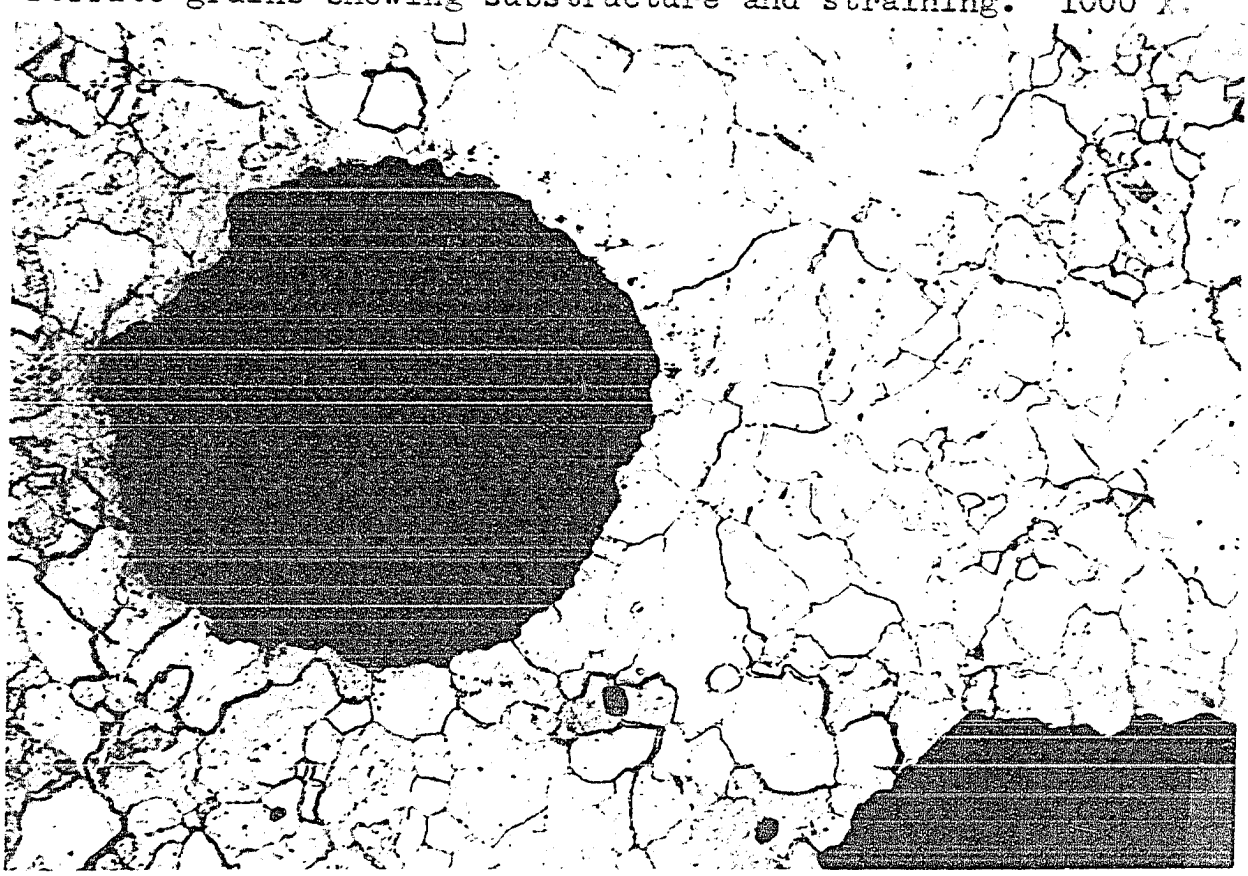

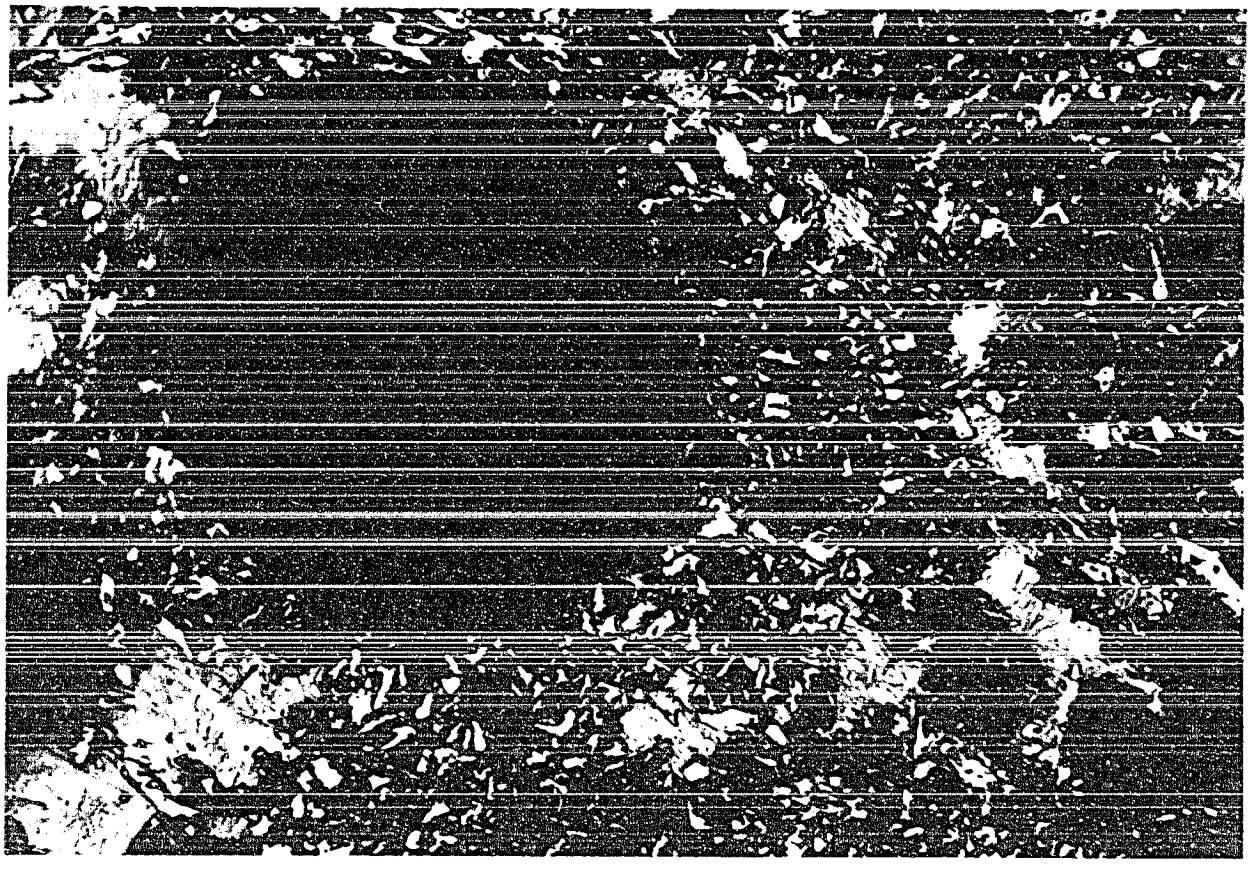

FIG. 41

Transformed at 1000°F for 15 minutes. Fine pearlite (dark) and martensite (gray). 1000 X.

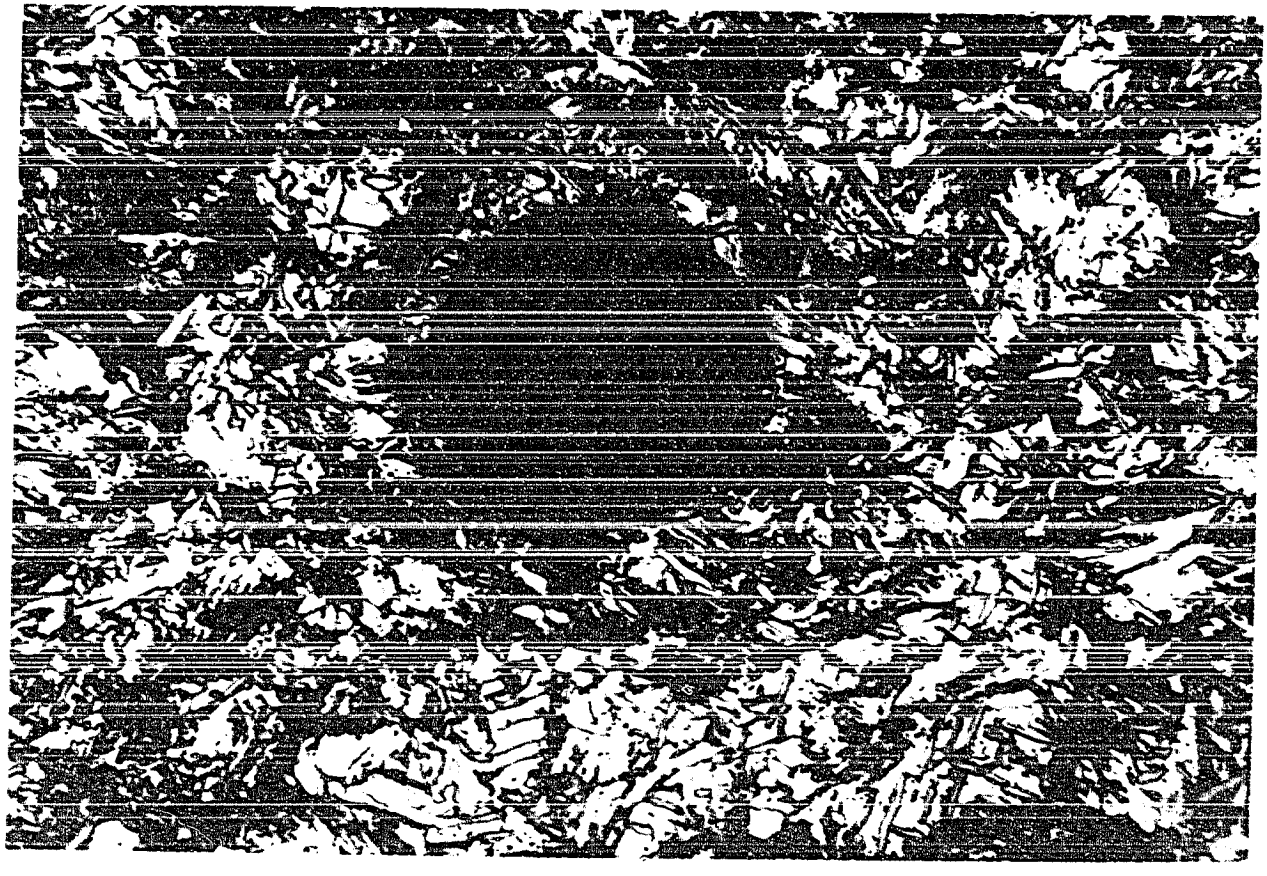

FIG. 42

Transformed at 900°F for 400 minutes. Fine pearlite (dark) in the grain boundaries and constituent "X" (speckled). 1000 X.

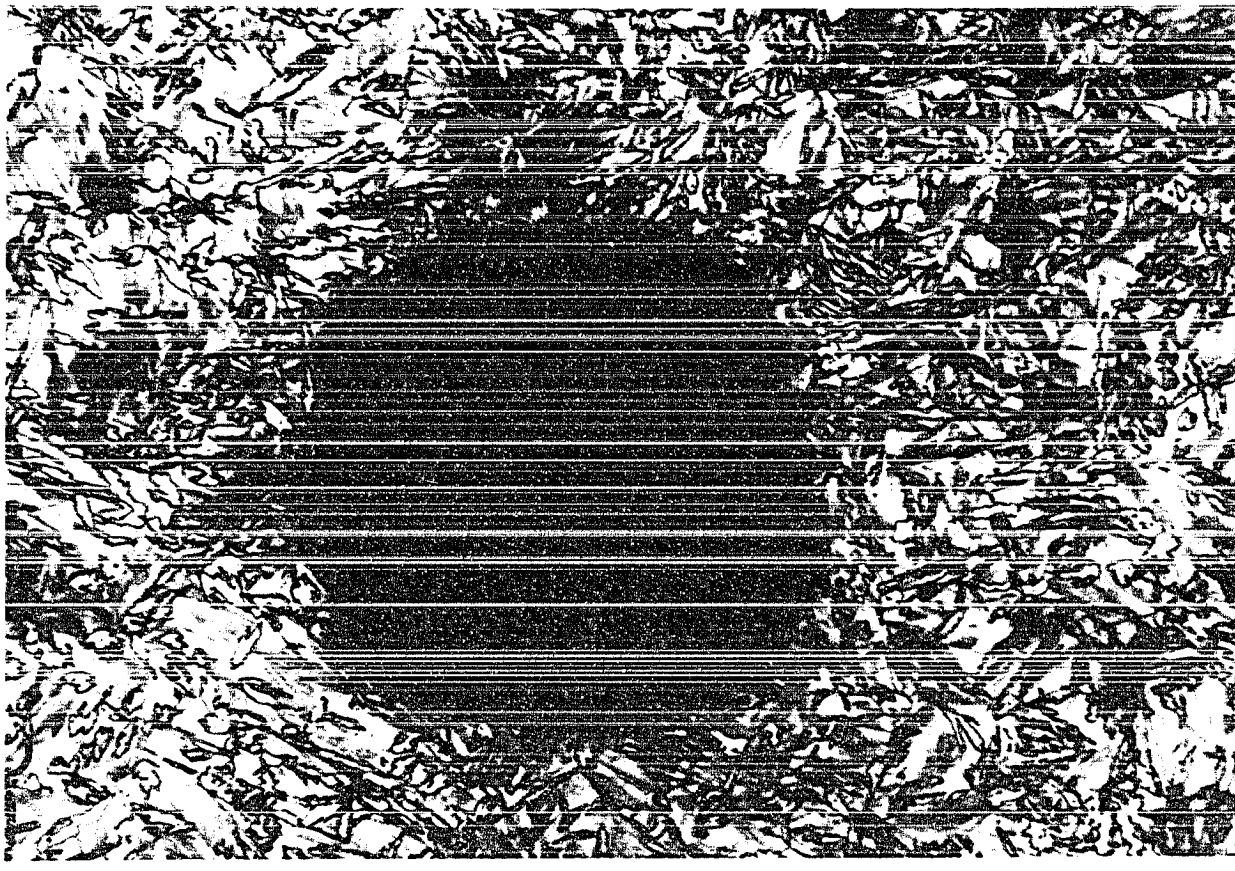

FIG. 43

Transformed at 800°F for 70 minutes. Feathers or needles of constituent "X" in a matrix of martensite. 1000 X.

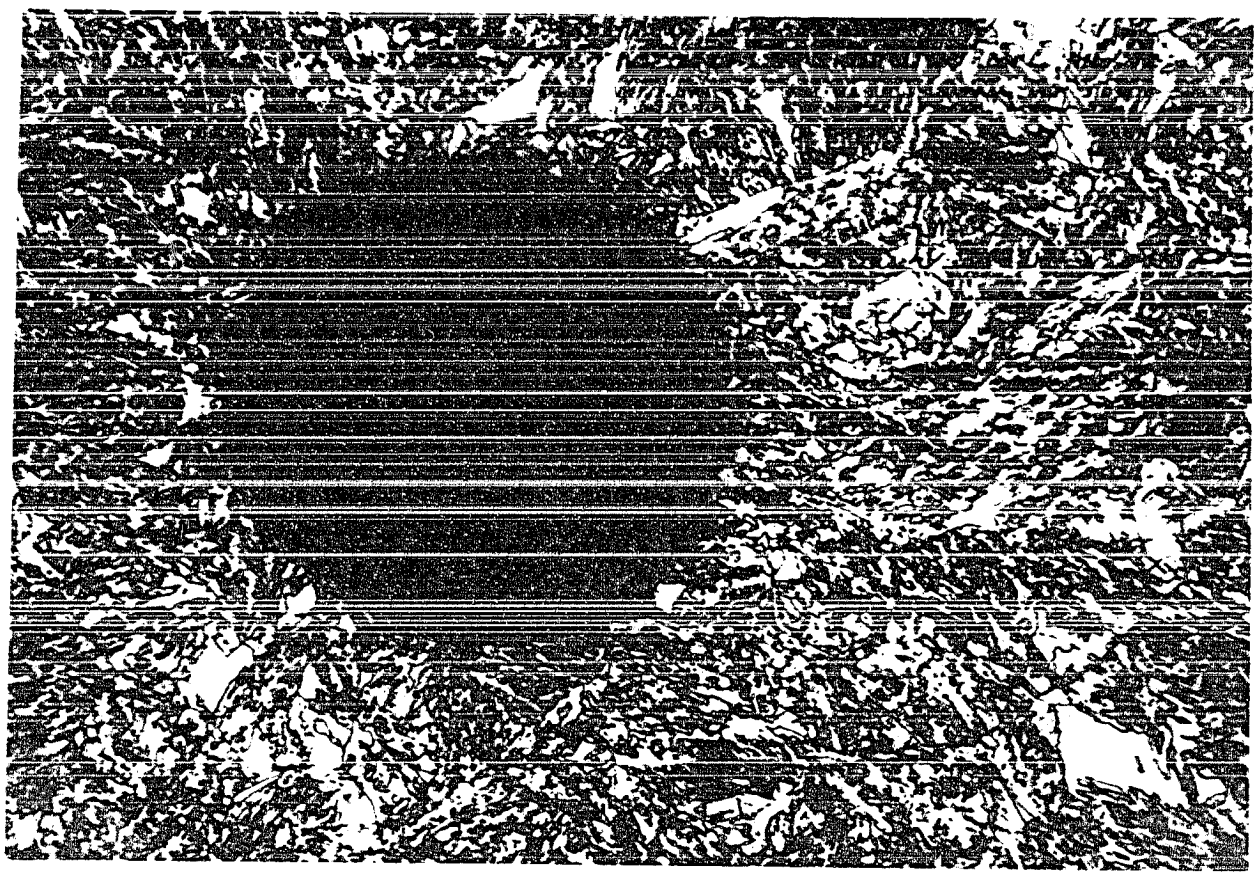

FIG. 44

Transformed at 700°F for 4,000 minutes. Constituent "X" (speckled) and several large white grains of martensite. 1000 X.

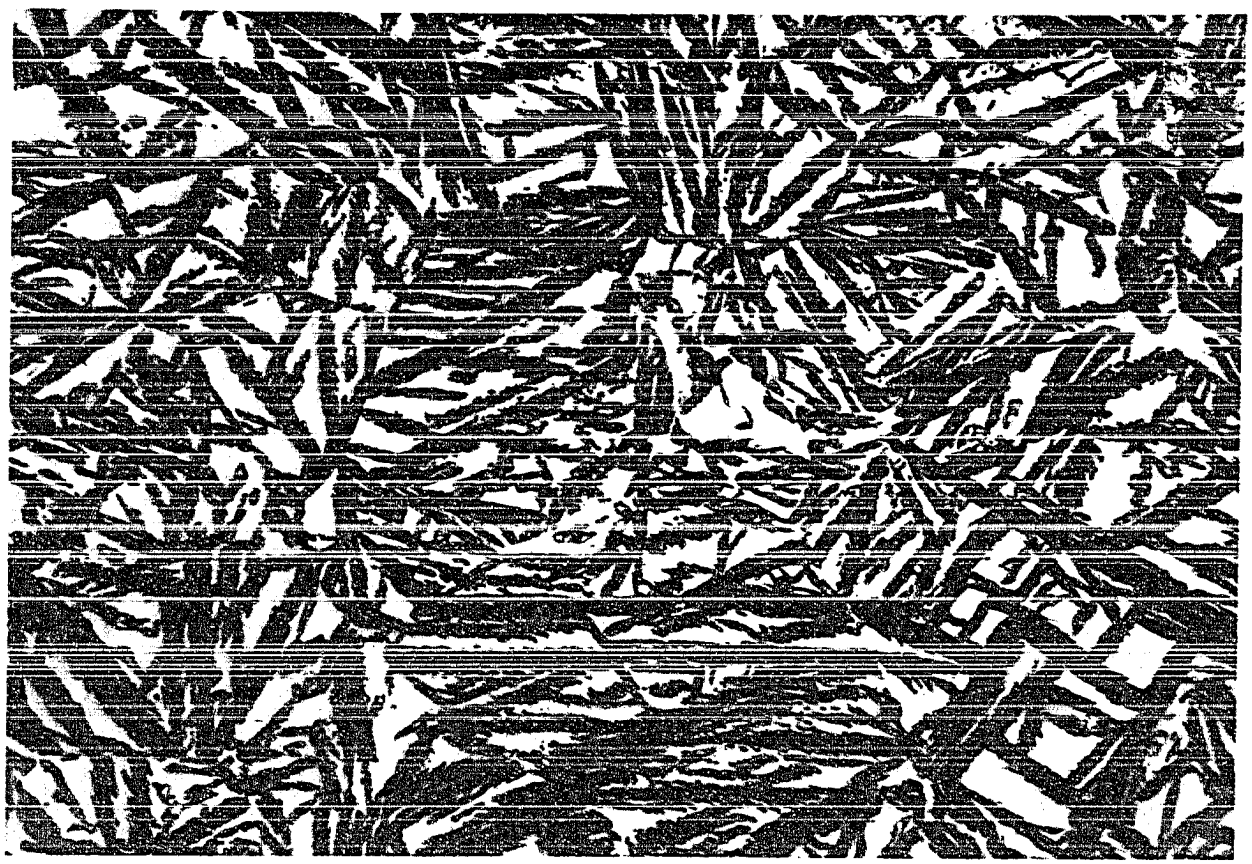

FIG. 45

Transformed at 600°F for 2,000 minutes. Feathers of bainite (dark) and martensite (white). 1000 X.

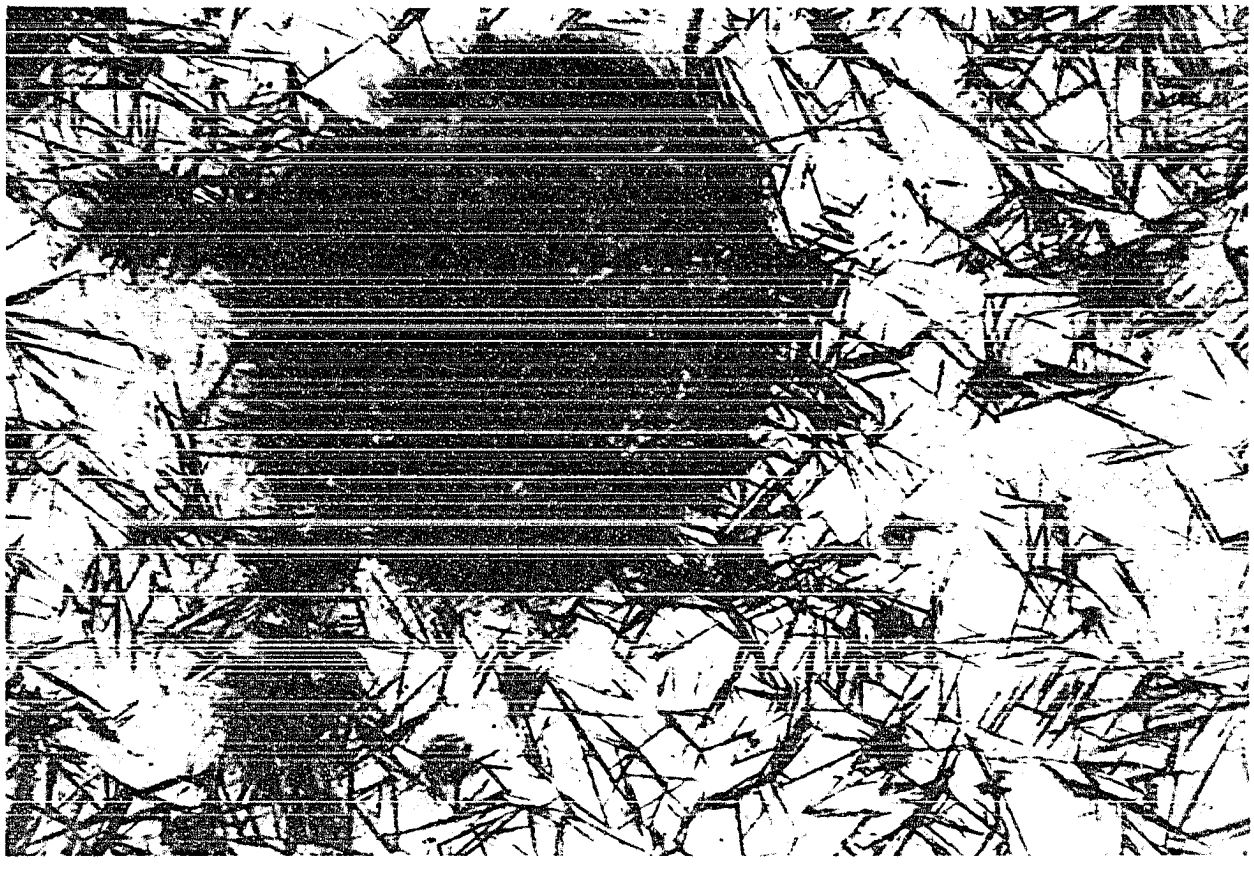

FIG. 46

Transformed at 500°F for 65 minutes. Needles of bainite (dark) and martensite (gray). 1000 X.

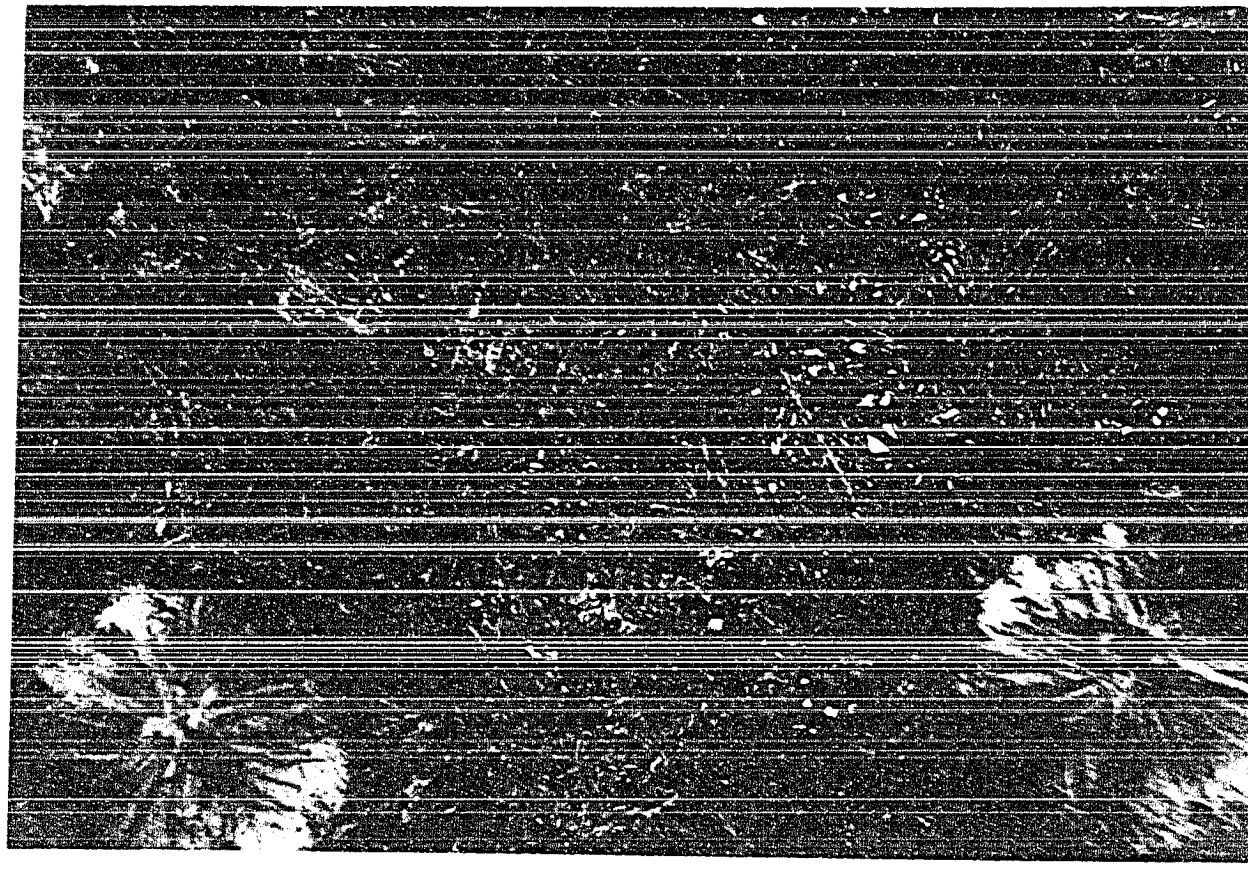

FIG. 47

Transformed at 400°F for 4,000 minutes. Fine acicular bainite (dark) and traces of martensite or untransformed austenite (white). 1000 X.

PHOTOMICROGRAPHS OF TRANSFORMATION STRUCTURES

FOR THE CAST IRON NO. 2

The structures were obtained after austenitizing at 1650°F, quenching and holding at the temperatures and times indicated, and finally quenching in water. The specimens were etched with nital.

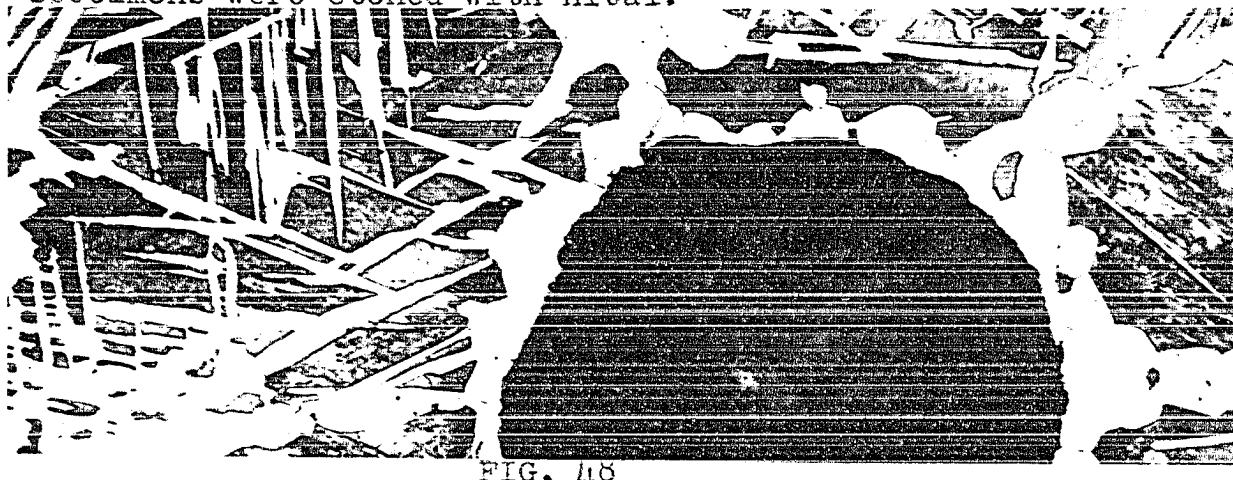

FIG. 48

Transformed at 1250°F for 6,300 minutes. Ferrite (white) is formed along the crystallographic planes (widmanstatten ferrite) and grain boundaries of austenite. Martensite is gray. 1000 X.

FIG. 49

Transformed at 1250°F for 10,000 minutes (1 week). Similar to Fig. 47 except that the time of transformation was longer, resulting in more ferrite. Ferrite (white) and martensite (gray). 1000 X

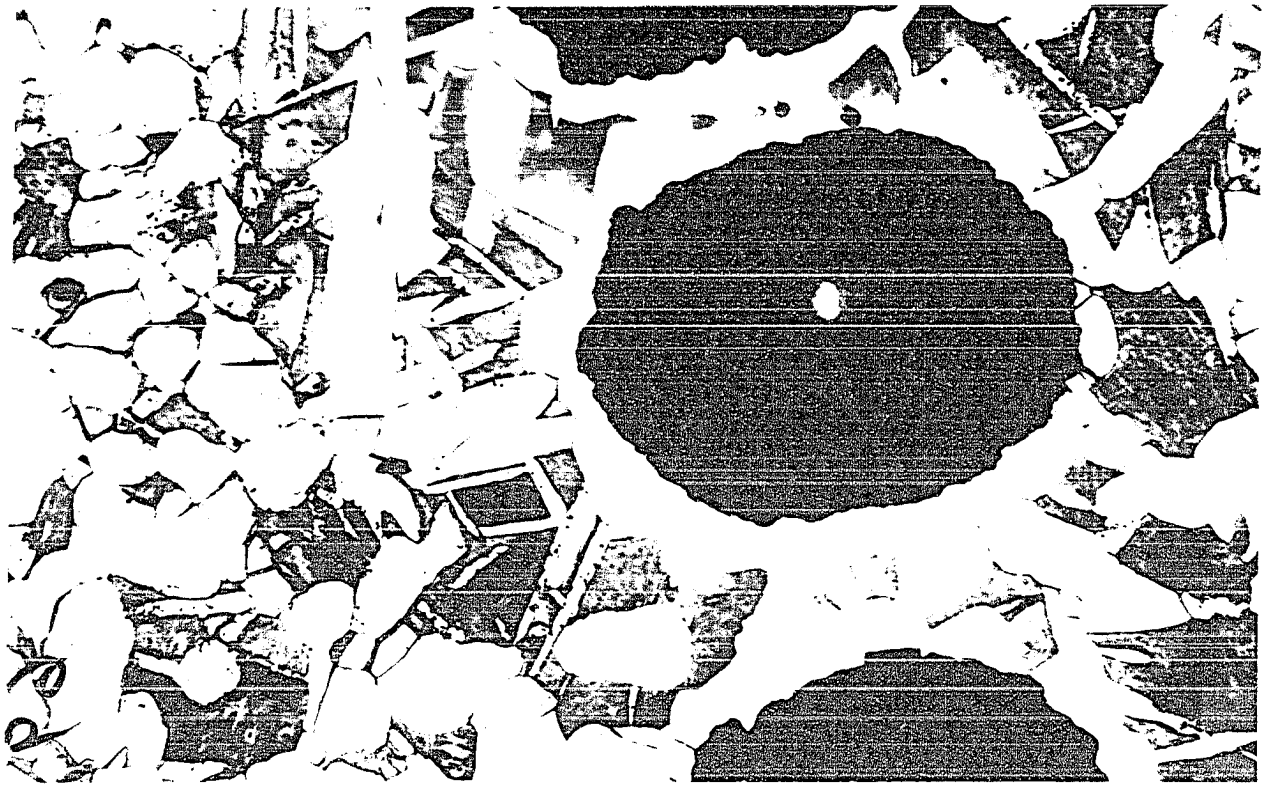

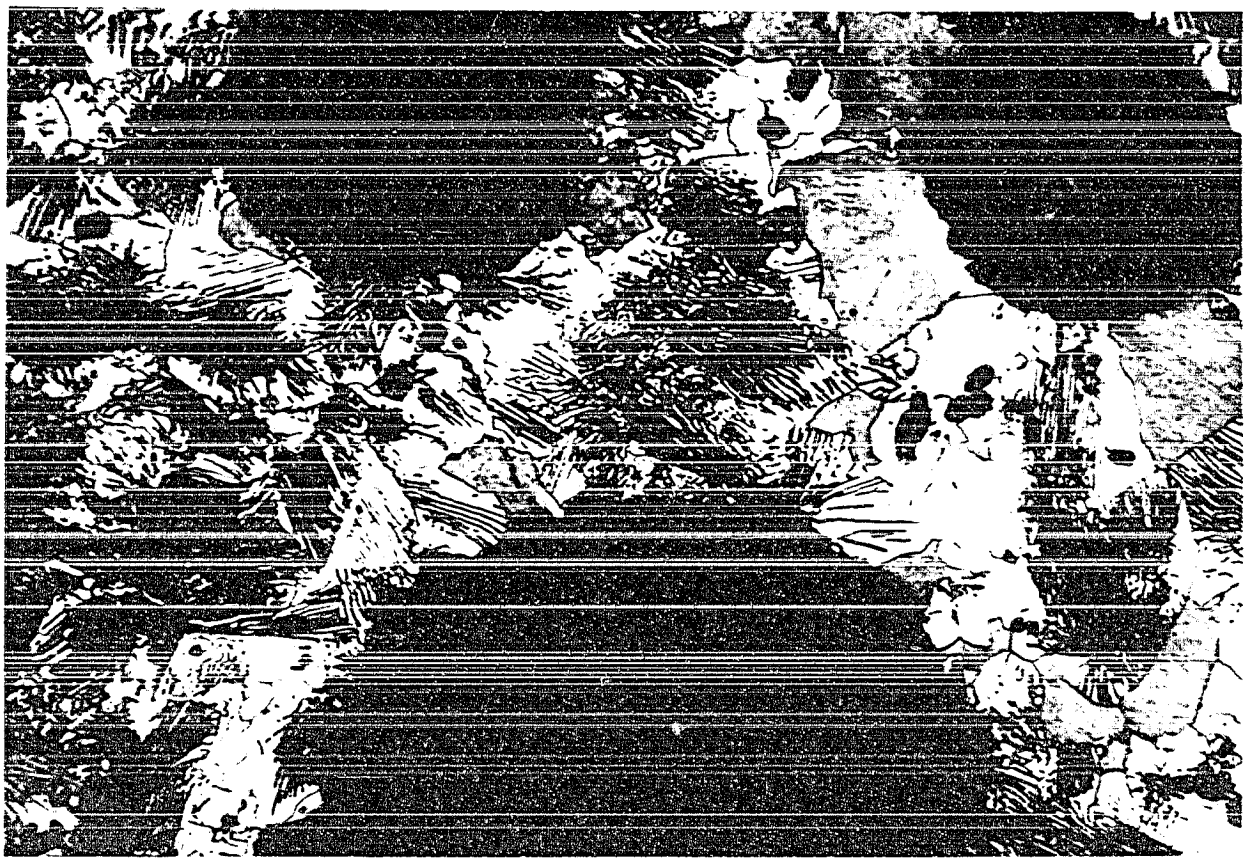

FIG. 50

Transformed at 1200°F for 20 minutes. Ferrite (white), coarse pearlite (lamellar) and martensite (gray). 1000 X.

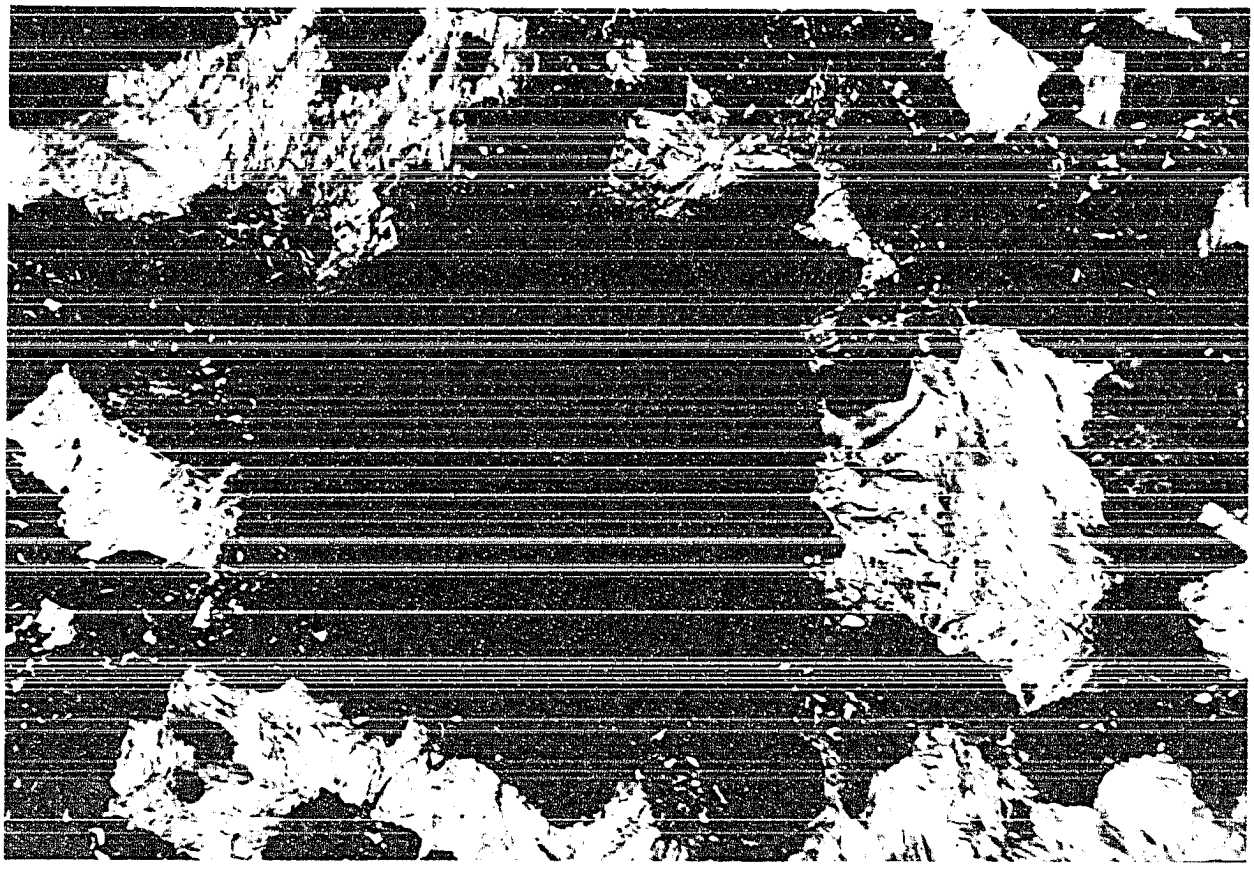

FIG. 51

Transformed at 1100°F for 4 minutes. Pearlite (dark) and martensite (gray). 1000 X.

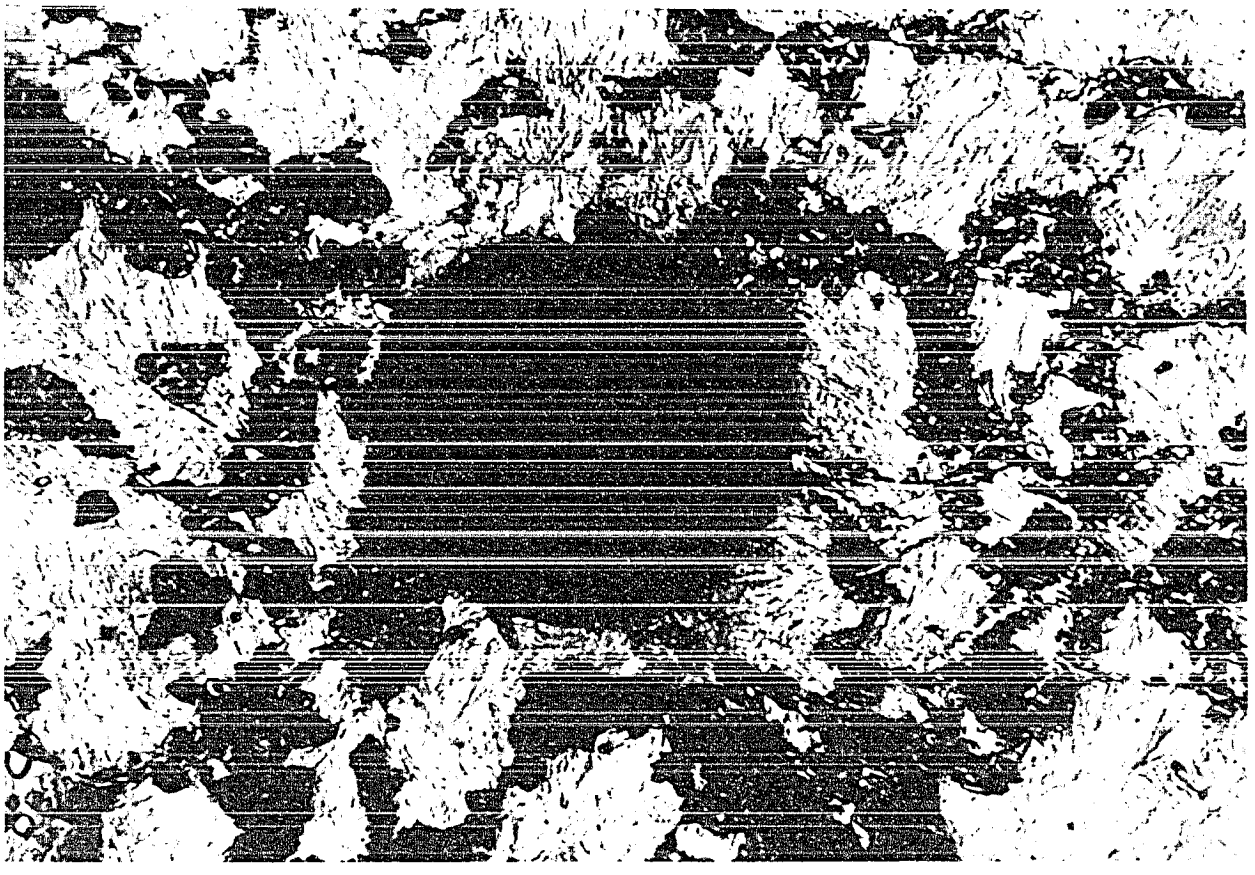

FIG. 52

Transformed at 1000°F for 15 minutes. Fine pearlite (dark) forms in the grain boundaries of austenite. Martensite is gray. 1000 X.

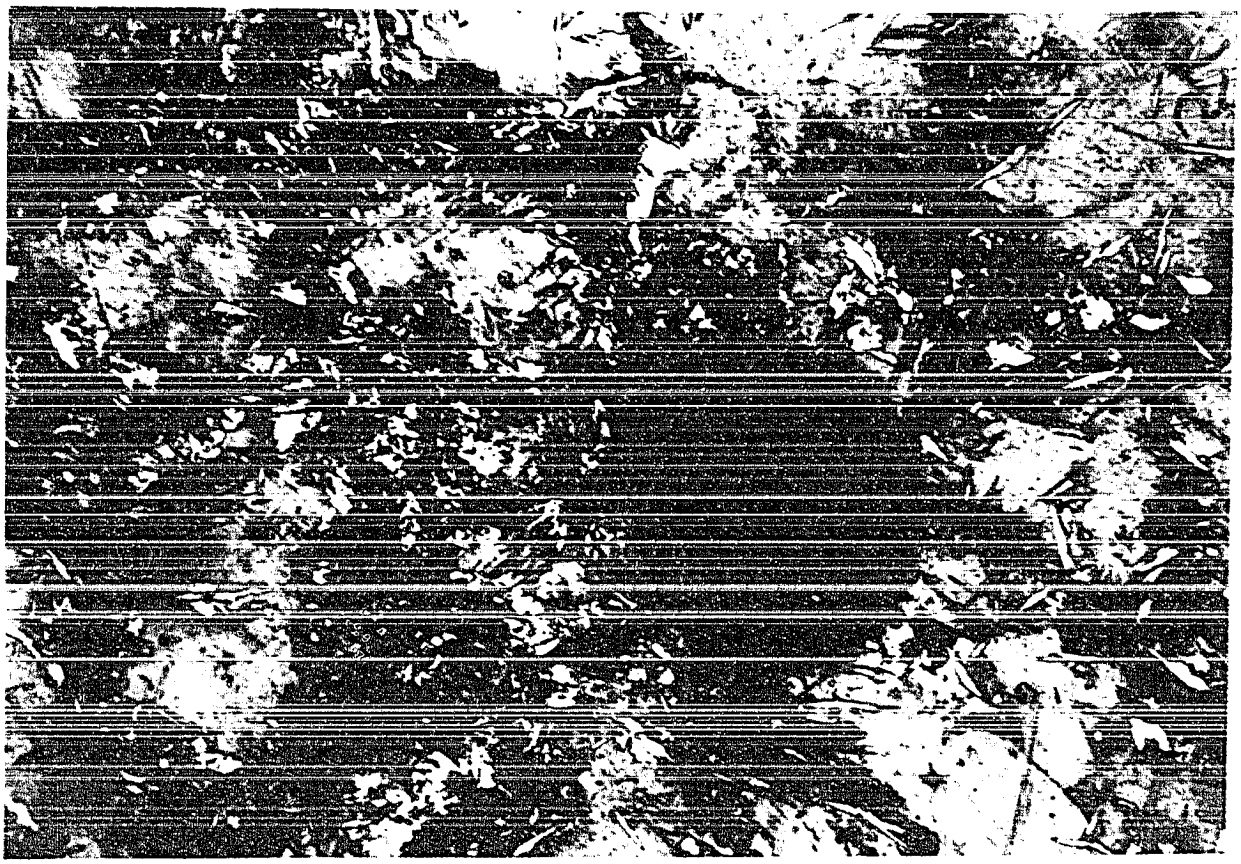

FIG. 53

Transformed at 900°F for 500 minutes. Fine pearlite (dark), needles of ferrite (white), constituent "X" (white and speckled) and martensite (gray). 1000 X.

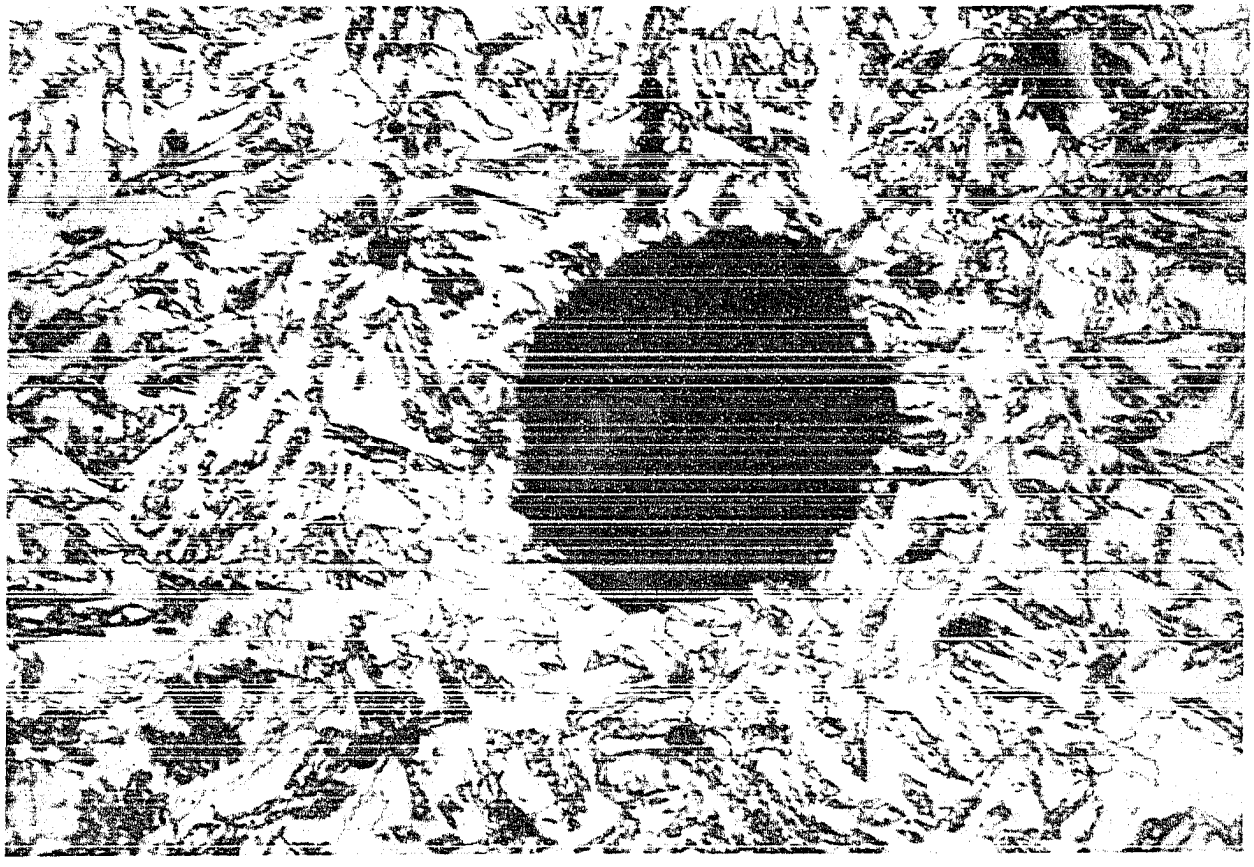

FIG. 54

Transformed at 700°F for 700 minutes. Constituent "X" (speckled feathers) in a matrix of martensite (light gray). 1000 X.

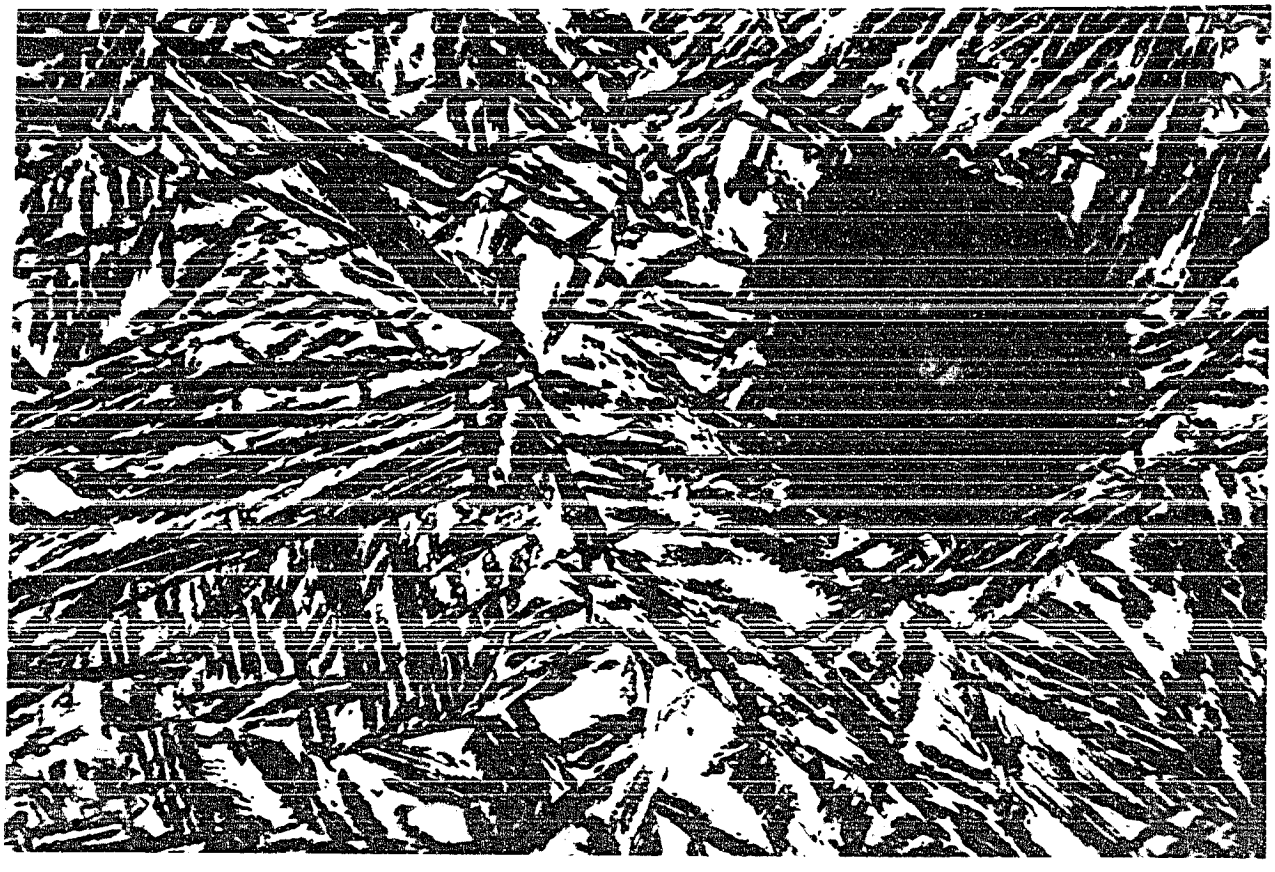

FIG. 55

Transformed at 600°F for 10,000 minutes (1 week).
Feathers of bainite (dark) and martensite (white). 1000 X.

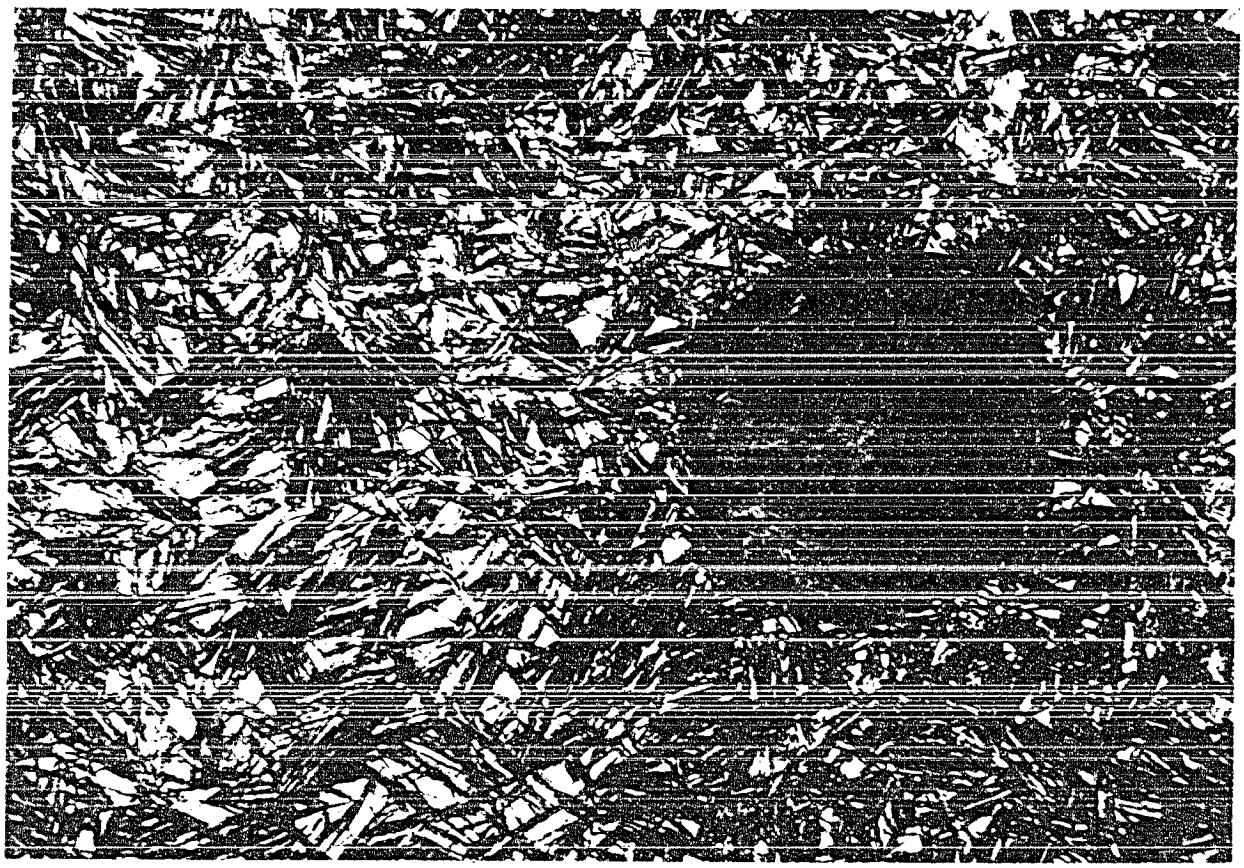

FIG. 56

Transformed at 500°F for 1350 minutes. Bainite (dark) and martensite (white). 1000 X.

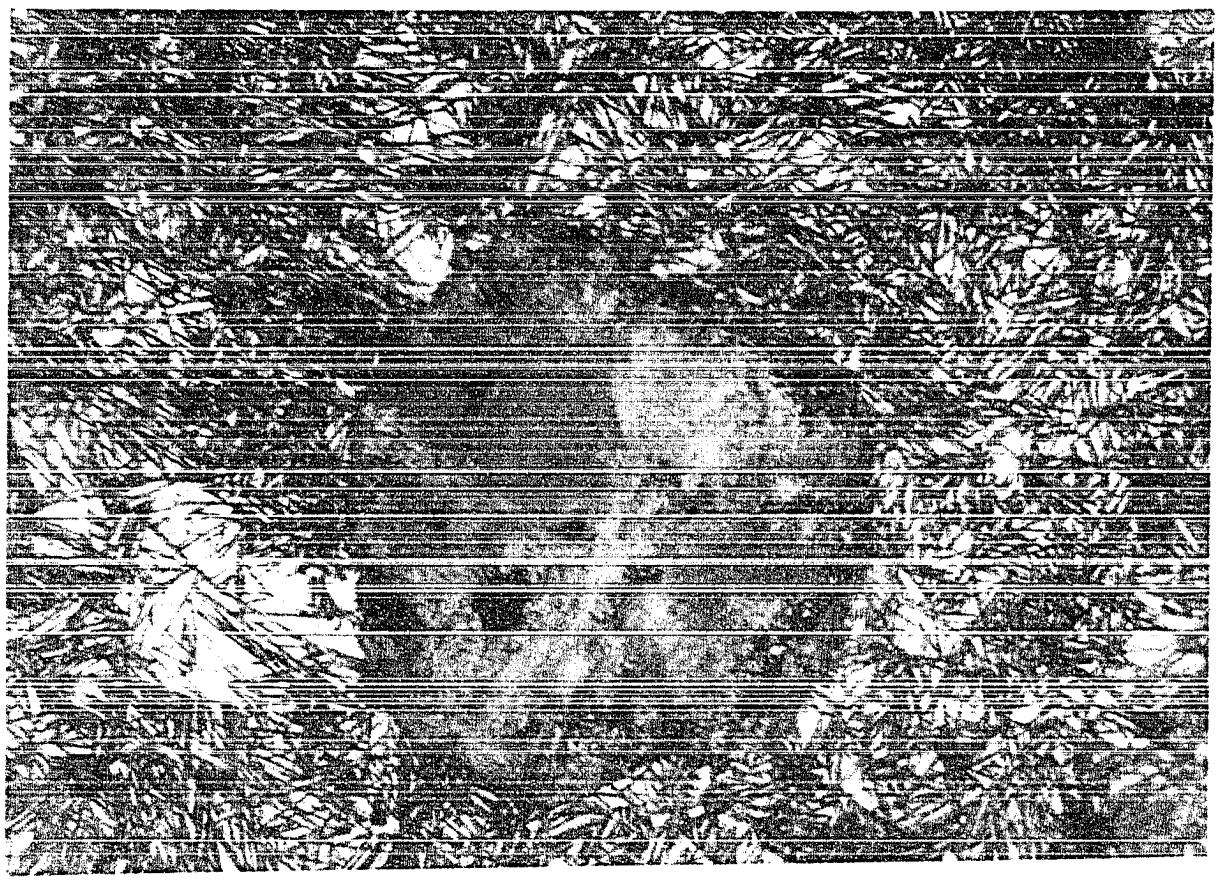

FIG. 57

Transformed at 300°F for 6,000 minutes. Needles of bainite (dark) and martensite (white). 1000 X.

PHOTOMICROGRAPHS OF TRANSFORMATION

STRUCTURES FOR THE CAST IRON NO. 3

The structures were obtained after austenitizing at 1650°F, quenching and holding at the temperatures and times indicated, and finally quenching in water. The specimens were etched with nital.

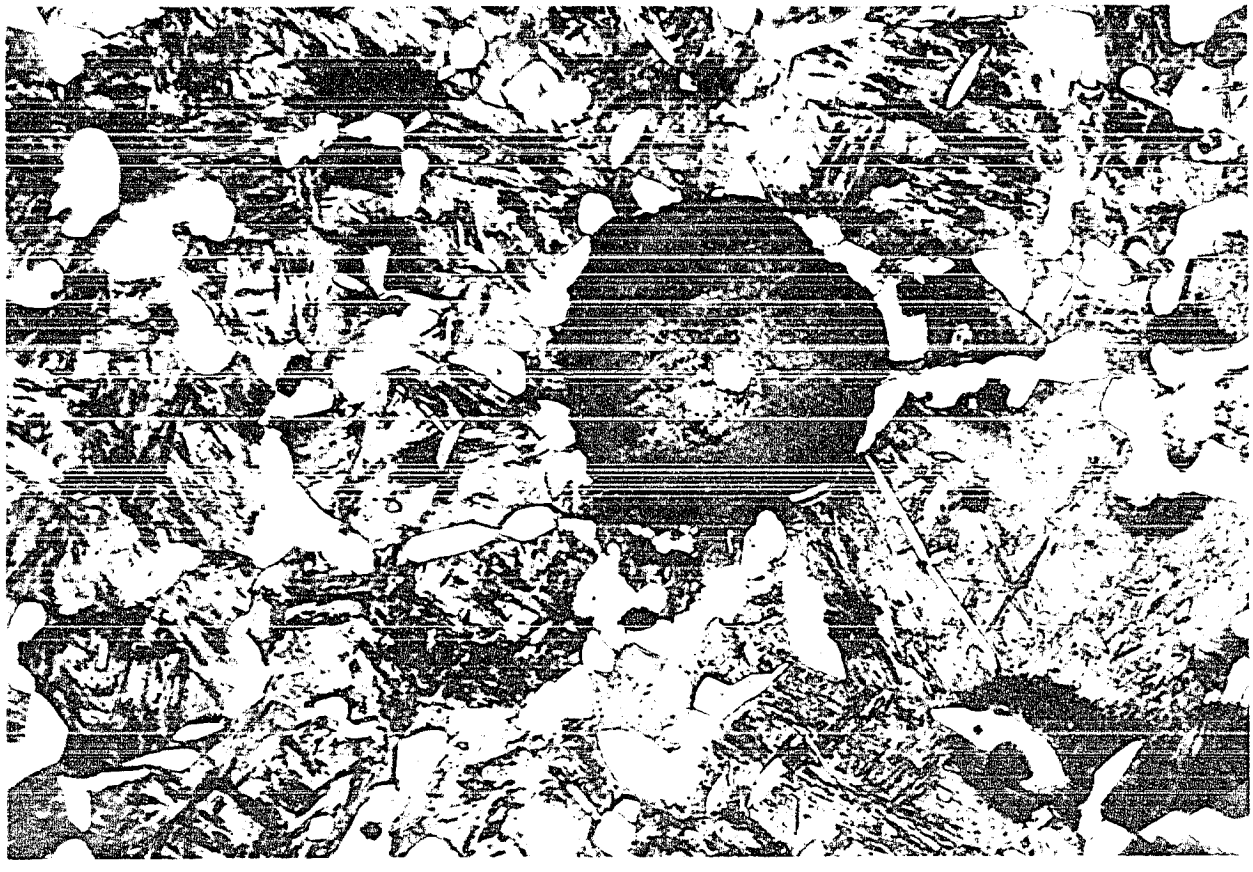

FIG. 58

Transformed at 1300°F for 10,000 minutes (1 week). Ferrite (white) along the grain boundaries and martensite (gray). 1000 X.

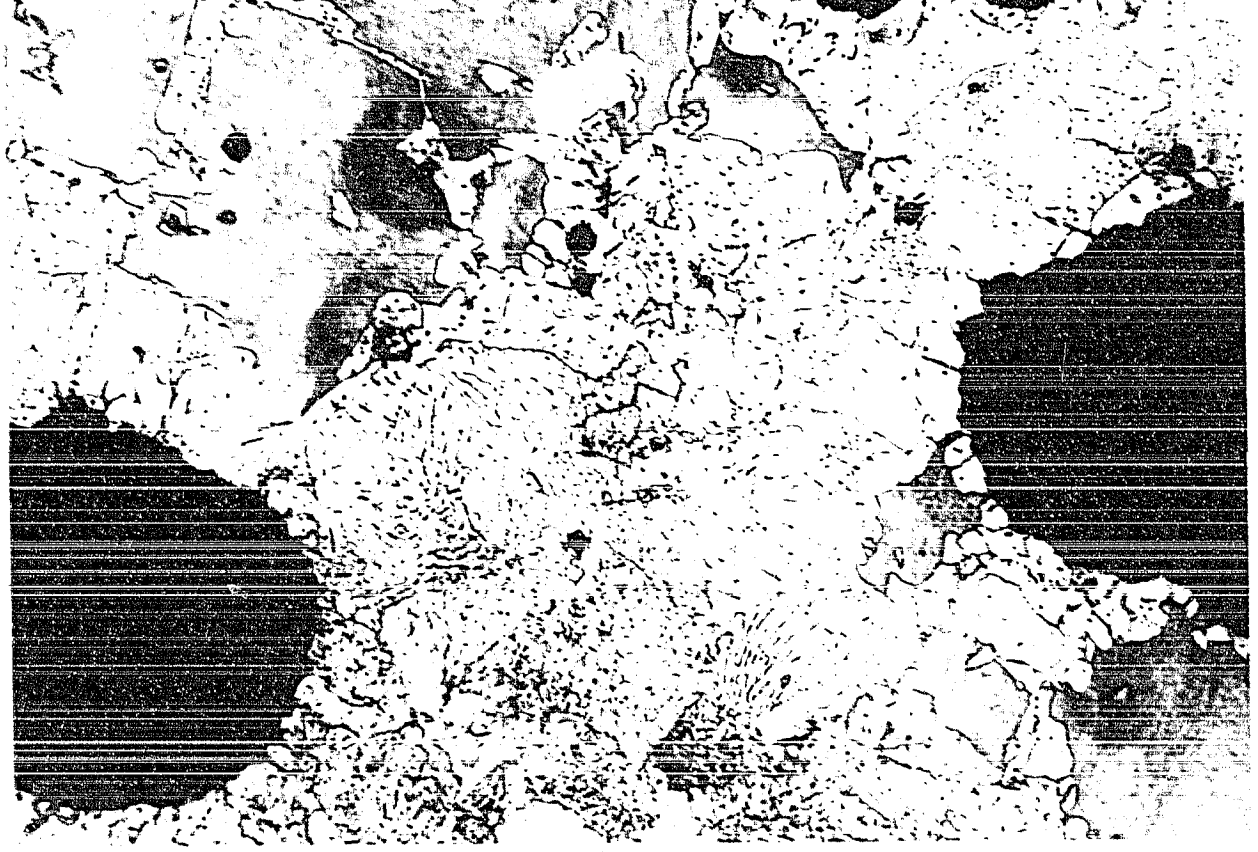

FIG. 59
Transformed at 1225°F for 1500 minutes (1 day). Ferrite grains with spheroidal carbides and very coarse lamellar pearlite. Martensite is gray. 1000 X.

FIG. 60
Transformed at 1225 for 10,000 minutes (1 week). Easily stained ferrite. 1000 X.

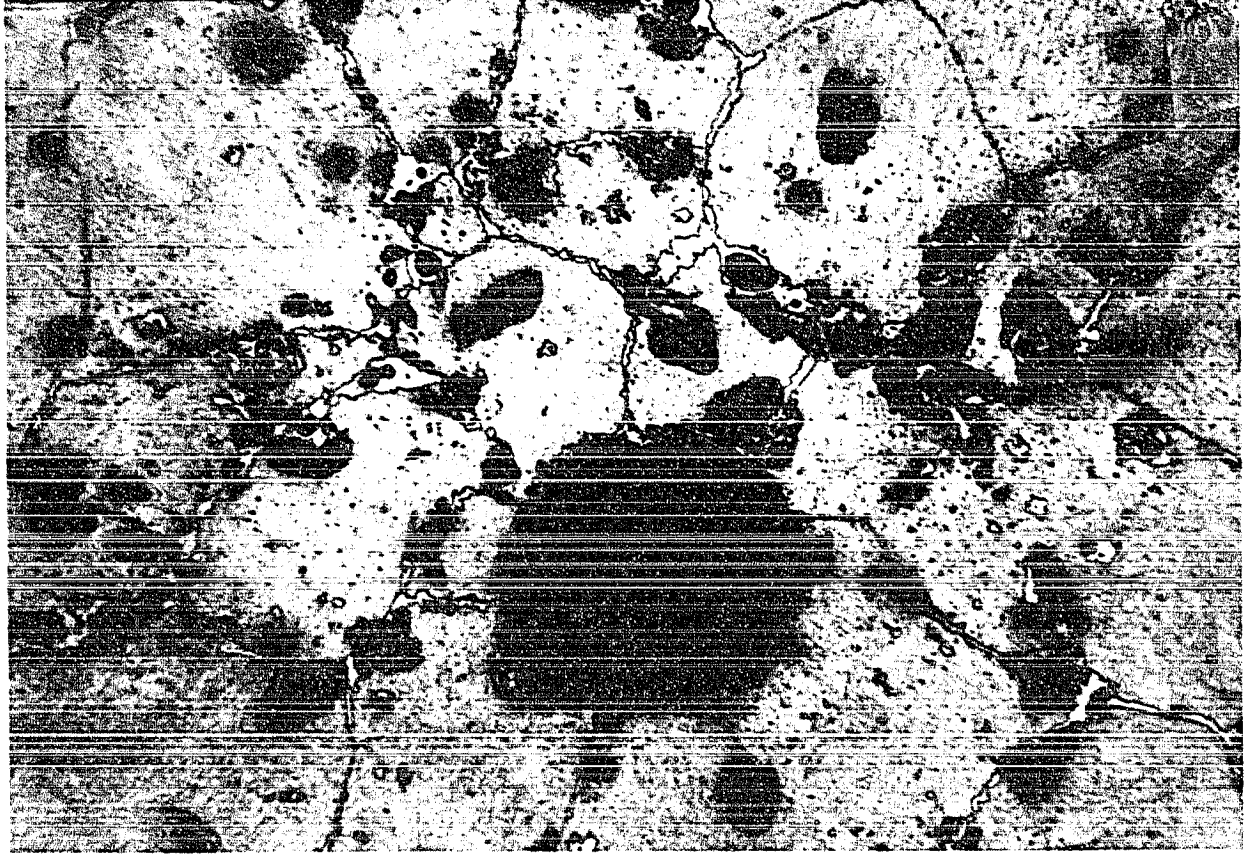

FIG. 61
Transformed at 1200°F for 60 minutes. Ferrite (white) along the grain boundaries. Nodules of pearlite (dark) and martensite (gray). 1000 X.

FIG. 62
Transformed at 1200°F for 1,100 minutes. Martensite (gray) and ferrite (white) with spherodized and elongated carbides. 1000 X.

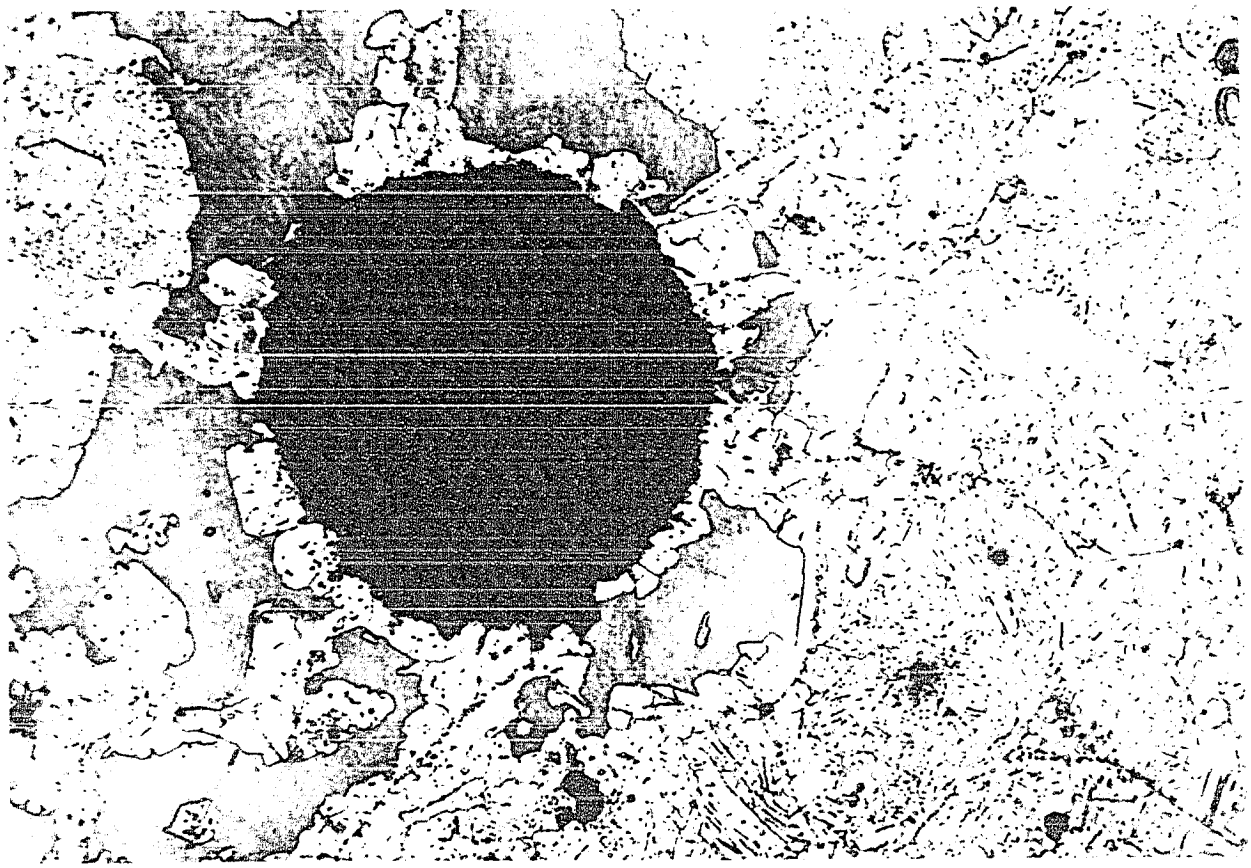

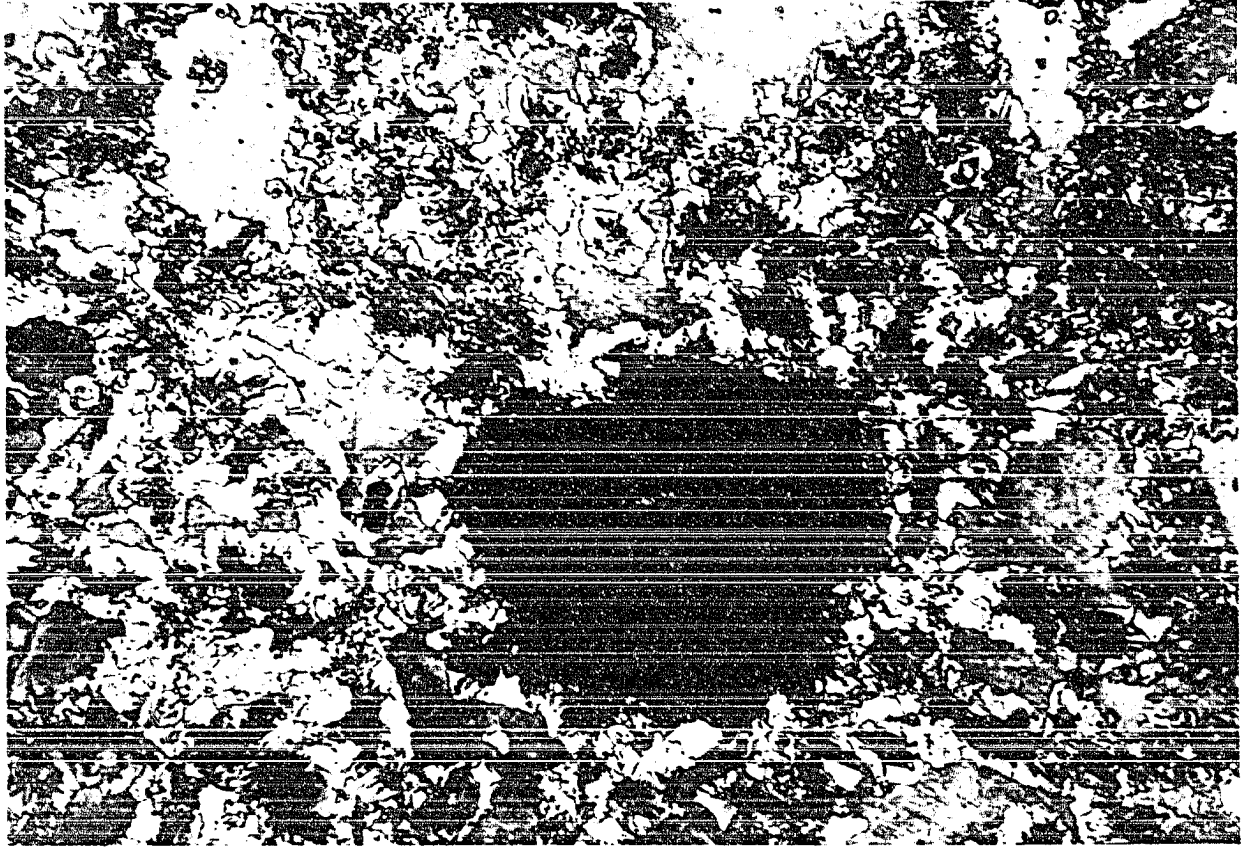

FIG. 63

Transformed at 1100°F for 400 minutes. Pearlite (dark), ferrite (white) and martensite (gray). 1000 X.

FIG. 64

Transformed at 1100°F for 10,000 minutes (1 week). Easily stained ferrite. 1000 X.

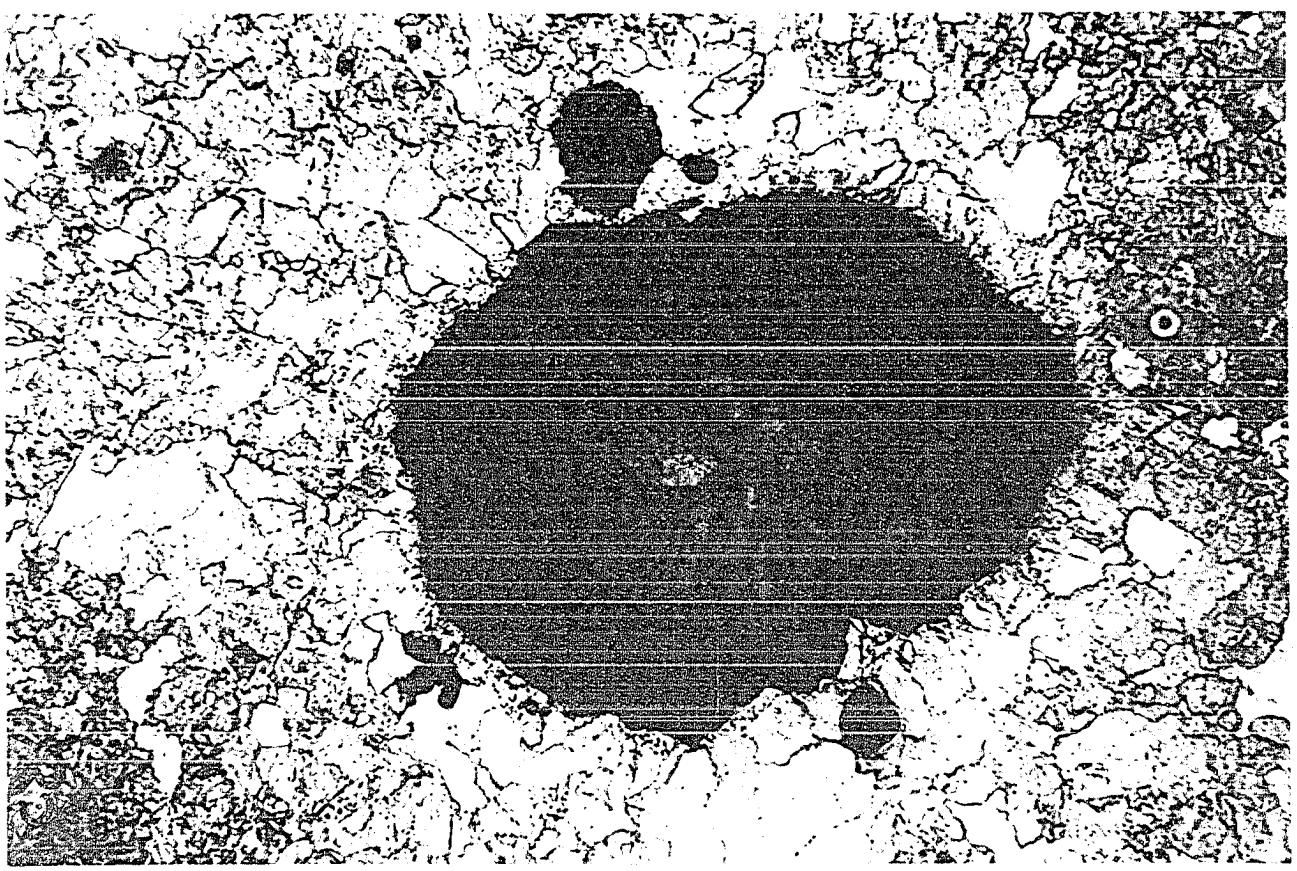

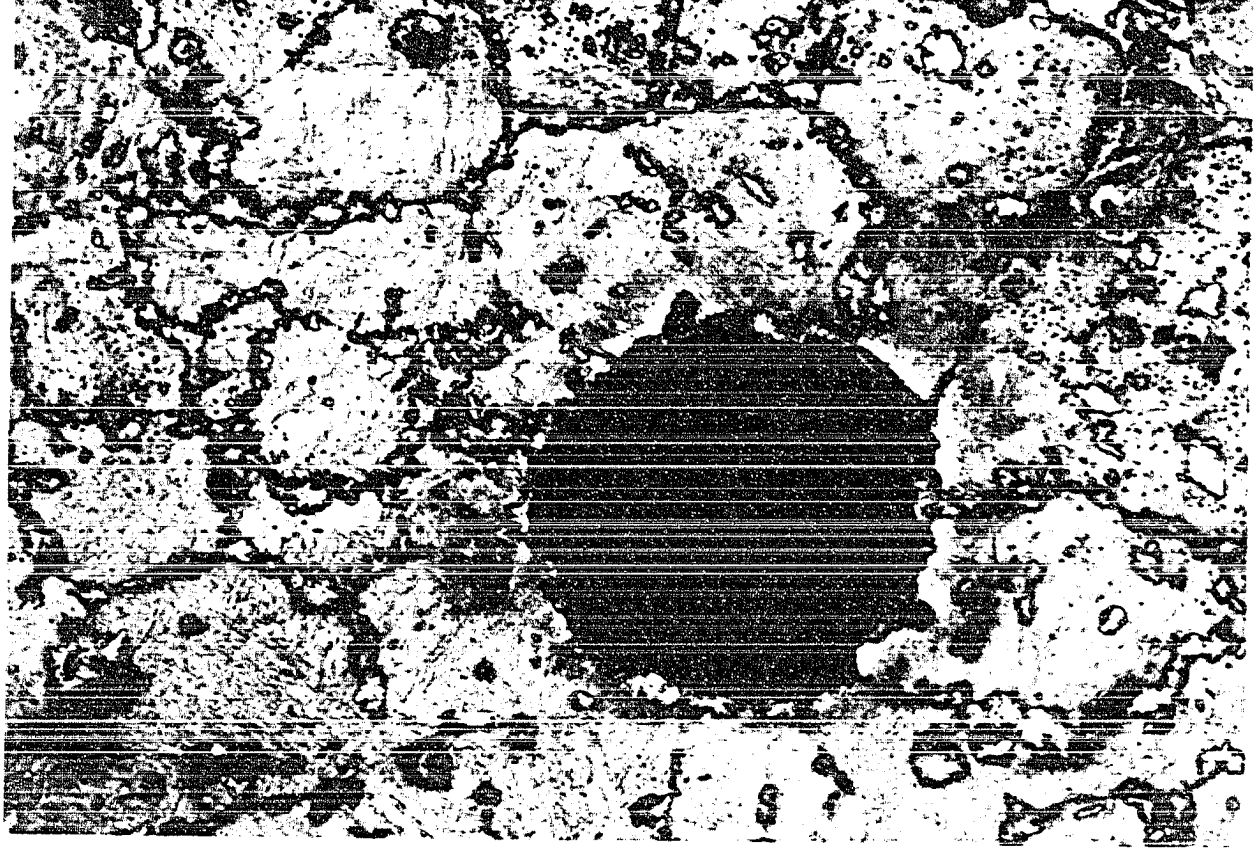

FIG. 65
Transformed at 1000°F for 700 minutes. A light etching phase or structure in the grain boundaries of austenite. The large grains are martensite. 1000 X.

FIG. 66
Transformed at 1000°F for 5,000 minutes. Fine pearlite (dark), ferrite (white) and martensite (gray). 1000 X.

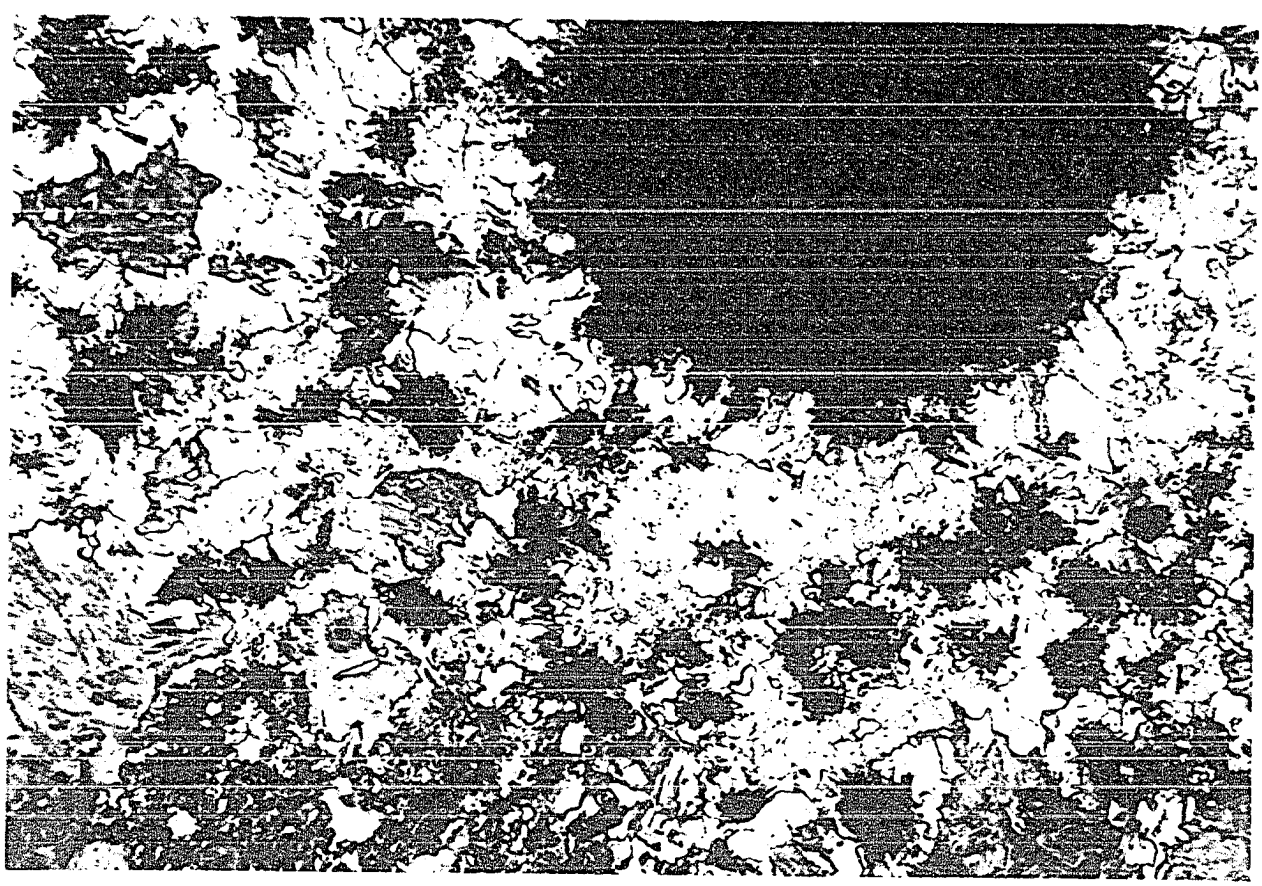

FIG. 67
Transformed at 900°F for 400 minutes. Needles of ferrite (white) and martensite (gray). 1000 X.

FIG. 68
Transformed at 900°F for 10,000 minutes (1 week). Needles of ferrite (white), pearlite in the grain boundaries (dark) and martensite (gray). 1000 X.

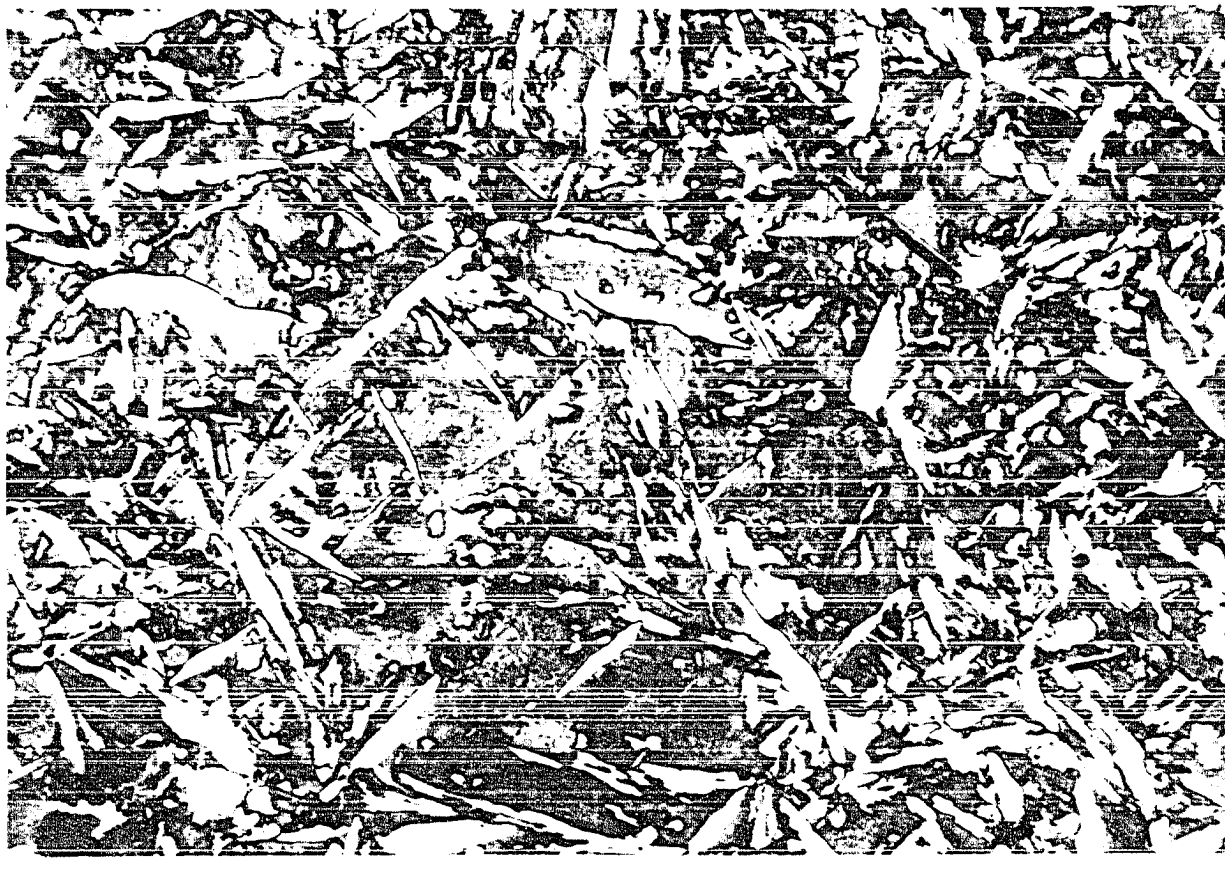

FIG. 69

Transformed at 800°F for 7,000 minutes. Ferrite needles (white), constituent "X" (speckled) and martensite (gray). 1000 X.

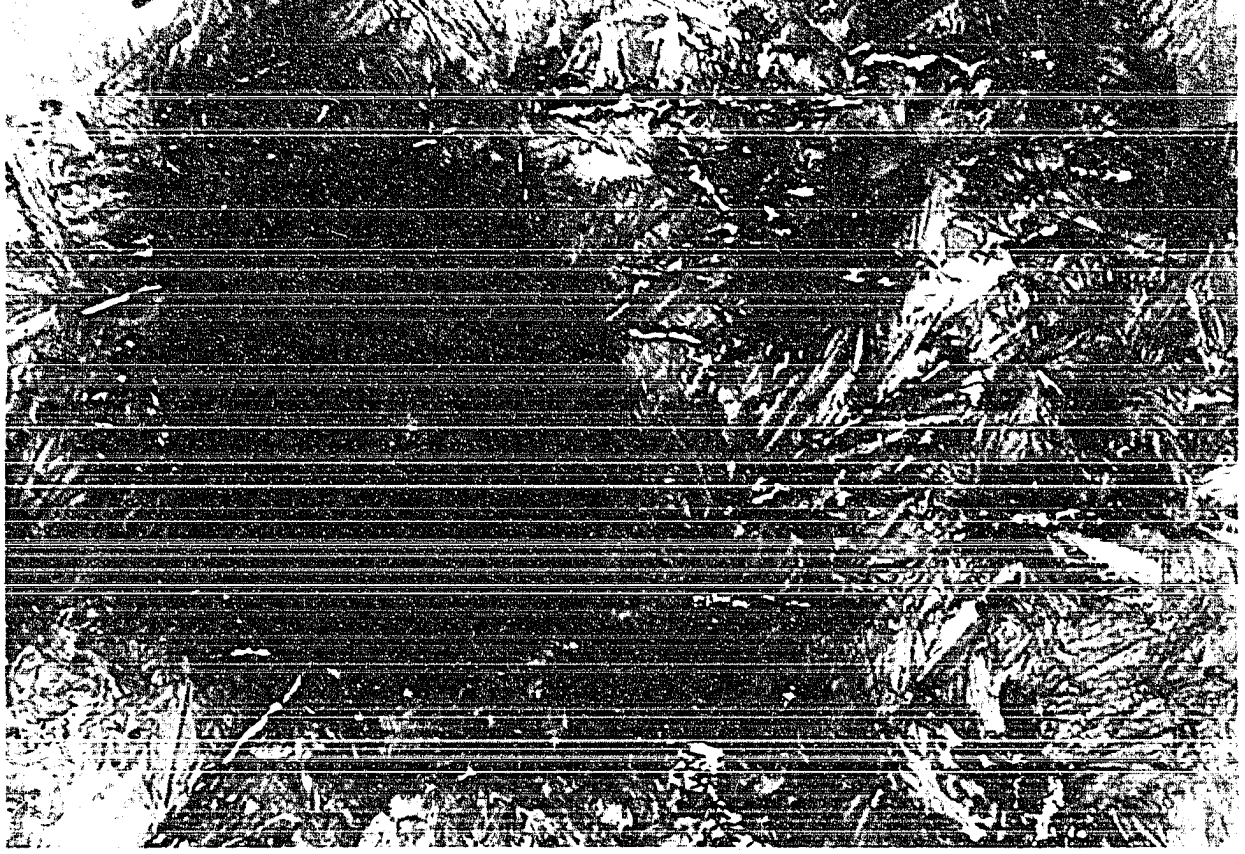

FIG. 70
Transformed at 700°F for 5,000 minutes. Constituent "X" in a martensitic matrix. 1000 X.

FIG. 71
Transformed at 700°F for 20,000 minutes (2 weeks). Constituent "X" (speckled) and martensitic matrix. 1000 X.

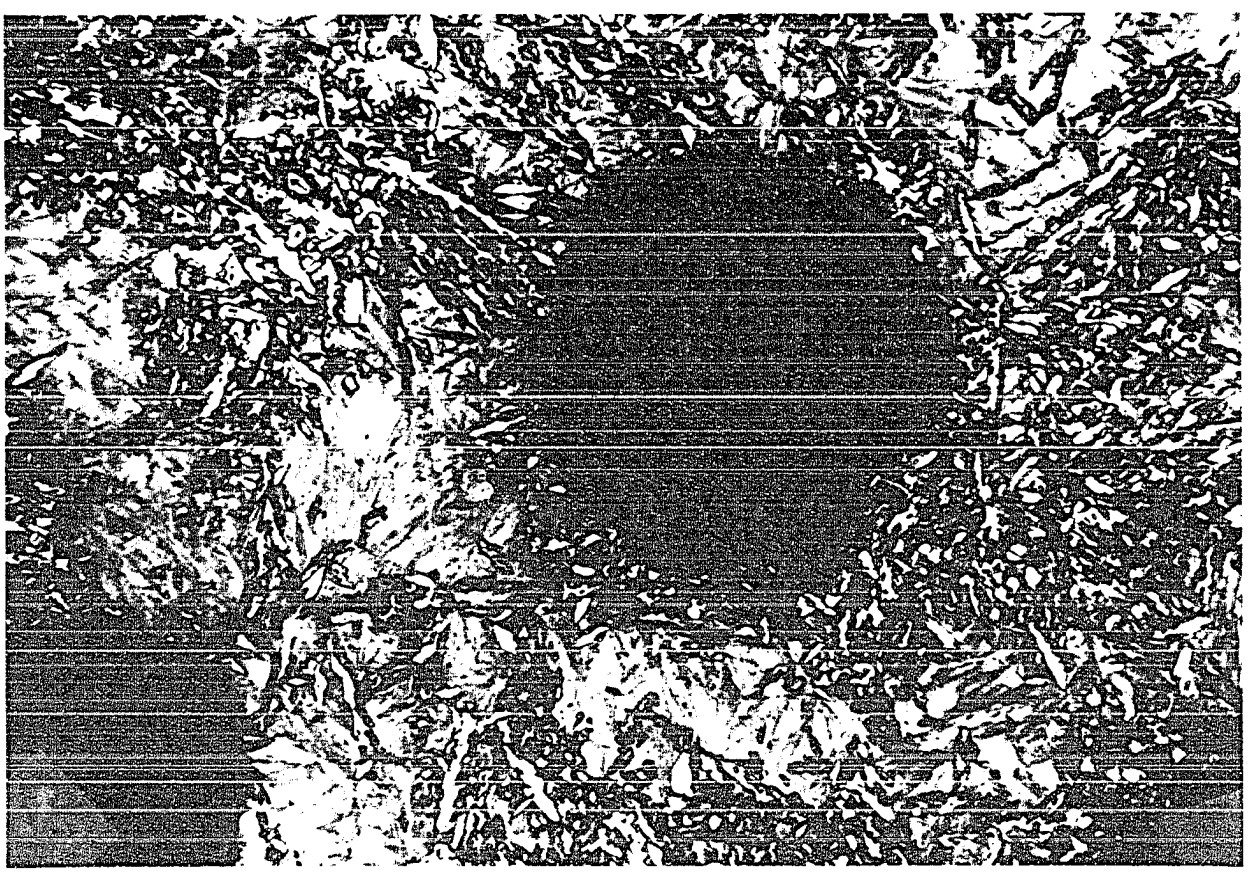

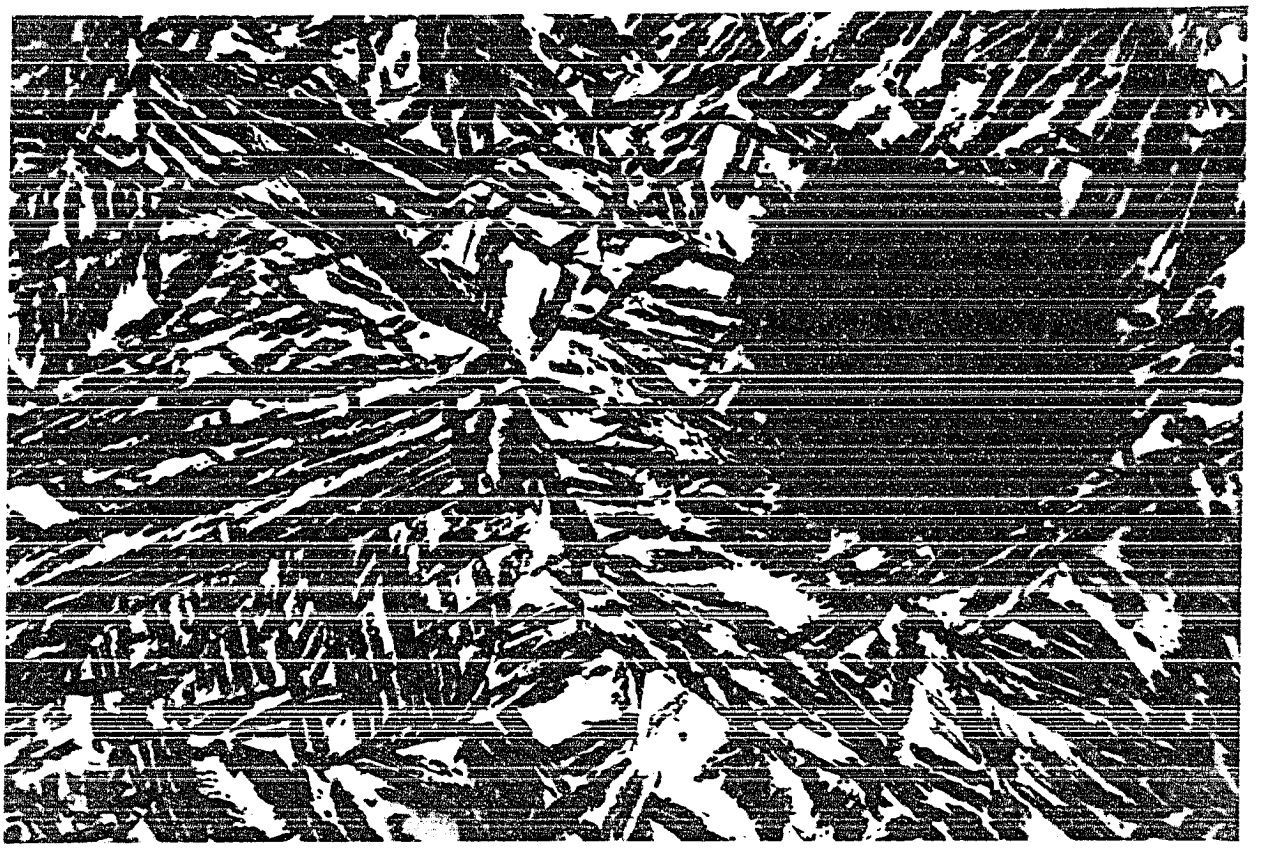

FIG. 72

Transformed at 600°F for 2,000 minutes. Feathers of bainite (dark) and martensite (white). 1000 X.

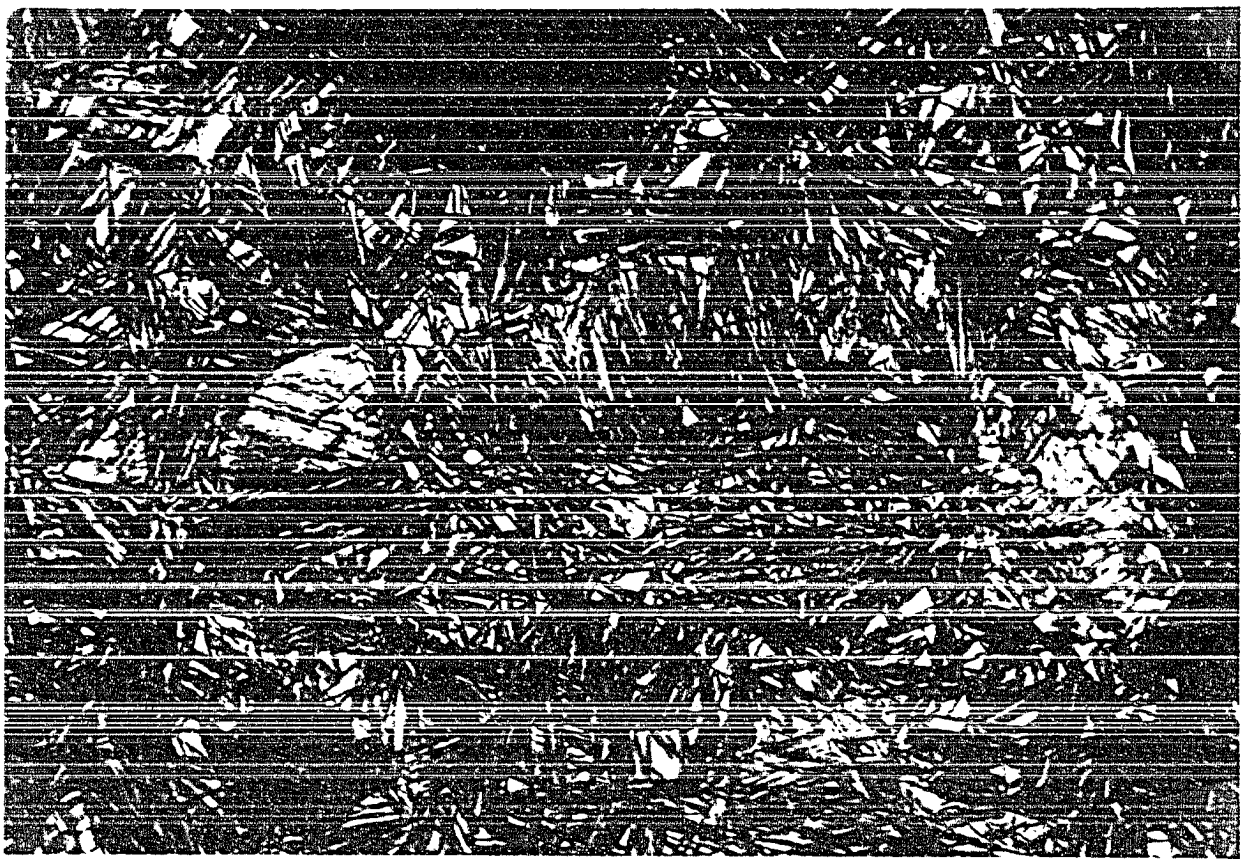

FIG. 73

Transformed at 500°F for 850 minutes. Bainite (dark) and martensite (white). 1000 X.

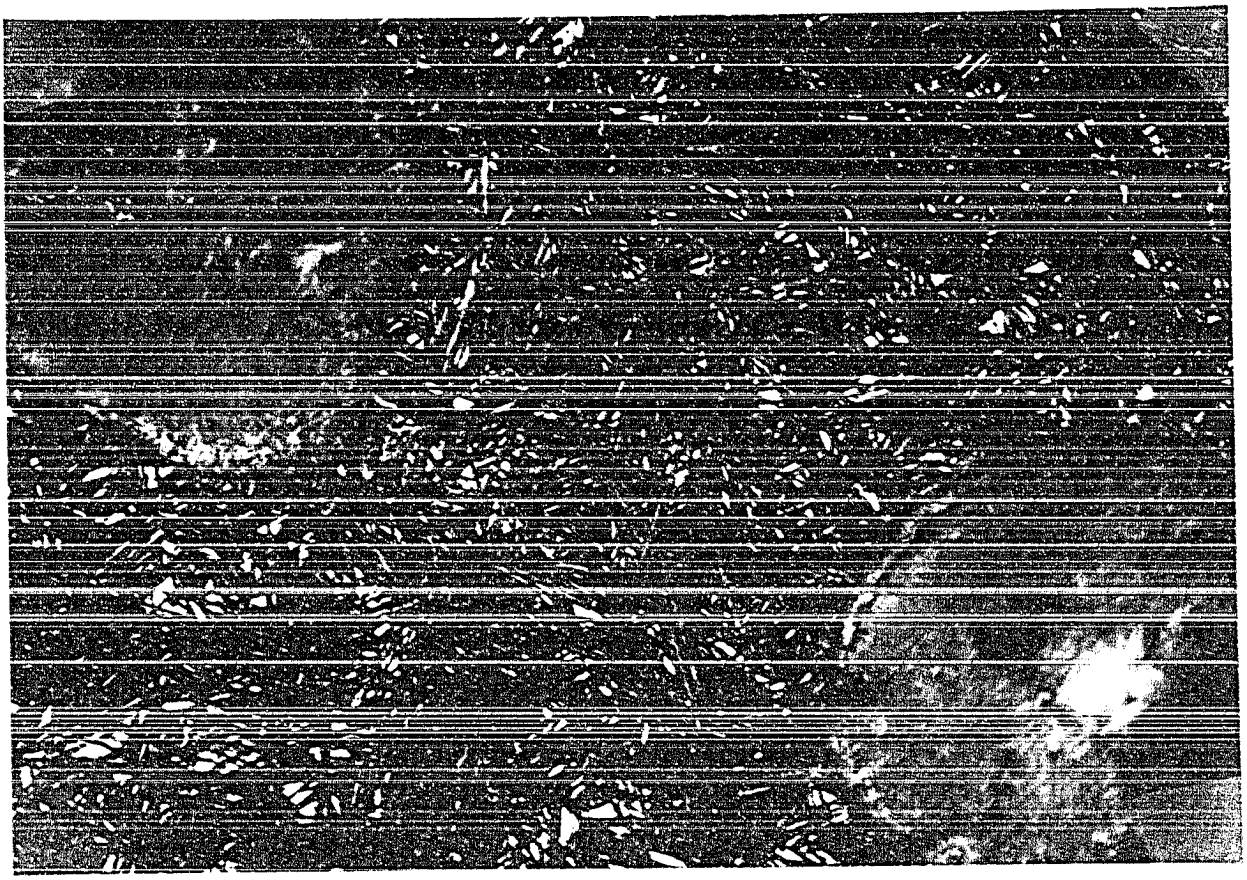

FIG. 74

Transformed at 400°F for 6,000 minutes. Bainite (dark) and martensite or untransformed austenite (white). 1000 X.

FIG. 75

Quenched to 200°F and held for two minutes, then tempered at 750°F for one minute. This figure shows the amount of martensite (dark) present at 200°F. 1000 X.

PHOTOMICROGRAPHS OF TRANSFORMATION

STRUCTURES FOR THE CAST IRON NO. 4

The structures were obtained after austenitizing at 1650°F, quenching and holding at the temperatures and times indicated, and finally quenching in water. The specimens were etched with nital.

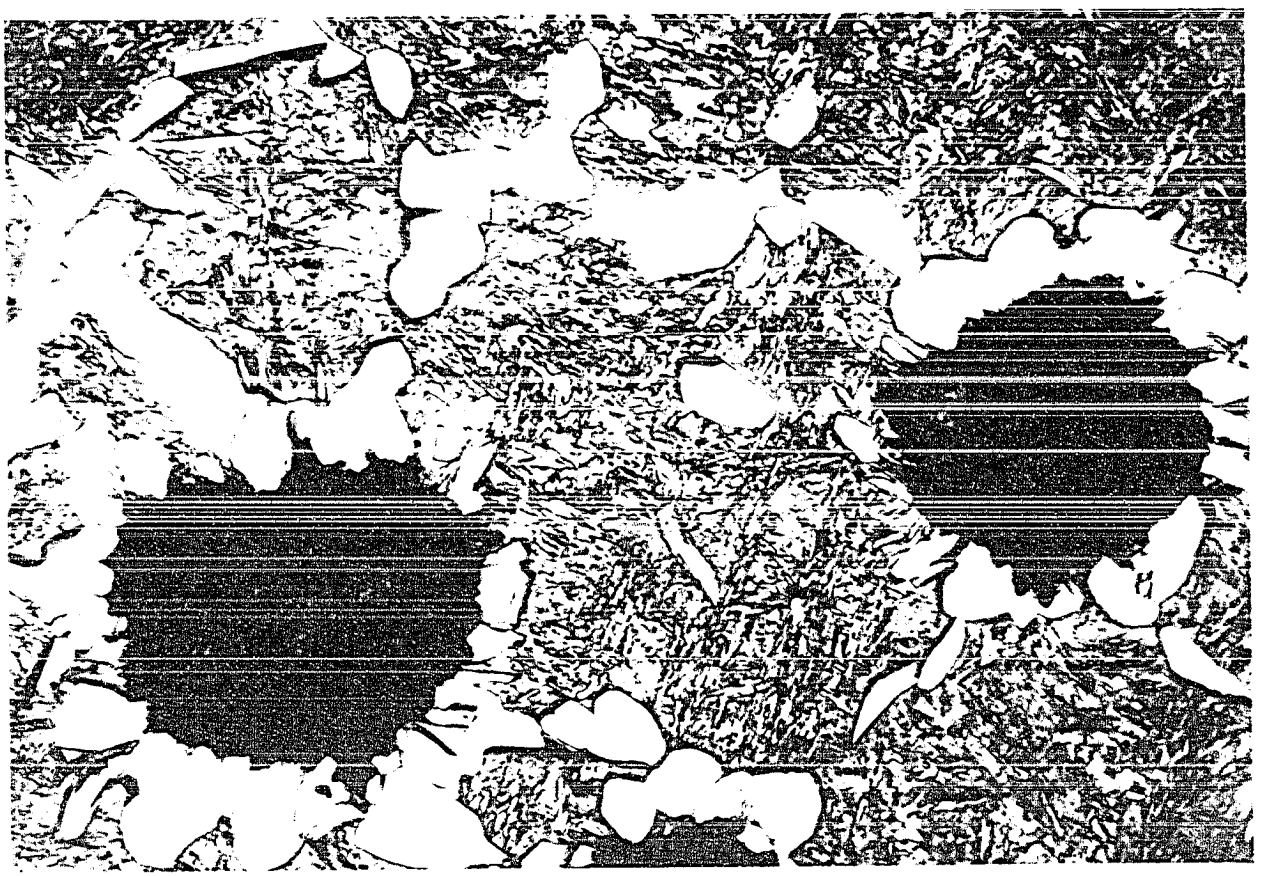

FIG. 76

Transformed at 1450°F for 330 minutes. Martensite (gray) and ferrite (white) along the grain boundaries and around the graphite nodules. 1000 X.

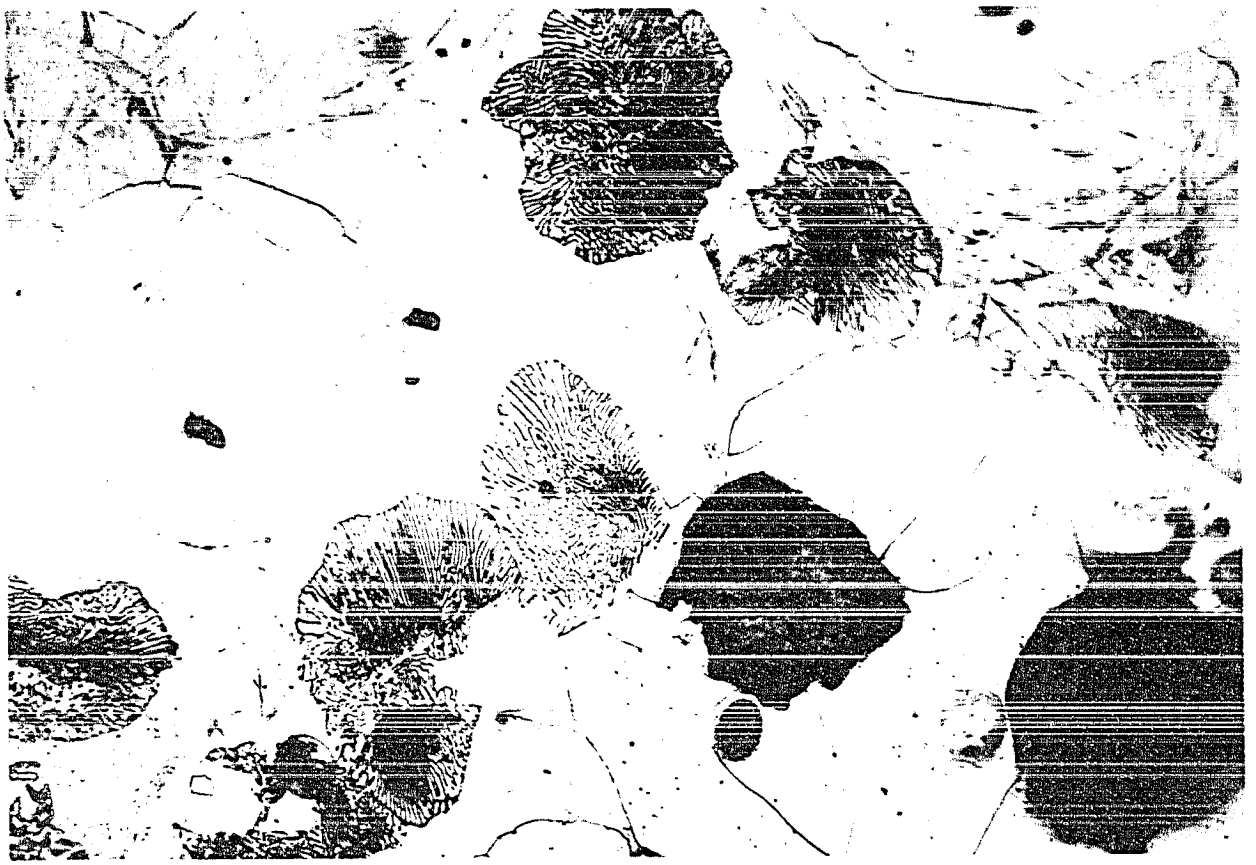

FIG. 77

Transformed at 1400°F for 15 minutes. Ferrite (white), nodules of coarse lamellar pearlite and martensite (gray). 1000 X.

FIG. 78

Transformed at 1350°F for 5 minutes. Ferrite (white) and martensite (gray). 1000 X.

FIG. 79

Transformed at 1300°F for 1.5 minutes. Pearlite (dark) several grains of ferrite (white) near the graphite nodules and martensite (white). 1000 X.

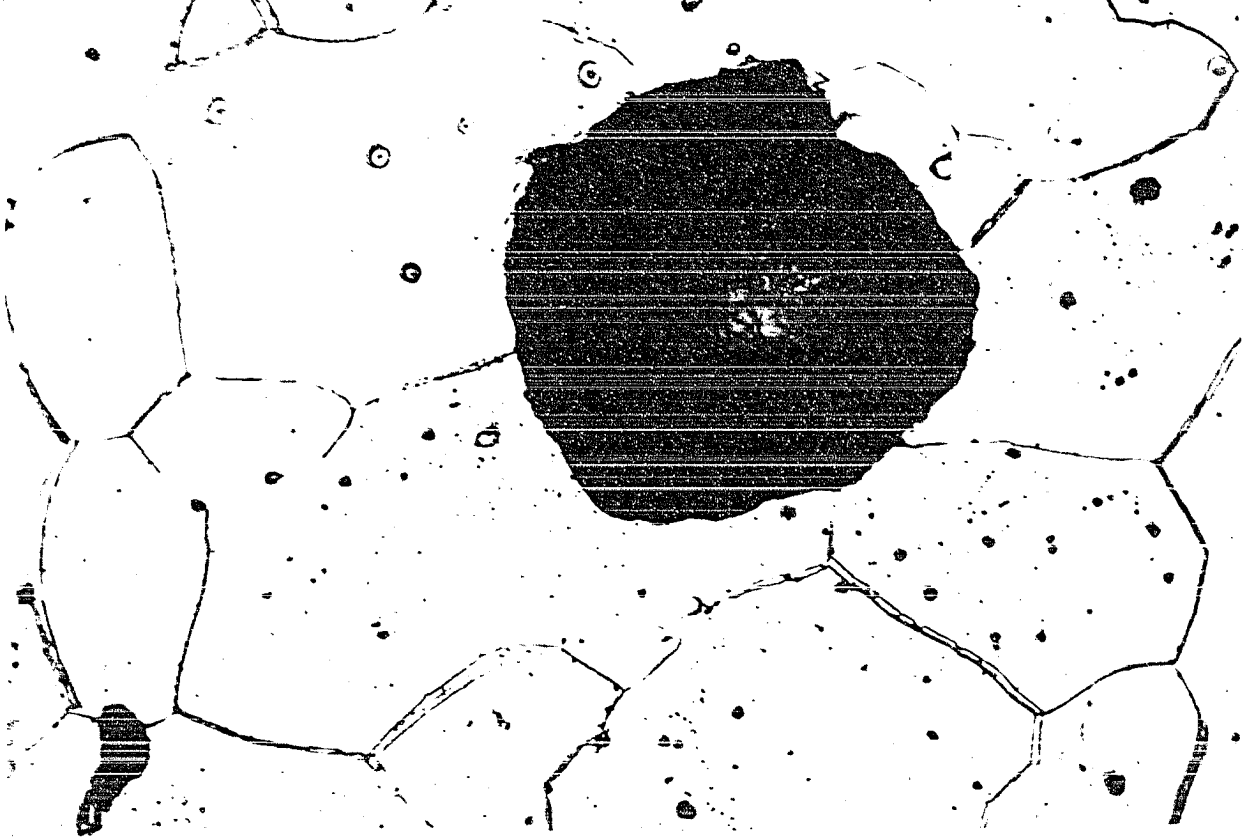

FIG. 80
Transformed at 1300°F for 1300 minutes. Large equiaxed ferrite grains without any substructure. Compare with Fig. 81. 1000 X.

FIG. 81
Transformed at 1200°F for 1,700 minutes. Ferrite grains showing substructure and straining. 1000 X.

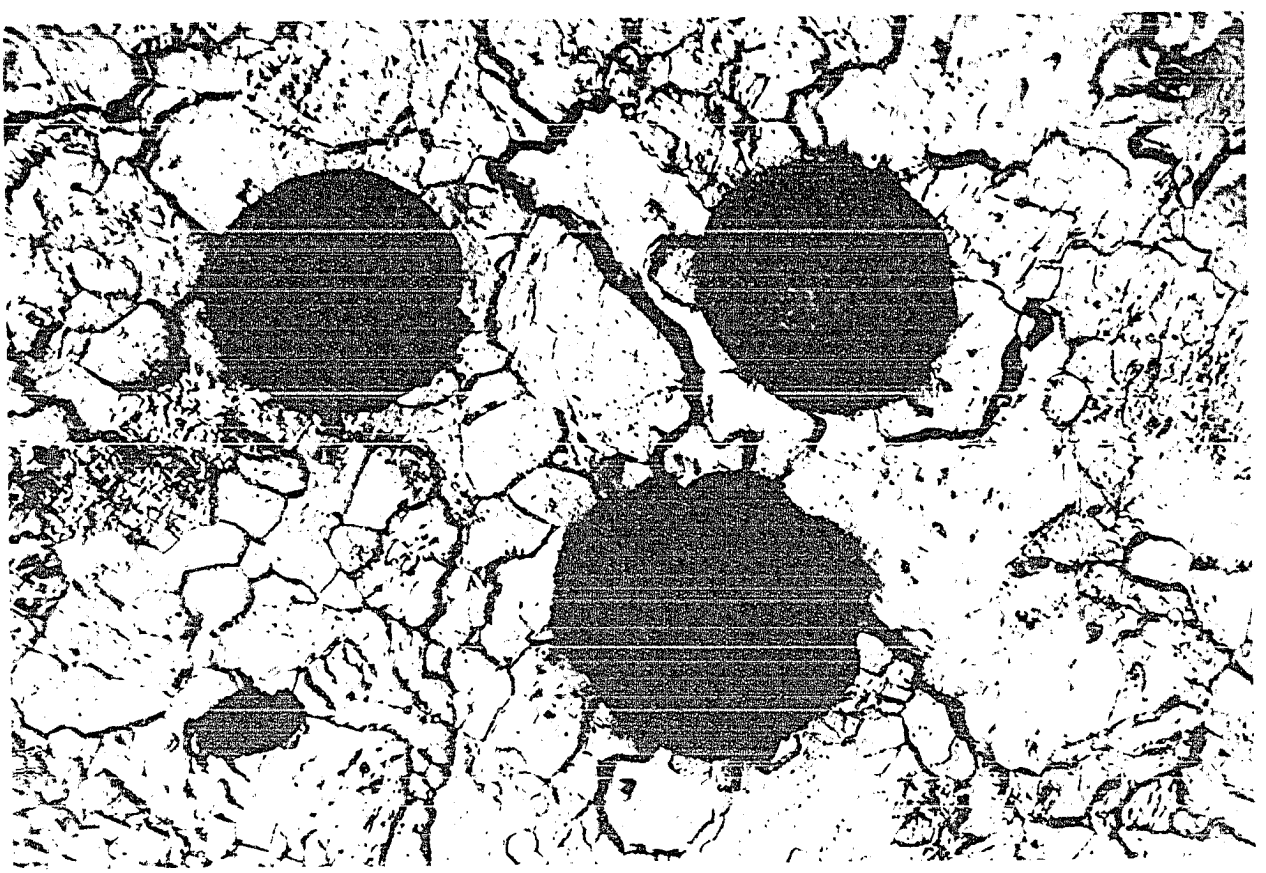

FIG. 82

Transformed at 1200°F for 20 seconds. Pearlite dark and martensite (white). 1000 X.

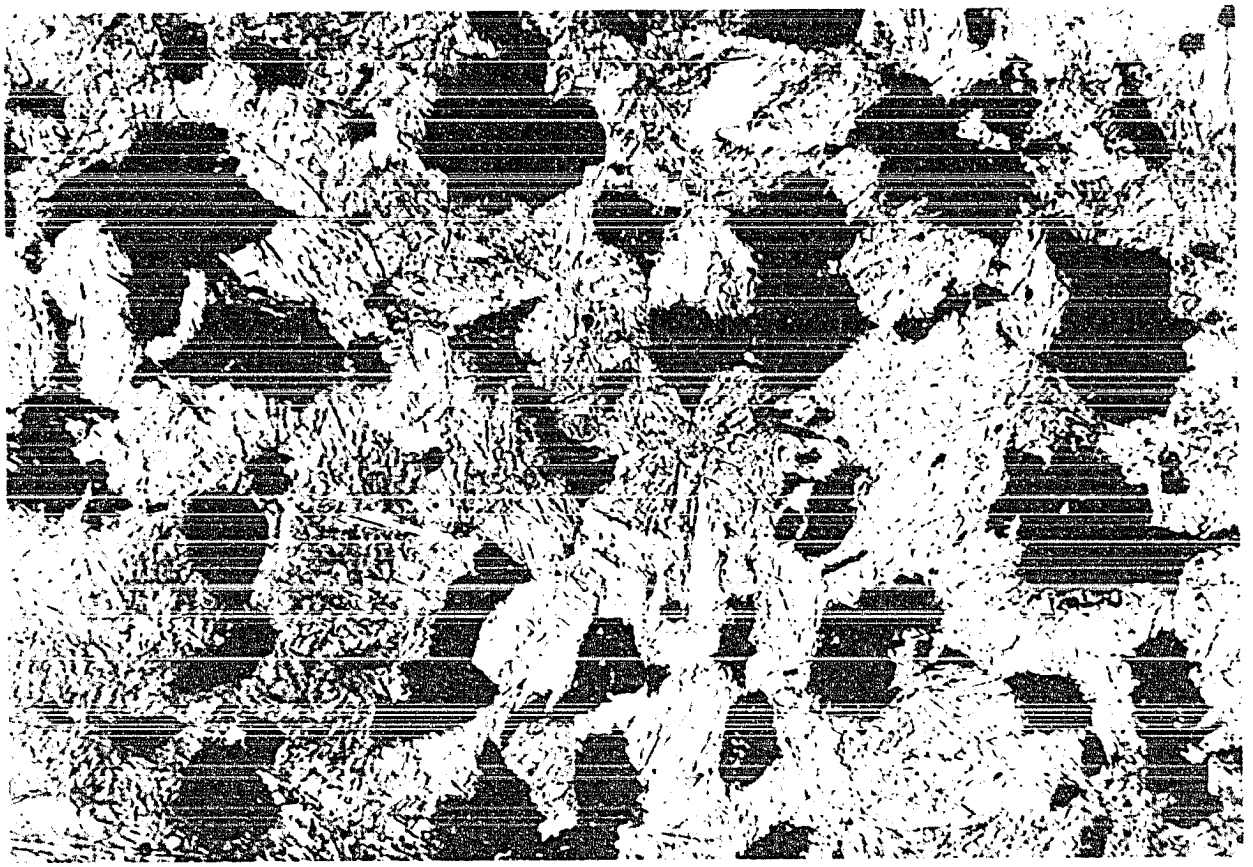

FIG. 83

Transformed at 1100°F for 50 seconds. Fine pearlite (dark) and martensite (gray). 1000 X.

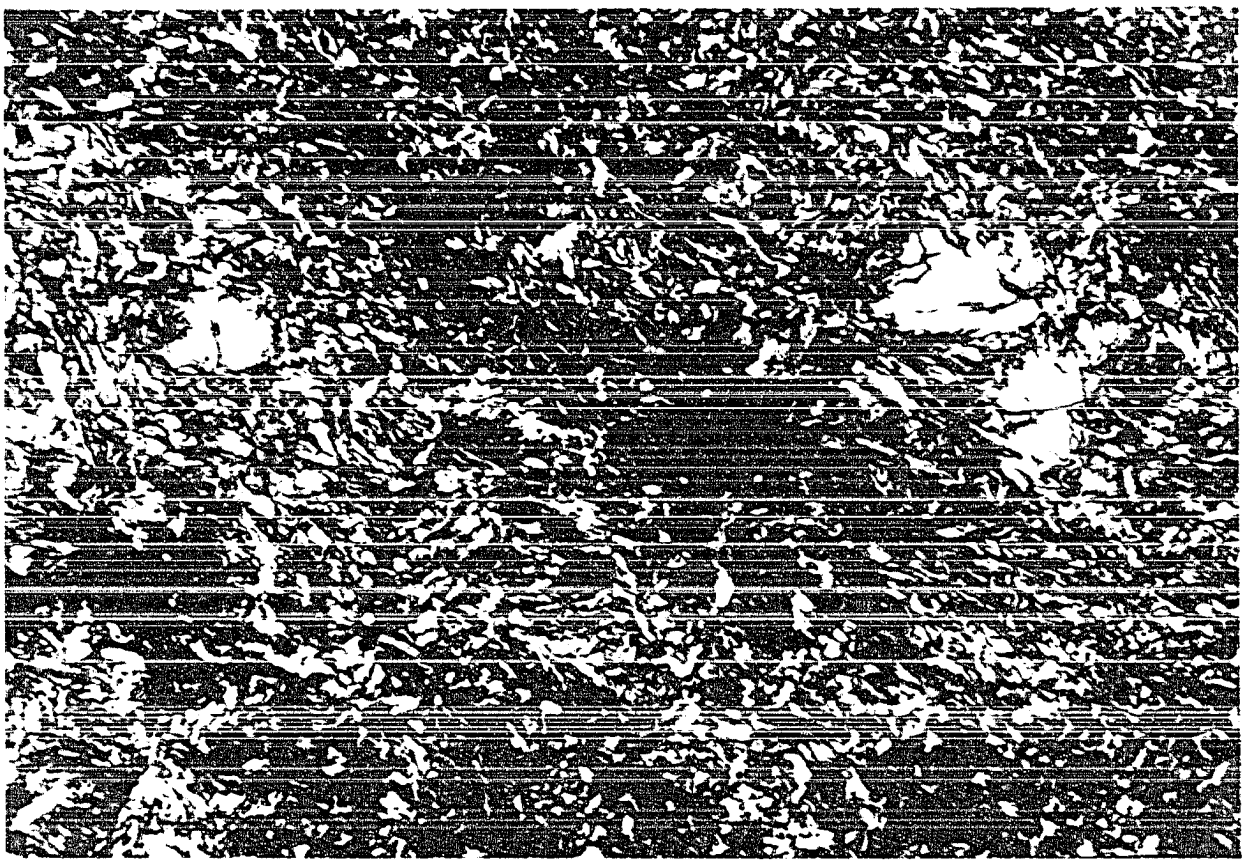

FIG. 84

Transformed at 1000°F for 10 minutes. Mostly constituent "X" (speckled), some pearlite (dark) and several grains of martensite (large white areas). 1000 X.

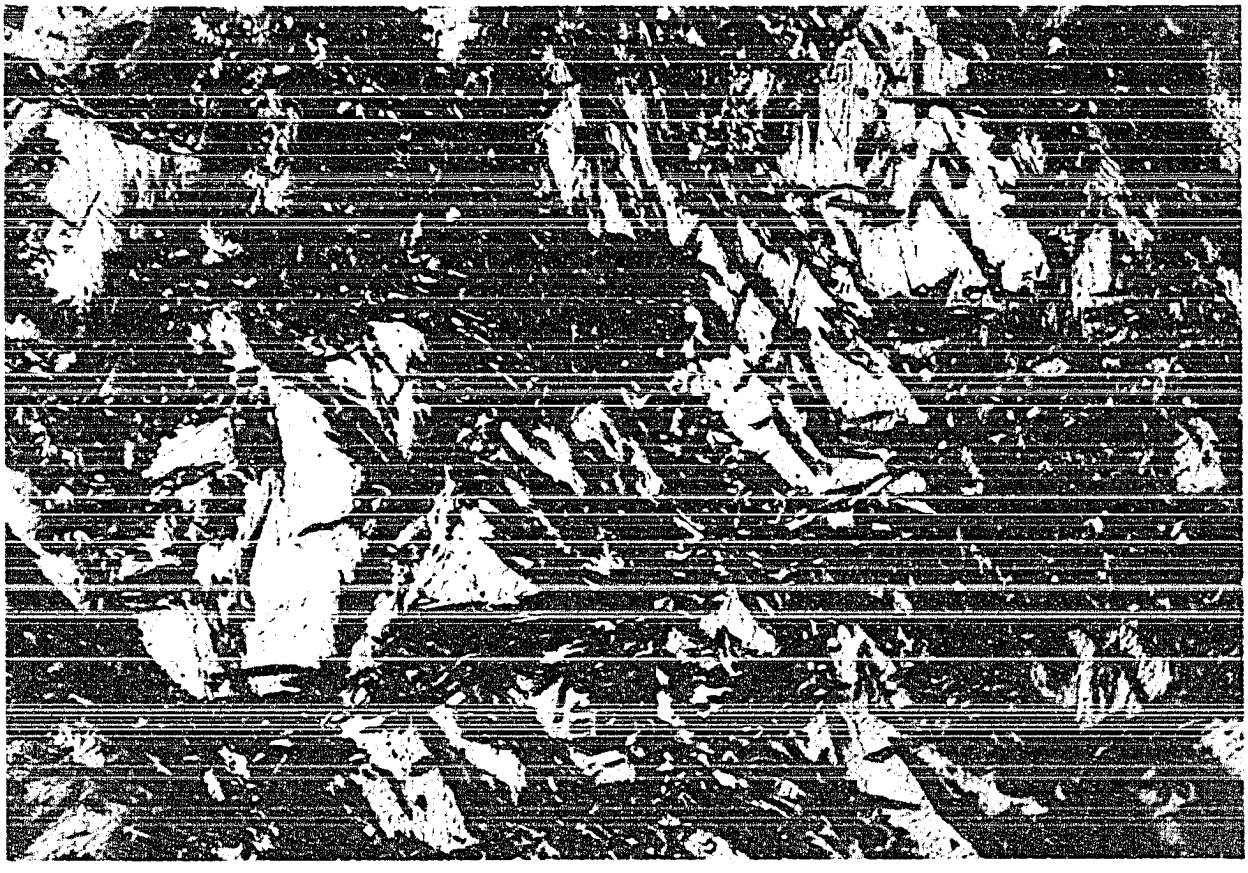

FIG. 85

Transformed at 900°F for 20 minutes. A transition structure (dark) between constituent "X" and bainite. White areas are martensite. 1000 X.

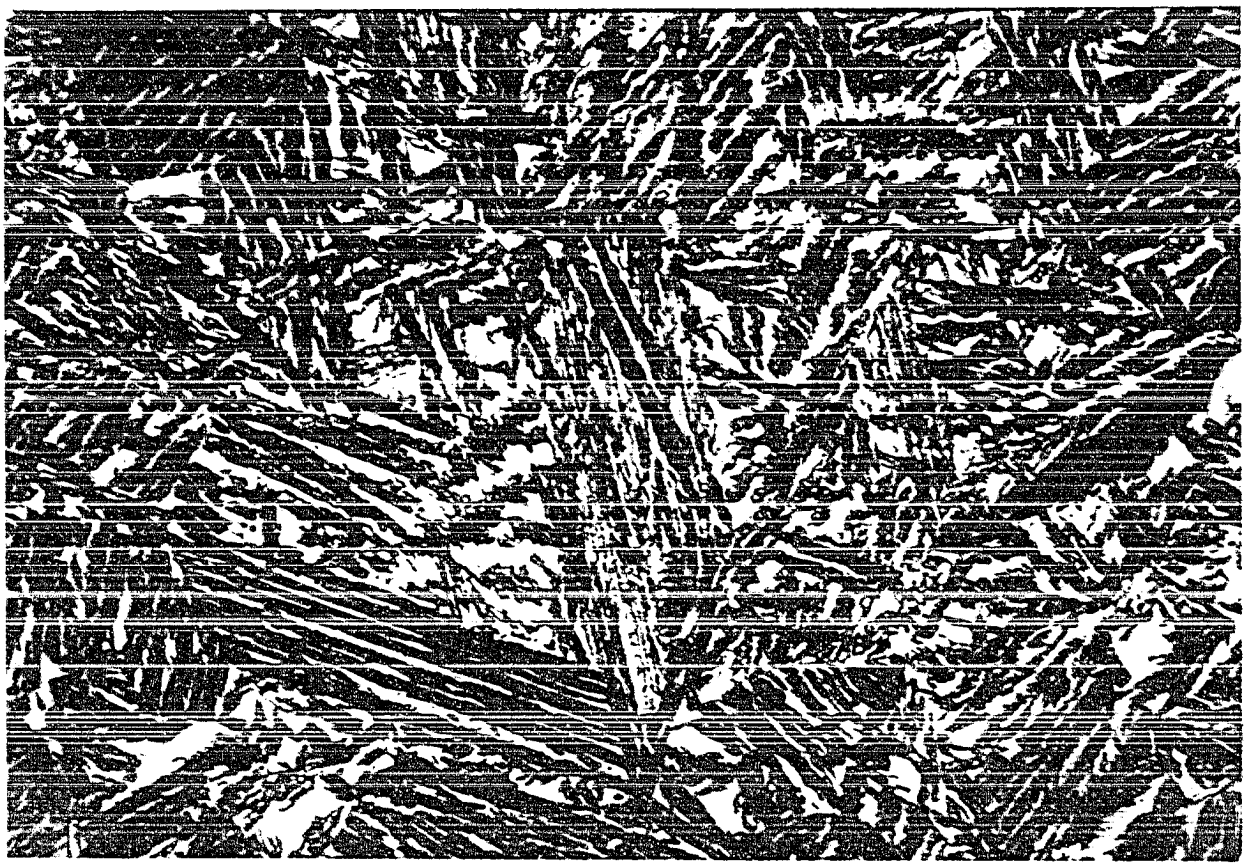

FIG. 86

Transformed at 800°F for 60 minutes. Feathers of bainite (dark) and martensite or untransformed austenite (white). 1000 X.

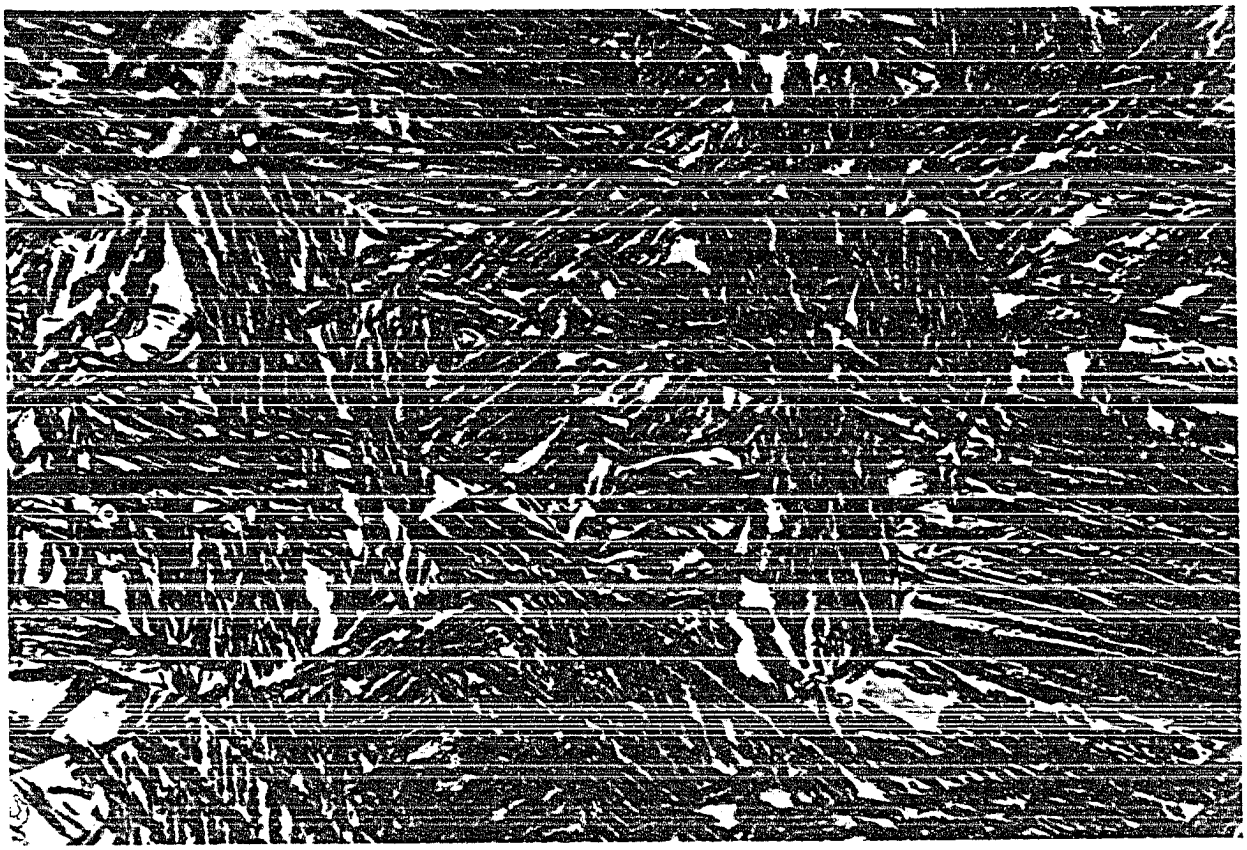

FIG. 87.

Transformed at 700°F for 200 minutes. Bainite (dark) mostly along crystallographic planes and martensite or untransformed austenite (white). 1000 X.

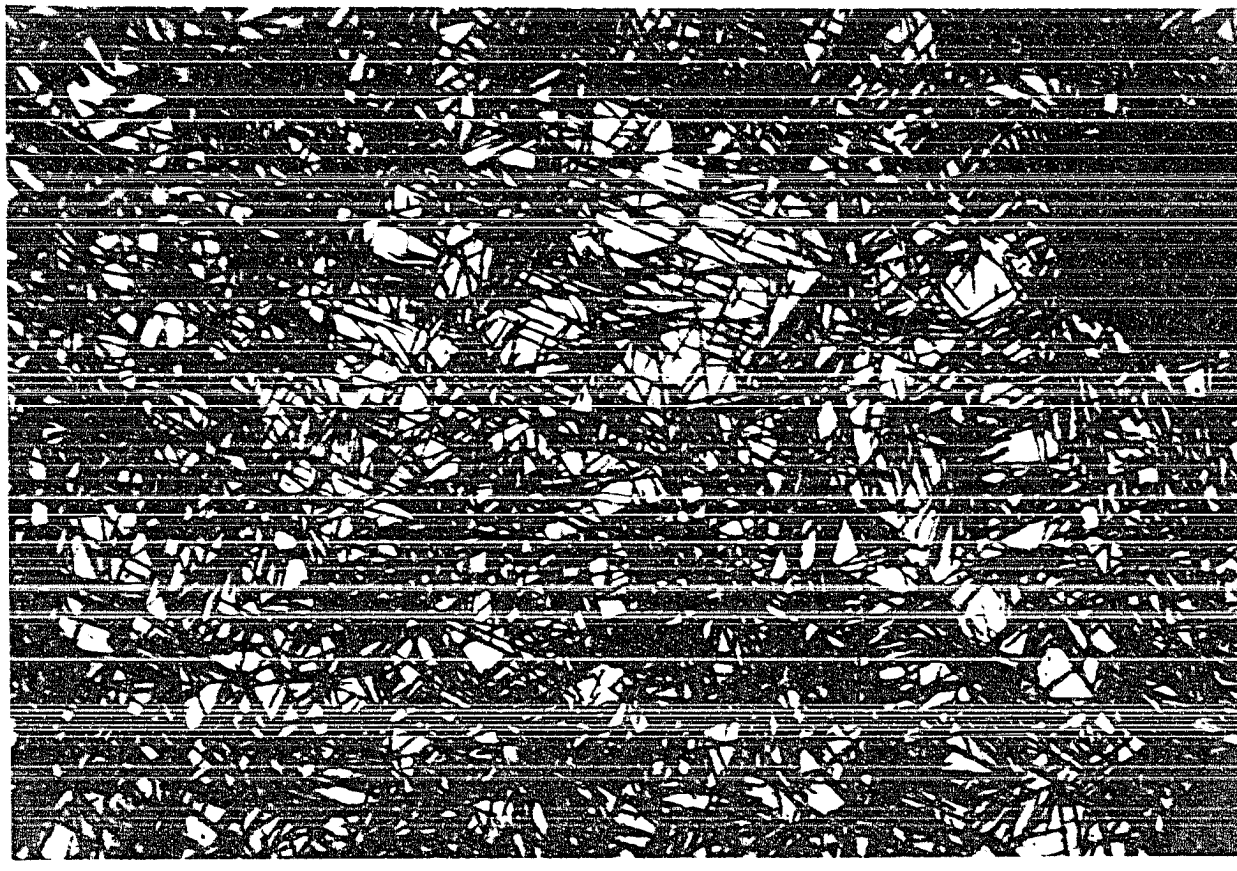

FIG. 88

Transformed at 500°F for 10 minutes. Fine bainite needles (dark) and martensite (white). 1000 X.

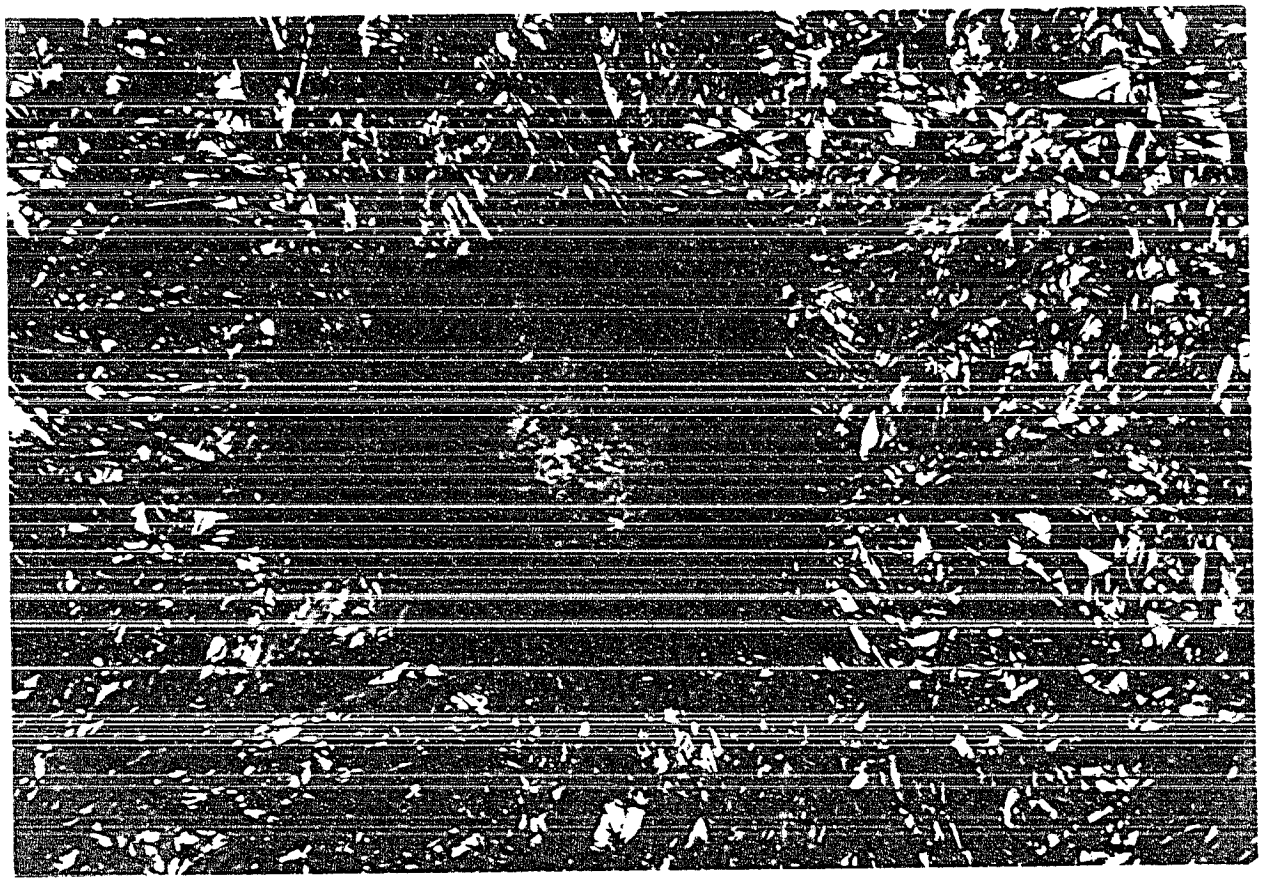

FIG. 89

Quenched to 200°F and held for one minute then tempered at 600°F for 30 seconds. This figure shows the amount of martensite (dark) present at 200°F. 1000 X.

PHOTOMICROGRAPHS FOR OTHER TOPICS

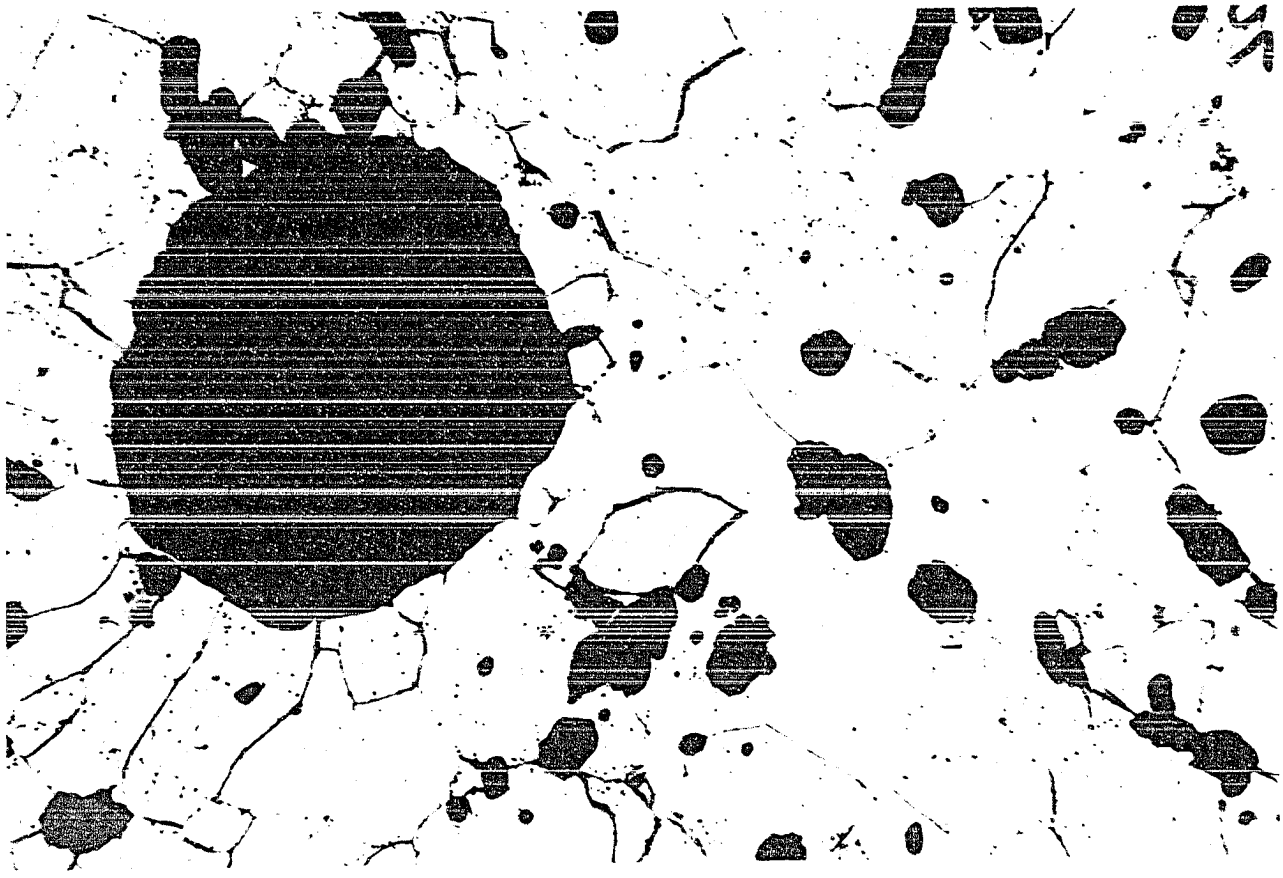

FIG. 90

Cast Iron No. 1. Homogenized at 1800°F for one week in order to produce small "semi-spheroidal" nodules and transformed at 1250°F for 10 hours. Ferrite (white) and many small "semi-nodules" of graphite (dark). Etched with nital. 1000 X.

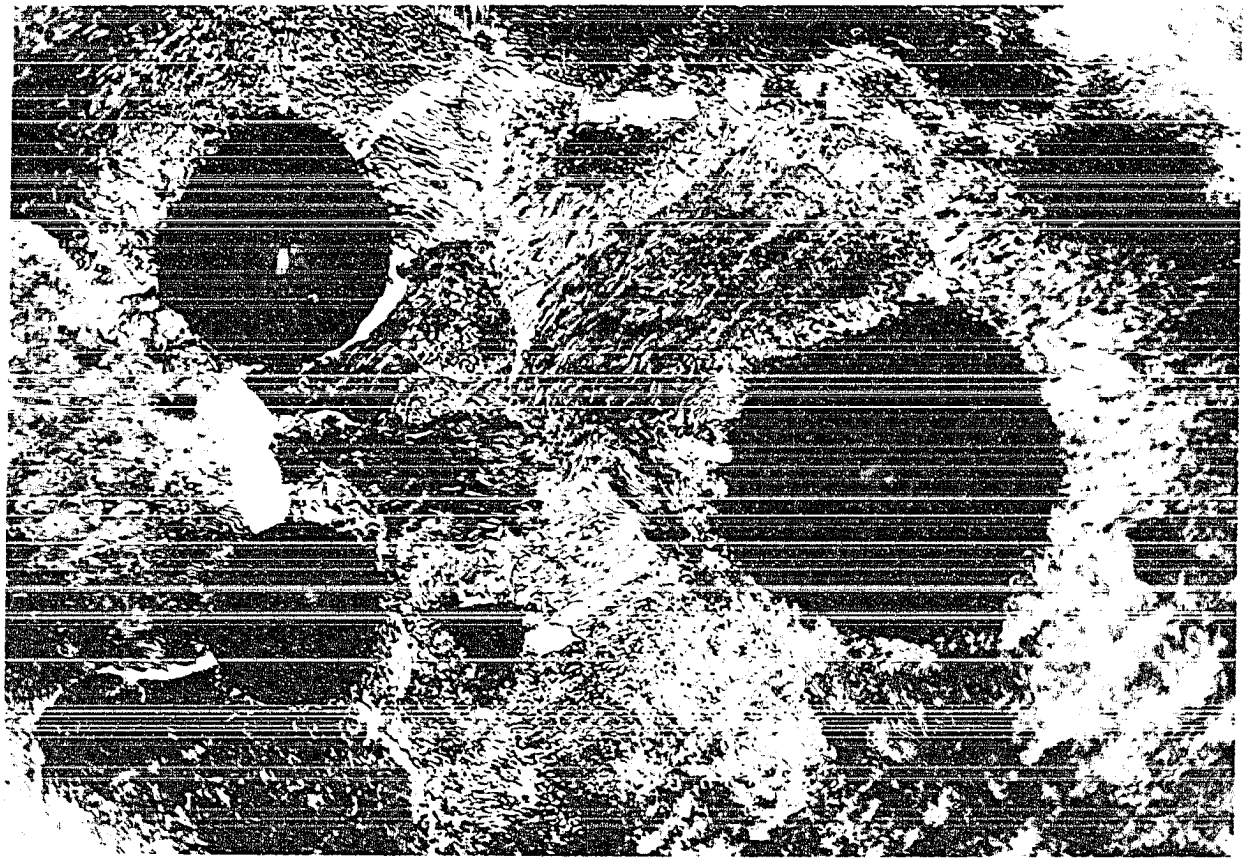

FIG. 91

Cast iron No. 1 in the as cast condition. Several ferrite grains (white) and lamellar pearlite. Cast iron No. 2 looks like No. 1 except it has no ferrite. Etched with nital. 1000 X.

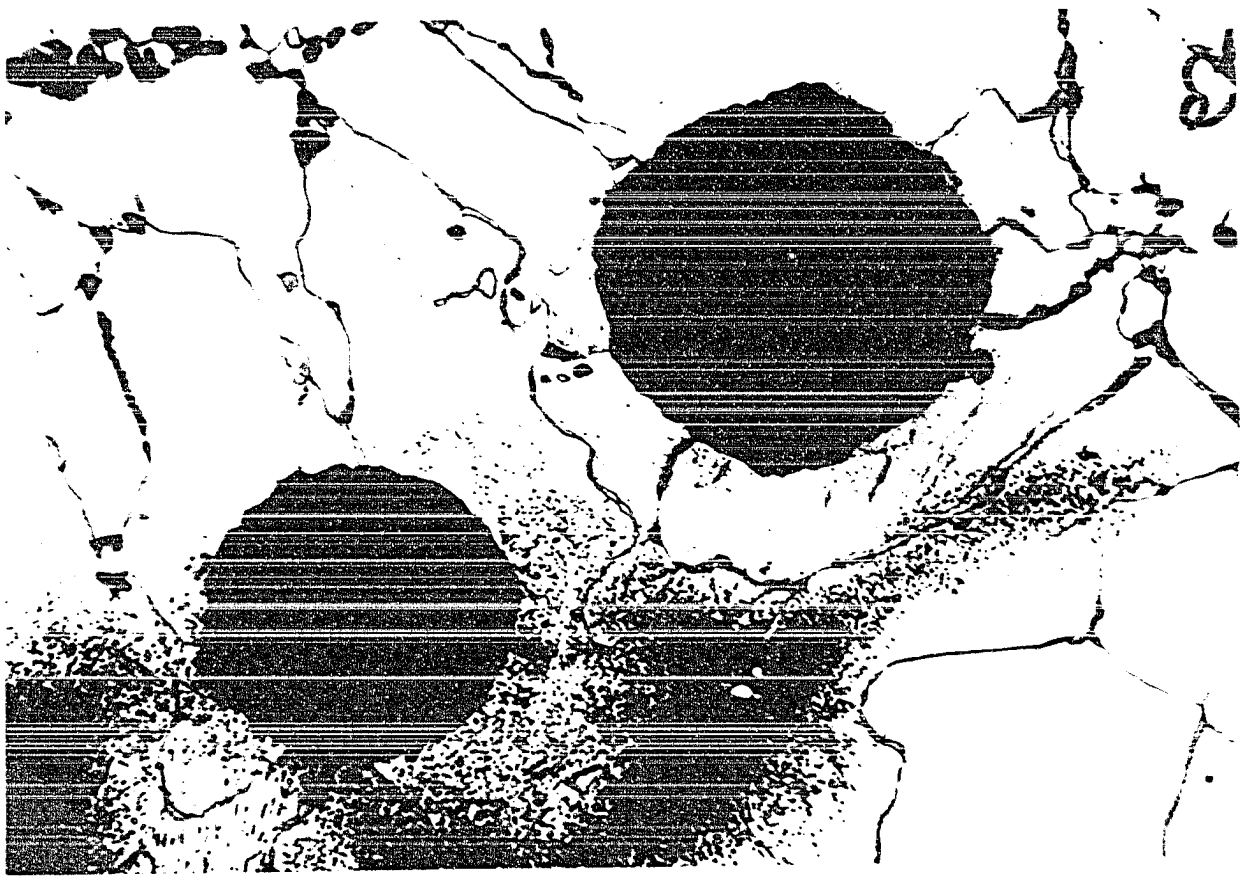

FIG. 92

Cast iron No. 1 which was annealed in the as cast condition (lamellar pearlite) at 1300°F in a lead bath for 150 minutes. The structure consists of large ferrite grains (white), small martensite grains in the grain boundaries (gray) and zones of spherodized pearlite. Etched with nital. 1000 X.

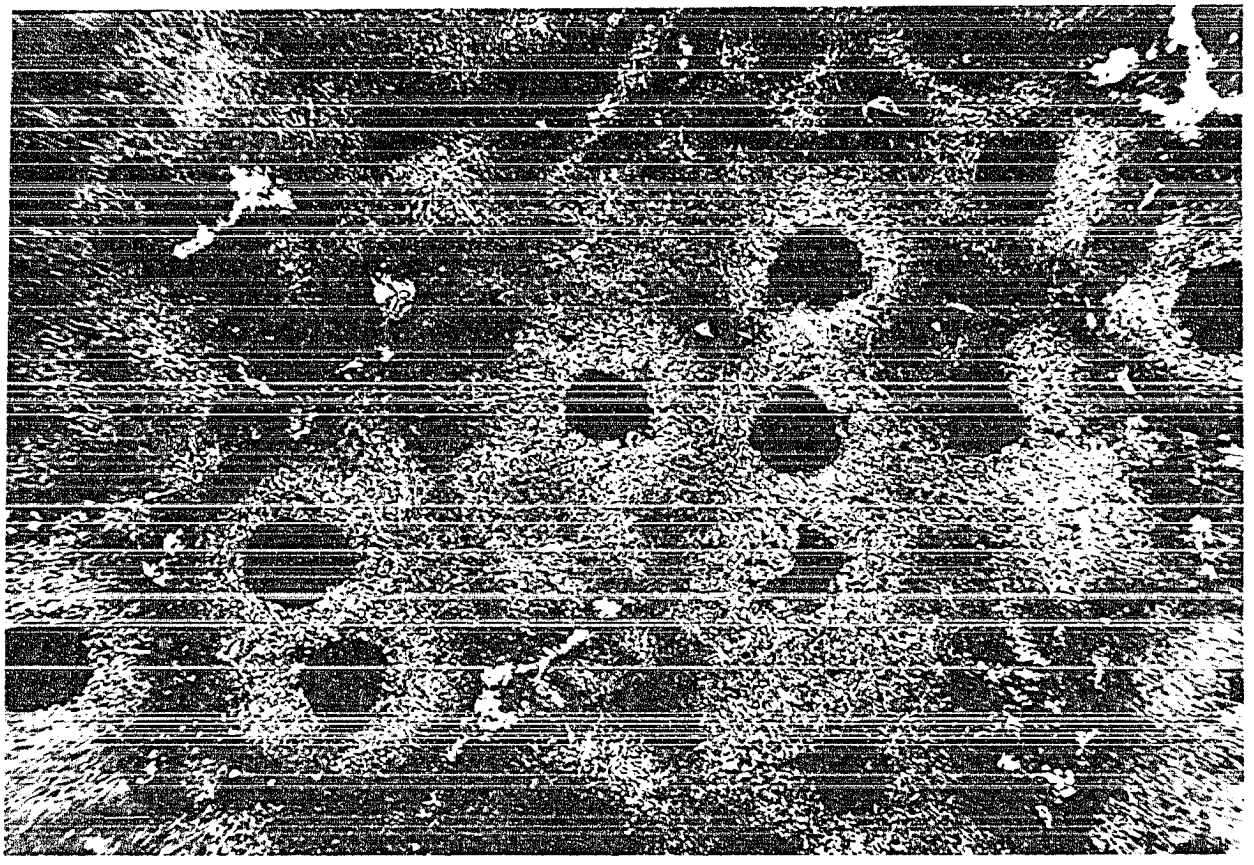

FIG. 93

Cast iron No. 3 which was annealed in the as cast condition (bainite and martensite) at 1200°F for one hour. The structure consists of spherodized pearlite and massive carbide (white) outlining the cellular structure. Etched with nital. 200 X.

FIG. 94

Cast iron No. 1 unetched. Examined under sensitive tint. Nodules show radial structure. 1000 X.

# CONCLUSIONS

1) Ferrite may form directly from the austenite at temperatures of about 150°F above the nose of the T-T-T diagram.

2) The three reactions, namely, austenite to graphite plus ferrite, austenite to pearlite, and pearlite to ferrite and graphite may go on simultaneously at temperatures of approximately 100°F above the "nose" of the T-T-T diagram.

3) There is a range of about 100°F where austenite, ferrite and graphite can co-exist without the complete disappearance of either ferrite or austenite.

4) The reaction for graphitization of pearlite is slower than the reaction for graphitization of austenite below the critical temperature.

5) Ferrite formed from the graphitization of pearlite shows a substructure and straining while ferrite formed directly from austenite does not show a substructure or straining.

6) Ferrite in nickel-molybdenum alloy cast irons stains readily and appears to have dispersed stable carbides.

7) Needles of ferrite appear below the nose of the T-T-T diagram in nickel-molybdenum and nickel-manganese alloy cast irons.

8) Manganese moves the T-T-T diagram to the right and slows down graphitization of both austenite and pearlite below the critical temperature.

9) An increase of manganese increases the time necessary for the beginning of the formation of constituent "X" to a greater extent than for the beginning of pearlite or acicular bainite. This gives a greater indentation in the middle of the T-T-T diagram and results in a more prominent "chin". In other words an increase in manganese results in a more prominent bainite curve.

10) Higher silicon and lower nickel content move the T-T-T diagram upward and to the left. The curve for the end of graphitization of austenite is moved upward considerably while the curve for the end of graphitization of pearlite is not affected appreciably. This results in the formation of ferrite at higher temperatures and shorter times. The critical temperatures and the $M_s$ and $M_f$ are also raised.

11) The constituent "X" type of structure forms very slowly in nickel-molybdenum cast iron and as a result the T-T-T diagram has a prominent "nose" and a prominent "chin".

12) Many small "semi-nodules" of graphite are formed on prolonged heating at high austenitizing temperature (1800°F)

as shown in Figure 90.

13) The longer the austenitizing or homogenizing time and the higher the temperature the greater the number of small "semi-nodules" formed.

14) Nodular cast irons are quite unhomogeneous and show concentration of alloying elements and impurities in the zones that outline the cellular boundaries. Pearlite in these zones is very difficult to decompose to graphite and ferrite.

15) The unhomogeneous zones due to their higher alloy content have a much lower Mf temperature then the rest of the material. This may result in retained austenite in these zones even in low alloy cast irons.

16) The unhomogeneous zones are usually away from the nodules and may contain some carbide.

17) The last 10% of pearlite takes a very long time to decompose and this is usually due to the unhomogeneous zones that contain carbide stabilizers.

18) If nodular cast iron specimen is austenitized and homogenized in air, there is some decarburization, and the surface zone of the specimen becomes depleated of carbon. The surface zone transforms more rapidly because of its lower carbon content, and therefore erroneous results may be obtained for the "beginning" and "end" of transformation.

# REFERENCES


1. S. Epstein, "The Alloys of Iron and Carbon", book, Vol. I - Constitution, 1936, McGraw-Hill Book Co.

2. C. Wells, "Graphitization in High Purity Iron-Carbon Alloys", Transactions, A.S.M. Vol. 26, 1938, p. 289.

3. H. Seltz, H. J. McDonald and C. Wells, "Heat Capacity of Iron Carbide from 68° to 298°K and the Thermodynamic Properties of Iron Carbide", Transactions, A.I.M.E. Vol. 140, 1940, p. 263.

4. A. L. Norbury, "Constitutional Diagrams for Cast Iron and Quenched Steels", J. Iron and Steel Institute, vol. 119, 1929, p. 443.

5. A. Boyles, "The Structure of Cast Iron", A.S.M. Book, 1946.

6. V. Delport, "Nodule Formation Discussed at International Foundry Congress", Foundry, Vol. 80, 1952, p. 200.

7. A. I. Krynitsky and H. Stern, "Experimental Production of Nodular Graphite in Cast Iron", Foundry, March, and April 1952.

8. I. Iitaka, "A Theory of Globular Graphite Formation in Cast Iron", Reports of the Casting Research Laboratory, No. 2, 1951, and No. 4, 1953.

9. K. P. Bounin and G. I. Ivantzoff, "On the Crystallization of Nodular Graphite in Cast Iron", Doklady Akademii Nauk, S.S.S.R., New Series Vol. 72, No. 6, 1950

10. A. De Sy, "Graphite Spherulite Formation and Growth", Foundry, Nov., 1953.

11. J. E. Rehder, "Nodules and Nuclei in Nodular Iron", American Foundryman, February and May, 1952.

12. H. F. Scobie, "Nodular Iron Symposium Shows We Still Have Long Way to Go", American Foundryman, October, 1950.

13. R. P. Dunphy and J. S. Pellini, "Nodular Genesis and Growth in Magnesium Treated Hypoeutectic Irons", Internation Foundry Congress, Brussels, September, 1951.

14. B. Chalmers, "Melting and Freezing", Journal of Metals, May, 1954.

15. A. Wittmoser, "Sur les Germes du Graphite Spheroidal", Congres International de Founderie, Paris, Septembre, 1953.

16. A. B. Greninger and A. R. Troiano, "Kinetics of the Austenite-Martensite Transformation in Steel", Transactions, American Society for Metals, Vol. 28, 1940, p. 537.

17. B. F. Brown and M. F. Hawkes, "Kinetics of Graphitization in Cast Iron", Transactions of the American Foundrymen's Society, Vol. 59, 1951, p. 181.